EUROPEAN AVIATION SAFETY AGENCY
AGENCE EUROPÉENNE DE LA SÉCURITÉ AÉRIENNE
EUROPÄISCHE AGENTUR FÜR FLUGSICHERHEIT

Research Project EASA.2009/2

MOSTDONT - Mode S Transponder in High Density Operational Environment

easa.europa.eu

Disclaimer

Research Project EASA.2009/2

MOSTDONT
Mode S Transponder in High Density Operational Environment

Final Report

Release 1.2

Submitted by the FAV-FCS consortium

Funkwerk Avionics GmbH
Riedweg 5
89081 Ulm
Germany

Tel. +49 731 93697-30
Fax +49 731 93697-79
e-mail: info@funkwerk-avionics.com

FCS Flight Calibration Services GmbH
Hermann-Blenk-Str. 32 A
38108 Braunschweig
Germany

+49 53123777-0
+49 53123777-99
e-mail: info@flightcalibration.de

Date: 21.10.2010

Authors:

Dr.-Ing. Jochen Bredemeyer, FCS Flight Calibration Services GmbH

Publicly certified expert for “Navigation and Radar Systems in Air Traffic Control”
by the Chamber of Engineers of Lower Saxony (IngKN) , Germany

Erik J. Wischmann, Funkwerk Avionics GmbH

Jens Gottstein, Technische Universität Braunschweig

Note:

The map images in this report were produced with OpenStreetMap (http://www.openstreetmap.org/)

Table of Contents

Executive Summary

This report documents the results of a study on Mode S signal-in-space characteristics and their impact on airborne transponders. The study was commissioned by the European Aviation Safety Agency (EASA, Tender EASA.2009.OP.20).

Mode S technology and its application for surveillance and airborne conflict prevention are specified in two standardisation documents: ICAO Annex 10 Volume IV, and EUROCAE ED-73C/RTCA DO-181D. The specifications for the signal-in-space characteristics in these documents, however, have several shortcomings that have led to problems in radar/transponder compatibility in the recent period.

Therefore, the main task of this study was to measure and analyse the actual signal-in-space as it exists in several parts of the European airspace with respect to radar and transponder performance. A dedicated measurement receiver was made available for this purpose that allows a detailed investigation of signals transmitted by conventional SSR facilities, TCAS (Traffic Alert and Collision Avoidance System) equipped aircraft and ground-based multilateration systems. This receiver was installed in a special mission flight inspection aircraft, operated by FCS Flight Calibration Services GmbH. This recorded interrogation signals during various FCS measurement campaigns, totalling more than 100 flight hours.

These airborne measurements were complemented by ground station recordings from an existing dual channel Mode S monitoring network, operated by the Technical University (TU) Braunschweig.

In addition to these investigations of real-world in-space RF signals, Funkwerk Avionics (FAV) performed laboratory tests to investigate to what extent signals generated by typical Mode S test equipment differed from the airborne measurements.

As a result of these analyses, a number of recommendations for improvements of the Mode S specifications (ICAO Annex 10 and ED-73C) were developed. These recommendations are aimed at ensuring that a transponder that successfully passed all ED-73C test cases and complies with the standards will actually work correctly in the Mode S operational environment.

The major findings of this study are:

- Most radar stations surveyed apply a phase modulation technique (I/Q modulation) that is not simulated by existing test equipment.
- The duration of Mode S phase reversals may exceed the maximum of 80 ns due to a number of effects (e.g. P5 side lobe suppression, multipath propagation). Existing test equipment cannot simulate such slow phase reversals.
- Transponder reply rates required in the current operational environment are well below the minimum reply rate capabilities specified in the standards.
- Non-diversity transponder installations with only one antenna (as applicable for most General Aviation aircraft), mounted below the fuselage, pose no significant problem for radar detection or TCAS communication.
- Some TCAS units perform interrogations that are not compliant with ICAO Annex 10 and ED-73C.
- There are some discrepancies between ICAO Annex 10 and ED-73C that need to be resolved; proposed resolutions are provided by this report.

1 INTRODUCTION

1.1 Document Overview

This document is the Final Project Report on the MOSTDONT (Mode S Transponder in High Density Operational Environment) study, launched by EASA and performed under contract by Funkwerk Avionics GmbH (FAV), Flight Calibration Services GmbH (FCS) and Technische Universität Braunschweig (TU BS). The study is aimed at identifying and investigating potential certification issues for Mode S transponders in high density operational environments.

The report has the following structure:

This **Section 1** contains the document overview, provides background on the reason for conducting the study, lists the study partners and their principal work share, and concludes with a list of reference documents and abbreviations.

Section 2 describes the study approach in detail and provides detailed work package descriptions explaining the tasks for each work package and the expected outcome.

The activities conducted within the study and the respective results are documented in **Section 3**.

Section 4 summarizes the major findings of the study and provides conclusions.

Supplemental information is provided in the **appendices**.

1.2 Background

After the first issue of the technical specifications for SSR (Secondary Surveillance Radar) Mode S in ICAO Annex 10 in 1987, it took nearly another two decades until a Mode S radar infrastructure was fully operational in central Europe and other areas of the world. During this extended period of Mode S ground infrastructure implementation, Mode S SSR transponders essentially served as mere TCAS responding devices. TCAS (an implementation of the ICAO-defined Airborne Collision Avoidance System "ACAS") was widespread in commercial aviation already 20 years ago and has been mandatory since the early 1990s (U.S.), and then later in other regions. A major change in information coding from Mode A/C to Mode S concerns the uplink interrogations on 1030 MHz. These are modulated in DPSK (Differential Phase Shift Keying) which makes detection more complex, while increasing sensitivity to interference sources such as multipath propagation.

The ICAO Annex 10-derived transponder MOPS ED-73C (EUROCAE) does not contain any information on the potential influence of realistic disturbance sources that may exist in operational environments, but mainly describes signals under laboratory-clean conditions. Consequently, transponder manufacturers have tended to implement detection algorithms and designs responding to clean signals as generated by a MOPS-compliant test generator. However, such a design is likely to have difficulties – to a varying degree – in coping with real world signals from radars in the field.

Mode S radars have now become very widespread and there are mandates for Mode S transponder equipage (ICAO ACAS II mandate for commercial transport, varying requirements for General Aviation across Europe, see EUROCONTROL web page http://www.eurocontrol.int/msa/public/standard_page/General_aviation_VFR.html).

The increasing amount of Mode S and Mode A/C, as well as TCAS transmissions, which are a consequence of the ever increasing number of transponder equipped aircraft due to these mandates, presents a formidable challenge for the correct operation of Mode S transponders. However, this correct functioning is essential for the provision of the ATC surveillance service, which depends on the data transmitted by Mode S transponders for the identification and positioning of controlled flights. The fact that new surveillance techniques such as multilateration (MLAT) and 1090 MHz Extended Squitter-based Automatic Dependent Surveillance – Broadcast (ADS-B) also rely on the correct functioning of Mode S transponders underlines the key importance of this study and its findings.

There is a range of issues associated with operating Mode S transponders – especially low-power, single antenna transponders for general aviation – in high density environments such as Terminal Management Areas (TMA) around major international airports:

- High rate of interrogations due to dense TCAS traffic

  The maximum rate of interrogations as required by current ED-73C may already be exceeded today in dense environments, mainly due to a large number of TCAS interrogations.

- Overlapping interrogations and replies

  In dense environments, the likelihood of interfering interrogations or replies increases. This is worsened by the parallel operation of Mode S and Mode A/C as present in most airspace today. The increasing use of ADS-B and multilateration surveillance systems further increases the channel load.

- Ground-induced disturbances (e.g. multipath effects) on interrogations and replies

  As previous measurements in real environments have shown, the effects of ground-induced multipath signal propagation are evident not only in the transponder replies received by the radar stations but also in the interrogations as received by the airborne transponder. Such effects may not be sufficiently addressed in the current standards (ICAO Annex 10 and EUROCAE ED-73C).

- Varying implementation at different radar sites

  Different radar sites may use quite different settings of certain parameters (e.g. Mode S lock-out criteria, side-lobe suppression characteristics, interrogation patterns, rotational frequencies). These parameters are often tuned in order to meet the ICAO criteria for minimum detection probability, using statistical evaluation of the entire traffic (including air transport aircraft). This poses the risk, however, that the probability of detection for low-power, non-diversity transponders as installed on smaller general aviation aircraft falls below those minima. As it is impractical to test each new transponder design against radar installations all over the world, the test requirements in ED-73 must give a fair representation of the real environments to ensure that a certified transponder will function correctly with all radar installations.

1.3 Study Partners and Work Distribution

The following work share was agreed upon:

1.3.1 Funkwerk Avionics GmbH (FAV)

Own work packages:

1100 Management

1300 Final Report

2200 Improved Test Signal Definition (with inputs by FCS)

3200 Active Interrogation Reduction

3300 Side Lobe Suppression

Subcontract: **Institute of Flight Guidance, TU Braunschweig**:

Support to WP2100

Work package 3100 Probability of Communication Frame Interference

1.3.2 FCS Flight Calibration Services GmbH

Own work packages:

1200 Scientific coordination and securing good scientific practice

2100 Evaluation of the characteristics of the signal in space

2200 Inputs to FAV (based on WP2100)

2300 TCAS analysis

2400 Influence of non-diversity antenna installations

1.4 Referenced Documents

[RD1] Specifications attached to the Invitation to Tender. EASA.2009.OP.20 MOSTDONT - Mode S Transponders in high density operational environment

[RD2] QUESTIONS AND ANSWERS PERTAINING TO THE TENDER PROCEDURE EASA.2009.OP.20. 11 November 2009.

[RD3] Minimum Operational Performance Specification for Secondary Surveillance Radar Mode S Transponders (EUROCAE ED-73C), September 2008, Paris/France

[RD4] Annex 10 to the Convention on International Civil Aviation: Aeronautical Telecommunications - Volume IV: Surveillance Radar and Collision Avoidance Systems (ICAO Annex 10, Volume IV), Third Edition, Amendment 80, July 2002

[RD5] Manual on the Secondary Surveillance Radar (SSR) Systems (ICAO Doc 9684 AN/951), Third Edition, Amendment 1, 2004.

[RD6] Bredemeyer, J.; Wischmann, E.: Challenges for Mode S transponders in a real radio field environment. International Radar Symposium IRS 2009. Hamburg, Germany, September 2009

[RD7] Bredemeyer, J.; Lauper, P.: Mode S Test Flights in Switzerland. In: Proceedings of International Radar Symposium (IRS 2007). Cologne, Germany , 05-07 September 2007

[RD8] Bredemeyer, J.; Kleine-Ostmann, T. ; Schrader, T. ; Münter, K. ; Ritter, J.: Airborne Field Strength Monitoring. In: Advances in Radio Science, Kleinheubacher Berichte Bd. 5, U.R.S.I., 2007

[RD9] Bredemeyer, J; Form, P.: Experimentally tested detection of interfered Mode S replies. In: Proceedings of International Radar Symposium (IRS 2003). Dresden, Germany, 30 September - 02 October 2003

[RD10] Bredemeyer, J.: Interferenz unkoordinierter Abfragen und Antworten von Transpondern der Luftfahrt. In: Proceedings of Symposium Transponder 2003. Hannover, Germany, 02-03 April 2003

[RD11] Bredemeyer, J.: Flight Inspection of the Secondary Surveillance Radar Signal-in-Space. In: Proceedings of 12th International Flight Inspection Symposium (IFIS 2002). Rome, Italy, 03-07 June 2002

[RD12] Bredemeyer, J.: Korrelationsanalyse im Sekundärradarfunkfeld. In: Ortung und Navigation (2001), Nr. 2, p. 71–83

[RD13] Gottstein,J; Form,P: EUROCONTROL Safety R&D Seminar 2009: Five Million Flight Hours Continuous Reception of ACAS - Communications and Reporting of TCAS-interventions in the German airspace. Munich, Germany, 21-22 October 2009

[RD14] Deutsche Forschungsgemeinschaft (DFG):
Proposals for Safeguarding Good Scientific Practice
Recommendation of the Commission on Professional Self-Regulation in Science
http://www.dfg.de/aktuelles/presse/reden_stellungnahmen/download/self_regulation_98.pdf

[RD15] Gottstein, J.; Burkert, A.; Form, P.: ACAS-Monitoring by an Experimental Ground Station in Braunschweig. DGON ESAVS 2007 Symposium, Bonn, Germany, March 2007

[RD16] Gottstein, J.; Form, P.: ACAS-Monitoring of 1.000.000 flight hours in the North German Airspace. Tyrrhenian International Workshop on Digital Communications, ESAVS 2008, Capri, Italy, 03-05 September 2008

[RD17] ICAO CNS Supplement - SSR Mode S Interrogator Code (IC) Allocations for the EUR Region, Edition 1.6, EUROCONTROL

[RD18] ICAO Document 8071 - Manual on Testing of Radio Navigation Aids, Volume III (Testing of Surveillance Radar Systems), First Edition 1998

1.5 Abbreviations

ACAS	Airborne Collision Avoidance System
ADS-B	Automatic Dependent Surveillance – Broadcast
AP	Address/Parity field (24 bits)
ASR	Airport Surveillance Radar
ASTERIX	All Purpose Structured Eurocontrol Surveillance Information Exchange
AWACS	Airborne Warning and Control System
DF	Downlink Format
DFG	Deutsche Forschungsgemeinschaft
DFS	Deutsche Flugsicherung GmbH
DPSK	Differential Phase Shift Keying
EASA	European Aviation Safety Agency
FAV	Funkwerk Avionics GmbH
FCS	FCS Flight Calibration Services GmbH
FIR	Finite Impulse Response
FIS	Flight Inspection System
GPS	Global Positioning System
I/Q	In-phase / Quadrature
IC	Interrogator Code
II	Interrogator Identifier
IF	Intermediate Frequency

ITT	Invitation To Tender
LVA	Large Vertical Aperture
LVNL	Luchtverkeersleiding Nederland
MLAT	Multilateration
MOPS	Minimum Operational Performance Standard
MSSR	Monopulse Secondary Surveillance Radar
PPS	Pulse Per Second
RD	Reference Document
RF	Radio Frequency
RMS	Root Mean Square
SI	Surveillance Identifier
SLS	Side Lobe Suppression
SPR	Sync Phase Reversal
SSR	Secondary Surveillance Radar
TCAS	Traffic Collision Avoidance System
TMA	Terminal Manoeuvring Area
TOA	Time Of Arrival
UF	Uplink Format
WP	Work Package
WAM	Wide Area Multilateration

2 STUDY APPROACH AND WORK PACKAGES

2.1 Overall Approach

The FAV-FCS team has divided the activities required by EASA's invitation to tender (ITT) into two main groups of activities:

- Those related to the Mode S signals-in-space on 1030 MHz and their characteristics;
- Those related to the transponder itself and its operational environment.

The study is based largely on data recordings which were collected during this study. Despite the availability of a vast set of recordings from previous studies, the FAV-FCS team believed that the questions to be answered by this study required dedicated measurement campaigns with special, non-standard receivers and a setup specifically designed to provide the data for the envisaged analysis tasks.

The signal-in-space (SIS) related activities conducted for this study comprised:

- Evaluation of the recordings with a focus on Mode S uplink signal characteristics, including timing related aspects, analysis of frequently observed disturbances of those signals (without interference with other signals). The various Mode S sources were ground Monopulse Secondary Surveillance Radar (MSSR) facilities, MLAT interrogators and airborne TCAS signals.
- These analyses lead to a number of proposals for a revised signal specification which may in the future be the basis for Mode S transponder testing.
- Analysis of the signal disturbances observed in aircraft-to-aircraft signals (TCAS).
- Assessment of the essential effects resulting from the use of non-diversity transponder installations on general aviation aircraft. This analysis covers the aspects of both aircraft-to-ground and aircraft-to-aircraft communication.

Activities summarised under operational aspects included:

- Evaluation of the probability of data communication frame interference. This was accomplished through analysis of recordings provided by an existing Mode S observation network.
- An analysis of existing ICAO and EUROCAE/RTCA specifications with respect to discrepancies, ambiguity, and incompleteness (e.g. definition of side lobe suppression characteristics).
- Investigation of existing limits in typical General Aviation Transponders when interrogated at rates exceeding the reply rates specified in EUROCAE ED-73C.

2.2 Work Packages (WP)

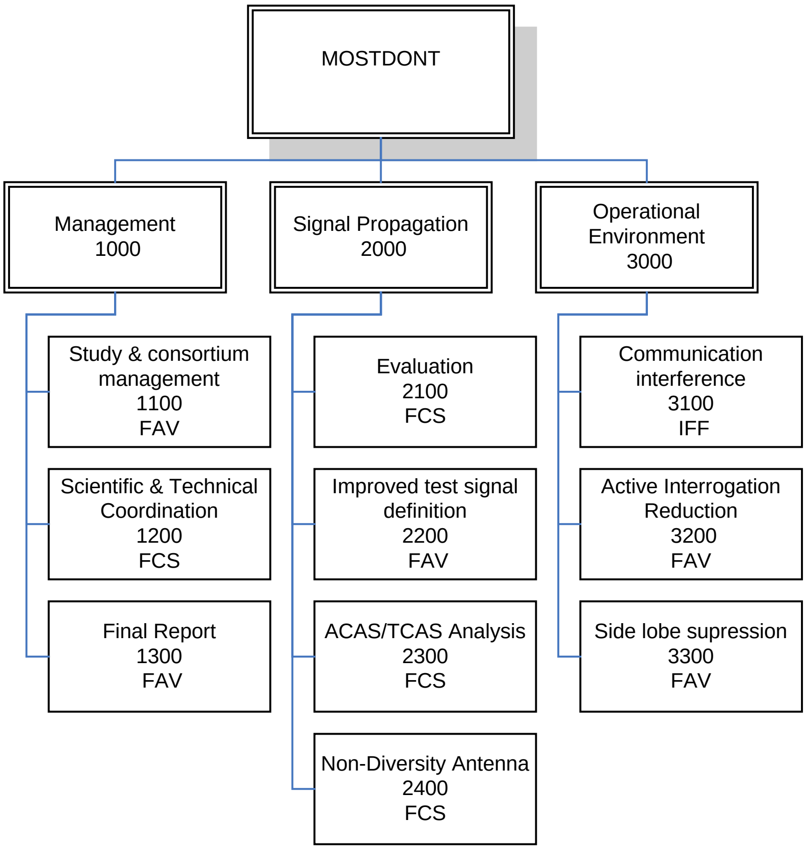

Figure 2-1: MOSTDONT Work Breakdown Structure

2.2.1 Management

2.2.1.1 WP 1100 Study and Consortium Management

The study was managed by the FAV project manager on behalf of the consortium. Activities in this WP comprised:

- Day-to-day management and coordination of the study work to ensure progress as planned
- Schedule control and tracking
- Coordination of work between all project participants
- Liaison with EASA
- Regular reporting in accordance with the project plan
- Identification of risks and timely initiation of suitable corrective actions

During the course of the project from February to August, 2010, several project meetings were held:

- Kick-Off meeting at EASA, Cologne — February 5th, 2010

  Presentation of study approach, setup of communications, scheduling

- 1st progress meeting at FCS, Braunschweig — March 31st, 2010

  Review of planning and preparation for flight measurements, initial measurement results, planning for interim report

- 2nd progress meeting at EASA, Cologne — May 4th, 2010

  Review of results from measurements (in-flight and on ground), review of interim report, outlook on outstanding work

- 3rd progress meeting at FAV, Ulm — June 10th, 2010

  Presentation of lab measurement results, review and discussion on study findings, preparations for final report

- Final project presentation at EASA, Cologne — August 30th, 2010

  Presentation of study results and recommendations regarding certification standards, delivery of final report

2.2.1.2 WP 1200 Scientific and Technical Coordination

The task of this WP was to control and ensure that the work of all packages was performed following the "Proposals for Safeguarding Good Scientific Practice" [RD14] of the Deutsche Forschungsgemeinschaft (DFG). The objective was to provide neutral, independent and unbiased answers to the questions of the ITT.

2.2.1.3 WP 1300 Reporting

This work package comprised all reporting activities towards EASA. Monthly progress reports were prepared that listed the activities and achievements in the reporting period as well as the planned activities in the following period. This was further supported by frequent phone calls and e-mails to keep EASA informed on the project progress.

2.2.2 Signal Propagation

2.2.2.1 WP 2100 Evaluation

The essential prerequisite for this task was the generation of a large database of signal-in-space records on the 1030 MHz SSR channel. The majority of the data had to be gained airborne, in order to evaluate the transponder's performance within the "Secondary Surveillance Radar" system. The following approach was taken for the generation of the database:

- The majority of data was collected during regular flight inspection missions of FCS Flight Calibration Services GmbH. These are regularly performed each week across central Europe. During normal operations, a single FCS flight inspection aircraft spends more than 25 hours a week on ferry and mission flights. Flight inspection missions of FCS cover, among others, dense areas as Frankfurt, Vienna and Zurich TMA.

- Other parts of the flight segment necessary for this study were performed by a Cessna-172 experimental aircraft of TU Braunschweig ("D-EMWF") carrying the FCS equipment. This covered a special mission flight to the Amsterdam TMA, were previous signal recordings had indicated potential problems for single-antenna aircraft.

Special attention within this essential work package in the context of the overall study was given to the receiving and recording technology employed. There is little value in the elaborate analysis of masked, corrupt or otherwise impaired data which does not fully correspond with the real signal-in-space radio frequency (RF) signal, due to unwanted and undocumented effects by the employed receiver.

As FCS had developed and tested various SSR 1030/1090 MHz experimental receivers on the ground and airborne in the past 8 years (see referenced documents), a highly suited and validated measurement receiver platform was available. This provides a high IF (intermediate frequency) bandwidth (>10 MHz) and an appropriate, tried and tested recording technology to autonomously save the essential signal components of all incoming Mode S interrogations.

2.2.2.2 WP 2200 Improved Test Signal Definition

EUROCAE ED-73C, section 1.6, defines the interrogation signals that a transponder must be able to process. The document states "The following paragraphs describe the signal in space expected to appear at the transponder antenna". Tolerances specified in the subsequent sections, as well as definition of interference signals (section 3.12) and pulse decoder characteristics (section 3.9), however, may not sufficiently take multipath effects and other disturbances into considerations that exist in the real environment.

The results from WP2100 provide a better understanding of typical characteristics of the signal in space as seen by the transponder antenna in real environments and the effects of disturbances on that signal.

Some vital characteristics were found in the recorded data that cannot be re-produced with the currently available industry standard test equipment (e.g. detailed method for DPSK phase shifting). Therefore, suitable enhancements and additions of the required test equipment will be proposed.

2.2.2.3 WP 2300 Interference of Radar and TCAS Interrogations

Within this WP, an existing algorithm will be applied to detect those uplink telegrams affected by multipath propagation. This serves to clarify in greater detail any effect of multipath propagation on the phase transition at the "Synchronisation Phase Reversal" (SPR) or single data bits.

Real radar data was used to evaluate the air-to-air transmission of TCAS during the flight trials. Since the positions and therefore the distance between two potential conflict partners are known, the signal-in-space quality of TCAS transmissions can be fully compared against transmissions from ground interrogators. A cross-correlation between TCAS broadcast Uplink Format (UF) 16 (includes 24 Bit Mode S address of aircraft) and UF00 (Short air-air surveillance without source identification) signal strength and frequency of occurrence allows a mutual allocation.

The UF00/ Downlink Format (DF) 00 short air-air surveillance communication is initially needed to determine the slant range and difference in altitude. In case of further convergence of two TCAS-equipped aircraft, they exchange a Traffic Advisory (TA) or Resolution Advisory (RA) on a UF16/DF16 basis. A repeatedly interfered UF16 would then result in a delayed or impossible detection of a TA or even RA. Hence, the focus must be on a detailed investigation of UF16 to conclude the impact on TCAS.

In summary, the outcome of WP2300 is designed to provide statistically based answers to the following questions:

- What is the total amount of radar and TCAS interrogations and its distribution?
- What is the percentage of multipath-affected Mode S interrogations in total?
- What is the distribution of affected radar and TCAS transmissions?
- At what altitudes and which distances from the radar, especially in TMAs, does the signal-in-space suffer from interferences?
- What is the relative frequency of interference between radar and TCAS replies?
- What is the relative frequency of an unrecognized UF00/UF16?

2.2.2.4 WP 2400 Non-Diversity Antenna

This work package is aimed at identifying any problems with radar or TCAS operation due to the non-diversity antenna installation on small GA aircraft.

All aircraft above 5700 kg are equipped with TCAS and are required to have diversity transponders which use two antennas (one at the top, one at the bottom of the fuselage). On smaller aircraft with non-diversity transponders, the mounting point of the single transponder antenna is usually at the bottom of the fuselage. Hence, it is possible that wave propagation between an TCAS-equipped aircraft and a smaller aircraft having a transponder only is impeded if the smaller aircraft flies below, since its antenna radiation above the fuselage is masked.

2.2.3 Operational Environment

2.2.3.1 WP 3100 Communication Interference

A TCAS monitoring network is operated by TU Braunschweig [RD10, RD12, RD13]. This scientific tool receives Mode S messages sent by Mode S equipped aircraft in the German airspace. The system has five 1030/1090 MHz receiver stations in four locations: Frankfurt airport, near Stuttgart, near Munich und two more at Braunschweig research airport, one looking in westerly direction, the other towards the east. All Mode S data received by these stations are transmitted via internet to Braunschweig. The data is continuously stored and analysed. Every TCAS incident is extracted and the TCAS communication is analysed bit by bit. Additionally, the underlying traffic situation and the reactions of the involved aircraft to the TCAS resolution advisories are reconstructed and documented.

To achieve this, the system checks the standard conformity of every Mode S message, checks its logical consistence and sequence, and collects all data in a database, which is necessary to validate the Mode S addresses as a check sum for the CRC check and for the content of each telegram. All standard and long Mode S formats used for SSR radar, for TCAS or ADS-B purposes can be included into the process to measure whether an interrogation is followed by a proper reply or whether squitters and broadcasts are repeated according to the standard. Such measurements provide the basis for in-depth statistics about the individual success of valid Mode S transmissions.

The two particularly designed stations at Braunschweig research airport and an experimental station in the laboratory provide the capability to feed artificial Mode S test telegrams into the stream of received signals. The rate per second and the power (in dBm) of the test signals can be varied to determine the general detection probability of Mode S communication versus received power in the uplink and downlink channel depending on the traffic load, the region, the season and the time of day, and to simulate a specific growth in traffic. Furthermore, the real traffic at one of the monitoring stations will be substituted by a second Mode S test signal generator to assess the overall performance of a Mode S - only environment.

Three target scenarios (mixed mode, high density mixed mode and Mode S only) will be created. This simulation approach by Mode S test signal generation covers the effects of physical propagation, traffic load, system inherent effects and the ability of receivers to overcome superimposition and disturbance. The tool is believed necessary because the influence of every individual effect cannot be reconstructed in a pure simulation environment.

As one of the ground stations of the monitoring network is located at Frankfurt airport, the actual dense air traffic environment of central Germany will be evaluated and the results will be taken into account for the simulation of growing air traffic environment. Data sets of WP2100 will be used to support the verification of the results.

This goal of this WP is to describe the real environment of Mode S transponders and their performance under these conditions.

If necessary, the monitoring system is able to identify and select Mode S addresses of incorrectly working transponders for further investigations of individual equipment and aircraft installations.

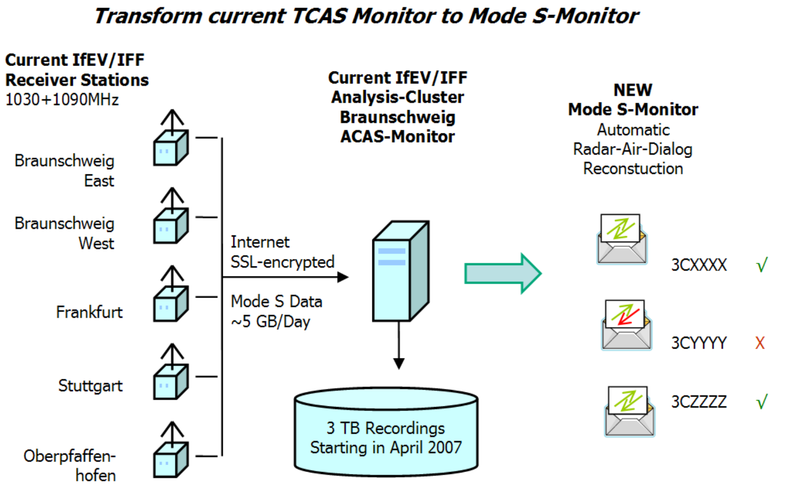

Figure 2-2: IFF Monitoring Approach

2.2.3.2 WP 3200 Active Interrogation Reduction

Simultaneous measurements of interrogation signals on 1030 MHz and respective transponder replies on 1090 MHz in real high-density environments can provide a first indication of potential reply reductions due to high interrogation load. Such measurements alone, however, will not suffice as various effects may contribute to transponder non-replies or non-reception on the ground.

Therefore, the scenarios as observed during the measurements were re-produced in a laboratory environment to create similar (and even higher) interrogation loads. Then, the effects of a reduction in number of replies by the transponder (if any) can be measured, such as reduction in sensitivity for Mode A/C interrogations. The behaviour may vary between different transponder models.

This task yields information on how close the interrogation load in real high-density environments is already to the threshold where transponders will start to limit their reply rates (or if this limit is already exceeded).

2.2.3.3 WP 3300 Side Lobe Suppression

Side lobe suppression requirements as given in EUROCAE ED-73C may not provide enough details on required transponder behaviour under certain circumstances. For example, the required reply behaviour for Mode S side lobe suppression with a difference between P5 and P6 in the range -12 dB to +3 dB is not defined, at all.

Another problem is that ICAO Annex 10, Volume 4 uses a different set of requirements, defining the maximum level of the P5 pulse within the desired arc of interrogation at -9 dB below the P6 pulse amplitude. These two different specifications are thus in contradiction.

Based on measurements of the side lobe suppression characteristics in the real radar environment and laboratory testing of existing transponder equipment, further supported by analysis of applicable standards for certification of radar stations, a modification of the requirements in ED-73C is proposed.

Special emphasis is also put on a clearer definition of phase requirements for the side lobe suppression tests.

Each proposal for a modification is supported by rationale for the respective change that includes sample measurements and an analysis of potential impact on test requirements and necessary test equipment.

3 ACTIVITIES AND RESULTS

3.1 Signal in Space Evaluation

3.1.1 Scope of Measurement Flights

Within a period of five months (March to July 2010), the FCS flight inspection aircraft "D-CFMD" was equipped with the 1030 MHz recording equipment for certain weeks. The missions flown are composed of ferry flights and flight inspections of terrestrial navigation aids and procedures across Germany, including major hubs such as Frankfurt, Munich and Berlin.

In total, the number of flight hours performed is above 100, which serves as a reliable database for the investigation of the signal-in-space (SIS). Moreover, a project-specific flight from Braunschweig to Amsterdam was performed using a *Cessna 172* owned by Technische Universität Braunschweig (TU BS).

3.1.2 Recording Equipment and Analysis Tools

3.1.2.1 Measurement Hardware and Software

Figure 3-1 shows a rough overview of the hardware section used as a receiving and recording platform. The original carrier frequency of 1030 MHz is mixed down to an intermediate frequency (IF) of 70 MHz and then sampled with a 14 Bit A/D converter producing a discrete bandpass signal y(t). It is under-sampled at a rate of 105 MSps/s (mega samples per second) resulting in a second IF of 35 MHz, which is adequate to comply with the Nyquist theorem since the system has to cover the channel bandwidth, not the IF carrier frequency. The RF/IF section of the recording device is designed to leave the original Mode S signal-in-space essentially untouched. However, the hardware is not a spectrum analyser but a measurement receiver. Its bandwidth is limited from using commercially available 1030 MHz RF and 70 MHz IF filters, resulting in a total 3 dB bandwidth of ±10 MHz around the centre frequency.

A state-of-the-art signal generator is used to calibrate the RMS signal strength of y(t) against a reference source within the level limits -80 dBm to -20 dBm.

Mode S uplink correlator, operating on y(t) in real-time then converts the IF to a baseband signal to detect the preamble pulses P1, P2 and the beginning of P6. This is implemented using an FPGA and stores the full bandpass signal y(t) of each detected interrogation on a hard disk, using 8 kB per single telegram. A rather tolerant configuration is required to detect as many interrogation-like signals as possible. Any further signal processing is done by software in a post process to extract derived signals used for this study.

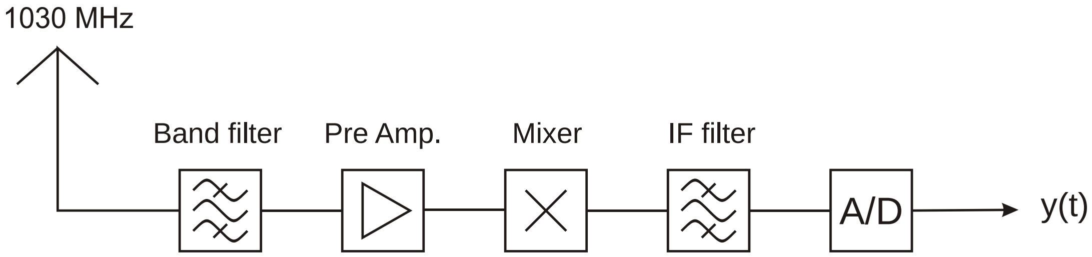

Figure 3-1: Block Schematics of RF/IF Unit

In general, the recording unit does not require any manual intervention during runtime. Recordings start as soon as DC power is provided with a maximum loss of 10 s on sudden power-off events, e.g. when power is switched off by the flight inspector. Any synchronization with the Flight Inspection System (FIS) aircraft positioning results is done via the GPS time pulse-per-second (PPS). Hence, the recorder has an internal GPS receiver from which the PPS and the autonomous rough position are taken.

Furthermore, the hardware is connected to the aircraft's ARINC suppression bus to obtain dead time information from airborne L band emissions of on-board avionics systems (DME, SSR, and TCAS). Once the system is running, it is designed to function without manual intervention. A front panel display provides system active status information, as well as usage of the internal hard disk.

Collected data can be analysed in various, generic ways. At first, the most important task is performing a time-synchronized data fusion between the Mode S data and flight path gained from the FIS.

A dedicated analysis software, written in "C++", was made available by FCS which performs all further signal operations, plots the relevant diagrams and does statistical work on the data. At first, the Mode S uplink telegram has to be demodulated to reveal its contents. The bandpass signal y(t) is recovered from hard disk and fed into a standard In-phase (I) and Quadrature (Q) demodulator as shown in Figure 3-2. The equal pair of succeeding I/Q bandpass filters is implemented as a linear-phase "Finite Impulse Response" (FIR) type, in order to avoid any phase distortion. These filters are needed to suppress the mirror frequency 2 * f_0 at the mixer outputs. Their parameters are selected to comply with the given bandwidth of the hardware section and are noise-optimized.

Some more floating point operations calculate three important signals:

1. $|y_T(t)|$ is the *baseband signal* (video), linearly demodulated from the input y(t), showing the interrogation pulses;
2. $\Phi(t)$ is the four-quadrant arcus tangens function showing the momentary phase. It allows to detect the direction towards which the phase turns and, consequently, to detect if frequency modulation is applied on the signal (see below);
3. An autocorrelation function (ACF) operating on the I/Q signals is applied to demodulate the telegram bits.

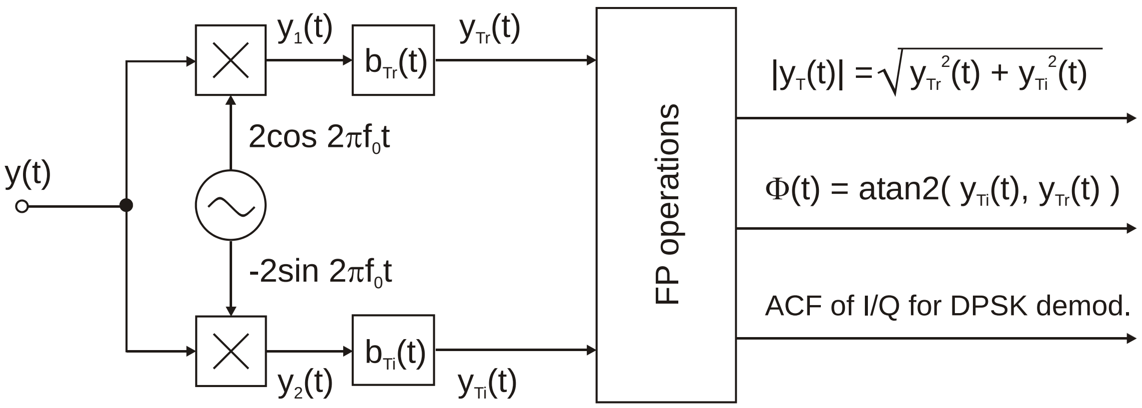

Figure 3-2: Software section of signal post processing

3.1.2.2 Basic Signal Processing Example

In this chapter some general results of signal processing on a prototype signal being recorded with the measurement system are presented. They give an overview on assessing the quality of a received Mode S interrogation. A reference example of an uplink format 00 (UF00, TCAS short air-air surveillance) is shown in Figure 3-3. The baseband (video) curve clearly indicates the pulse train P1, P2, P6 at an average level of -63 dBm. On the x-axis, the time in microseconds starts before P1, whereas the amplitude in true Root Mean Square (RMS) millivolts, which is compliant with the level value, is linearly mapped to the y-axis. At the beginning of P6 the 1.25 µs continuous wave (CW) "training sequence" precedes the sync phase reversal (SPR). It is used to determine the initial phase and setting it to zero. This behaviour is known from a *Costas Loop* which tunes the phase to synchronize the argument of the cosine function with the incoming phase of y(t). However, in our case it is used only to reset the initial value for the phase. At the SPR moment the phase curve then performs a 180° step for the first time, followed by further phase reversals when there are "1"-bits in the telegram.

The actual DPSK demodulation is very sophisticated and performed by a complex autocorrelation function ACF which operates on the combined I/Q signals. It makes use of the full energy given by the Mode S chip length of 250 ns for the data bits, and even uses nearly 500 ns to detect the SPR since there is a two chip-length gap between SPR and the first data bit. Each phase reversal is expressed by a clear maximum of the ACF curve.

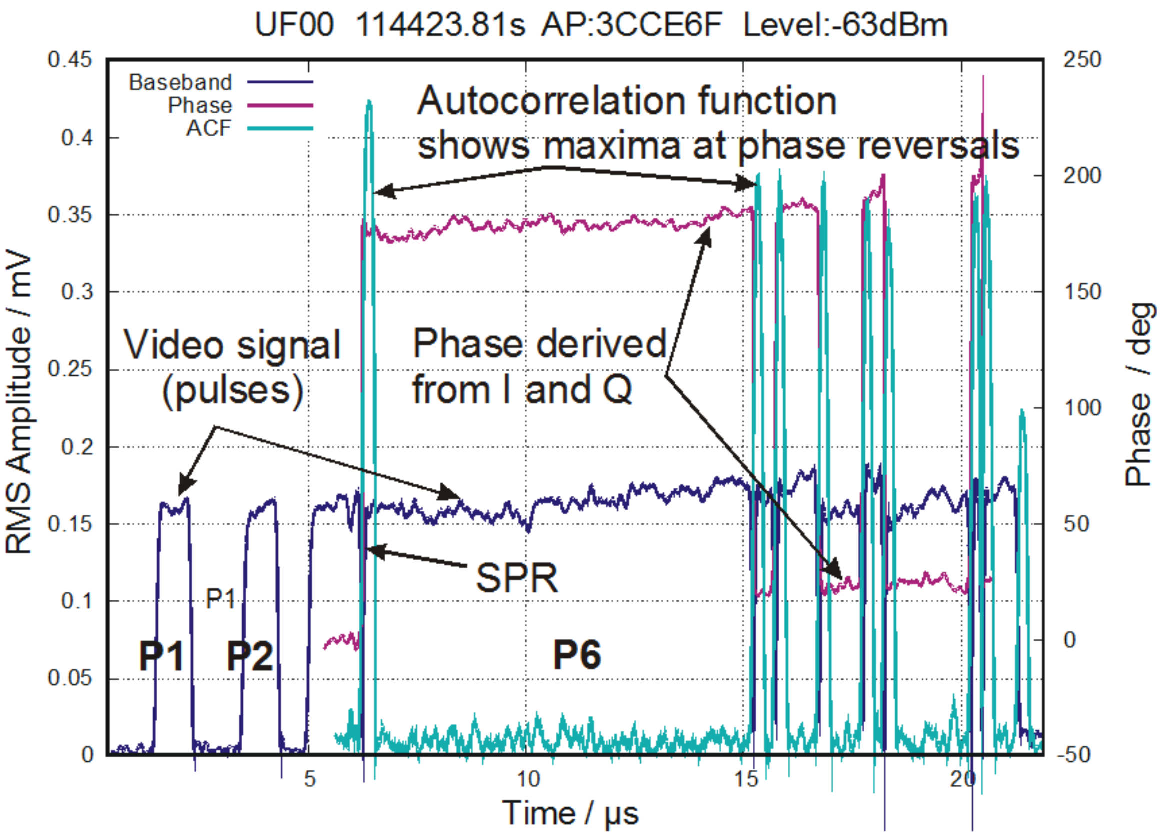

Figure 3-3: Curves computed from a Mode S bandpass signal

As known from Mode S uplink telegram basics, the sync phase reversal is the most important part of the pulse P6, since it starts the bit clock for the later decoding. After having detected P1, P2 and P6 from the incoming pulse train, a transponder usually activates a time window within which the SPR must occur, starting somewhere in the 1.25 µs CW training sequence. The boundaries of that time window are tolerant enough to cope with even interfered P1/P2/P6 pulse amplitude characteristics. But a demodulator's ability to determine the exact moment of its occurrence is the fundamental prerequisite for the correct detection of all data bits. One single bit error makes the telegram content completely unusable and would prevent a transponder from replying. Therefore, the central focus of all analyses and interpretations is placed on the SPR quality.

The next Figure 3-4 presents a temporal zoom of the SPR region showing its baseband and phase signal. During the quick phase transition from 0° to 180° the video signal is subject to a deep notch which pulls down the amplitude close to zero. This typical behaviour of a hard phase shift keying can also be observed in the polar plot of the SPR given by Figure 3-5: The phase starts with 0° at the beginning of P6, crosses zero amplitude within one sample (1 / 105 MHz = 9.5 ns) and settles in the 180° domain.

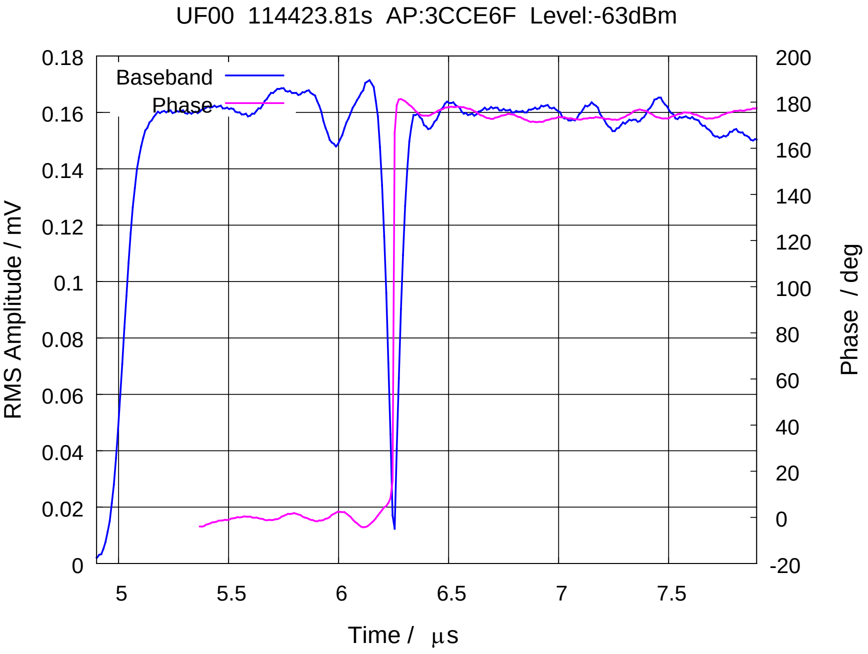

Figure 3-4: Sync Phase Reversal at higher temporal resolution

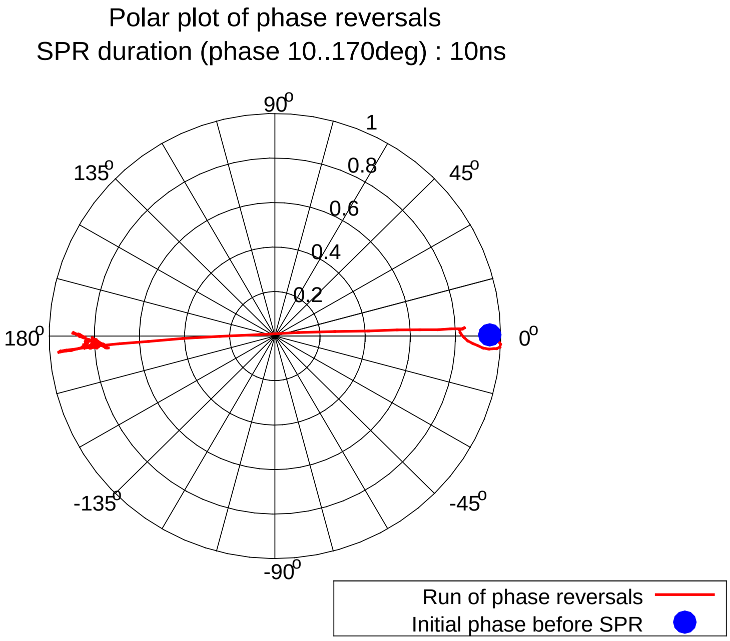

Figure 3-5: Phase before and after SPR

3.1.2.3 Spectrum Issues

Apart from using the bandpass signal y(t) for I/Q demodulation, it can also be the source to feed a *Discrete Fourier Transformation* (DFT) to obtain a frequency spectrum. When transforming a signal from time into frequency domain one has to be very careful determining the correct boundary conditions.

Considering a single phase reversal region (SPR or the Mode S data bit "1"), the momentary frequency shift can be derived from differential phase and time values, e.g. using values given by Figure 3-5:

$$\Delta f = \frac{1}{2\pi}\frac{\partial\varphi}{\partial t} = \frac{1°}{360°}\frac{170°\text{-}10°}{10\,\text{ns}} = 44.4\,\text{MHz}$$

This high deviation does not represent the actually required interrogation bandwidth since it is limited to the reversal duration where the amplitude crosses zero as seen above in the polar plot.

An amplitude drop down close to zero can be observed in the video plot, but due to the limited temporal discretisation of 9.5 ns the actual value within the region of interest is hard to determine. To evaluate the entire interrogation spectrum of a Mode S transmission, a time window for a n-DFT must range from the beginning of P1 to the end of P6. Consequently, the parameter "n" then is the telegram length multiplied by the sampling rate 105 MHz. In Figure 3-3 we can observe 8 phase reversals within P6 of possible 57 in total. The resulting spectrum shown in Figure 3-6 is well below the ICAO spectrum limits (blue curve, see ICAO Annex 10 Vol. IV, Figure 3-2) and mainly formed by the number of set data bits in P6 and the steepness of the pulses P1, P2 and P6. As stated before, the total receiver IF 3 dB bandwidth is 2 * 10 MHz. A corrected spectrum limit against the actual receiver bandwidth is given by the green curve. The spectrum is still well below that curve.

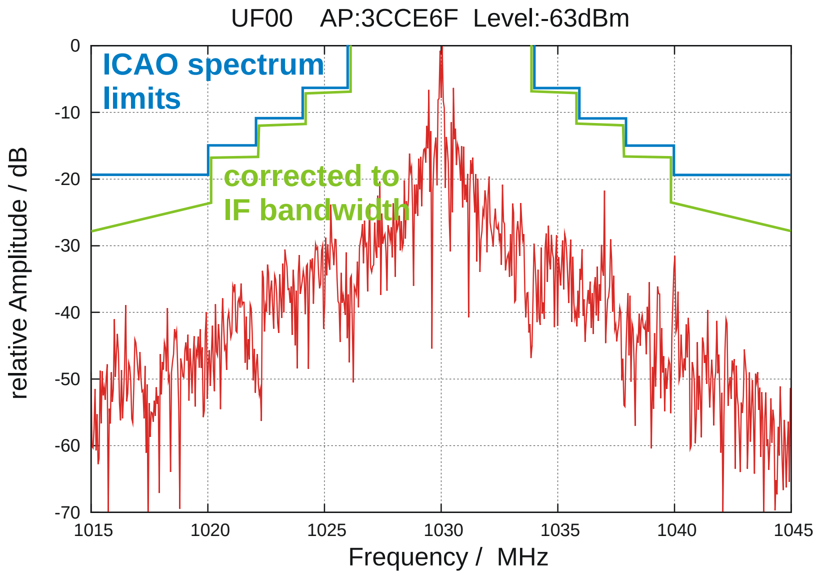

Figure 3-6: Frequency spectrum of y(t) over telegram duration

3.1.2.4 Phase Modulators

3.1.2.4.1 Theoretical Approach

An emitted signal u(t) at a peak amplitude a_0 using phase angle modulation can generally be expressed as

$$u(t) = \mathrm{Re}\left\{a_0 \cdot \exp\left(j\,\psi(t)\right)\right\} = a_0 \cdot \cos\left(\psi(t)\right)$$

This is the real – and therefore actually radiated – part of a complex bandpass signal. In case of Binary Phase Shift Keying (BPSK), the phase angle is composed of the linear phase part according to the carrier frequency f_0 and of the hard phase shift keying 180° weighted by b_k:

$$\psi(t) = 2\pi f_0 t + \pi \cdot \mathrm{b_k}$$

Since I and Q demodulation outputs are signed values, a four quadrant arcus tangens (atan2 function, e.g. in "C") reveals the direction towards which the phase turns.

The most simple technical implementation is realized by an RF switch and a single 180° delay line resulting in $b_k \in \{0,1\}$. Related plots of a prototype UF00 interrogation were already shown in section 3.1.2.2 (see Figure 3-3).

Assuming signed integer values are the range of b_k, the following theoretical sequences are conceivable if consecutive phase reversals occur every increment k:

- $\mathrm{b_k}(1) = \{0, +1, 0, +1, 0, +1, \ldots\}$
- $\mathrm{b_k}(2) = \{0, -1, 0, -1, 0, -1, \ldots\}$
- $\mathrm{b_k}(3) = \{0, +1, 0, -1, 0, +1, 0, \ldots\}$
- $\mathrm{b_k}(4) = \{0, -1, 0, +1, 0, -1, 0, \ldots\}$
- $\mathrm{b_k}(5) = \{0, +1, +2, +3, +4, +5, +6, \ldots\}$
- $\mathrm{b_k}(6) = \{0, -1, -2, -3, -4, -5, -6, \ldots\}$

$b_k(1)$ and $b_k(2)$ could use the delay line implementation since the total phase stroke is 180°, whereas the others require different techniques.

3.1.2.4.2 Quadrature Modulation and Filter Issues

A quadrature modulator and demodulator are complementary designs to generate complex bandpass signals and to recover complex baseband signals. Hence, the block schematic of the modulator is given by the inverse schematics of Figure 3-2. The variation of the two scalar inputs "Inphase" (I) and "Quadrature" (Q) then allows to reach every two-dimensional point in a polar diagram like Figure 3-5, not only points on the real axis.

A simulation of I and Q modulation signals was performed to observe the resulting magnitude and phase as an output of the software post-processing. The theoretical modulation signals were fed into the same FIR filter actually used for analysing the recorded bandpass signal y(t).

In the upper sub-figure of Figure 3-7 an I/Q signal combination of a hard phase keying ($b_k(1)$ or $b_k(2)$) is used as input values. Hence, a 180° phase reversal ("orig. phase") is given by a 1 to -1 step of "Inphase" (see legend of the plot) within one increment 1/105 MHz, whereas "Quadrature" remains zero. In the software post-processing, linear-phase FIR filters are implemented to recover I and Q. The filter group delay is therefore a constant time delay of roughly 150 ns which affects the input signals while the phase remains undistorted.

Due to low-pass filtering the steepness of the outputs is reduced (here: "FIR In."). However, the resulting phase duration ("FIR phase" curve) is as short as the unfiltered value. Where the amplitude of "FIR In." crosses zero, the absolute magnitude ("FIR video") has a zero dip.

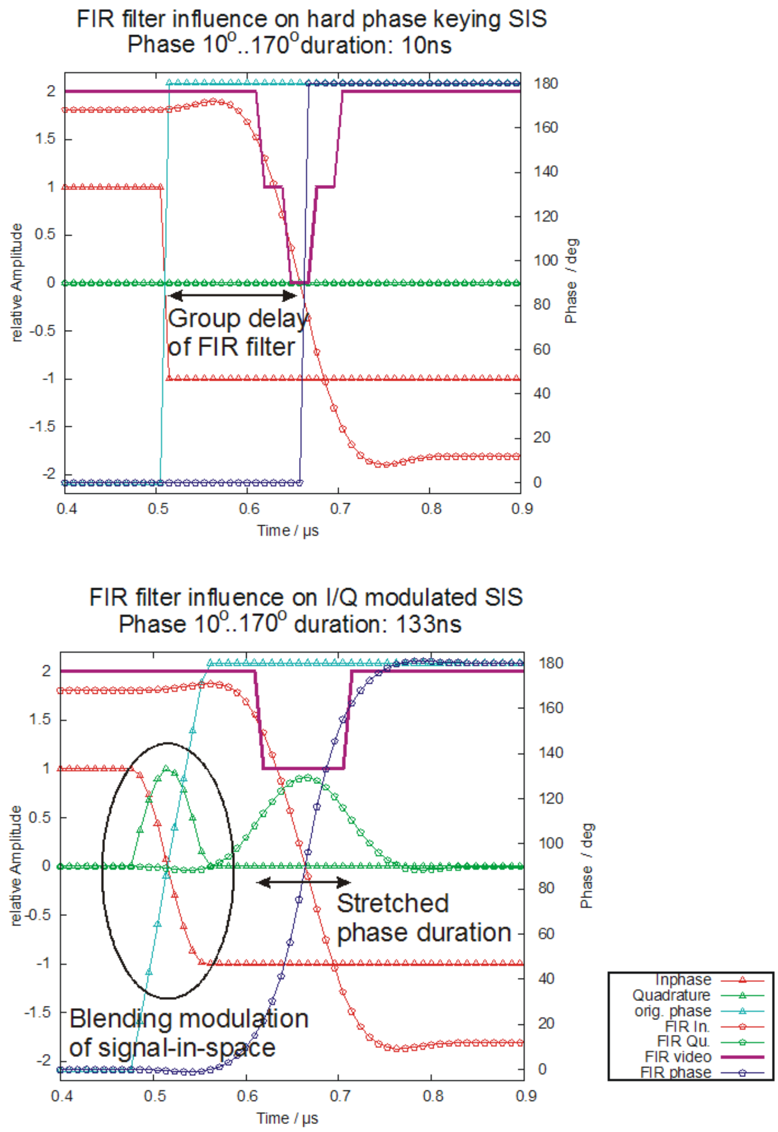

Figure 3-7: FIR filter influence on hard phase keying and blending I/Q modulation

A common method to reduce the required bandwidth of the signal-in-space and to minimize the amplitude dips is to perform a *blending modulation* within the acceptable P6 phase reversal duration of 80 ns (ICAO Annex 10, Part IV, 3.1.2). Typically, the I-and Q-input signals are intended to be real quadrature components. For example, if I were a digital cosine wave of frequency f_m, and Q were a digital sine wave of the same frequency, then the output of the quadrature modulator would be a single-sideband tone with a frequency of 1030 MHz + f_m. In the prototype blending modulation shown in the lower sub-figure, f_m = 6.25 MHz is selected over a period of 80 ns, resulting in a 180° phase stroke of the original signal-in-space. However, the output of the FIR baseband filter slightly deforms the blending signals ("FIR In." and "FIR Qu.") and the derived phase curve gets round corners and stretches over time, so the computed phase duration is now 133 ns. Generally, the FIR filter parameters are adapted to match the bandwidth of the given IF hardware bandwidth, which results in a noise-optimized overall performance. The benefit is an increased detection probability of the ACF-based DPSK demodulation process. To perform more realistic time measurements, however, these parameters must be changed. This will be discussed in section 3.1.3.5.

Generally, a quadrature modulator is capable of generating all imaginable sequences $b_k(1)$ to $b_k(6)$. For scenarios other than shown in Figure 3-7, simple modifications to I and Q could be required. For example, a negative phase stroke, expressed by a lower sideband of 1030 MHz - f_m during phase transition, can be generated by simply changing the sign of one blending modulation signal.

The blending modulation is actually a frequency modulation of the carrier over a certain period, within which the carrier frequency is shifted either to positive or negative deviations. In the software section of the measurement system, the deviation sign of each phase reversal is identified using the four-quadrant inverse tangent. Therefore, the total phase accumulation over the telegram length can be computed. It was interesting to observe during the measurement campaign, that different Mode S Interrogators have their specific phase "signatures".

3.1.2.4.3 Measurement Examples of different Modulation Techniques

Examples of different modulation "signatures" will be listed in the following.

At first glance, a very similar phase curve compared to Figures 3-3 to 3-5 is depicted in the next Figure 3-8. However, both the zoomed video and the polar plot reveal that the amplitude notch is not as deep as in the preceding example of $b_k(1)$. As stated in the preceding paragraph, this is the intended behaviour of the blending I/Q modulator type which forces the curve in the polar plot to stay on the unit circle without loss of amplitude during the phase reversal on the transmitting site. As explained before, the FIR filter reduces the bandwidth and therefore the amplitude during phase transition. This example matches the simulated phase duration of 133 ns in Figure 3-7 which originally was 80 ns in the signal-in-space.

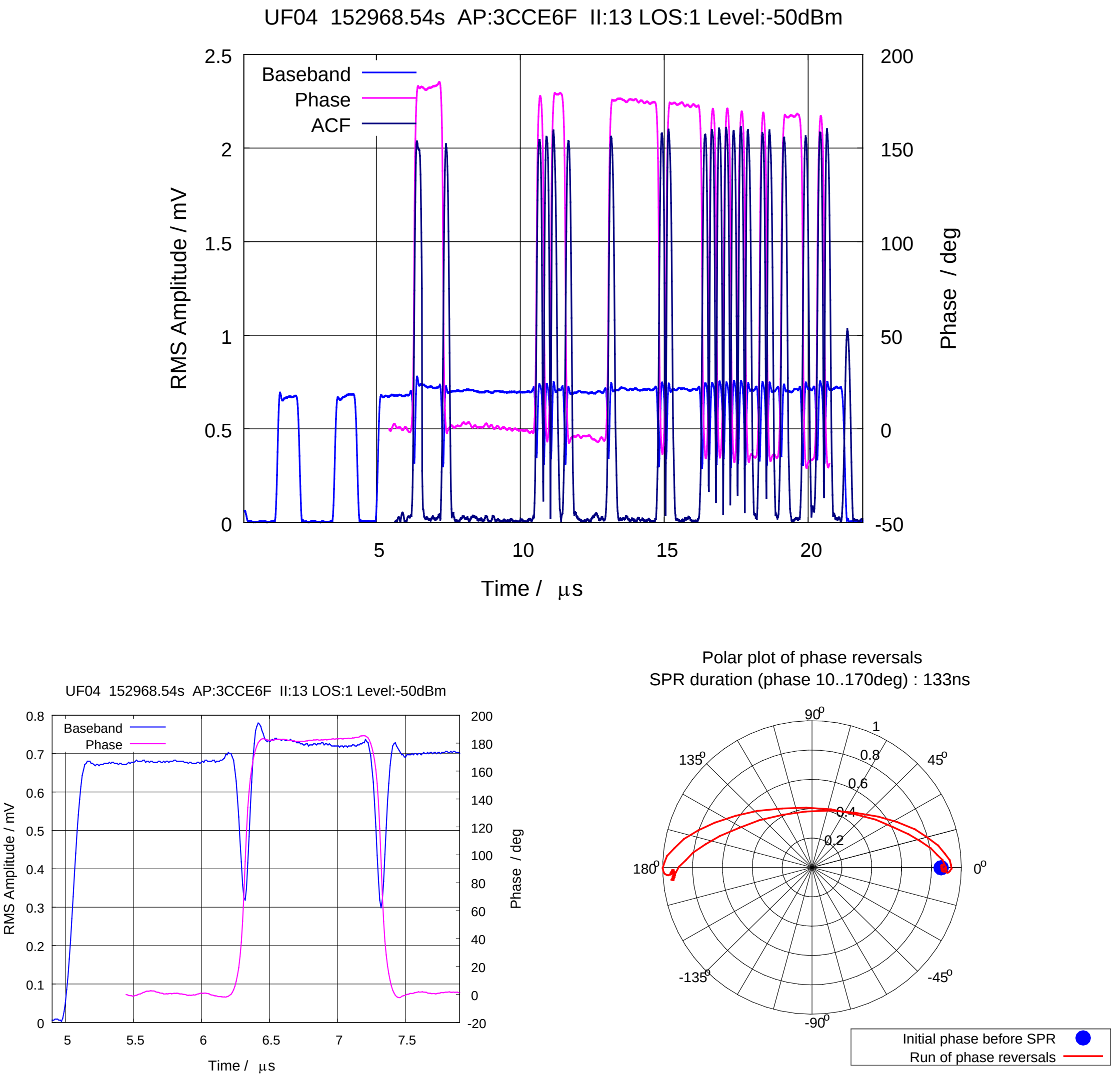

Figure 3-8: Plot of I/Q modulated UF04 of II13, zoom into SPR region and polar diagram

Figure 3-9 reveals an I/Q modulated UF04 having alternating positive and negative 180° increments around the initial phase as given by sequence $b_k(4)$. The SPR region at higher resolution again shows the rounded corners whilst the polar plot has dips similar to the preceding example.

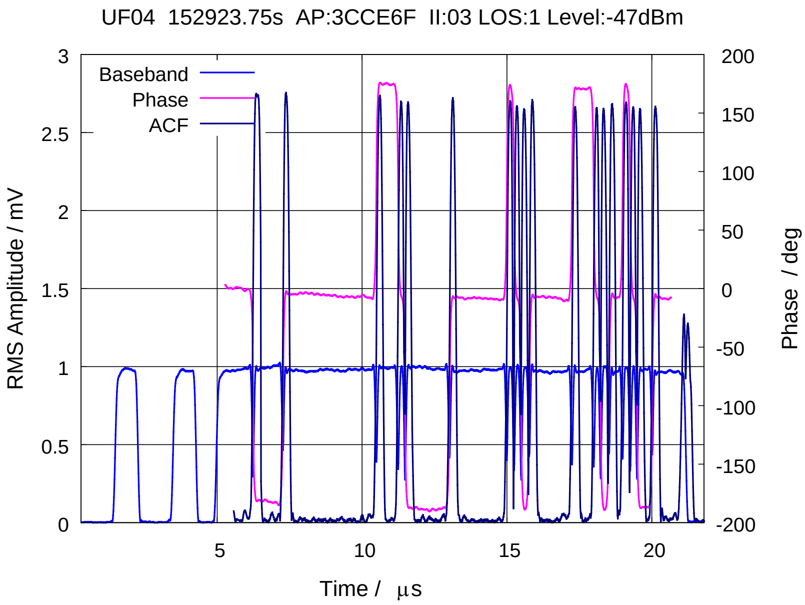

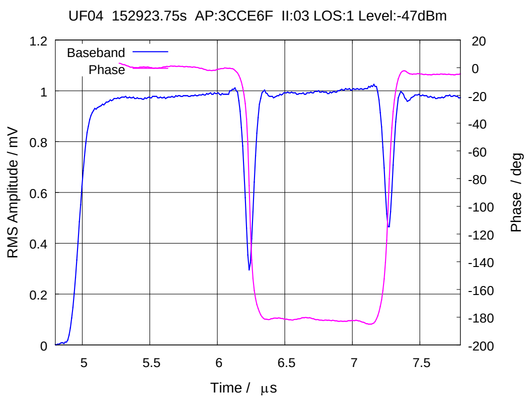

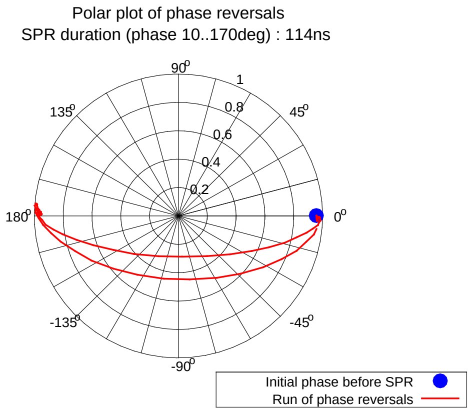

Figure 3-9: Plot of I/Q modulated UF04 of II03, zoom into SPR region and polar diagram

Approximately the same appearance is shown by another interrogator (Frankfurt airspace, II10) as depicted in Figure 3-10. The phase curve slightly differs from that in the preceding example: From the initial CW segment the phase turns twice into negative direction and then returns. Hence, the polar diagram with two reversals, starting from the SPR on, maps a full circle.

II10 is currently in use by the new German PAM-FRA Wide Area Multilateration (WAM) system.

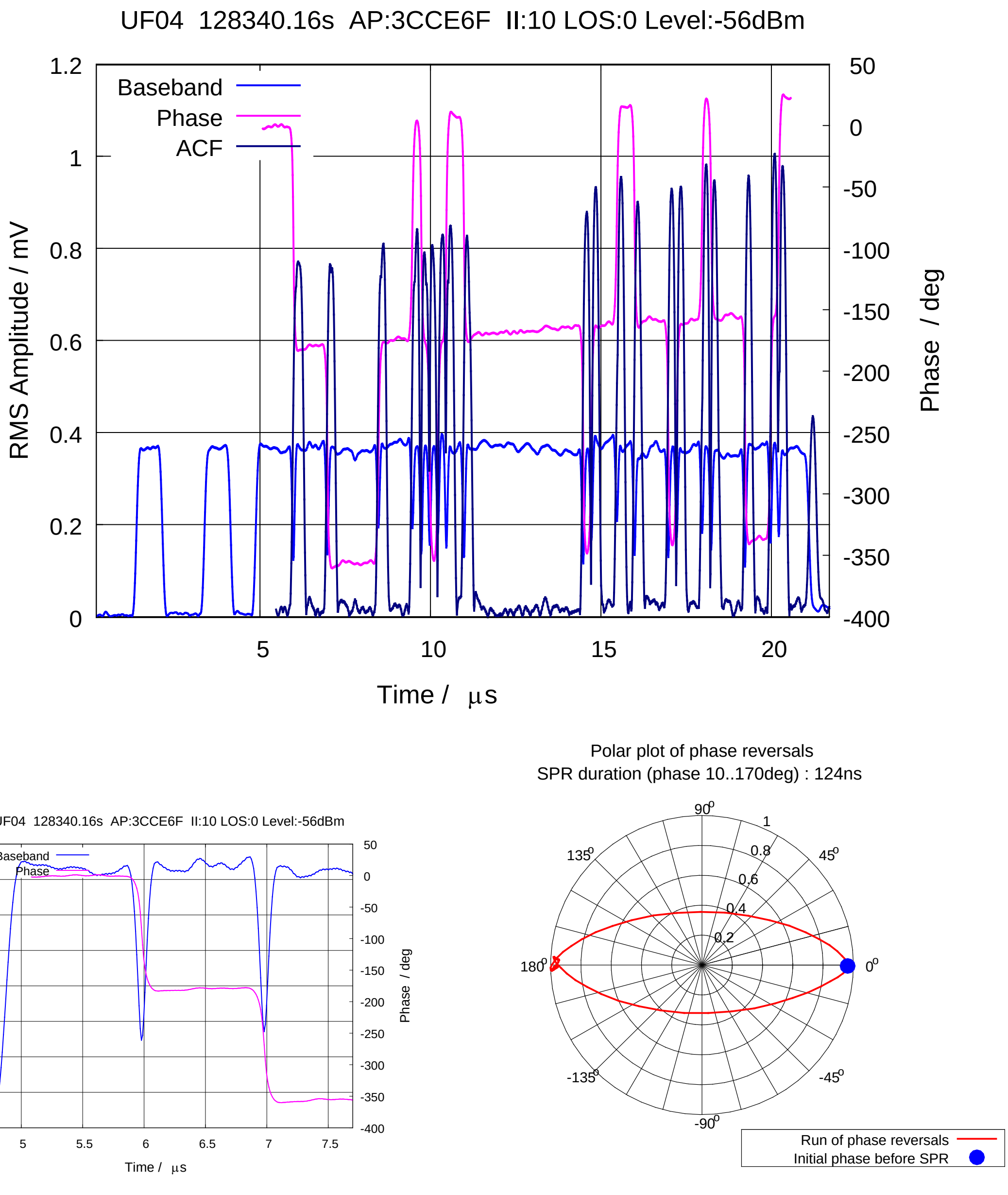

Figure 3-10: PAM-FRA interrogator phase signature

An I/Q modulator also allows to advance the phase continuously to one direction as can be seen in Figure 3-11, which complies with $b_k(6)$. At each of the eight phase reversals, 180° is subtracted from the starting value so in total we compute a phase shift of 1440°. The frequency deviation in the course of P6 can thus be expressed as

$$\Delta f = \frac{1}{2\pi}\frac{\partial\varphi}{\partial t} = \frac{1°}{360°}\frac{1440°}{14\mu s} = 296\,\mathrm{kHz}$$

Strictly speaking, the frequency tolerance window of 10 kHz according ICAO Annex 10 is violated. However, since the phase remains stable between two "1" bits, this should actually not cause any problems for receiving transponders.

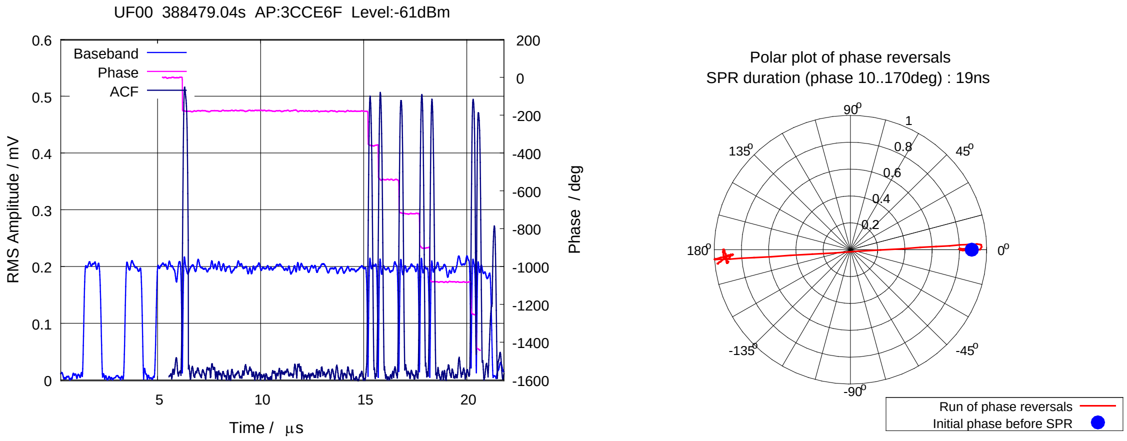

Figure 3-11: TCAS interrogation with incremental phase and short reversal duration

In the polar plot we observe a short 19 ns SPR duration with the curve crossing zero, which is accompanied by a zero amplitude dip of the amplitude.

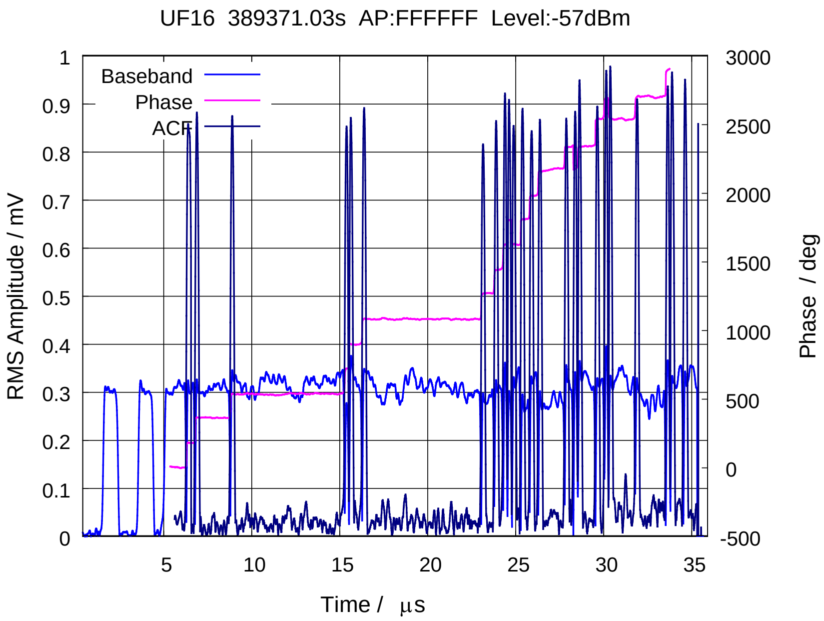

Figure 3-12: UF16 TCAS broadcast with a positive phase accumulation

A phase accumulation into positive direction only (sequence $b_k(6)$) can be observed at the UF16 TCAS broadcast shown in Figure 3-12.

These examples of "phase signatures" help to identify and to follow up transmissions of a certain interrogator, even if there are two or more share e.g. the same interrogation identifier code.

3.1.3 Analysis of the Radar Signal-in-space

This section will cover various flights performed as ferry or mission flights by the FCS "D-CFMD" aircraft and the dedicated flight to Amsterdam of the TU Braunschweig "D-EMWF" Cessna 172.

3.1.3.1 Measurement System Setup

A spare L-band antenna mounted at the bottom of the fuselage of the flight inspection aircraft was used to feed the measurement system. A photo of "D-CFMD" is shown in Figure 3-13 below, while Figure 3-14 shows a part of the fuselage with the antenna-in-use.

Figure 3-13: Photo of Beech King Air B300 “D-CFMD” of FCS

Figure 3-14: Fuselage and spare L-band antenna

3.1.3.2 Introduction

The analysis in this section covers both radar interrogators with mechanically turning antennas and fixed interrogators operated within multilateration systems.

Since the measurement equipment is mounted in an aircraft equipped with an aviation-certified Mode S transponder it makes sense to evaluate those interrogations selective to this particular aircraft, and those that are broadcast transmissions either from radars or other TCAS equipped aircraft. The aircraft's own technical Mode S address serves as the 24 bit Address/parity (AP) field to be computed from the 56/112 telegram bits via the Mode S uplink generator polynomial. This technique can be applied to both UF00 (TCAS) and UF04/05/20/21 (radar) transmissions.

In case of a broadcast message (radar UF11 all-call, TCAS UF16-32) the decoded AP field has all bits set to one. This is thus also well suited to obtain error-free uplink telegrams.

Some general statistics on received interrogations from various sources are given before presenting the analysis of radar interrogation patterns and the radiated signal-in-space.

To do so, the radar beam sweeps are analysed in detail to point out interrogator characteristics, revealing the specific signal degradation effects that might occur.

3.1.3.3 General Statistics on Radar Interrogations

This section gives an overview on the number of received selective interrogations during various measurements and mission flights. The radar source is identified by the interrogator code, and TCAS short air-air surveillance of which the requesting aircraft cannot be allocated in general.

Figure 3-15 presents the selective interrogation statistics of a ferry flight from Braunschweig to Berlin. Within the elapsed time all selective interrogations have been accumulated against different interrogators to be seen on the x-axis. The right bar of each interrogator shows the total number of received telegrams below the -73 dBm minimum trigger level (MTL) of a transponder – this is to find out how many weak transmissions have been received in relation to the total number.

Starting in Braunschweig on April 24th, 06:43h UTC, the aircraft mainly receives interrogations from the Brocken radar with its test code II14, the "German North Cluster Main" II03, the "German Air Force Cluster Main" II13 and short air-air surveillance interrogations UF00 from airborne TCAS devices. Interrogator Code 00 is not associated to a cluster but frequently used by multilateration surveillance systems and sometimes by radars, as many measurements have shown during the campaign. A few II02 interrogations seem to originate from the Deutsche Flugsicherung (DFS) Nordholz radar.

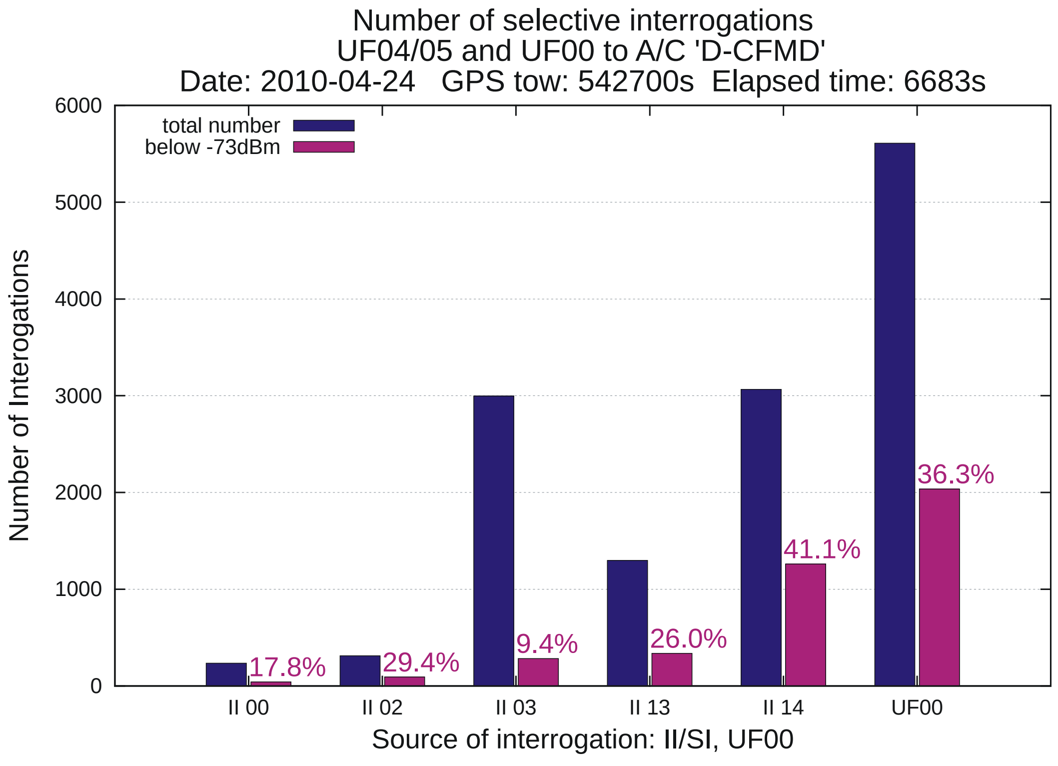

Figure 3-15: Ferry flight #1 from Braunschweig to Berlin and some ILS measurements

In total, the number of accumulated radar interrogations exceeds the number of TCAS UF00 calls.

The remarkable portion of weak TCAS interrogations which is continuously observed during all flights at a range from 10% to 40% can be explained by the following: The aircraft transponder radiates its DF11 short squitter alternately from the bottom and top antennas. Other aircraft flying above on their part radiate TCAS selective UF00 or broadcast UF16 interrogations which will be better received by the top antenna of the flight inspection aircraft, so the signal received at the bottom antenna has a low reception level. Since the measurement system is connected to a bottom antenna only, it receives only weak signal levels from these high-flying aircraft.

With the exception of some military aircraft equipped with electrically generated antenna rotation and equipped with Mode S surveillance capabilities, all rotating radars operate from the ground. So do the fixed interrogators as part of a multilateration system.

Note: This does not provide any answers to the question if a diversity-antenna operation is strictly needed or not. Arguments and interpretations regarding that issue are given in section 3.6.

By consulting the numbers of Figure 3-16, the telegram traffic volume seems to be well reproducible on the same air route to Berlin, starting in Braunschweig at 07:24 h UTC. Due to subsequent ILS measurements in Berlin the elapsed time is longer than in the preceding figure.

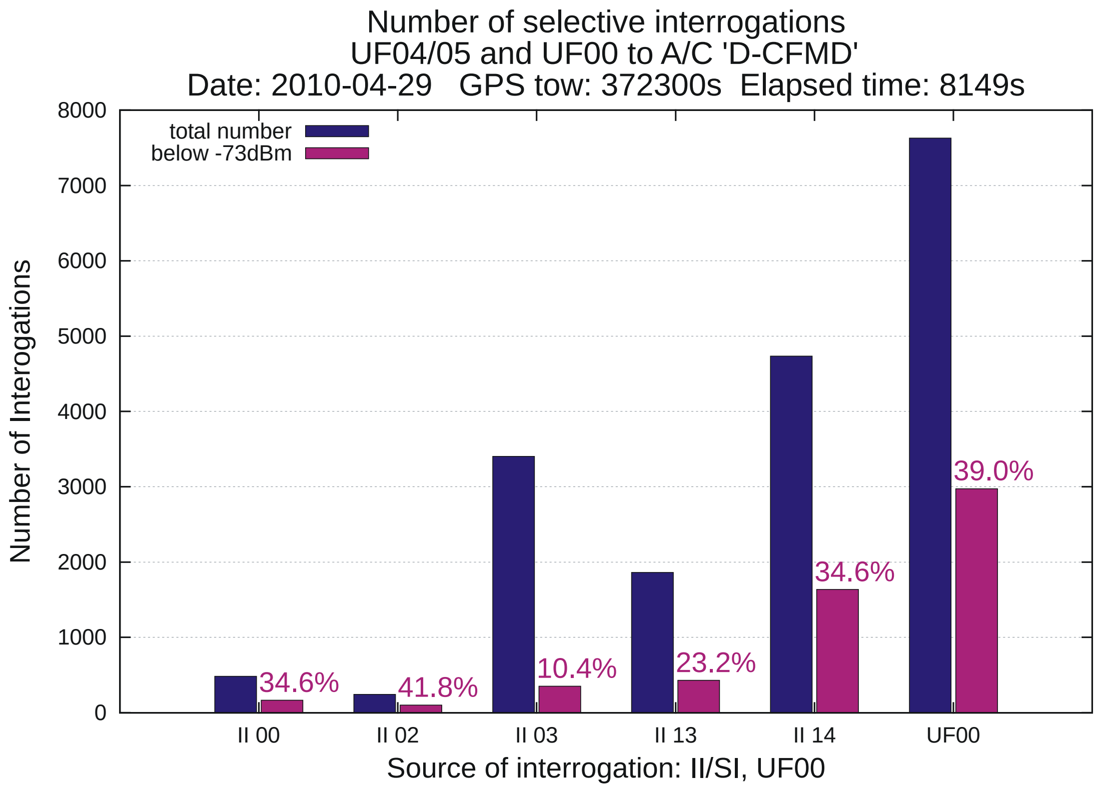

Figure 3-16: Ferry flight #2 from Braunschweig to Berlin and subsequent ILS measurements

Much higher air traffic was detected on a ferry flight to a following inspection programme of Instrument Landing Systems (ILS) in Frankfurt, starting at 16:50h UTC in Braunschweig. Here, the number of incoming UF00 is larger than all accumulated radar interrogations as shown in Figure 3-17. Most radar activity is induced by the

"German South Cluster Main" II11 and the test radar "Götzenhain" II14, in the vicinity of Frankfurt.

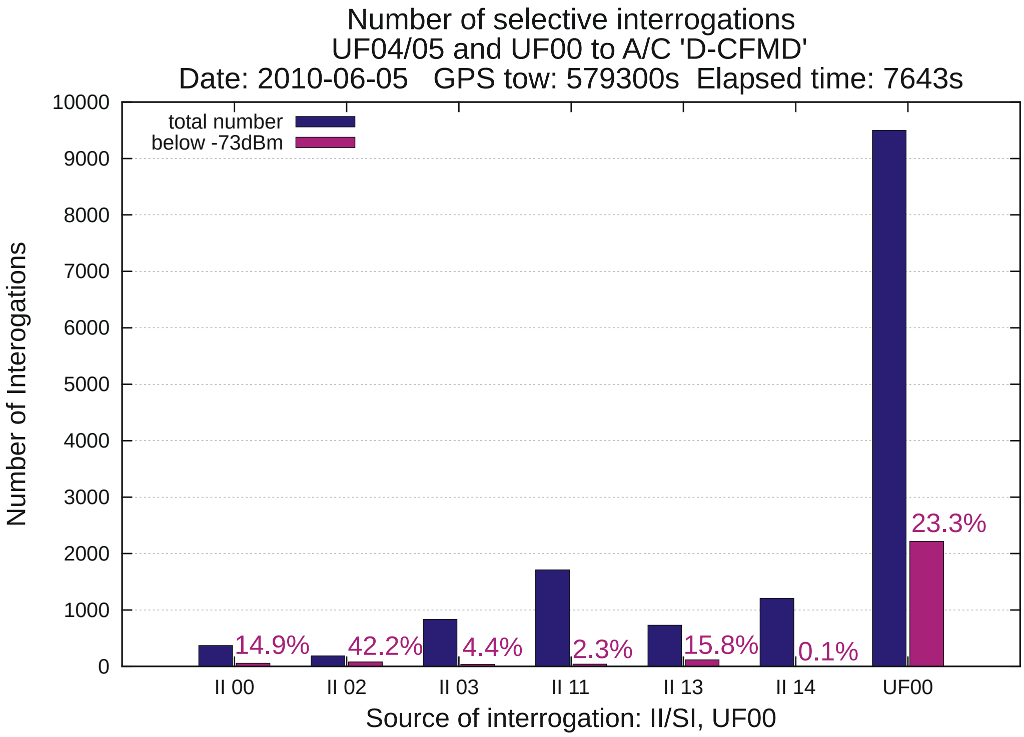

Figure 3-17: Ferry flight to Frankfurt and subsequent ILS measurements

Another example of a ferry flight with the destination of Munich airport is given by Figure 3-18. Since the distance is larger and the aircraft was close to the Czech Republic in mid-flight, more radar stations were observed. However, the most conspicuous characteristic of that graph is the low number of UF00 TCAS interrogations in contrast to all other figures, which is an indirect measure of the air traffic volume. During April 2010, a drop of traffic was caused by the volcanic ash cloud over northern Europe. On April 19th, the German airports were still closed for airline traffic until the next day.

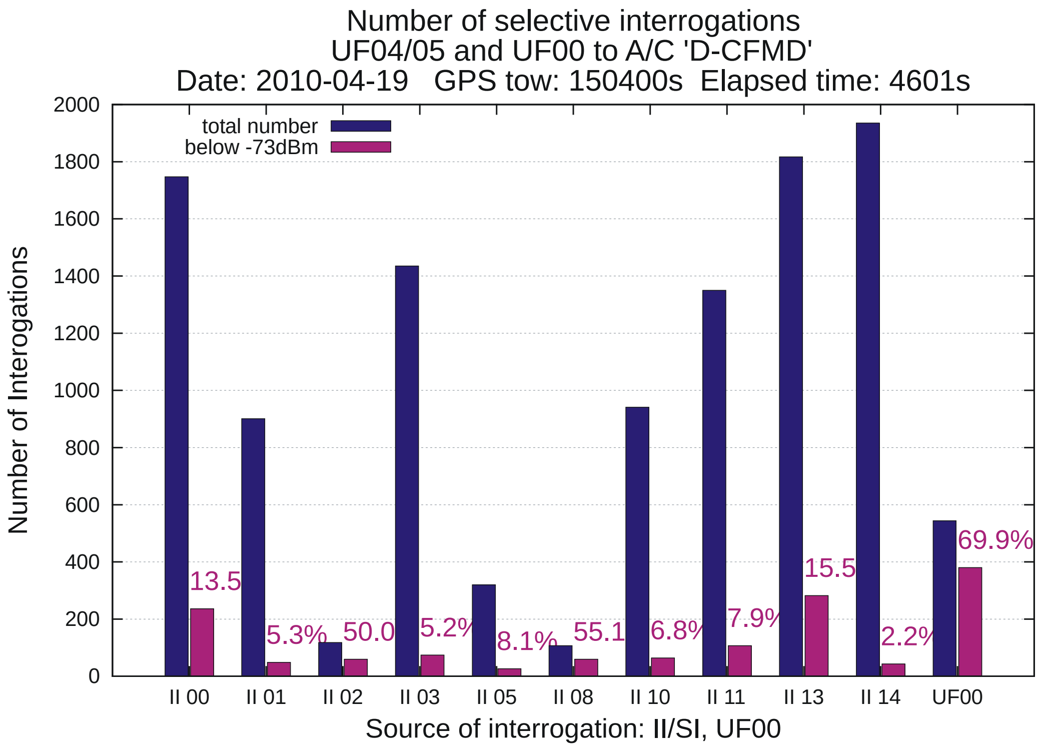

Figure 3-18: Interrogations during ferry flight to Munich

3.1.3.4 Analysis of Radar Sweeps

Since most interrogations can be assigned to certain radars due to the known interrogator codes, their individual characteristics during beam sweeps can be monitored using the time stamps of each single Mode S telegram. With reference to the mentioned ferry flight to Munich (Figure 3-18) it is interesting to observe which radars are interrogating at what frequency across the time scale. Over a period of 100s, the signal level distribution is shown in Figure 3-19, in which each dot represents one selective interrogation to the flight inspection aircraft. It can be easily identified that the antenna rotation periods of II01, II10 and II14 are five seconds, which is a typical value for airport radars. Mid- and long-range radars have longer periods of 10s, which is the case for interrogators II03, II05 and II13. Every radar sweep shows a distribution of received signal levels on the y-axis. It is remarkable that the levels of radars II01, II05, II10 are within 5 dB, whereas others are spread over a higher dynamic range, e.g. code II13 and II14.

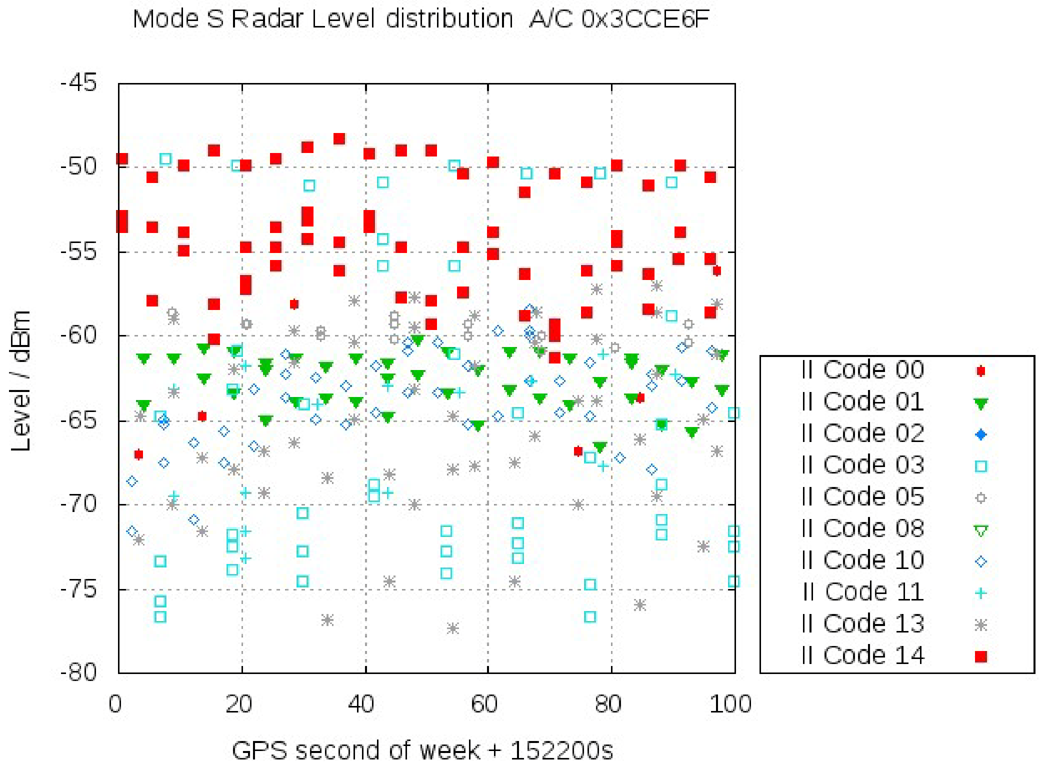

Figure 3-19: Level distribution of selective interrogations on ferry flight to Munich

A more detailed analysis requires zooming into antenna sweeps of an individual interrogator. In Figure 3-20 the interrogations of II01 are shown over a one-minute period. In addition to the selective UF04/05 calls all available UF11 telegrams of the Mode S all-call period are shown which should be statistically distributed around the antenna boresight, defined as the direction of maximum gain of the directional radar antenna. It can be clearly seen that the antenna rotation duration is five seconds and the selective calls mostly occur close to the maximum gain. To probe further we examine two consecutive beam sweeps at a highly extended temporal resolution as shown in Figure 3-21. Since the UF11 all-call interrogations all always transmitted at the same power level, their temporal and level distribution can be used to compute the 3 dB beam angle, reading roughly 40 ns for a 3 dB drop from maximum:

$$\Delta\Phi_A = 40\,\text{ms} * 360° / 5\,\text{s} = 2.9°$$

The selective interrogations occur at the rising gain during beam dwell time. This is appropriate, since in case of dense airspace re-interrogations might be necessary which then also could be performed on the falling gain side. For calculating the target off-boresight angle the incidence direction means no difference to the Monopulse SSR (MSSR) principle.

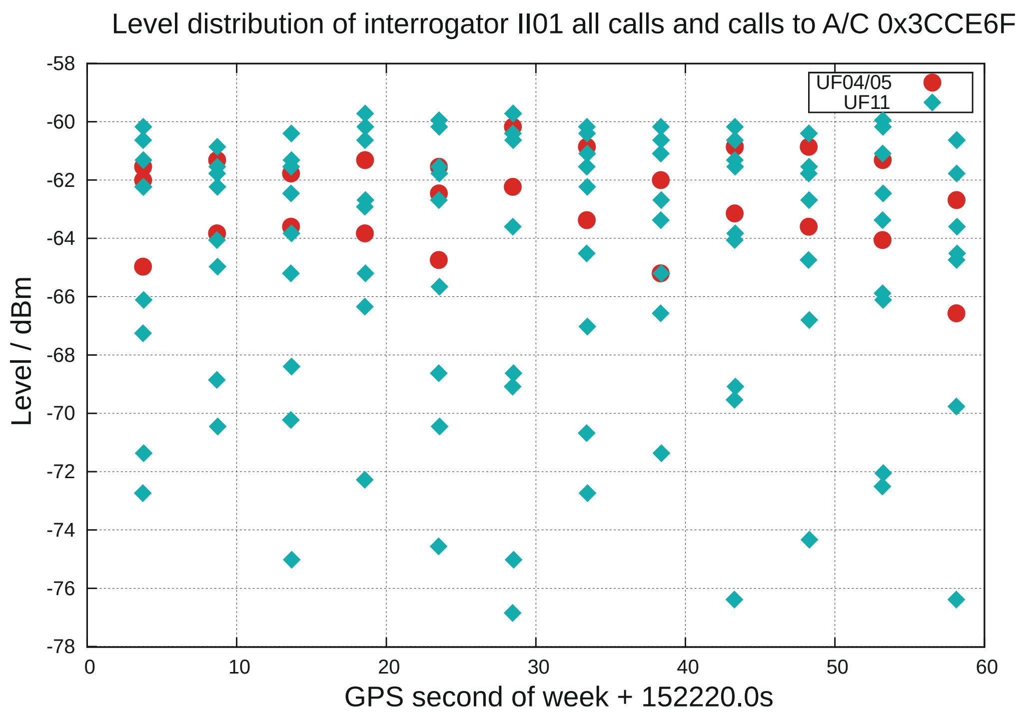

Figure 3-20: Antenna rotation and sweeps of radar II01

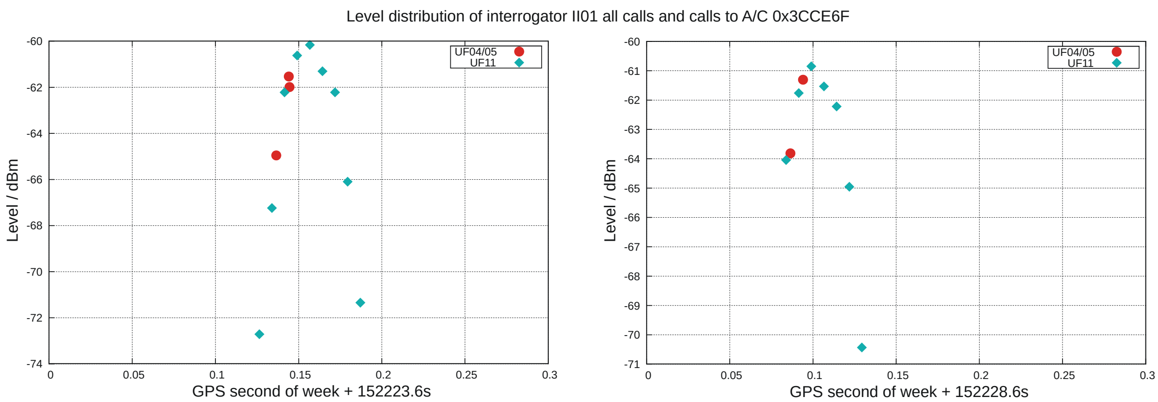

Figure 3-21: Zoom into two consecutive sweeps of II01

Another example shown in Figure 3-22 has interrogator II10 which reveals similar beam sweeps as in the preceding example. The only noticeable difference is the slightly increased frequency of UF11 all-calls within each beam sweep.

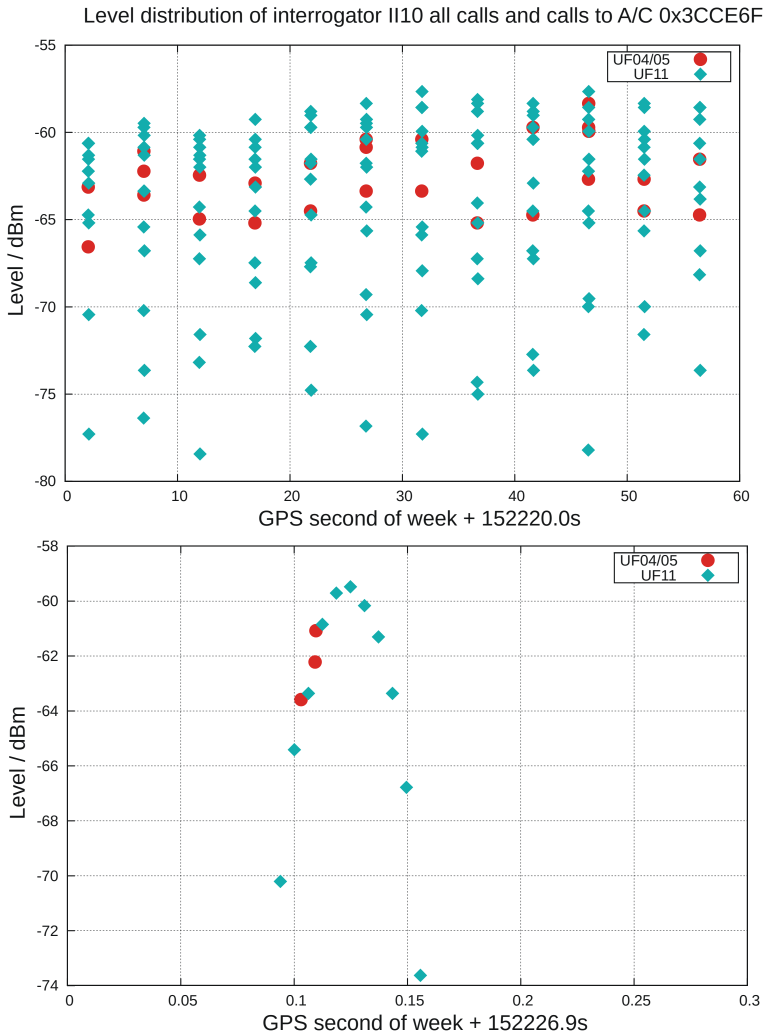

Figure 3-22: Antenna sweeps of II10 at low and high resolution

The same period is now evaluated for II13 as depicted in Figure 3-23. It can be observed that interrogations of three radars are received, two of these (Radar #1 and #2) address our aircraft that is not within the range coverage of #3 the signal levels of which are weak. Generally, the military radar II13 seems to regularly perform a threefold interrogation per radar sweep, since this behaviour was observed during all flights within coverage.

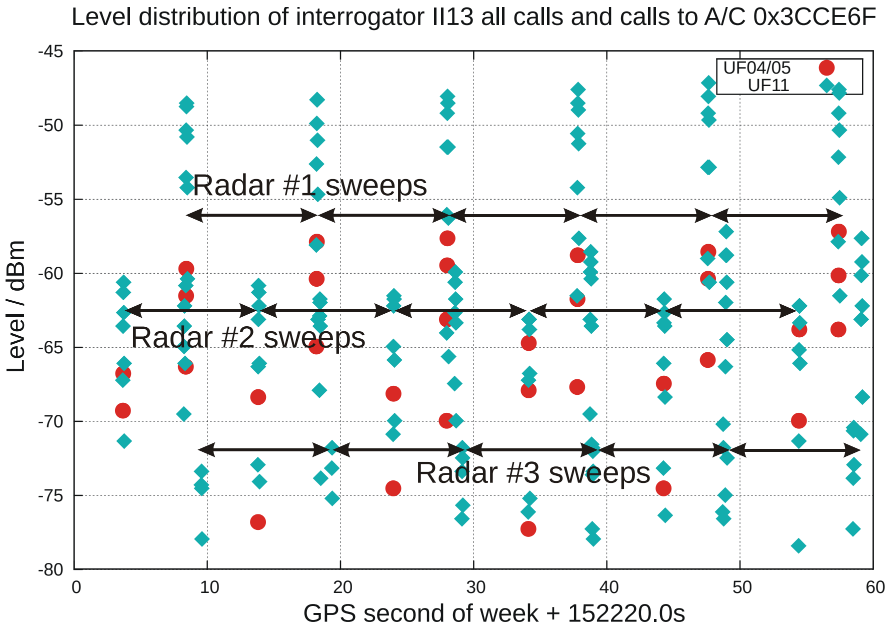

Figure 3-23: Interrogations II13 from three different radars

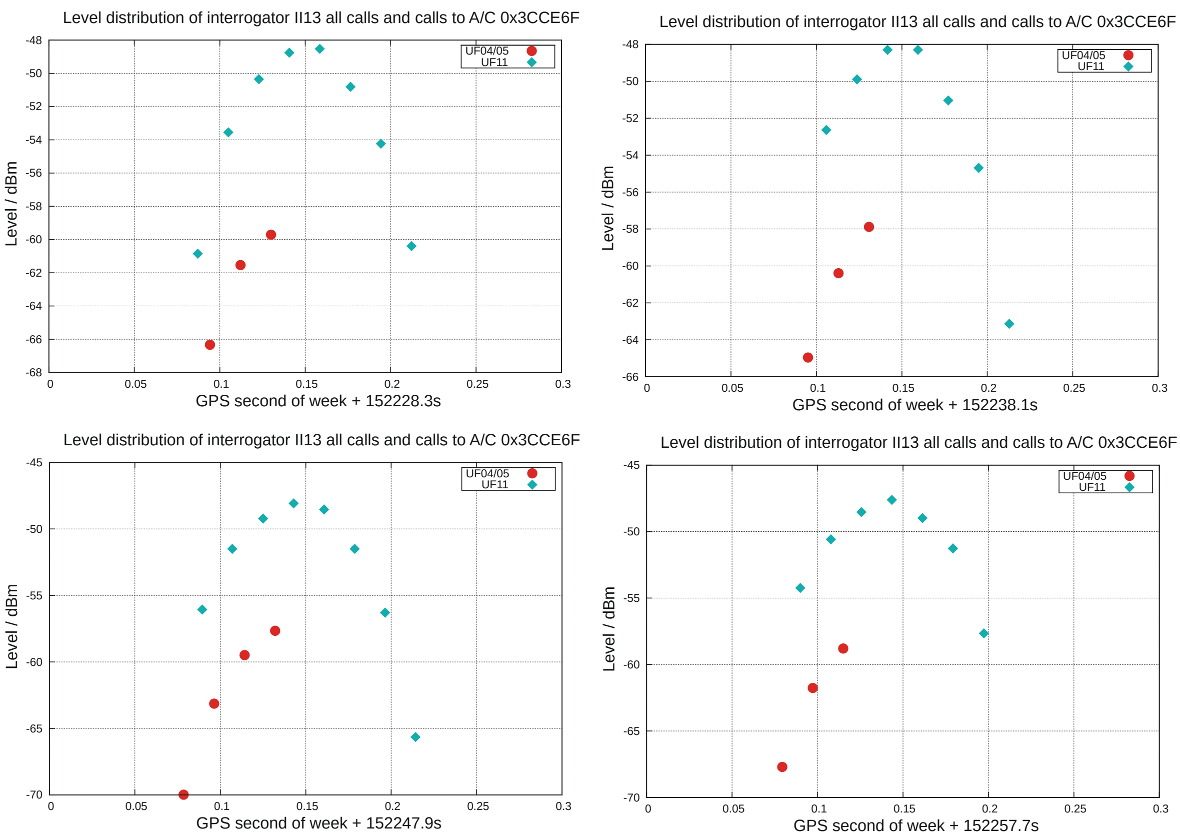

Figure 3-24: II13 interrogations within four consecutive sweeps

A high resolution graph of four consecutive beam sweeps of #1 are shown in Figure 3-24. Again, the level distribution of UF11 all-calls over time expresses the antenna beam angle. The most remarkable difference to the sweeps seen before is that the signal level of selective interrogations is significantly reduced by 8 to 10 dB compared to the nearby time UF11. Furthermore, the each very first interrogation is sent out at the beginning of the beam dwell down by 20 dB below the maximum level of the antenna boresight. Those single uplink telegrams of subfigure #3 will now be investigated by examining the video plots.

As shown in the UF04 telegram in Figure 3-25 ff. there is a P5 Side Lobe Suppression (SLS) leaking through P6, which is strongest in the first plot as expected, since this is the most off-boresight angle. At the beginning of P6 a level raising and falling around the SPR takes effect influencing also the phase, to be seen better in the lower left subfigure (zoom) and the polar plot. The original phase step 180° is reduced to 140° within 100 ns and consequently, the SPR phase transition 10° to 170° is further delayed up to 270 ns (more time measurements are performed in section 3.1.3.5).

Any DPSK demodulation process is sensitive to phase deviations, and so is the applied software autocorrelation process. Around the SPR the ACF curve shows two side lobes, the preceding having roughly 20% of the main lobe energy.

This particular military radar applies an active power management which reduces the selective interrogation signal power to a suitable threshold in compliance with [RD4] (ICAO Annex 10, 3.1.2.11.2 *INTERROGATOR-EFFECTIVE RADIATED POWER*). Both the selective interrogation power and the SLS power is reduced, as to be seen in Figure 3-29 which shows the most nearby preceding UF11 to the second UF04. However, the measured SPR duration of the UF11 is shorter than that of UF04, which may result from a different phase shift between SLS and the main beam to that specific off-boresight angle.

Since the measurement system does not include a dedicated 1090 MHz receiver there is no direct verification method if the local transponder gave a reply or not. However, the data of the existing Mode S 1030/1090MHz monitoring network operated by TU Braunschweig is available to perform the analysis. It provides all recorded up- and downlink formats of all aircraft within coverage of each sensor. For further information about this network refer to the detailed description in section 3.2.

It is important to understand in what way the reception on 1090 MHz of the interrogating radar differs from that of the network sensor. The radar beam is highly directional and expects the reply within the beam dwell right after the interrogation, masking all other sectors outside the 3° beam width. In contrast to this, the network sensor antenna pattern is nearly omnidirectional and draws a much higher transponder radio field load from full 360°. So in total there is a much lower signal-to-noise ratio on the network sensor site due to the lower antenna gain on the one hand, while, on the other hand, there is a high probability of telegram interference. For this reason, during most of the performed flights too many downlink telegrams of D-CFMD were lost, resulting in large gaps in the downlink telegram lists. As a result, a continuous correlation between airborne recorded interrogations and detected replies on ground was not viable.

However, during the flight measurement campaign the volcanic ash cloud came up and grounded much of the air traffic, as already stated above. On April 19th this helped to reduce the 1090 MHz channel load to such an extent that the correlation between the two data sources was successful at least for that day. The corresponding selective interrogations and replies of the beam sweeps as of Figure 3-24 were correlated and drawn up in a single list:

Sweep #1

```
UF04 GPS:152228.394296s 0x2001D040C3FB4B 00000000000000 AP:3CCE6F DI:1 II:13
DF04 0x200011903CCE6F00000000000000

UF04 GPS:152228.412149s 0x2001D040C3FB4B 00000000000000 AP:3CCE6F DI:1 II:13
DF04 0x200011903CCE6F00000000000000

UF04 GPS:152228.430002s 0x2001D040C3FB4B 00000000000000 AP:3CCE6F DI:1 II:13
No reply received!
```

Sweep #2

```
UF04 GPS:152238.195097s 0x208FD7404184E8 00000000000000 AP:3CCE6F DI:7 II:13
DF20 0xA0001190FE81E3000000003CCE6F

UF04 GPS:152238.212949s 0x208FD7404184E8 00000000000000 AP:3CCE6F DI:7 II:13
DF20 0xA0001190FE81E3000000003CCE6F

UF04 GPS:152238.230801s 0x208FD7404184E8 00000000000000 AP:3CCE6F DI:7 II:13
DF20 0xA0001190FE81E3000000003CCE6F
```

Sweep #3

```
UF04 GPS:152247.978553s 0x2001D040C3FB4B 00000000000000 AP:3CCE6F DI:1 II:13
DF04 0x200011903CCE6F00000000000000

UF04 GPS:152247.996406s 0x2001D040C3FB4B 00000000000000 AP:3CCE6F DI:1 II:13
DF04 0x200011903CCE6F00000000000000

UF04 GPS:152248.014259s 0x2001D040C3FB4B 00000000000000 AP:3CCE6F DI:1 II:13
DF04 0x200011903CCE6F00000000000000

UF04 GPS:152248.032112s 0x2001D040C3FB4B 00000000000000 AP:3CCE6F DI:1 II:13
DF04 0x200011903CCE6F00000000000000
```

Sweep #4

```
UF04 GPS:152257.779356s 0x2001D040C3FB4B 00000000000000 AP:3CCE6F DI:1 II:13
No reply received!

UF04 GPS:152257.797208s 0x2001D040C3FB4B 00000000000000 AP:3CCE6F DI:1 II:13
DF04 0x200011903CCE6F00000000000000

UF04 GPS:152257.815060s 0x2001D040C3FB4B 00000000000000 AP:3CCE6F DI:1 II:13
DF04 0x200011903CCE6F00000000000000
```

Within all four beam sweeps, the UF04 measured airborne and the associated reply (DF04 or DF20) detected on ground are listed. These ground replies were all contributed by the sensor station “Oberpfaffenhofen” (see section 3.2). The reply format itself depends on the uplink *designator identification* (DI) field. If the value is set to 7, a Comm-B reply (DF20) is requested to be seen in Sweep #2. Within Sweep #1 and #4 there is one missing reply each, which is likely to be due to an unreadable reply on the ground (the measurement receiver on the ground has a lower detection probability compared to a radar station due to its non-directional antenna installation).

From this analysis one can safely conclude that the transponder installed in the flight inspection aircraft has obviously no problems recognizing all interrogations, either sent from greater off-boresight angles having stronger SLS, or from the beam maximum.

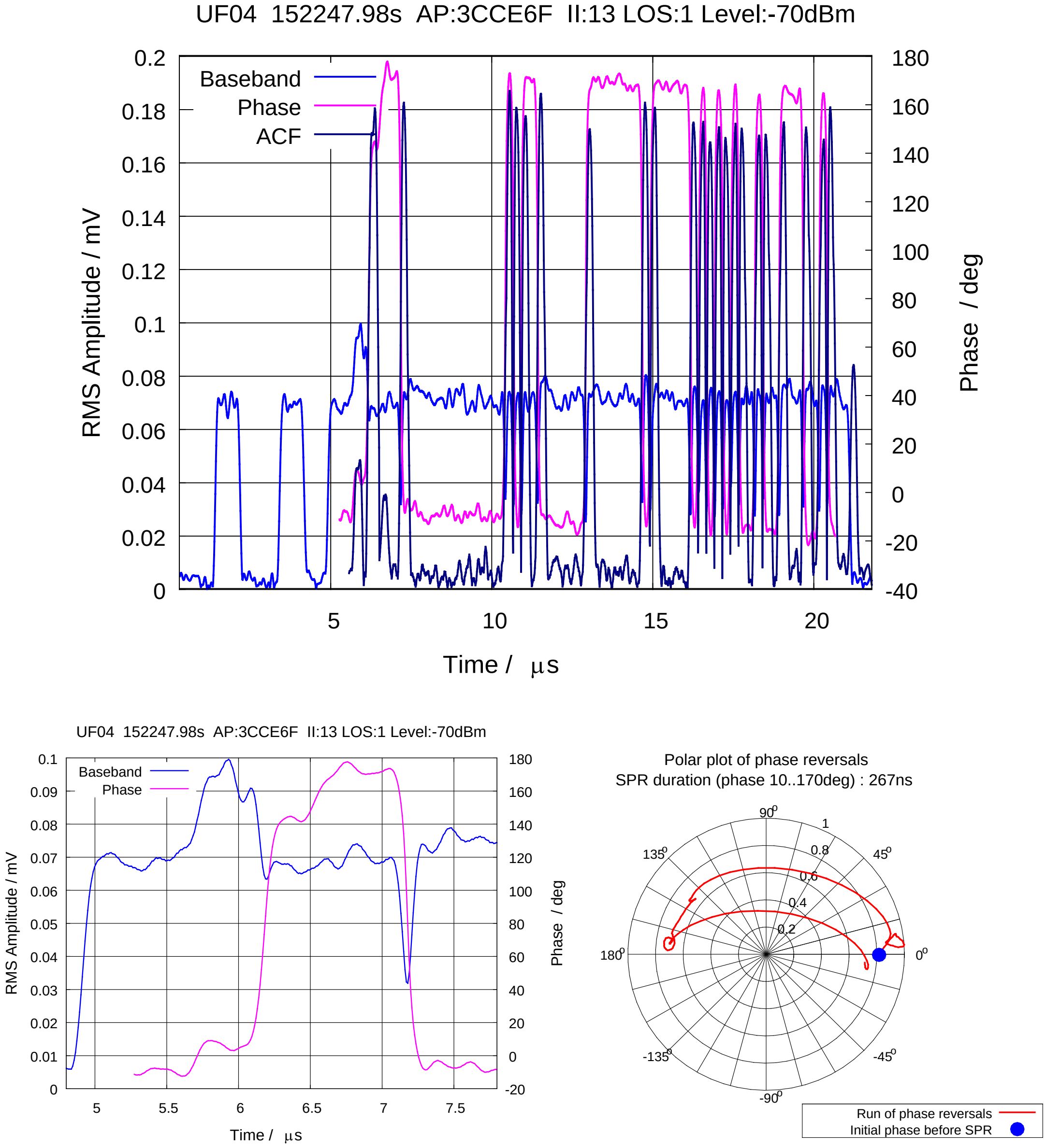

Figure 3-25: Interrogation UF04, 1 of 4 within one beam dwell of II13

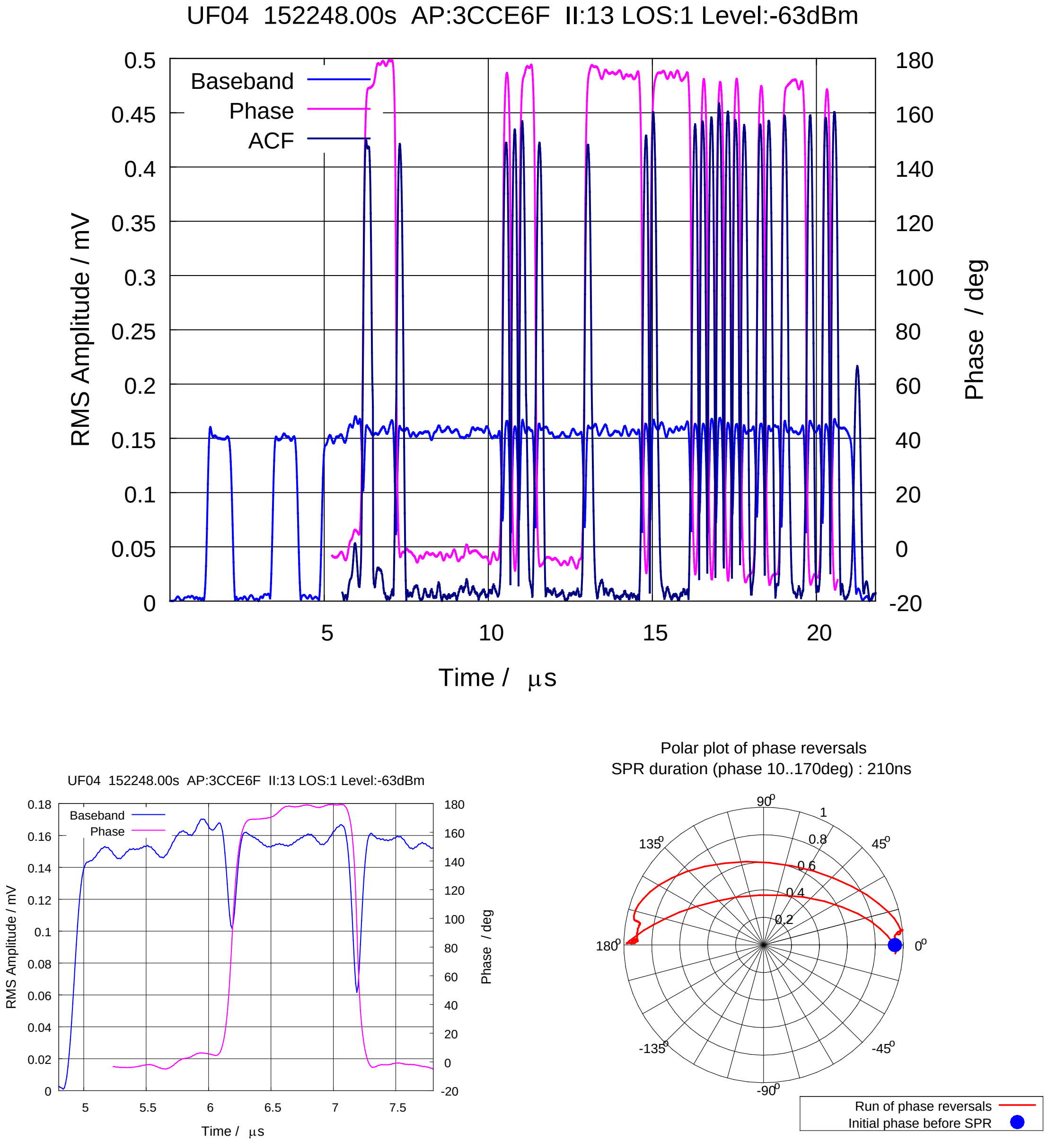

Figure 3-26: Interrogation UF04, 2 of 4

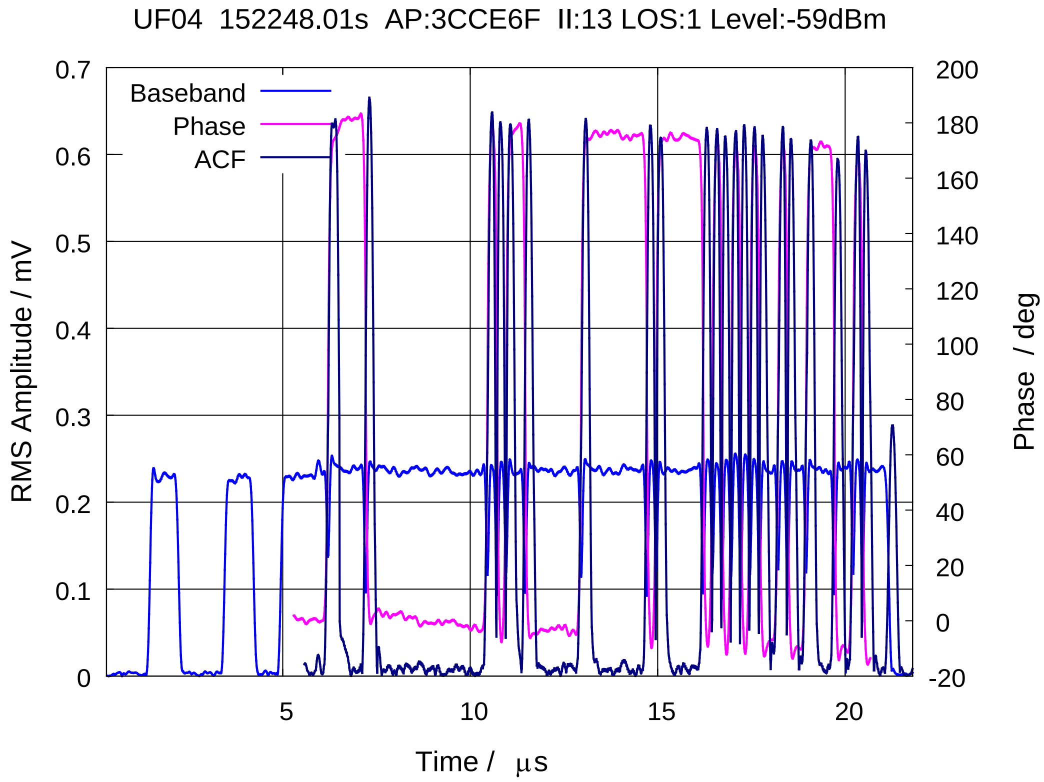

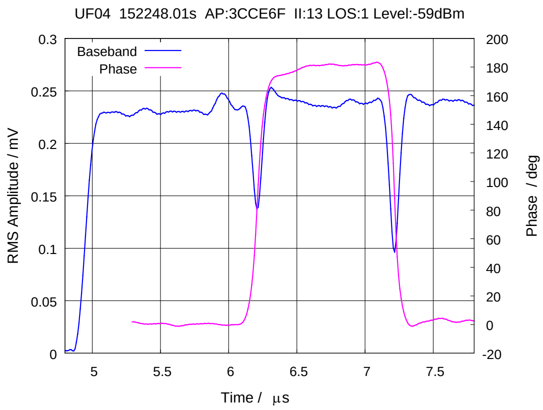

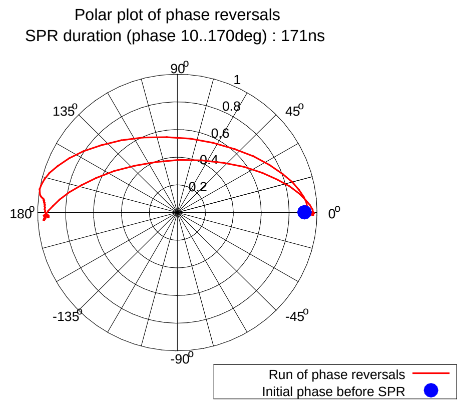

Figure 3-27: Interrogation UF04, 3 of 4

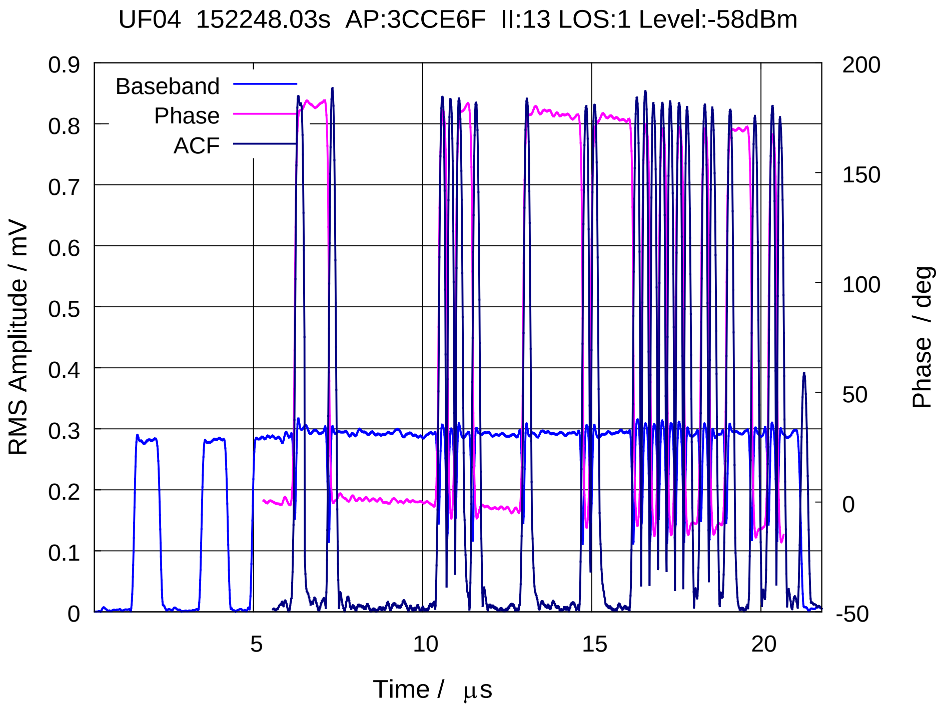

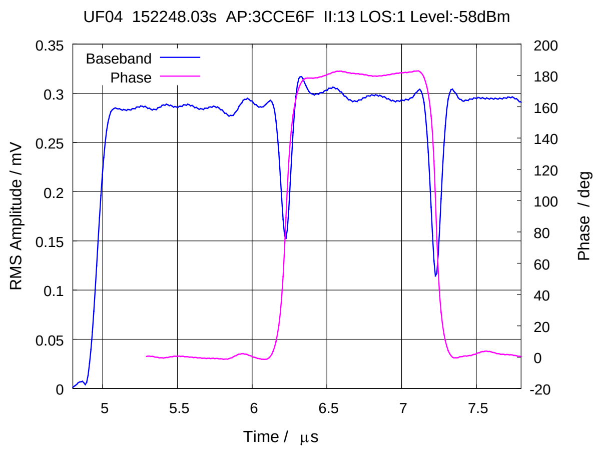

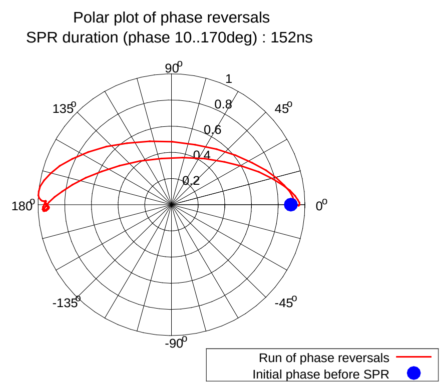

Figure 3-28: Interrogation UF04, 4 of 4

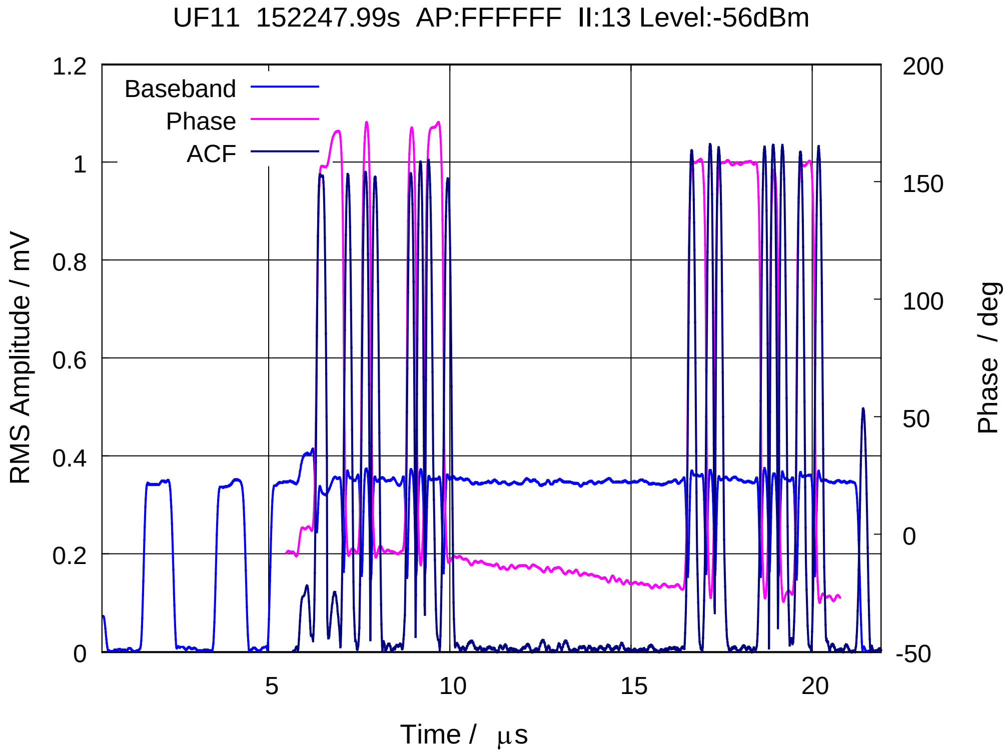

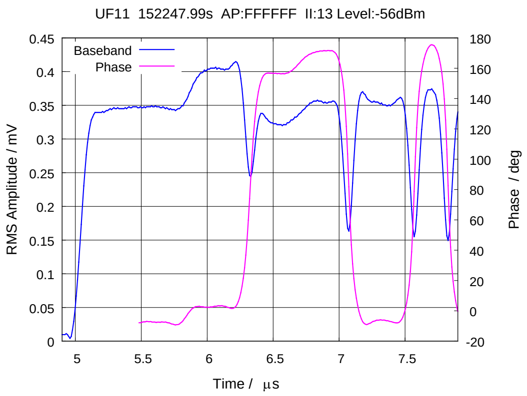

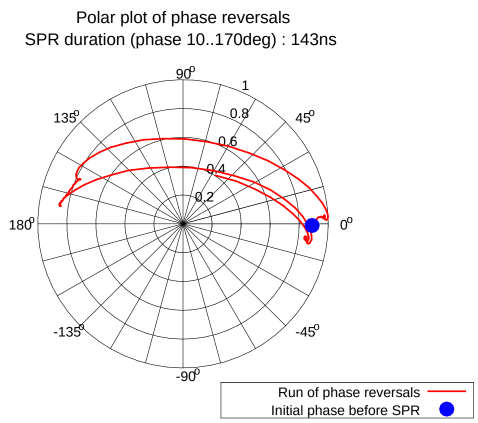

Figure 3-29: Interrogation UF11 close to second UF04 (2 of 4)

An even more drastic version of the SLS leakage effect seen at a different time is shown in the zoomed video and phase plot of Figure 3-30. The extension of the duration time is much higher than a 250 ns chip length which is normally used for detecting SPR and data bits in a transponder.

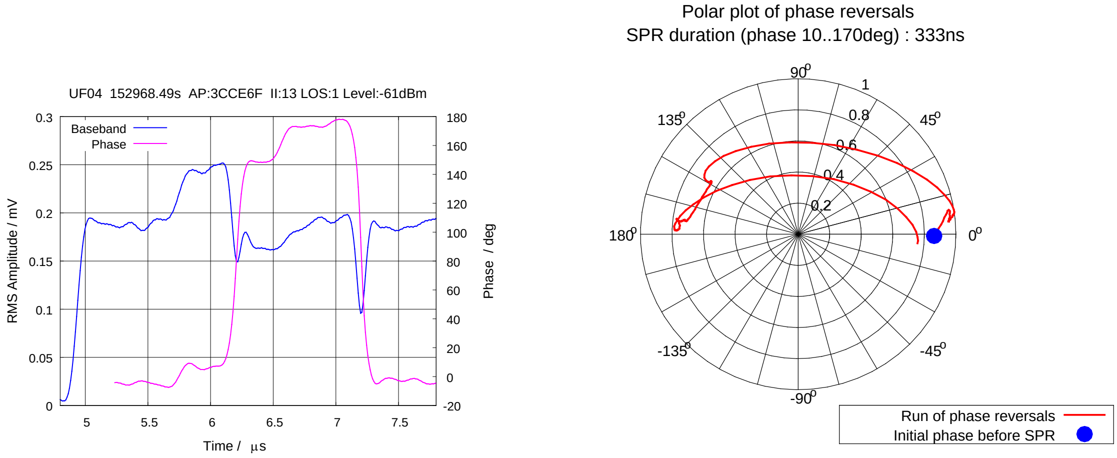

Figure 3-30: Interrogation II13 having more P5 SLS influence

In some areas the flight inspection aircraft received interrogations from numerous radars using the same II code, making it hard to distinguish between certain facilities. The constant antenna rotation periods however help to identify them in the diagram. On a ferry flight from Braunschweig to Cuxhaven-Nordholz (North Sea) five radars of the German *North Cluster Main* were received, four of which (Radar #1 to #4) radiated levels well above the transponder MTL as seen in the one-minute plot of Figure 3-31. Selective interrogations were received from #1 and #2. Radar #2 mostly interrogates once a beam sweep, whereas #1 does it two or three times.

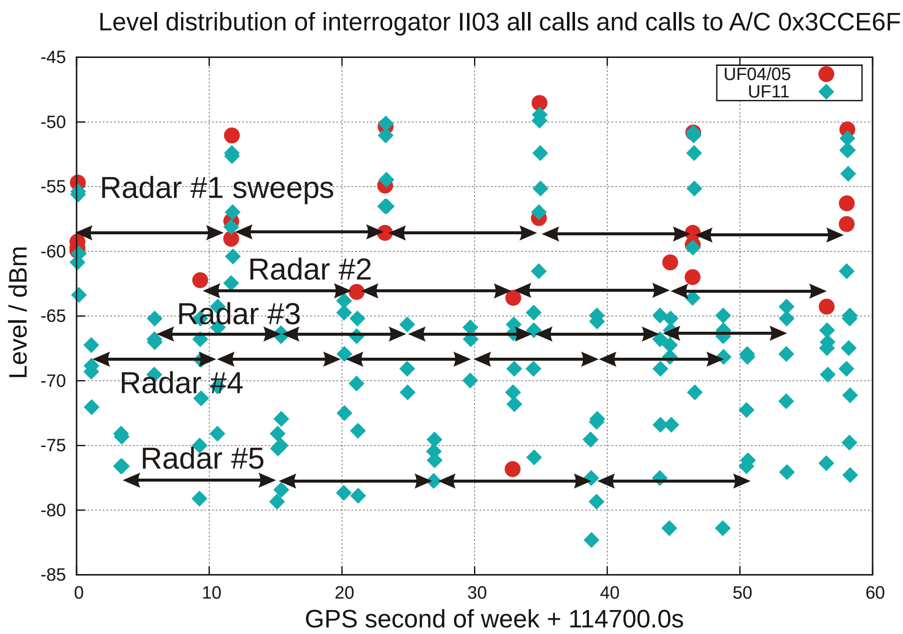

Figure 3-31: Interrogations II03 from five different radars

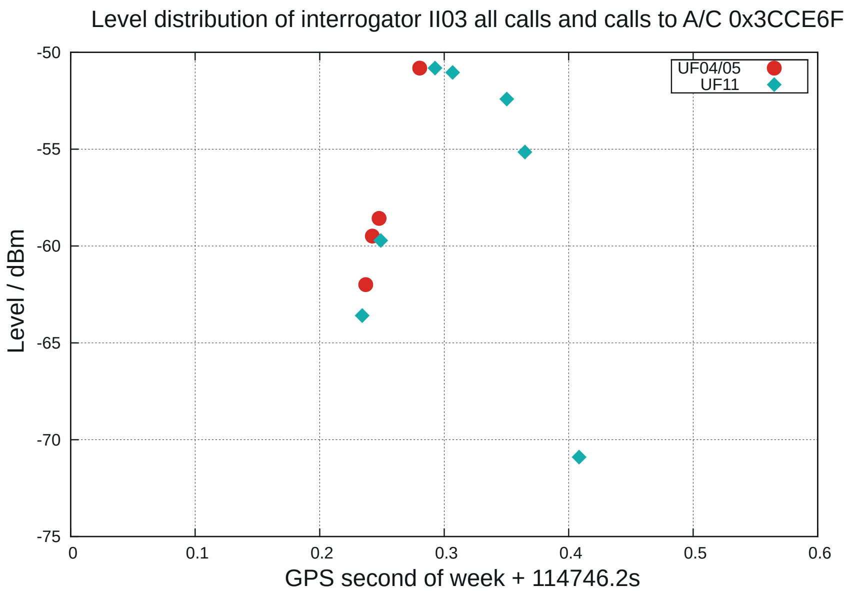

Figure 3-32: Interrogations within one sweep II03

Again, the zoom into one beam sweep reveals the level distribution over time (Figure 3-32). This radar performs the first interrogation at the beam boundary, but there is one interrogation close to the antenna boresight, which is continuously shown in Figure 3-31.

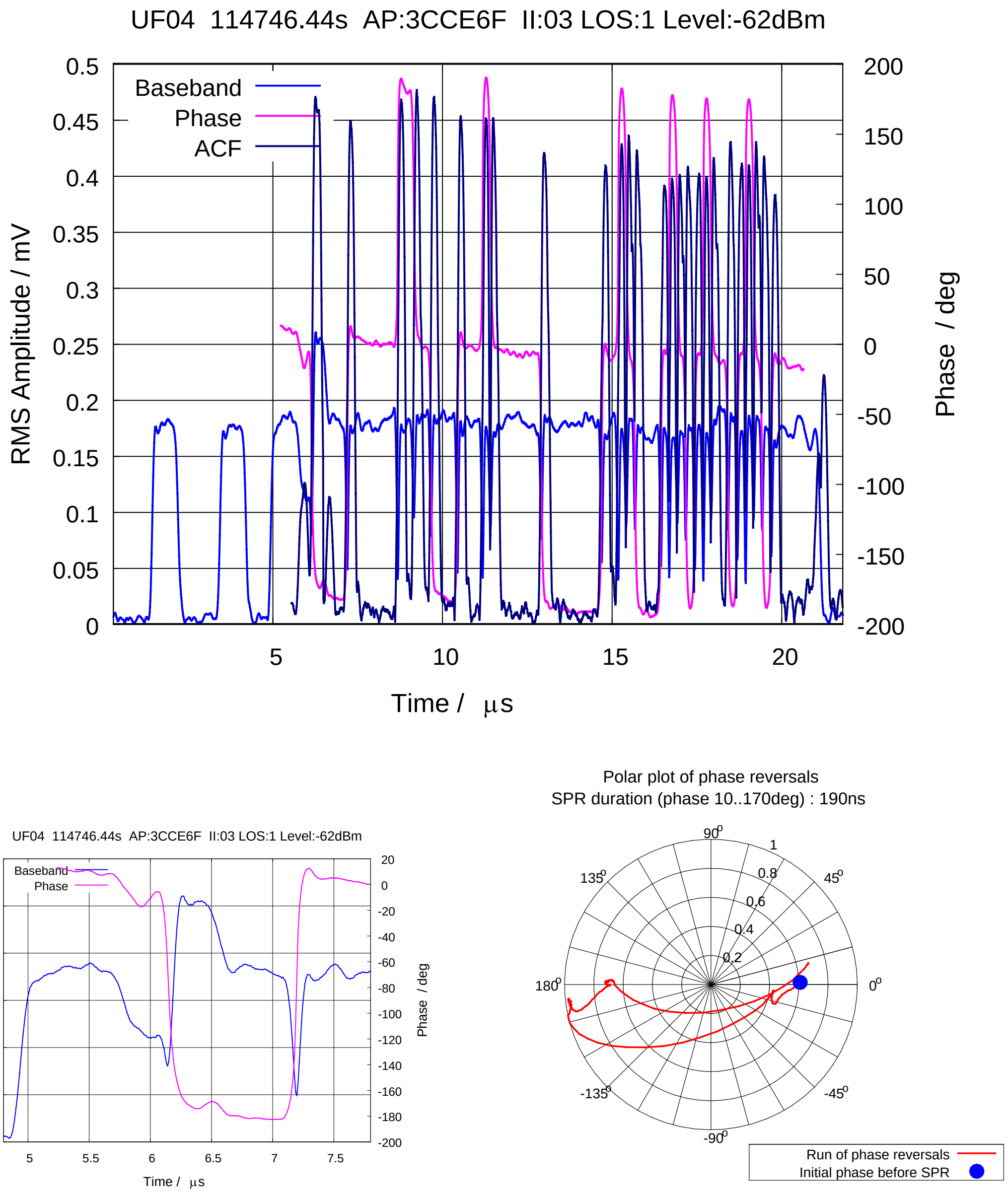

Figure 3-33: UF04 of interrogator II03 affected by SLS

As seen before, the interrogators maintain their interrogation patterns during beam sweeps. This could mean that a radar station interrogates twice, alternately UF04 and UF05, close to the antenna boresight, which was also observed during an ILS coverage flight of Saarbrücken and in the vicinity of Luxemburg. In Figure 3-34 the constant double interrogation within only 2 dB per sweep of II02 along the 100s period is visible, whereas the two clustered II11 and especially II05 show larger level variations.

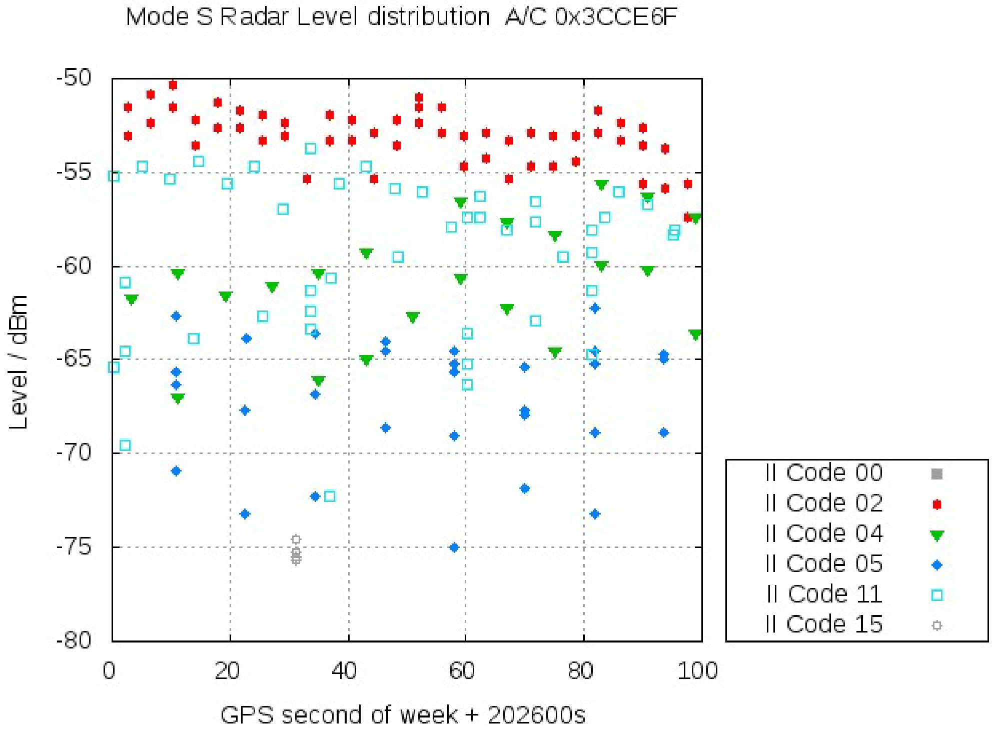

Figure 3-34: Interrogations during coverage flight of Saarbrücken ILS

Interrogator II02 deserves mentioning since its phase reversals are continuously fast and free of interferences. In Figure 3-35 we observe an I/Q modulation to negative phase direction being performed very quickly, as the zoom into the SPR region (lower left) reveals. The polar plot (lower right) emphasizes a phase reversal which has amplitude dips but is consistent without interferences from multipath and superimposed interrogations.

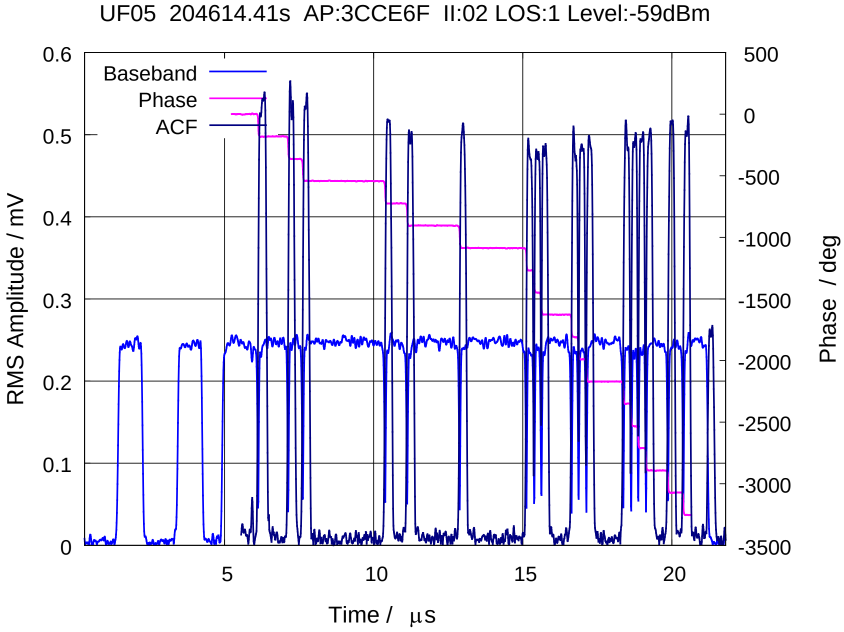

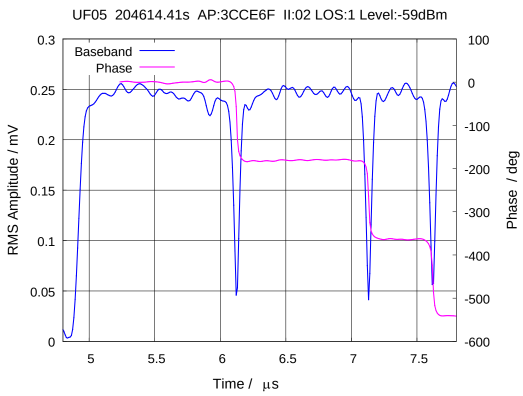

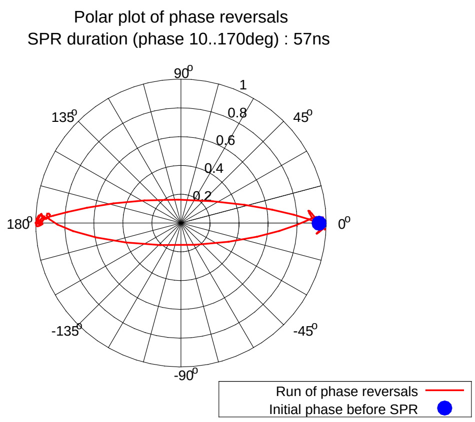

Figure 3-35: Fast and clean SPR of UF05 received from interrogator II02

3.1.3.5 Measurement of the Sync Phase Reversal Duration

As already stated in section 3.1.2.4 it is difficult to perform true signal-ins-space measurements focussing on time-critical signal characteristics due to hardware bandwidth constraints. The software FIR bandpass filters are normally optimized to comply with the IF bandwidth to reduce noise as much as possible, intending to assist the ACF DPSK demodulation process. Effectively, the noise-matched FIR filter stretches the actual phase reversal duration by a certain factor, as shown in section 3.1.2.4.

In order to improve the temporal behaviour for certain analysis, other time-optimized filter parameters were chosen at the cost of increased noise and therefore lower telegram detection probability.

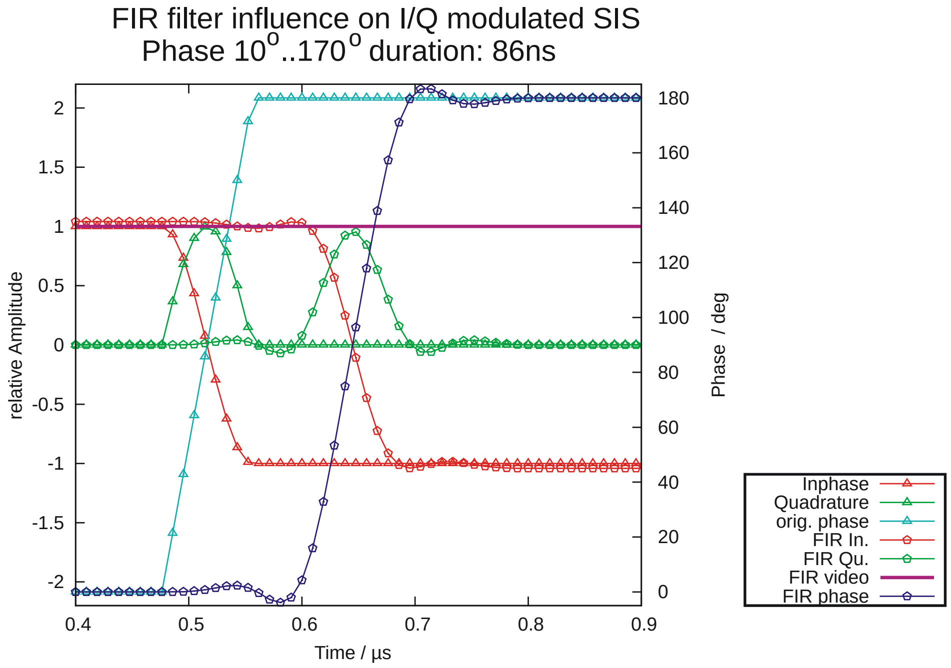

Figure 3-36: Time-optimized FIR bandpass filter

For the filter simulation, the same I/Q blending phase modulation was used as before. At the FIR filter outputs the signal shape now resembles the input values more closely. Finally, the steepness of the phase curve ("FIR phase") is only slightly decreased which stretches the original phase duration by a smaller factor than the noise-optimized filter.

Note: All SPR duration measurements presented here are influenced by the originally transmitted signal, the channel noise and the receiver characteristics. The receiver, as seen before, plays a major role in the quality of the final result. Hence, while values computed here are very close to the real signal-in-space characteristics they may still slightly vary from the real signal shape. Therefore, care must be applied when disqualifying certain interrogators, even if the ICAO limit of 80 ns per phase duration is partially exceeded.

In Figure 3-37 we observe a distribution of computed SPR durations separated for all interrogators named by their codes, taken from the Saarbrücken ILS coverage flight. Since the temporal resolution is limited to 9.5 ns, there is an accumulation of interrogations per each discrete 9.5 ns step on the x-axis. Most interrogations II02, II04, II04 perform well below the given ICAO limit 80 ns. The majority of II11 signals is a little above this value, but as already explained, this type of I/Q modulation is slightly decelerated from 80 ns to 86 ns due to the filter constraints.

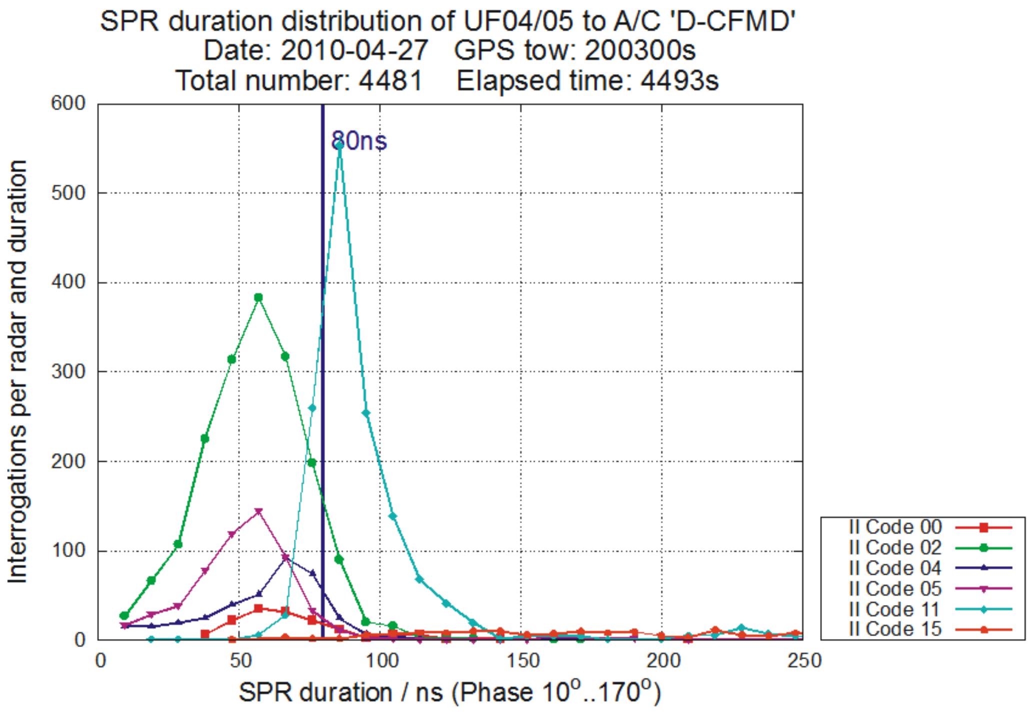

Figure 3-37: Radar SPR duration measured at ILS Saarbrücken coverage flight

Around the maximum, the curves seem to have approximately an equally distributed SPR duration, which resembles a Gaussian distribution. This behaviour needs to be explained in detail, using II02 as a prototype. The interrogator II02 is the same as referenced in Figure 3-35, having SPR durations of mostly 57 ns. As generally shown in section 3.1.3.4, the P5 SLS takes effect at larger off-boresight angles and leaks through P6, mostly inducing a *longer* SPR phase transition as seen at full length in Figure 3-25 and so on. The same happens to II02 as can be seen in Figure 3-38 increasing the consumed time beyond 100 ns. However, the P5 SLS can also have exactly the opposite effect: In Figure 3-39 we observe a P5 influence in the video plot and also in the autocorrelation curve revealing two side lobes. Compared with the polar plot of Figure 3-35 the amplitude during phase transition has decreased close to zero-crossing, and the resulting SPR transition time then is 19 ns, which is considerably less than 57 ns.

Both effects happen randomly and distribute the actually used time for the SPR transition around the most frequently observed discrete duration (here: 57 ns). This effect applies for all radar interrogations and is highlighted best if the number of interrogations is very large so that the curves have a clear maximum.

As an SLS-independent incident, multipath propagation degrades the signal-in-space in general, as depicted by an UF05 of the same radar shown in Figure 3-40. The main difference to the SLS influence is that the duration of *all phase reversals* is increased as shown by the zoomed video plot. During that flight, the altitude was constantly around 6,000 ft due to an ILS flight inspection pattern. Generally, multipath effects of that magnitude can only be observed during low altitude flights in certain areas. Multipath effects generally cannot be reproduced as well as the SLS effect.

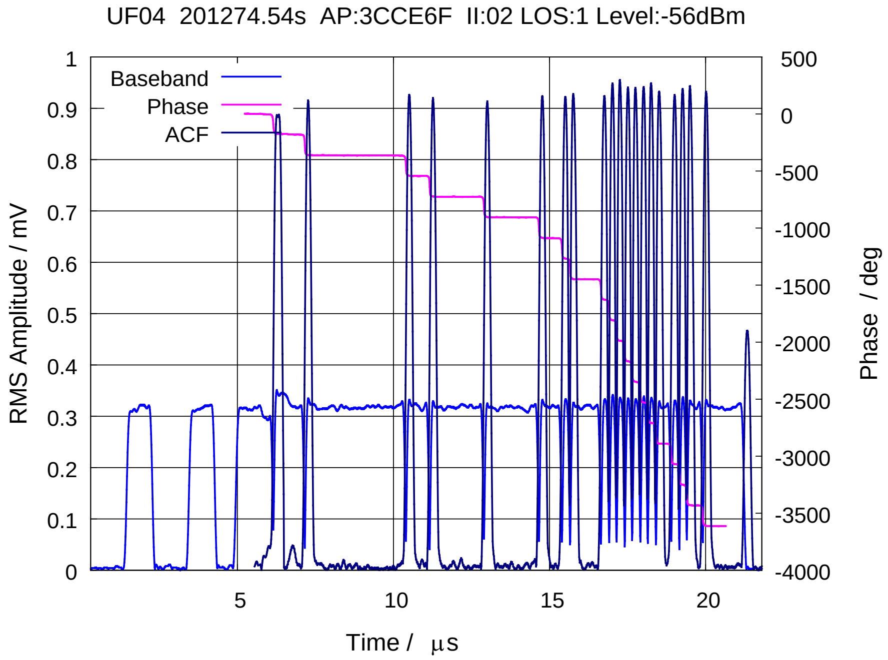

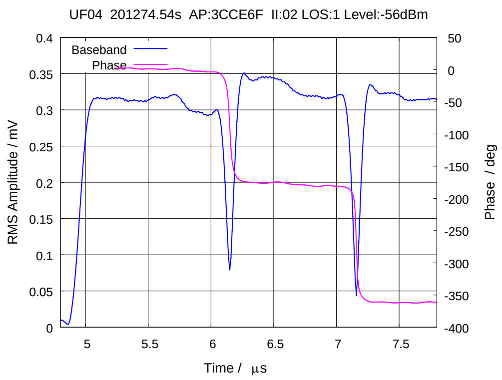

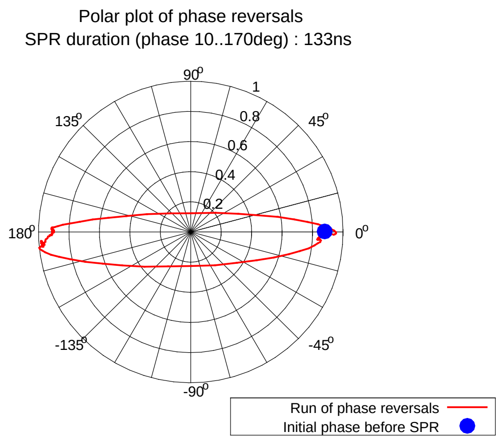

Figure 3-38: P5 SLS decelerating SPR duration of II02

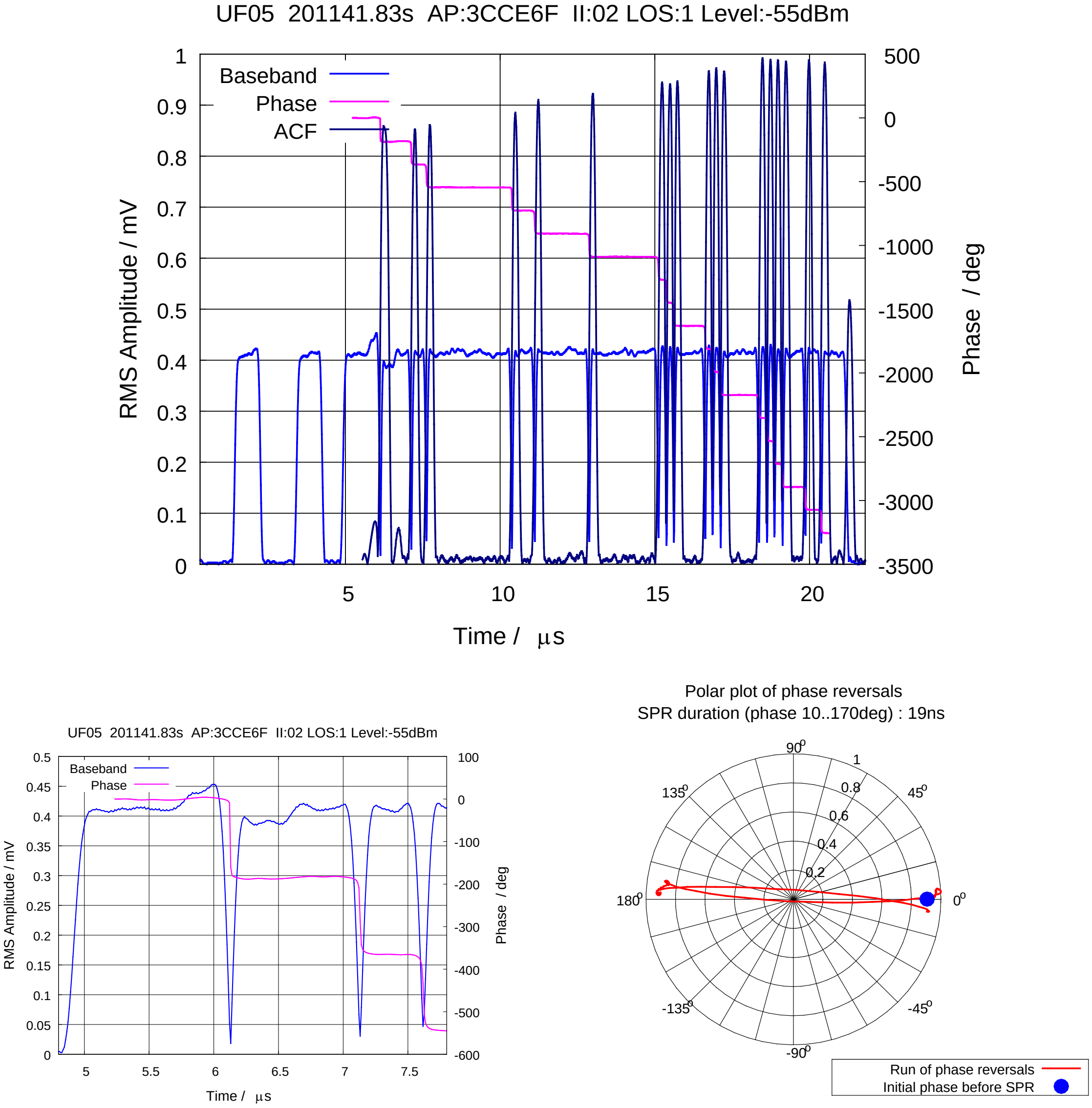

Figure 3-39: P5 SLS accelerating SPR duration of II02

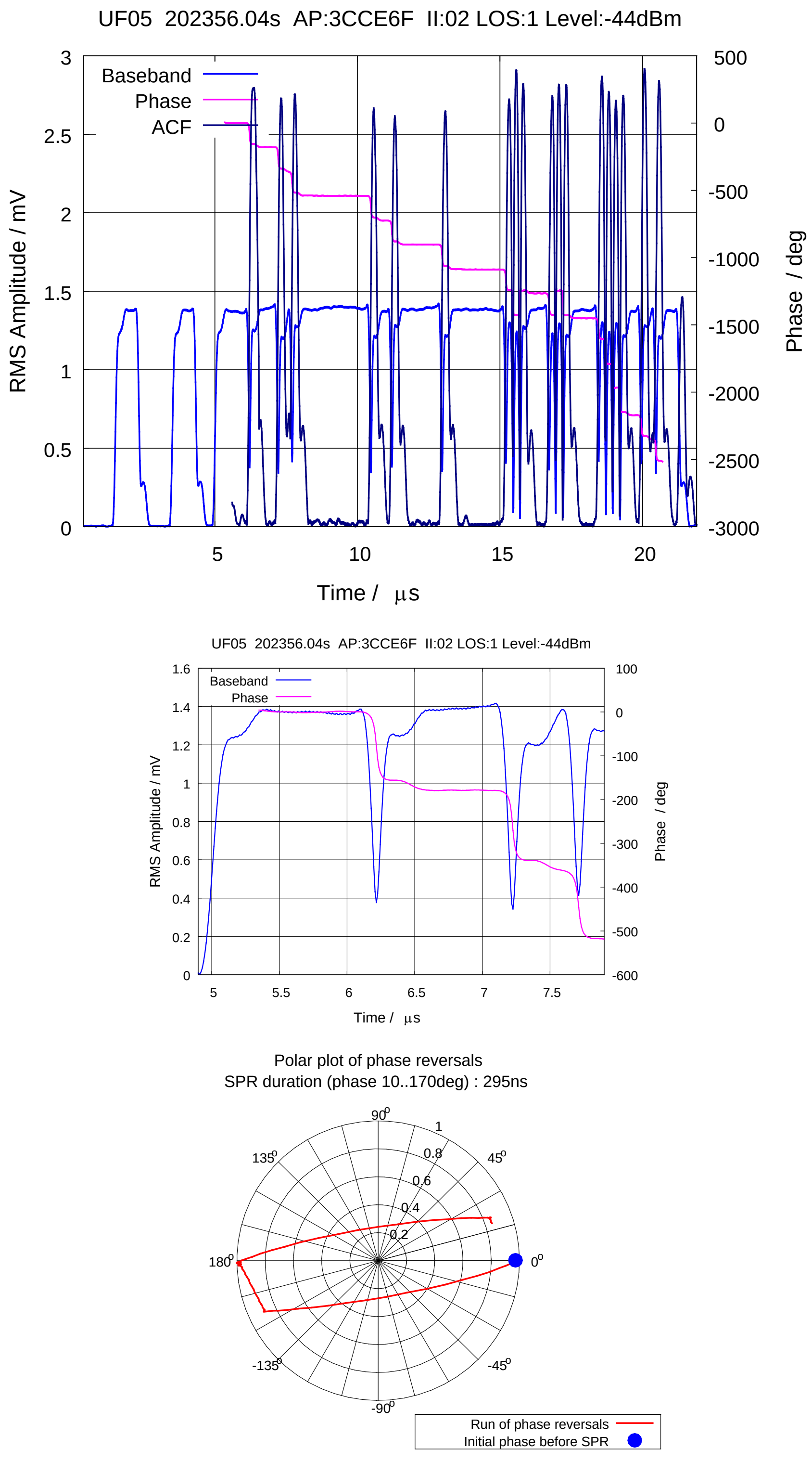

Figure 3-40: Multipath propagation effecting all phase reversals of UF05

Regarding TCAS, an individual curve of the SPR duration distribution is plotted in Figure 3-41. Most of the phase reversals are performed quickly, well below the theoretical limit of 80 ns. This curve cannot be directly compared to those gained from radar interrogators, since a specific source Mode S address is not part of the message in case of UF00 (for more on TCAS refer to section 3.1.4).

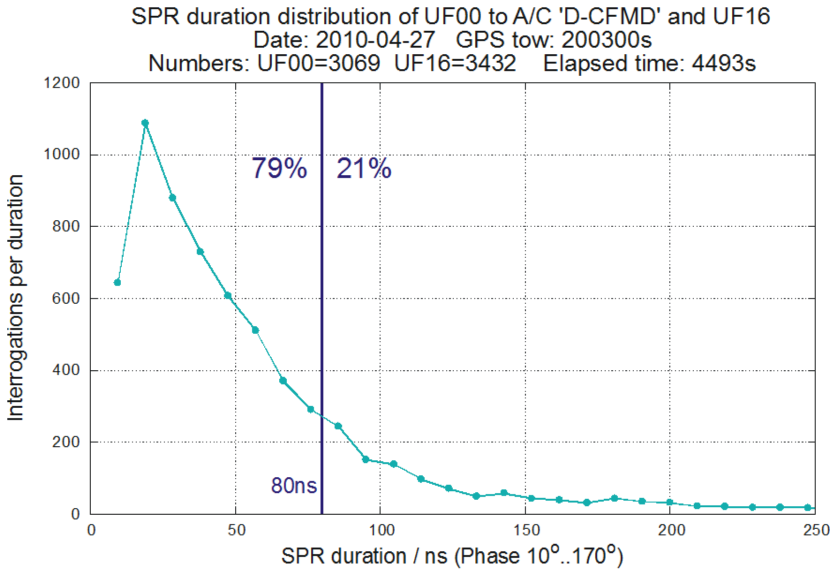

Figure 3-41: TCAS SPR duration

An additional type of statistics is presented in Figure 3-42, showing the percentage of short and long SPR durations. A boundary value for "fast phase reversal" was arbitrarily set to 100 ns so that the slight effect of FIR filter deceleration will be compensated. The bar diagram shows that apart from interrogator II15 the vast majority of phase reversals seems to be quick enough. However, there is a noticeable portion of extremely slow reversals above 250 ns represented by the right sub-bar. Interrogator II15 is assumed to be of military nature, which could even be a mobile type. Its mean phase reversal duration is the longest on that specific measurement flight.

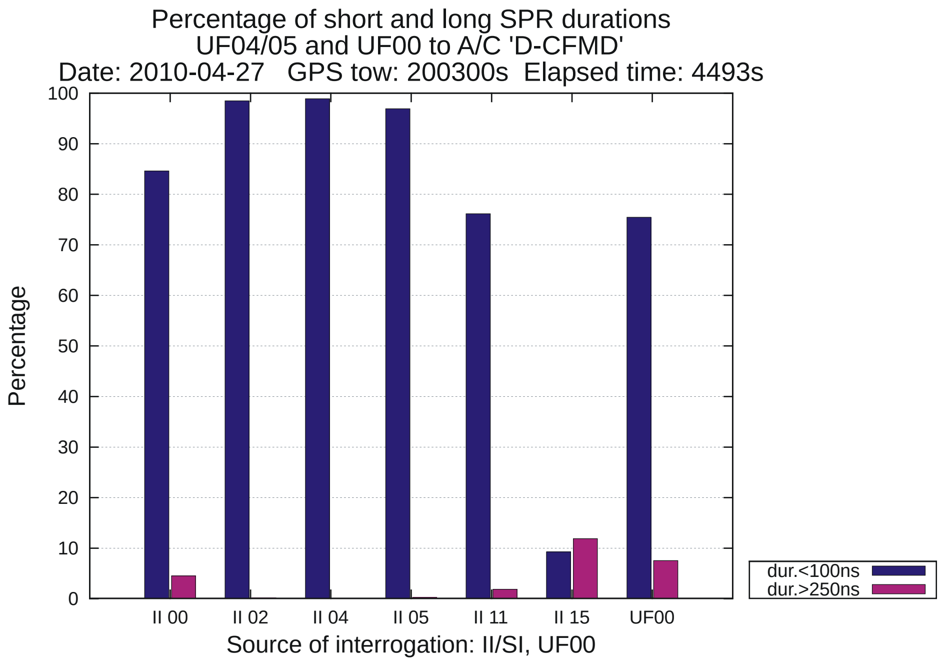

Figure 3-42: Interrogators with slow and fast SPRs observed during Saarbrücken flight

On a ferry flight from Braunschweig to Munich within coverage of mostly German radars (civil and long range military), mostly interrogator types transmitting phase reversal durations slightly above 80 ns are detected, which is shown in Figure 3-43.

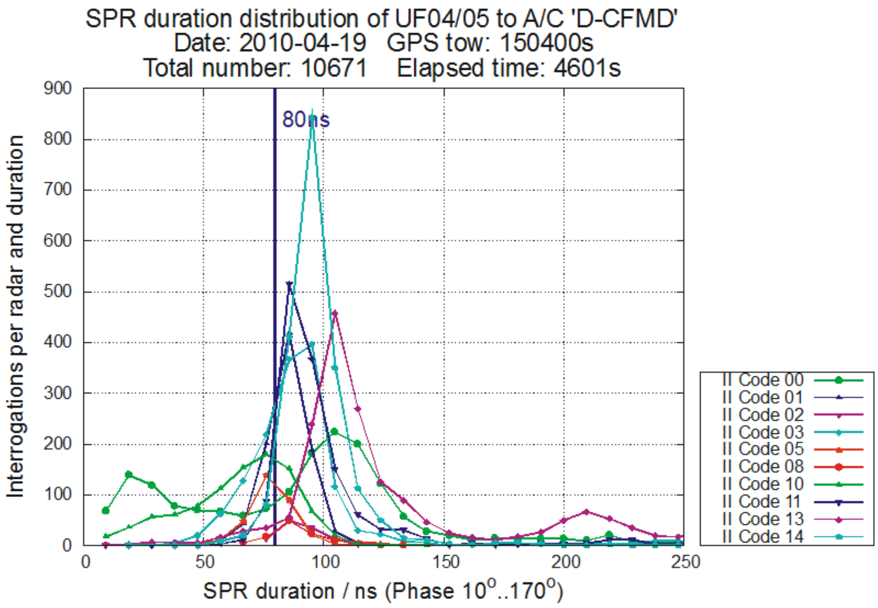

Figure 3-43: SPR duration measured during ferry flight to Munich

Using the 100 ns limit, we observe in the succeeding bar diagram of Figure 3-44 that most interrogations have a quick phase reversal, but there is a substantial portion of extremely slow values transmitted by II13, as already stated in section 3.1.3.4. The distribution of this portion forms a side lobe maximum around 220 ns.

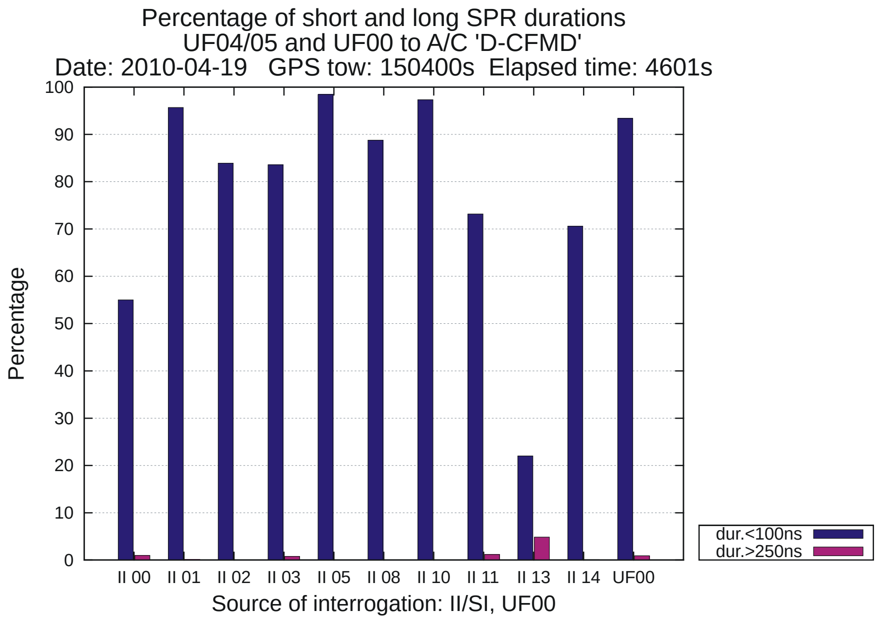

Figure 3-44: Fast and slow SPR durations measured during ferry flight to Munich

Once again, the explanation is given by examining the video plots as in Figure 3-45: Some selective interrogations towards the aircraft were transmitted at the boundary area of the antenna beam, so the P5 SLS takes effect and leaks through P6, which shifts the phase duration to much longer values. The resulting phase reversal is rather a step function than a strict monotonous increase, to be seen in the zoom and the polar plot. Generally, this effect takes place multiple times with certain radars, e.g. at all German II13 interrogators; this effect can be fully reproduced.

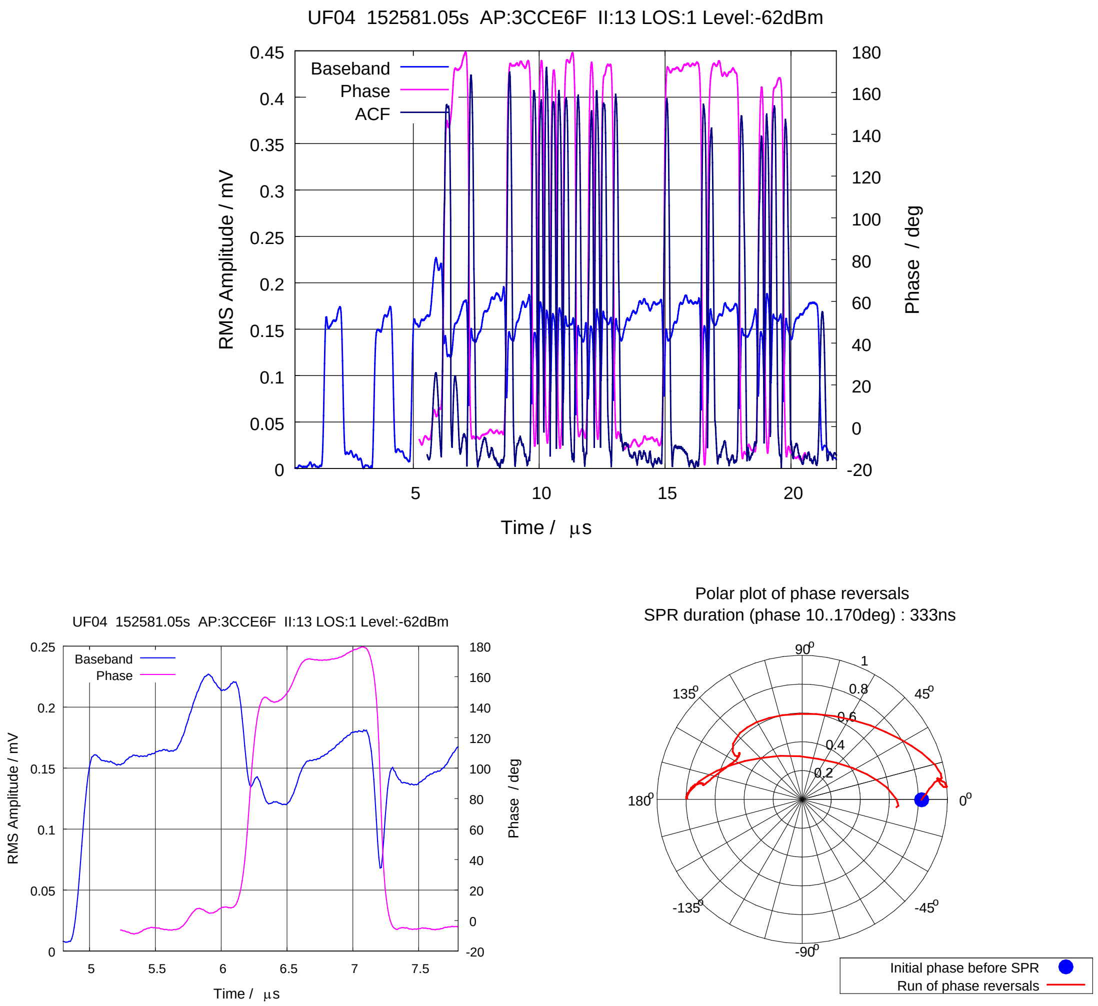

Figure 3-45: Strong P5 leaking through P6 at main beam boundary

A flight inspection of the Munich ILS was taking place a couple of hours later. A flight pattern of the northern runway is shown in Figure 3-46. The amount of time typically used for that kind of inspection is 4.5 hours. It consists of numerous approaches to the runway, so the aircraft is within the range of the airport radars, as well as of the multilateration interrogators.

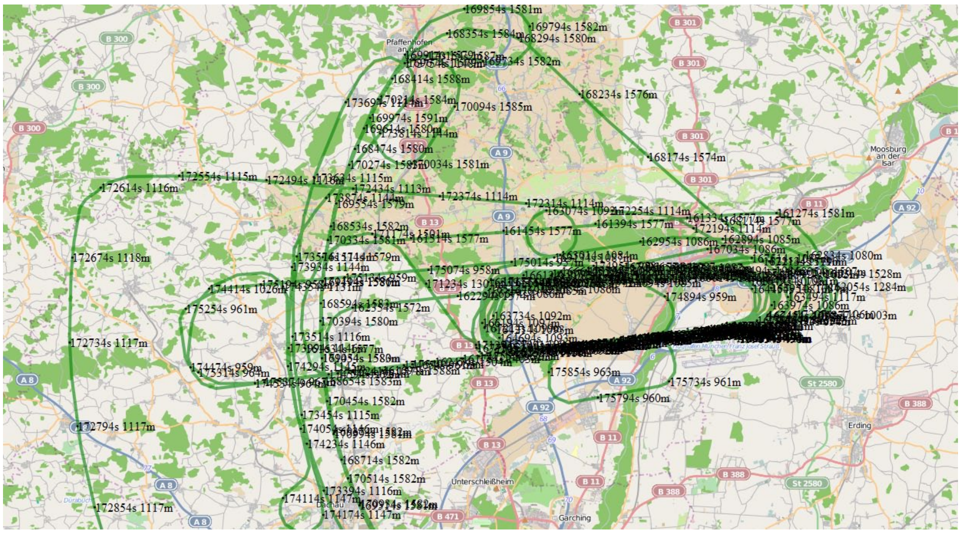

Figure 3-46: ILS flight inspection pattern of Munich airport

It can be seen in Figure 3-47 and Figure 3-48 that II11 and II13 perform as formerly stated. Most interrogations, however, originate from II00. It is known that there is a radar test facility near Munich which normally uses II14, but the received signal levels and interrogator signature reveals that also II00 is partly used by that facility.

As already seen in Figure 3-43 for II13, there is again a secondary maximum in Figure 3-47 at 220 ns for the same interrogator type II00. Another source of II00 is the multilateration interrogator on ground which mainly shows fast SPR transitions in case of multipath-free wave propagation.

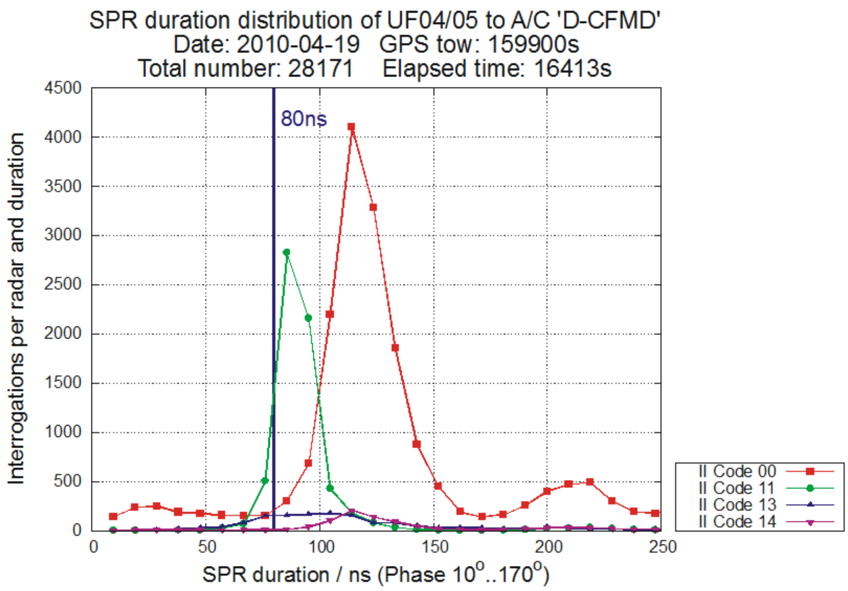

Figure 3-47: SPR duration measured during Munich ILS inspection

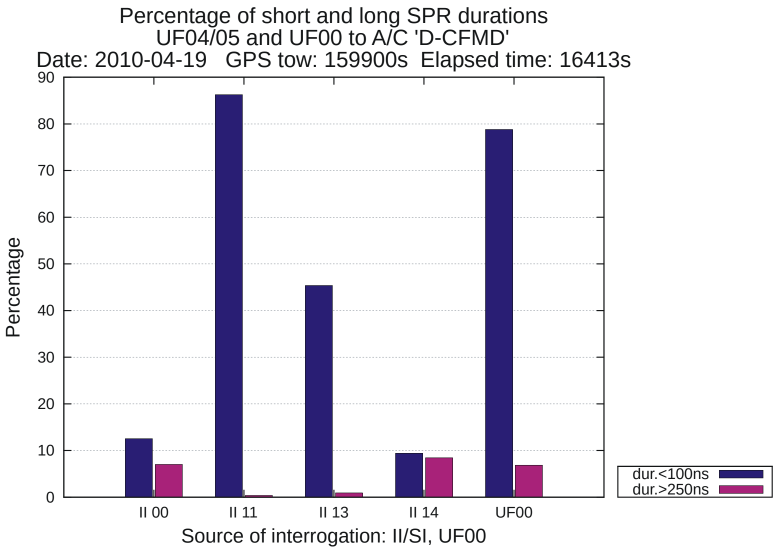

Figure 3-48: Fast and slow SPRs during Munich ILS inspection

The next example was taken from a ferry flight to Frankfurt with subsequent ILS measurements made at night. Again in Figure 3-49, the German clusters II03 and II11 behave the same as seen before, and so does II13 of German Air Force cluster. The high number of interrogations from II14 originates from the DFS Brocken radar (in test mode) on the one hand, and from the DFS Götzenhain test radar, located near Frankfurt, on the other.

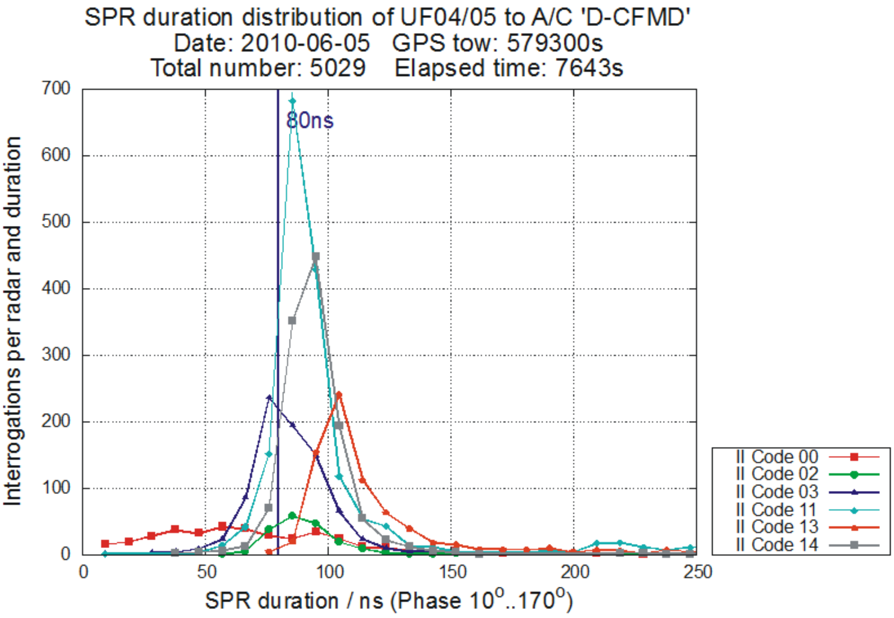

Figure 3-49: SPR durations during ferry flight to Frankfurt and subsequent ILS measurements

Several ILS "glide path level run" measurements in Frankfurt with a flight pattern shown in Figure 3-50 were performed two days later, followed by the return ferry flight Braunschweig. A similar plot of distributed SPR durations is presented in Figure 3-51 (note: the colours of II have changed!), again receiving most interrogations from airport radar II11. Due to the manoeuvres with sharp turns and higher bank angles the radar interrogations are degraded by some multipath propagation, and there were a number of interrogations at higher off-boresight angles having a P5 SLS effect. This explains the increased number of slow phase reversals in the bar diagram Figure 3-52.

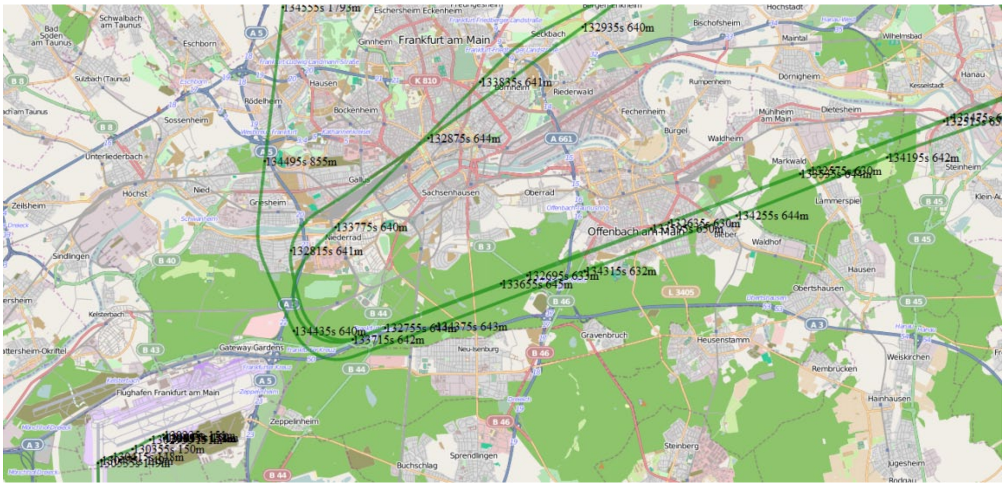

Figure 3-50: Flight pattern of ILS glide path level runs

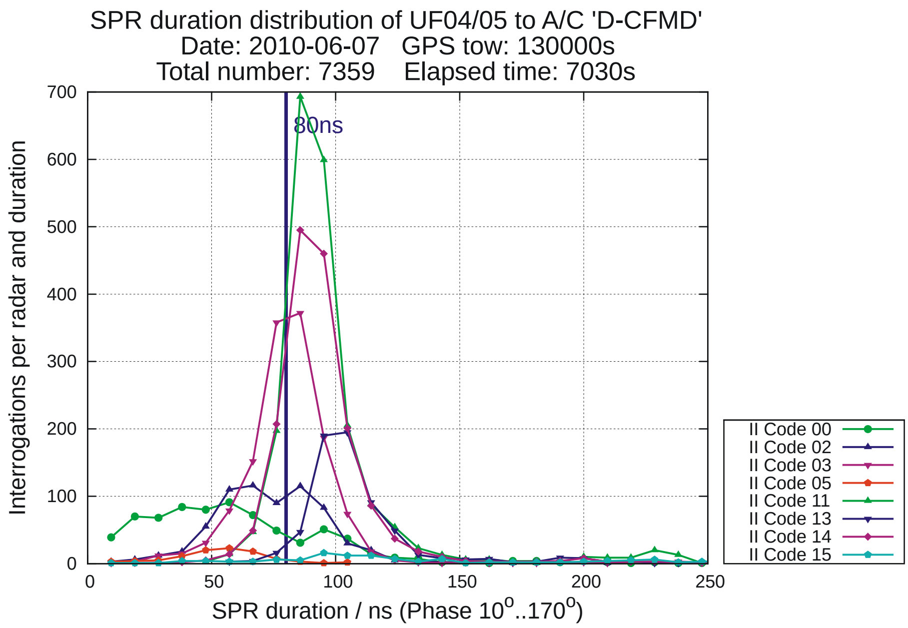

Figure 3-51: SPR durations during Frankfurt ILS measurements and ferry flight to Braunschweig

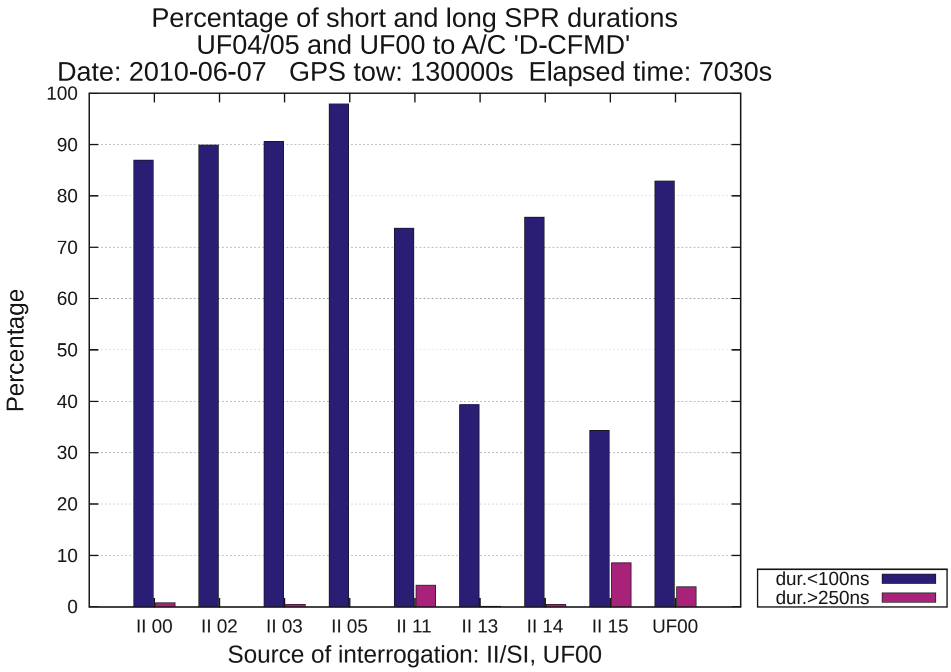

Figure 3-52: Fast and slow SPR duration during Frankfurt ILS measurements

3.1.3.6 Signal-in-space Measurements on a Dedicated Flight to Amsterdam

The dedicated flight to Amsterdam EHAM runway 22 using the small experimental *Cessna 172* "D-EMWF" aircraft (Mode S address: 0x3D2699) was performed mainly at 3000 ft altitude and below on May 28th 2010. In Figure 3-53 the aircraft is shown with a zoom of the lower fuselage section where a spare L-band antenna was mounted which fed into the measurement system.

Figure 3-53: Cessna 172 with spare L-band antenna

The aircraft was mostly interrogated by TCAS devices as shown in the UF00 bars of Figure 3-54. Aircraft equipped with TCAS fly at higher altitudes, so the aircraft antenna mounted at the bottom of the fuselage has lobes pointing to lower elevation angles. A statistical analysis on that issue is given in section 3.6 using the radar data kindly supplied by Luchtverkeersleiding Nederland (LVNL).

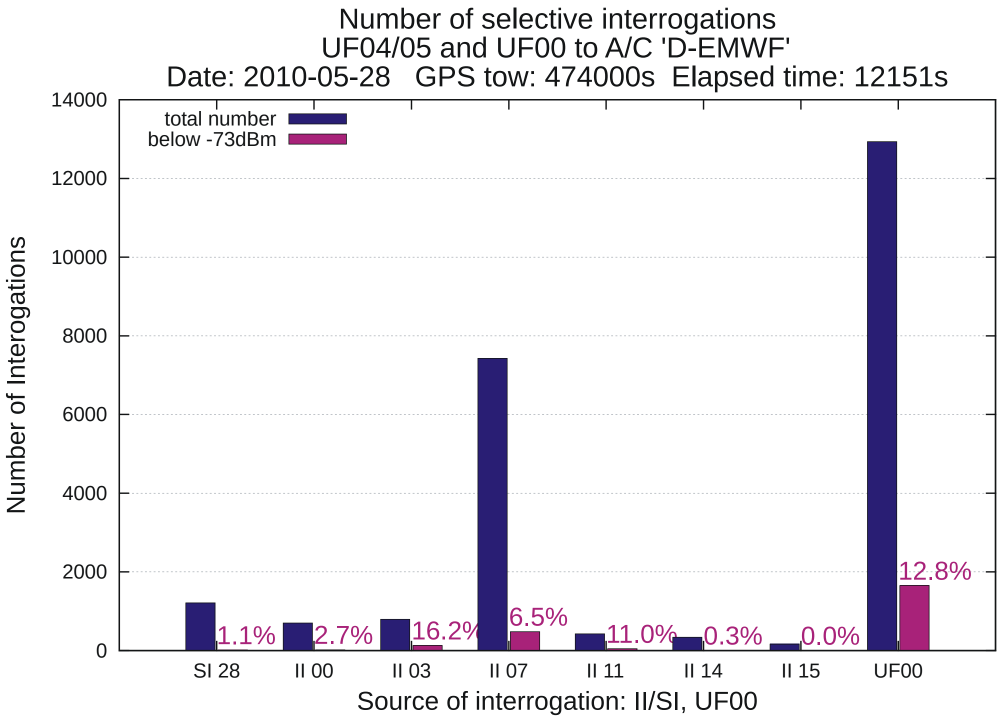

Figure 3-54: Enumeration of all selective interrogations and codes

In the Netherlands, a nationwide clustered network of II code 07 is used, and an additional Airport Surveillance Radar (ASR) using SI28 is operating at Amsterdam airport. This fact is reflected in the high total number of interrogations in the figure.

Most interrogations show fast phase reversals as shown in Figure 3-55, except for the already mentioned military interrogators II15 and some of the II00 interrogators, which can be subdivided into multilateration devices and an unknown radar source.

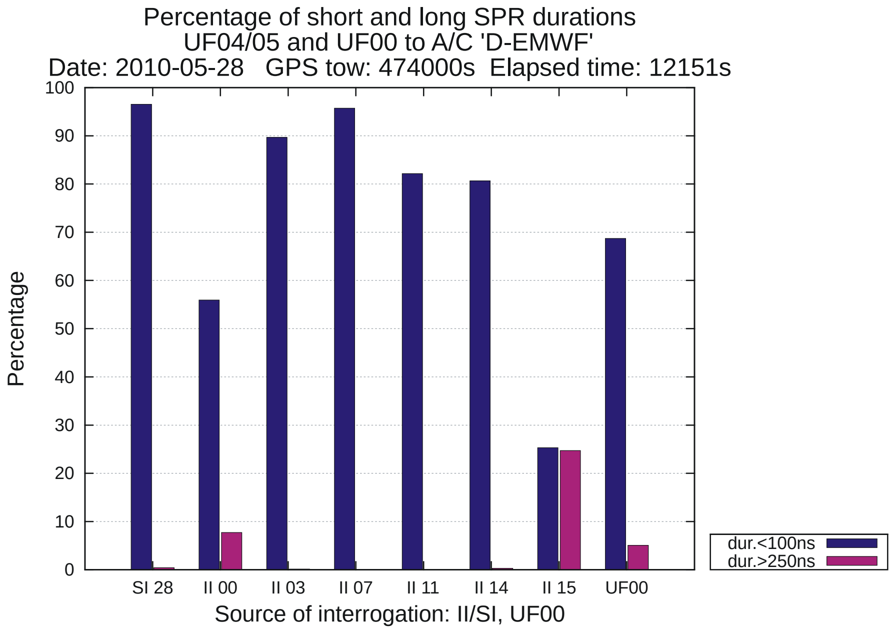

Figure 3-55: Fast and slow SPRs during Amsterdam flight

The approach to Amsterdam runway 22 was carried out above the *Markermeer* as shown in the map Figure 3-56 at low altitude (see labels in map).

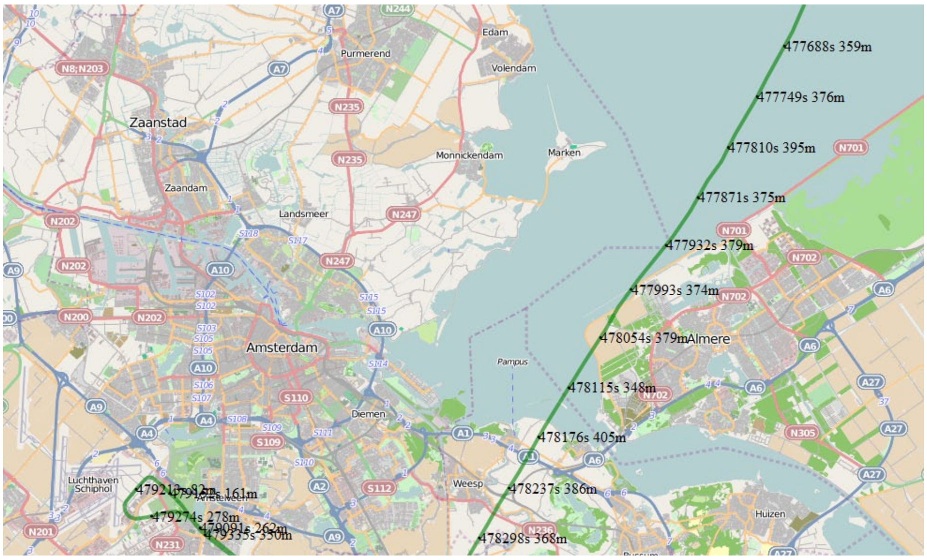

Figure 3-56: Approach to EHAM RWY22 across the Markermeer

In the following plots the effect of a conducting sea surface can be observed. Observing the radar interrogations II00 as in Figure 3-57, we notice some reflections following P1 and P2 of the uplink telegram, which also affect the data pulse P6.

Additionally, the SPR is heavily distorted by the P5 SLS leaking through. As a result, a significant deceleration of the SPR speed is computed and shown in the zoomed video plot and the polar plot.

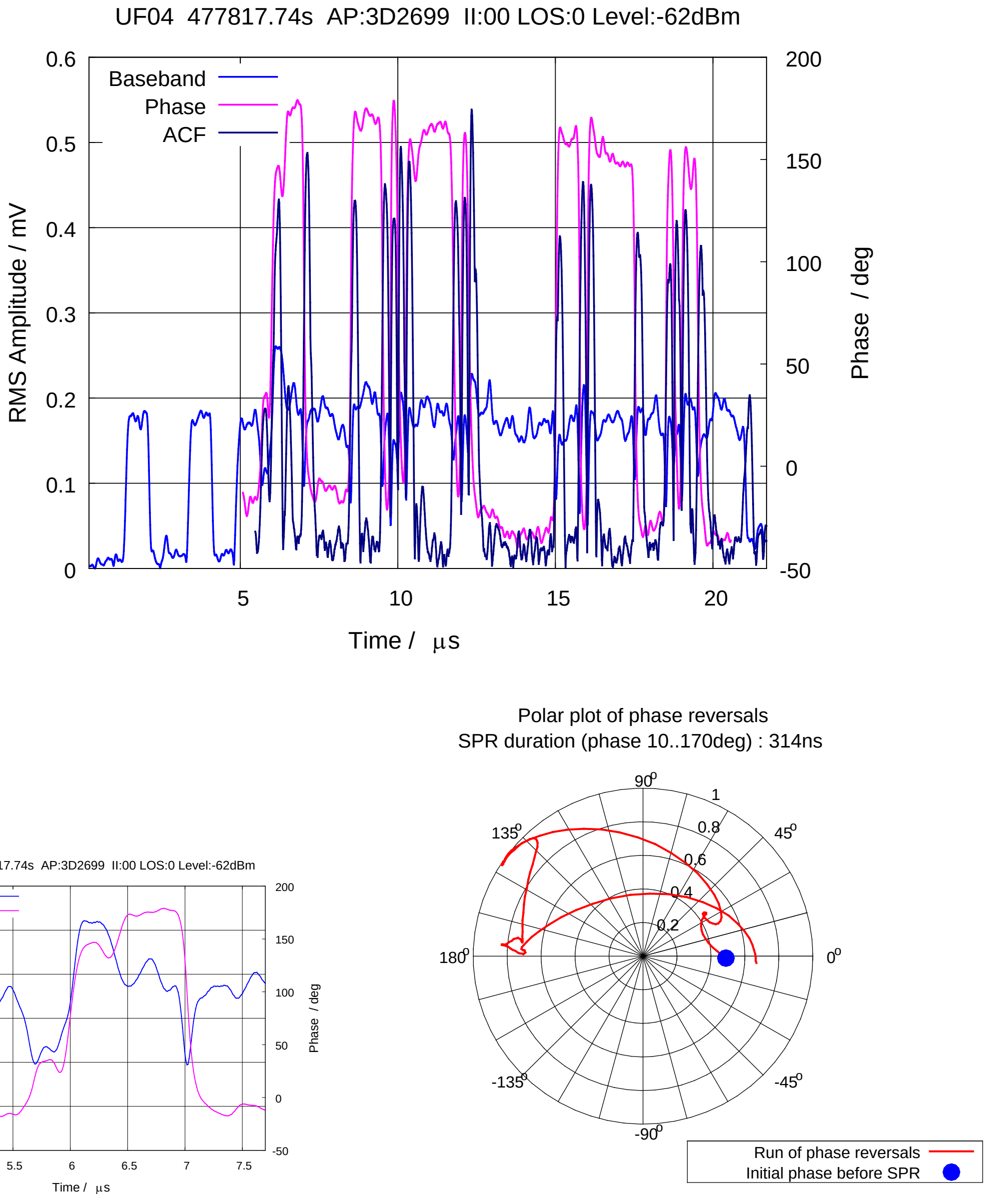

Figure 3-57: SLS and multipath propagation affect SPR of radar II00

In the vicinity of the airport the aircraft is interrogated by the multilateration (MLAT) system starting from GPS time 479000 s (see time labels in Figure 3-56). Due to different phase signatures of interrogators having II00, its source can be clearly distinguished. The MLAT system applies a phase decrease to one direction as the phase curve reveals in Figure 3-58, in contrast to the radar interrogator II00 as seen before. Generally, there is no side lobe suppression used with the non-rotating MLAT antennas, since their pattern is either omni-directional or wide aperture. Compared to directional radar antennas the MLAT radiation is more susceptible to multipath propagation of signals due to reflectors on the ground, which can be seen in the video plot. The zoomed run of the phase curve shows a delayed SPR. In the polar plot it can be observed that the multipath interference ties the phase at around -160° before letting it advance to -180°.

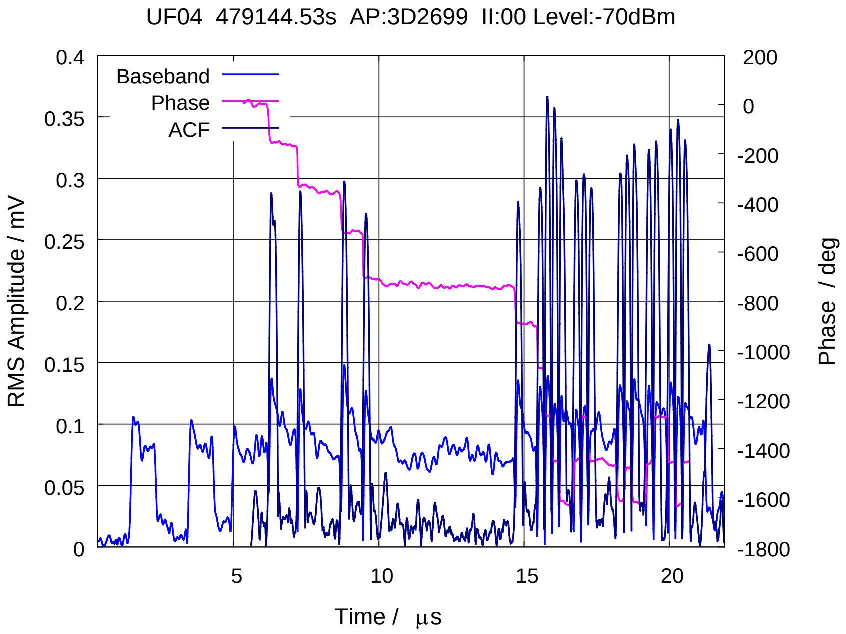

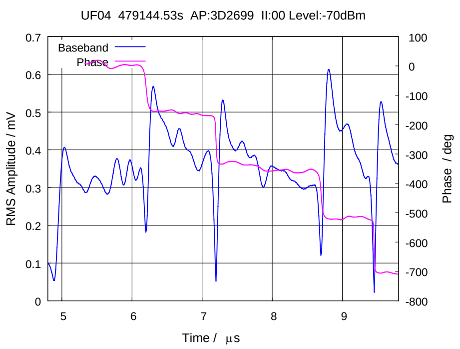

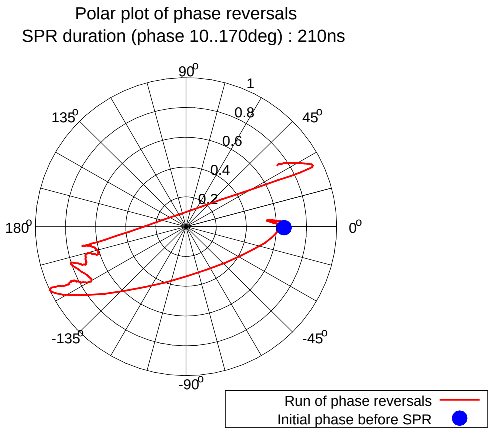

Figure 3-58: Multipath propagation affects SPR of MLAT interrogator I100

As stated before, the flight altitude to Amsterdam was mostly below 3000 ft with large segments between 1000 ft and 1500 ft (see Figure 3-112 for an altitude profile of that flight). The signal strength decreases dramatically if the low-elevation border of the vertical radar antenna pattern becomes effective because the antenna gain is low.

The analysis software performs a time-stamped demodulation of each Mode S uplink telegram it can decode. It is therefore possible to investigate re-interrogations within one radar sweep. If a bit-identical content telegram is transmitted within a few milliseconds, it is very likely that the radar did not get a reply at the first attempt and then retries to get one. This in turn means that either the transponder did not accept the interrogation or the radar did not decode the reply. In a certain area of the flight close to the sea, as depicted by the flight path in Figure 3-59, such repeated interrogations occurred very frequently.

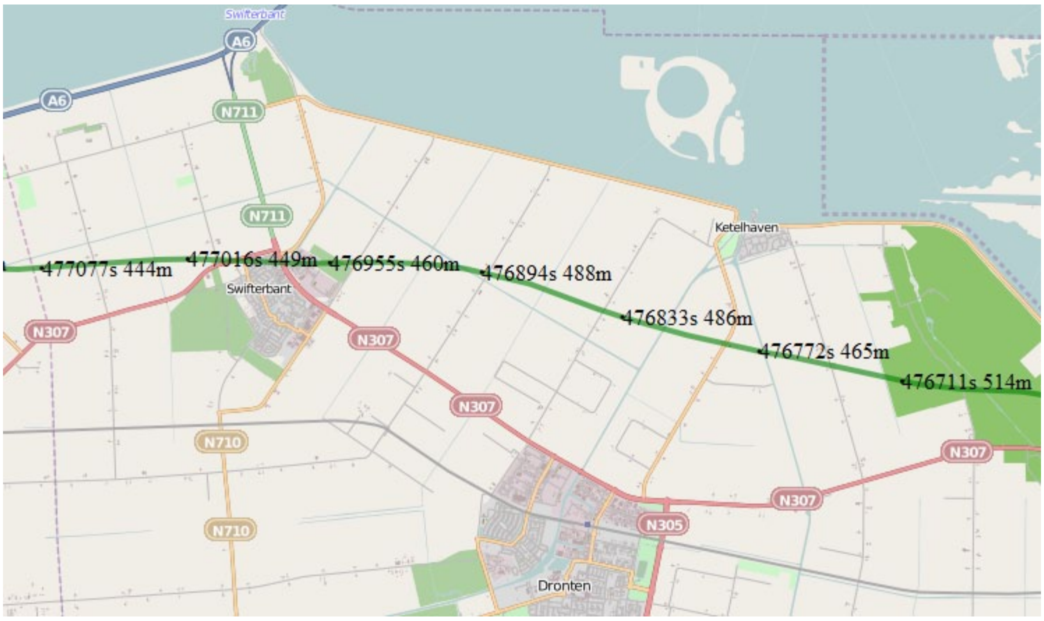

Figure 3-59: Area of frequent re-interrogations of radar II07

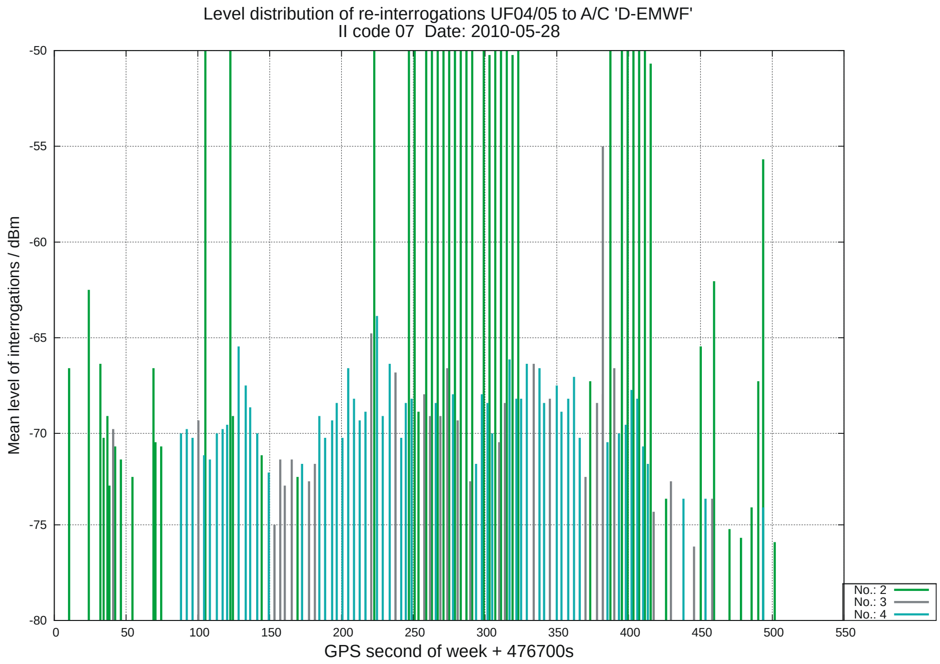

Figure 3-60: Level distribution and times of re-interrogations

It is interesting to note that many re-interrogations (three or more) take place when the signal strength is close to the transponder MTL of -73 dBm or even lower. Therefore, it is likely that the aircraft transponder refused to accept the interrogation due to weak signal levels. A more detailed analysis would require action on the radar site in order to evaluate if certain Mode S interrogations were not replied to by the transponder.

A detailed analysis of the Amsterdam Schiphol ASR “TAR1” (surveillance identifier SI28) interrogations in combination with corresponding ASTERIX radar data is presented in section 3.6.3.

3.1.4 TCAS Signal-in-space

Generally, most incoming Mode S interrogations are of the TCAS type as shown in the statistical plots above. It is therefore important to know the quality range of these signals, since they are directly used to avoid mid-air collisions, independently from any Air Traffic Control or radar intervention.

As shown before, the duration of the SPR is good indicator for the quality of Mode S uplink telegrams. The majority of interrogations seem to be of good quality, judged by plotting a statistic lasting for a few hours. In Figure 3-61 it can be seen that 91% of SPR durations are faster than 80 ns. Only those telegrams were used which either selectively address our aircraft or are UF16 broadcast having all bits set in the AP field, this ensuring the exclusion of errors. A further example is given by the following graph in Figure 3-62. It shows a curve resulting in a similar SPR duration distribution.

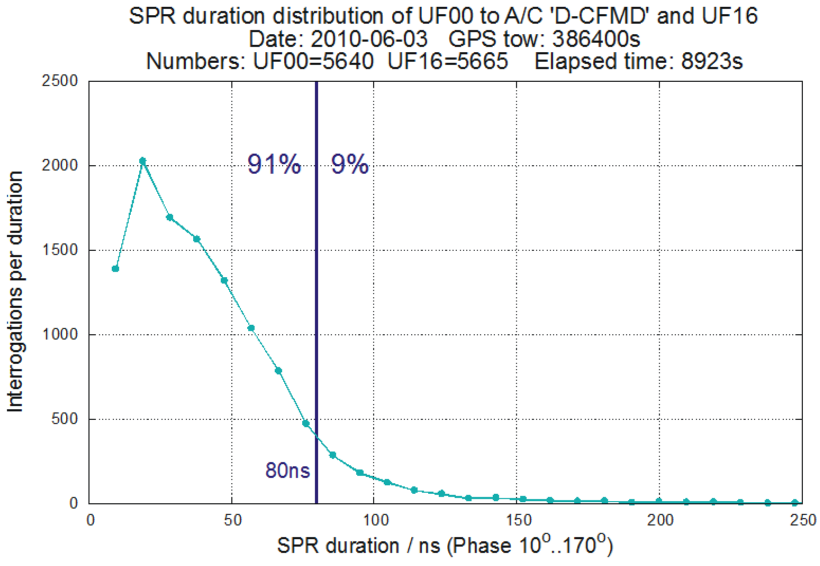

Figure 3-61: TCAS SPR duration during VOR flight inspection flying orbits

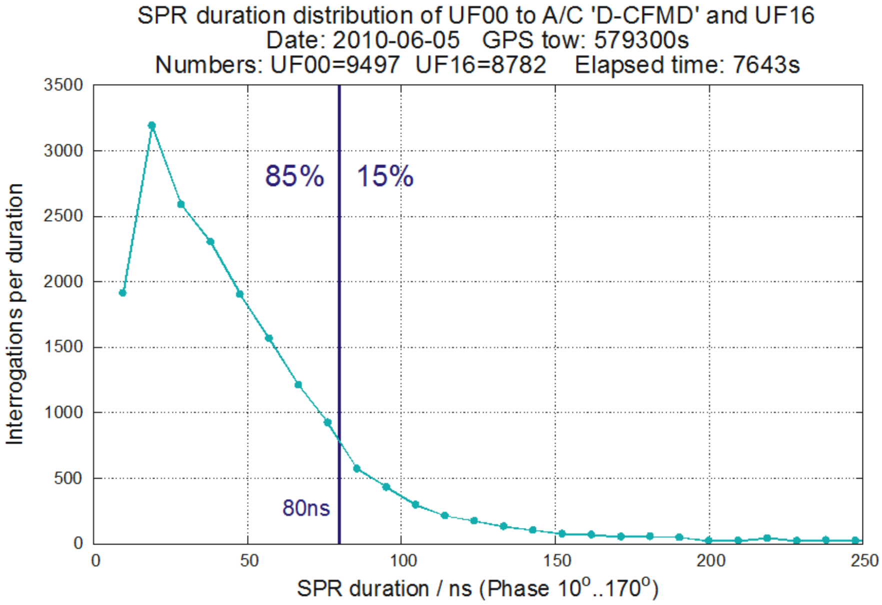

Figure 3-62: TCAS SPR durations on ferry flight to Frankfurt and ILS coverage measurements

Generally, these UF00 distributions are assembled from all different types of airborne TCAS interrogators which are receivable during flight time. So this figure is not associated with a specific TCAS device, but expresses the general frequency of occurrence gained from some flight hours.

Most TCAS interrogations apply a quick phase reversal mechanism, either a simple phase switch or a fast I/Q modulator, refer also to section 3.1.2.4.

In Figure 3-63 an TCAS I/Q modulator with fast switching phase characteristic is shown. Both the amplitude and the phase are stable over the telegram duration.

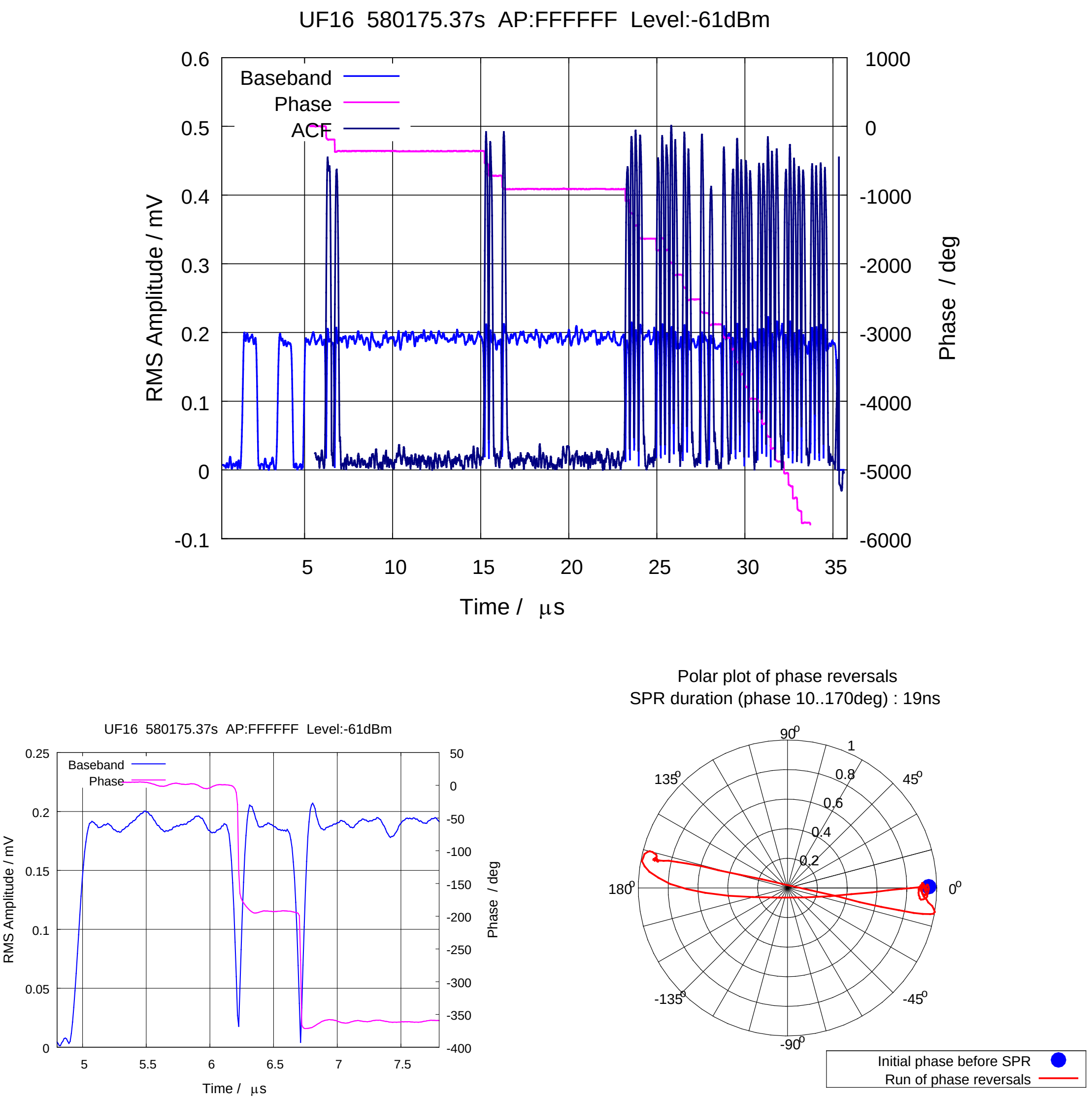

Figure 3-63: Good quality UF16 broadcast with negative phase advance

However, some signal anomalies of TCAS devices were detected. These transmissions would probably not have been accepted by any transponder, since the DPSK demodulation devices working in real time are assumed to be less sophisticated than the post-processing measurement system implemented for this study.

A very impressive example of a probably unreadable interrogation is shown in Figure 3-64. Regarding the ACF curve we notice a monotonous phase advance throughout

P6, but the zoom of the first SPR region including the first format data bit reveals a double 90°-step function instead of a 180° per each phase reversal. Moreover, the time consumption is nearly a full data chip length. Within the polar plot both phase reversals together nearly form a square function. These four phase conditions resemble a 4-PSK rather than a 2-PSK modulation.

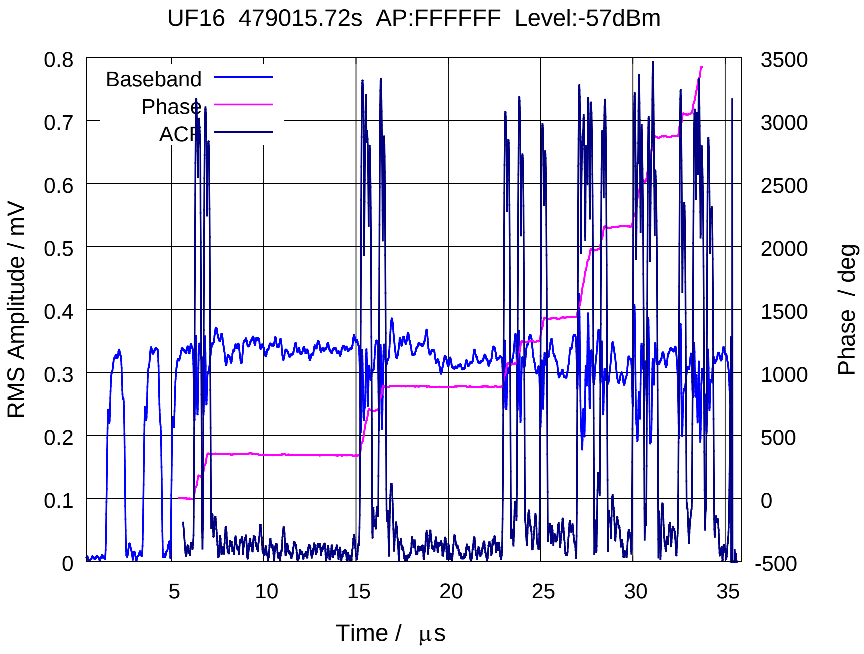

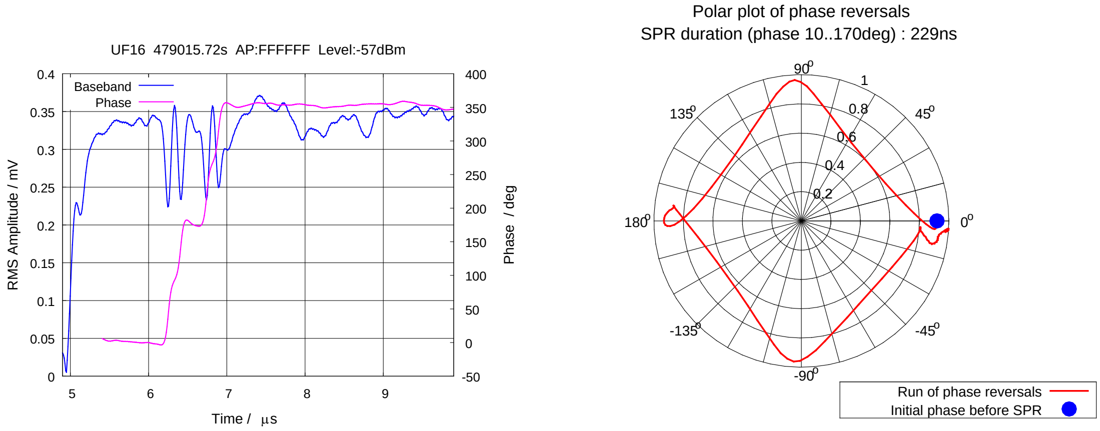

Figure 3-64: Poor quality UF16 broadcast having nearly 4-PSK characteristics

Some sporadic TCAS modulators definitely have problems to fulfil a 180° phase step. In Figure 3-65 the graph shows the baseband and the phase around the SPR and the first format bit of an UF16 broadcast. The modulator is of an RF switching type, probably using a delay line to cause the phase difference. It can be easily observed that the phase hardly reaches 150°, which leads to the assumption that the delay line might be too short.

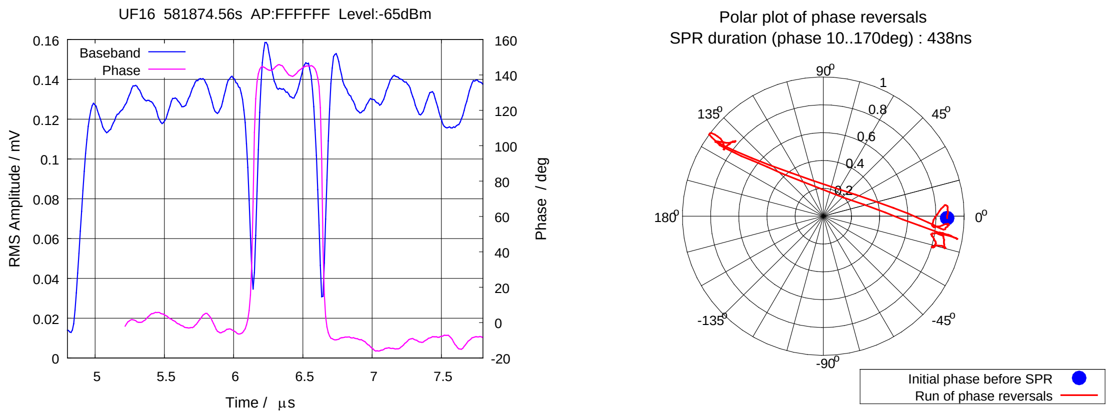

Figure 3-65: UF16 broadcast performing phase steps of only 150°

There are no clean 180° phase conditions transmitted from an TCAS shown in the next example in Figure 3-66. The phase spends only one discrete moment (9.5 ns) in-between the SPR and the next phase condition which is the first format data bit.

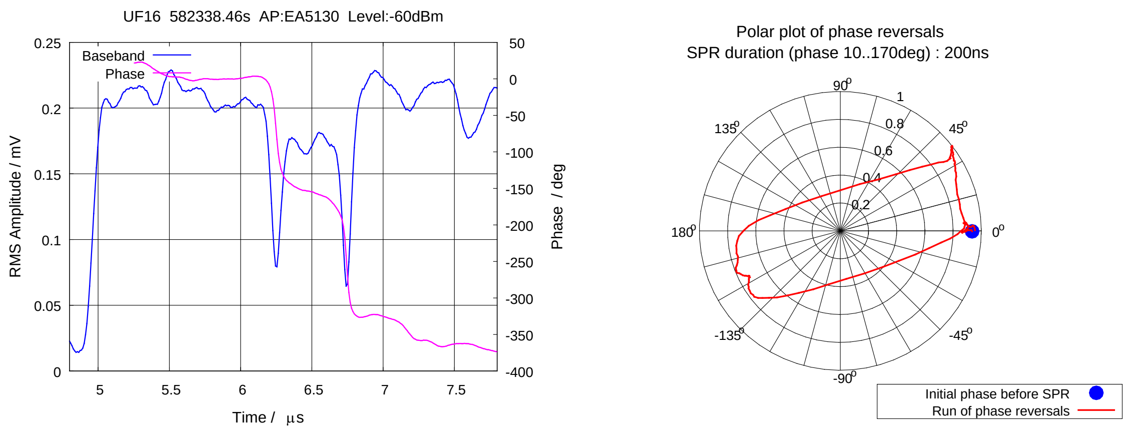

Figure 3-66: UF16 having poor phase conditions

Another phase step function of an UF00 is given by Figure 3-67. The phase climbs up to 140° and remains there for nearly 500 ns, then advancing to the final 180°. If two consecutive "1"-bits of this quality occur within the telegram then the decoding process is very likely to fail.

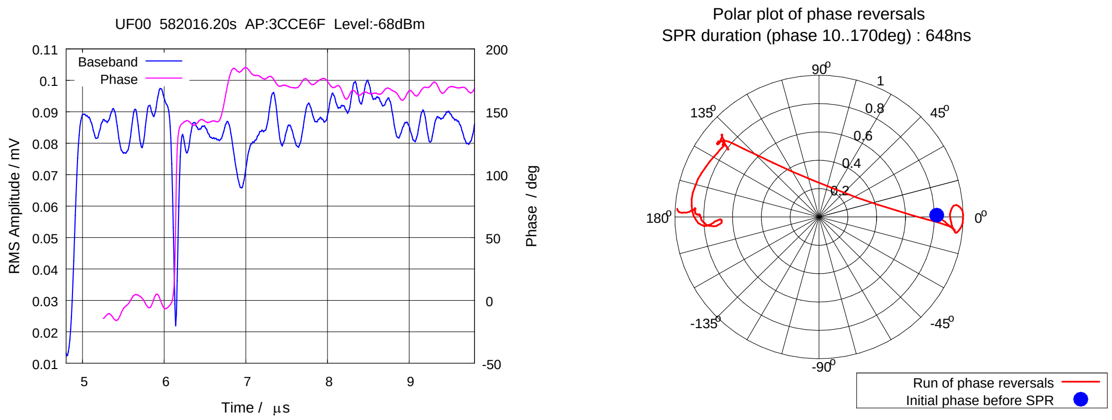

Figure 3-67: UF00 performing two phase steps to reach 180°

Apart from insufficient phase advances from one chip to another, some devices have poor amplitude stability throughout the telegram runtime. This is revealed in particular in the long 112 bit telegram UF16. In Figure 3-68 we observe an TCAS broadcast having more than 6 dB of amplitude modulation starting from the SPR on. It is probably a weak power amplifier or power supply leading to such effects.

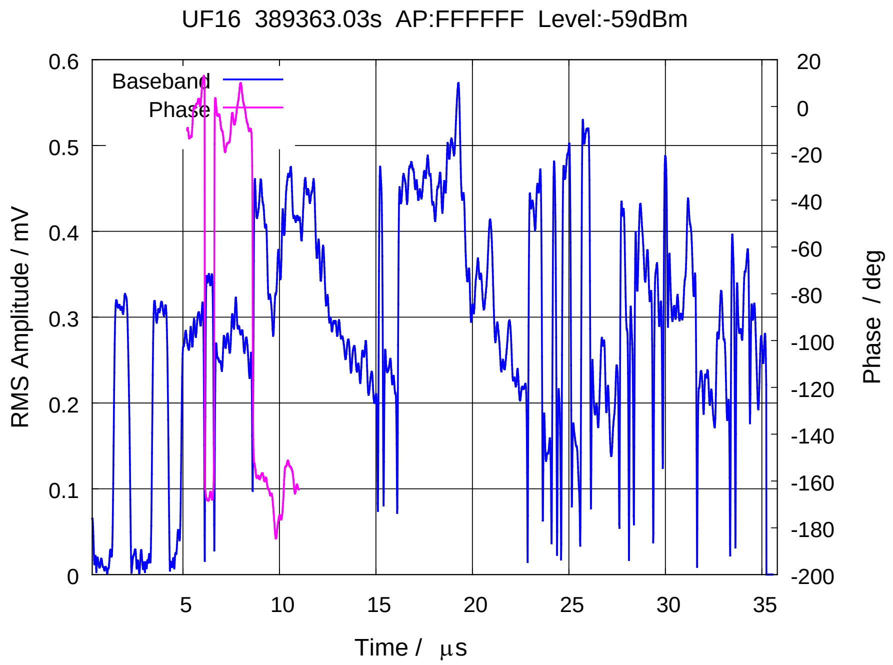

Figure 3-68: TCAS having power stability problems

Apart from power problems also the transmitted carrier frequency may differ from the requirements. In Figure 3-69 a mean negative phase amount of 350° can be observed during the run of P6. Since the frequency deviation depends on the phase this can be calculated as:

$$\Delta f = \frac{1}{2\pi}\frac{\partial\varphi}{\partial t} = \frac{1}{360°}\frac{-350°}{14\mu s} = -70\,\mathrm{kHz}$$

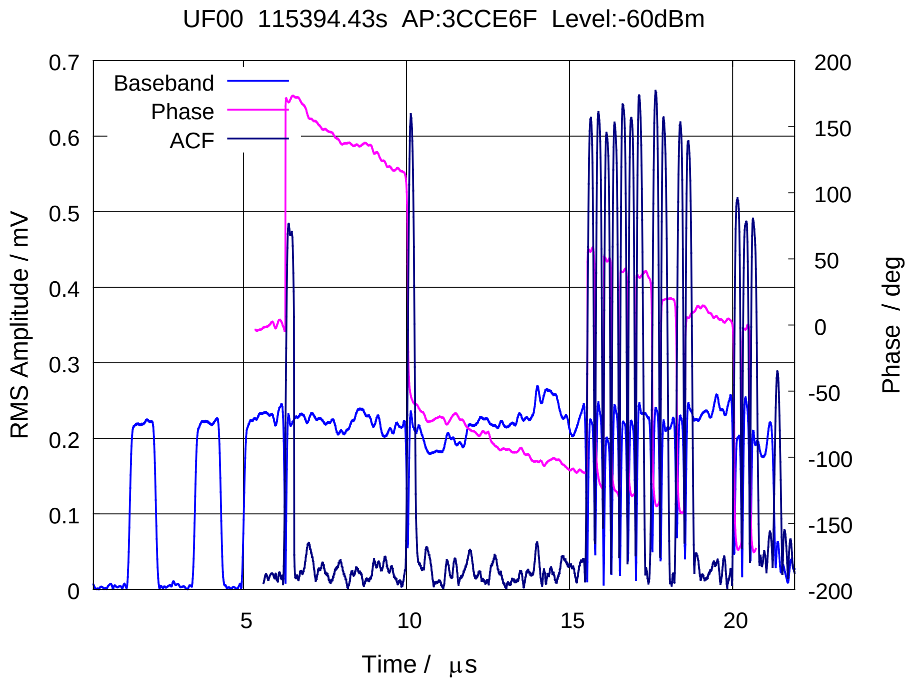

Figure 3-69: TCAS having carrier frequency far below 1030 MHz

During the raw data evaluation many aircraft were detected transmitting TCAS signals of poor quality. In many cases, the measurement system in combination with the fault-tolerant software could successfully decode the Mode S address of the respective aircraft. These are traceable only if the parity check sequence of a UF16-32 (TCAS broadcast) has all one-bits, then depicting the “Announced Address” correctly. A list of non-complying aircraft that does not claim to be complete was provided to EASA.

3.1.5 Summary of Findings

The selective Mode S calls to the aircraft received from MSSR interrogators were mostly stable, clean and only disturbed within the SPR signal area by the leaking effect of the SLS pulse P5, as shown in various subsections of 3.1.3. This effect strongly depends on the interrogator type. It potentially boosts the required SPR duration to more than a chip length which may then be far beyond the ICAO 80 ns requirement for the transition from 10° to 170°.

However, as revealed by the analysis of various radar sweeps covering several interrogators (section 3.1.3.4), the installed transponders of “D-CFMD” and “D-EMWF” aircraft correctly detected the vast majority of MSSR interrogations. That section also presents a more detailed beam sweep analysis to derive the power distribution and moments of selective and all-call interrogations, which also allowed determining the 3 dB beam width.

No selective interrogations at levels less than -6 dB below boresight maximum strength were found in signals from II01 (Figure 3-20), II10 (Figure 3-22) which perform a repetitive double interrogation within one sweep, this also being the case for II02 as shown in Figure 3-34. Radars II03 and II11 (German Clusters) start their first interrogation earlier in the beam dwell (Figure 3-32) at -12 dB so there is a stronger leakage of P5 through P6 (Figure 3-33), resulting in a prolonged SPR phase transition. II13 (German Air Force Cluster) is similar but has an additional power reduction feature (Figure 3-24). All radars within coverage of the performed flights radiate P5 also for selective calls UF04/05, which is not required but permitted according to ICAO Annex 10 (3.1.2.1.5.2.1 Note 2).

In order to reconstruct the signal-in-space SPR duration more accurately, it was necessary to use time-optimized instead of noise-optimised baseband FIR filters as explained in section 3.1.3.5. Figure 3-36 depicts that the achieved results are only slightly above the given simulated filter inputs. It was shown in the figures showing the “SPR duration distribution” (e.g. Figure 3-37, Figure 3-43, Figure 3-47) that there are significant differences in the SPR duration of various interrogators.

Problems with radars were found resulting in numerous re-interrogations from II07 (Figure 3-60) during the Amsterdam flight of “D-EMWF”, described in section 3.1.3.6. In specific regions the SSR channels are multipath-affected due to reflections from the sea surface or due to partially shadowed line-of-sight at lower flight altitudes.

In contrast to MSSR rotating interrogators, the facilities of a MLAT system have fixed antennas and inherently need no SLS mechanism. However, due to their nature of a wide aperture radiation, they are more susceptible to multipath propagation, since potential scatterers receive intensified signal portions. Hence, there is a high risk and likelihood that not only the SLS is affected but that all data phase reversals within P6 will also be interfered with. One example among the numerous found is given in Figure 3-58.

Obstacles from the ground represent the major source of multipath interference by far. Since TCAS is used to avoid mid-air collisions, the air-to-air interrogations UF00 remain multipath-free in the relevant airspace. Most TCAS devices were found to generate fast SPRs (see video example in Figure 3-5, statistics in Figure 3-61, Figure 3-62) which should be clearly detected by all transponders. However, there were numerous aircraft identified showing poor phase reversals, or weak phase and power stability of P1/P1/P6 as shown in the examples in section 3.1.4. These problems may be due to poor design of affected TCAS units or caused by defective hardware.

3.2 Communication Interference

The TU BS Mode S monitor network consists of 5 stations, each housing a 1030 MHz uplink receiver and a 1090 MHz downlink receiver. The locations of these stations are: Braunschweig NW, Braunschweig SE, Frankfurt, Oberpfaffenhofen, and Stuttgart. These stations are totally passive, i.e. they are only listening into communications on the Mode S channels. Received communications include Mode S radar interrogations and replies, TCAS-communications and Mode S squitters.

The stations transmit all received Mode S signals encrypted via the Internet to the TU Braunschweig monitoring facility. For the MOSTDONT project the stations had been reconfigured to also transmit radar interrogations which were discarded before. Therefore, the network link capacities, the computation power, the storage in Braunschweig and networking software had to be reviewed and extended.

An experimental software tool was made available by TU BS to accommodate analysis of Mode S radar communications. The core of the software is formed by a constantly updated model of the traffic situation. This model is derived from squitters and TCAS-communications. All received messages are CRC-checked and repeatedly received 3 times before being taken into account. Besides other information, the model contains the address and altitude of every Mode S aircraft within range and the positions of ADS-B equipped aircraft.

In relation to that model, multiple specialized analyses can be performed. One of the questions investigated was which radar station is received by the network under which circumstances. Therefore, all UF04, UF05, UF20, and UF21 radar interrogations were analysed. For every interrogation the requested aircraft address was checked. Additionally, the ADS-B position and the altitude of the aircraft were plotted on a map.

The analysis software generates interactive maps as html files, which can be viewed, zoomed and parameterized using a web browser. This document provides only screen-shots of these maps.

Initially, the following assumptions were made:

1) A receiver station is only able to receive a radar interrogation when the radar is aiming towards the monitor station. Mode S radars should only interrogate an aircraft when its antenna is pointing towards that aircraft. Therefore, the monitor station and the aircraft have to be in the radar beam at the same time – radar, monitor station and aircraft thus have to be on a straight line.
2) Since the receiver station and the radar are on ground, a receiver can only see radars relatively close by due to the spherical shape of the earth.

The results, however, were not quite as expected, i.e. the monitoring receivers were able to sometimes decode interrogations even when the radar was not pointing at the receiver. Apparently, the receivers, although respecting side lobe suppression, received stray interrogations outside the main radar beam dwell.

3.2.1 Received Interrogations and Aircraft Altitudes

This chapter presents an overview of the ground recordings. It shows the received radar interrogations corresponding to altitude bands. The monitor network is constantly collecting and storing all received Mode S signals. Arbitrarily, the data of March 10th, 2010 was chosen to base the following analysis on.

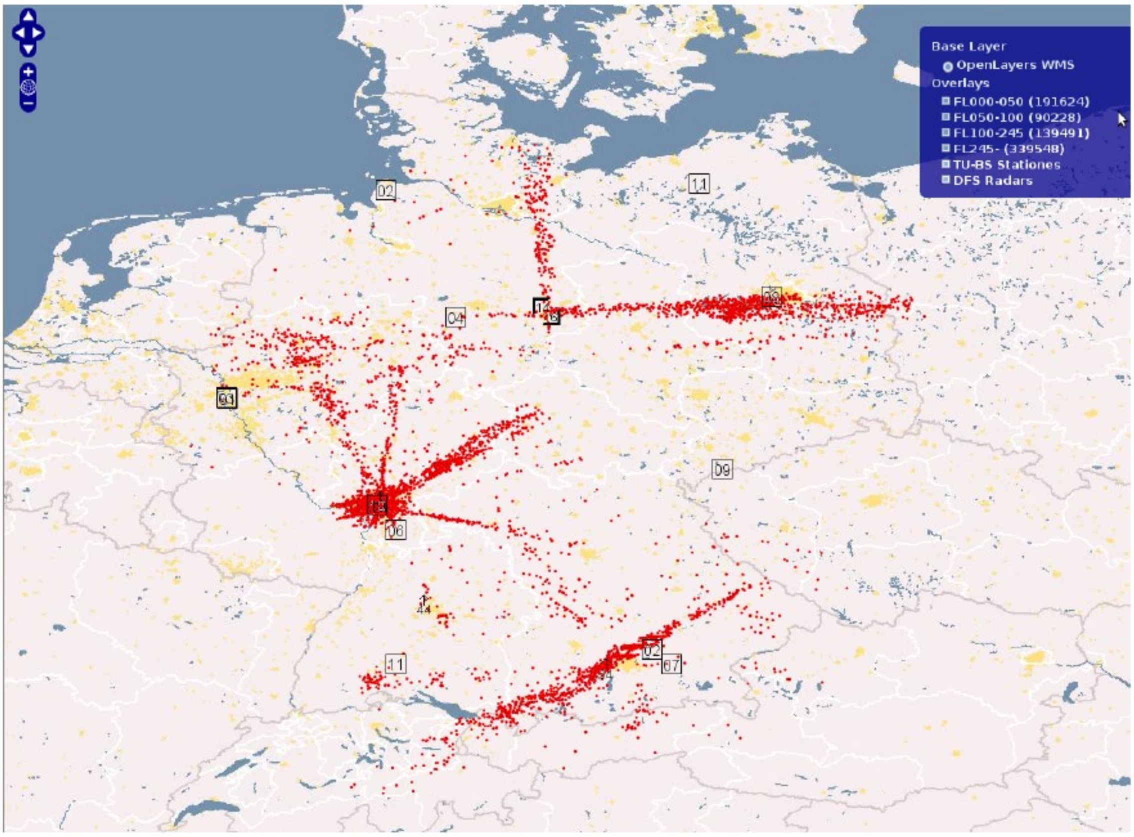

Figure 3-70: Positions of interrogated Aircraft in all altitudes

In every map the radar stations are marked with larger squares in grey, compare above Figure 3-70. Each square contains the radars II code (some of these II codes are out-dated, however). Besides the radars, the map shows the TU BS receiver stations with their System Identification Codes (SIC). The stations in Braunschweig are labelled 14 and 16, Frankfurt uses 24 (hidden behind the radar label 12), Oberpfaffenhofen 34, and Stuttgart 44.

Figure 3-70 also shows the positions of interrogated aircraft for all controlled traffic as red dots. During the whole day approximately 650,000 interrogations of ADS-B equipped aircraft within range were detected. The picture shows 4,000 interrogations randomly chosen from the whole day. Figure 3-71 to Figure 3-74 depict the positions of aircraft being interrogated per altitude band.

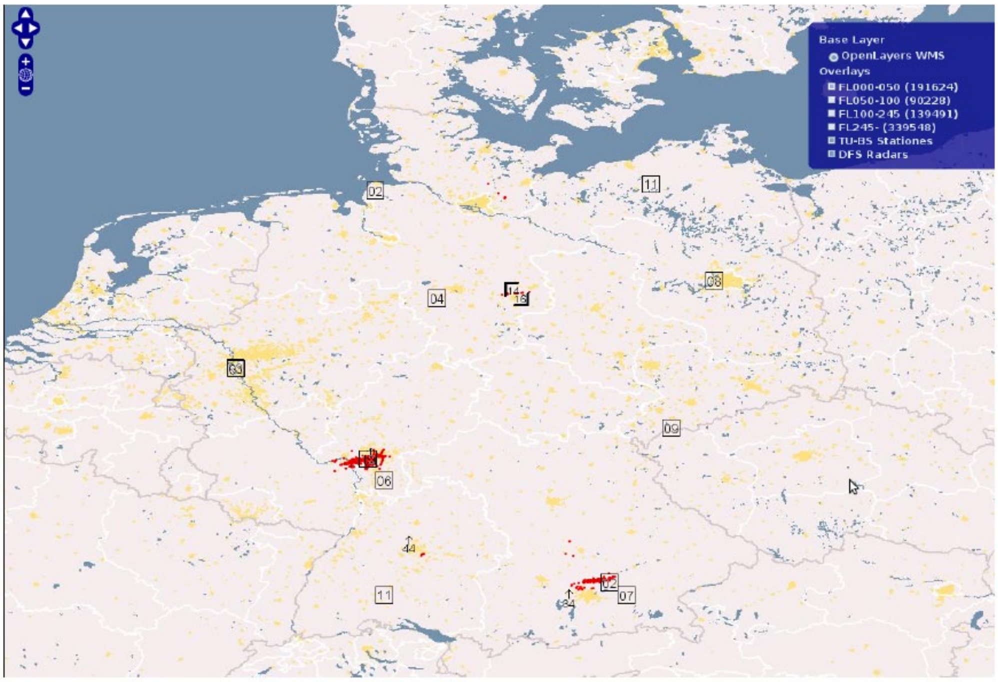

Figure 3-71: Positions of interrogated Aircraft up to FL50

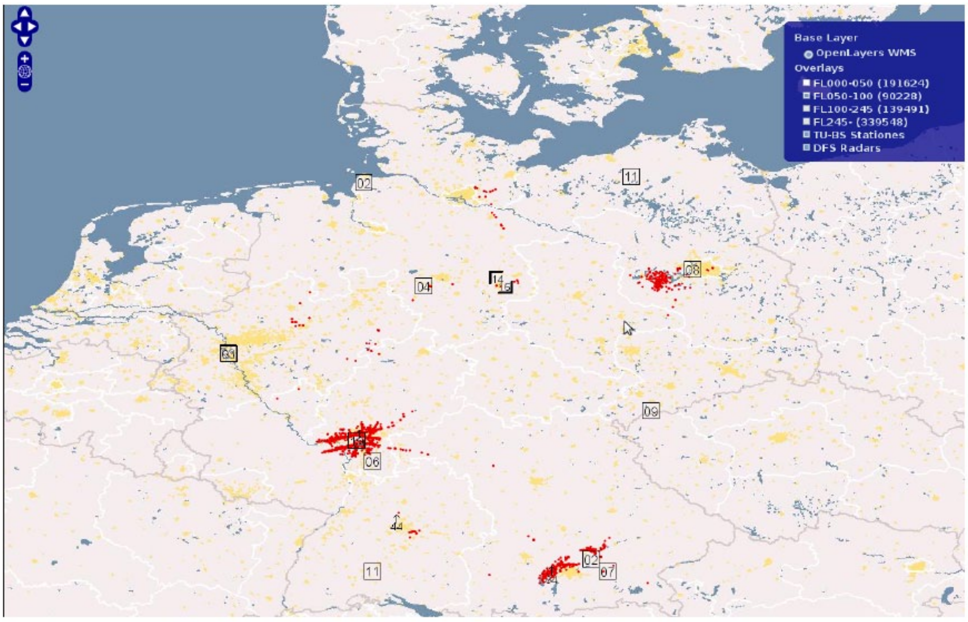

Figure 3-72: Positions of interrogated Aircraft between FL50 and FL100

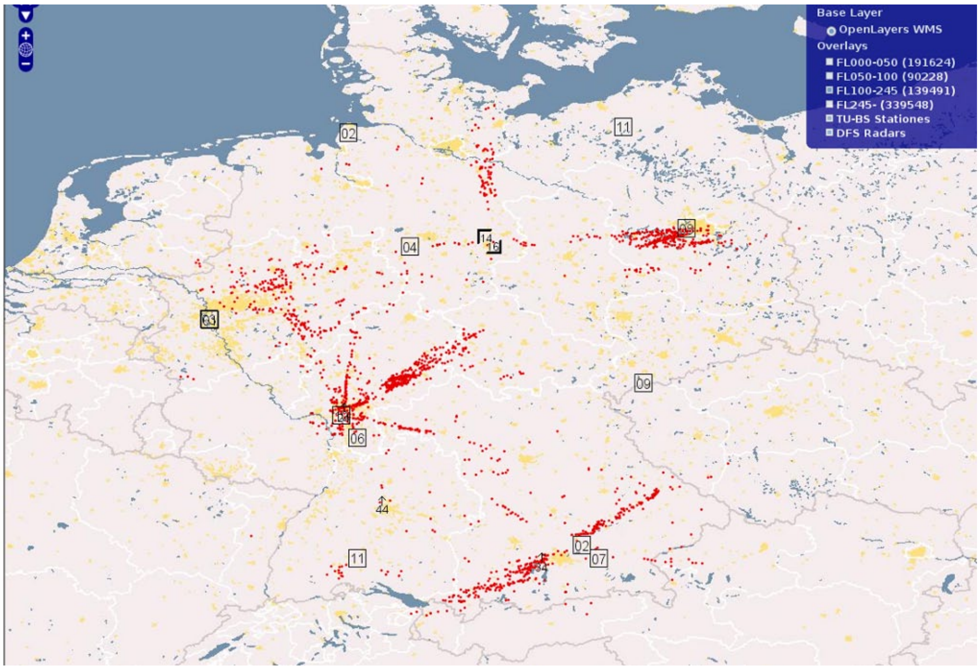

Figure 3-73: Positions of interrogated Aircraft above FL100 up to FL245

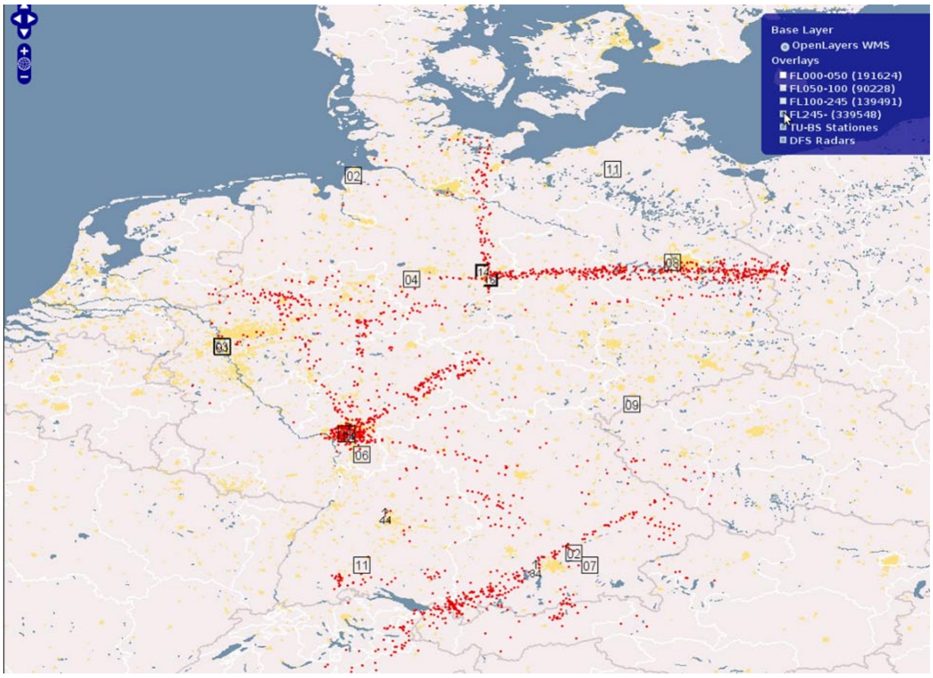

Figure 3-74: Positions of interrogated Aircraft above FL245

3.2.2 II Codes

Radars have 4-bit II codes (Interrogator Identifier) assigned in a way so that the coverage regions of radars with the same II code do not overlap. Therefore, at any point in the airspace, a certain II code should be used by one radar station only, unless clustering is applied. A Mode S transponder uses the II code to keep track of which radar has already acquired this transponder.

This section of the document shows the position of aircraft that were interrogated by radars with specific II codes.

Note: A second technique for unique identification of interrogators is the use of Surveillance Identifier (SI) codes, e.g. as applied by the Amsterdam ASR. This provides for 63 different codes instead of the 16 different codes offered by the II method.

3.2.2.1 Positions of Aircraft interrogated with II Code 00

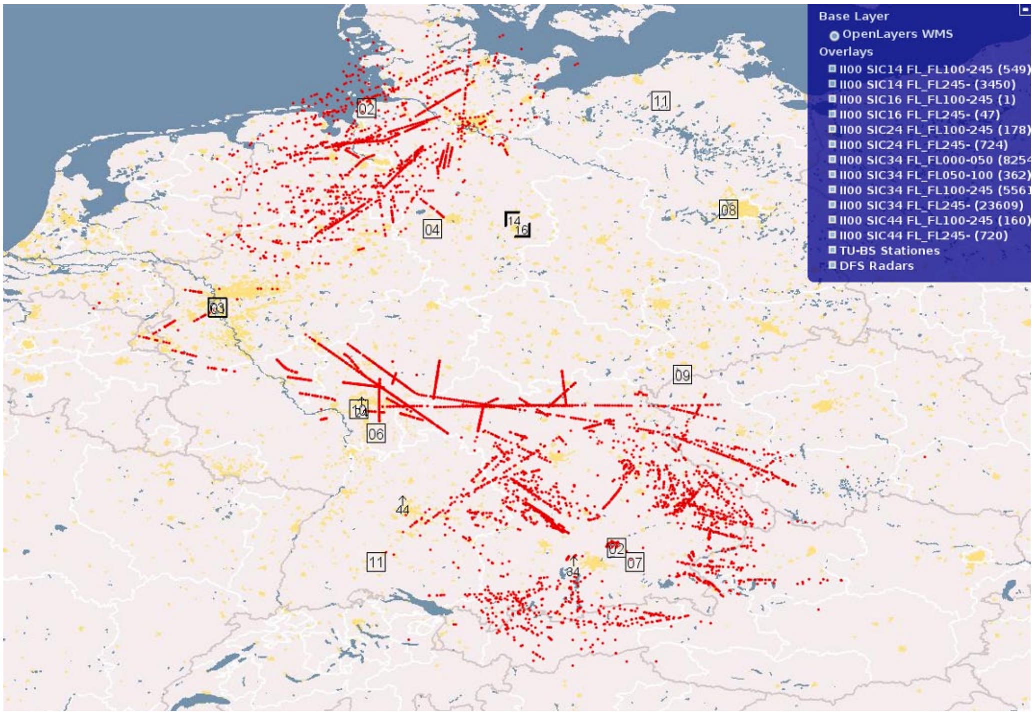

Figure 3-75: Positions of Aircraft interrogated with II Code 00

II code 00 is not assigned to a single radar station but reserved for mobile military interrogators, some MLAT systems are using this as well. Figure 3-75 shows that there are mobile military interrogators operating within the reception range. Since the Braunschweig SE (SIC16) and the Frankfurt (SIC24) stations received only a few interrogations during the day, tracks of single aircraft or aircraft using airways can be identified.

3.2.2.2 Positions of Aircraft interrogated with II Code 01

On 10.03.2010 there were no interrogations with II code 01.

3.2.2.3 Positions of Aircraft interrogated with II Code 02

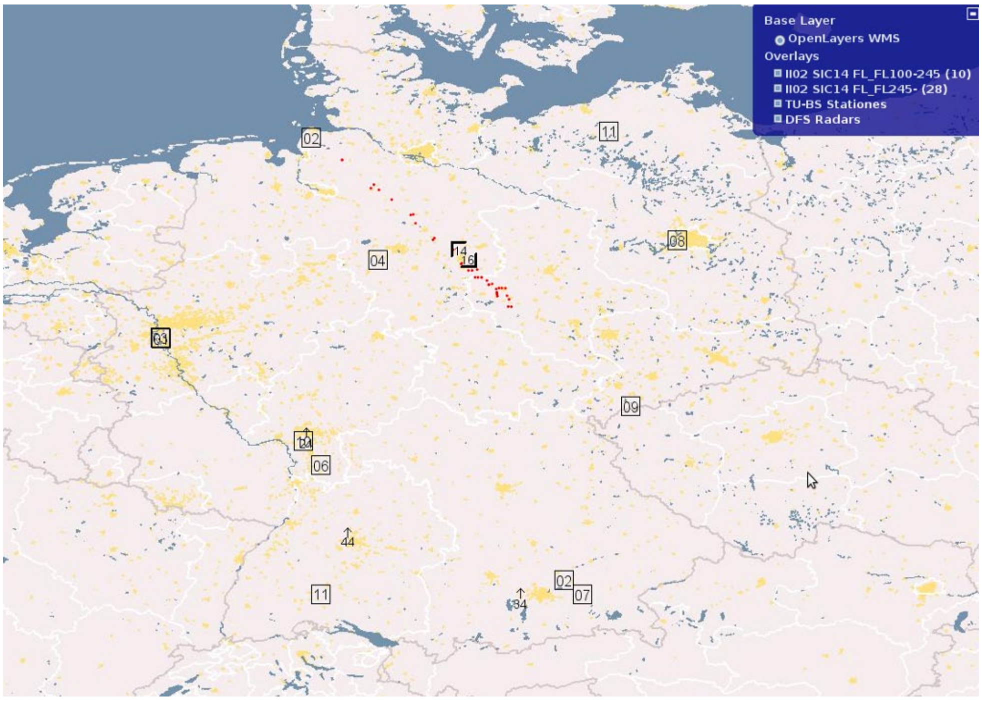

Figure 3-76: Positions of Aircraft interrogated with II Code 02

Figure 3-76 shows that the Nordholz radar station is interrogating with II code 02 and the Braunschweig monitor station is able to receive some stray interrogations although it is not visible from Braunschweig.

3.2.2.4 Positions of Aircraft interrogated with II Code 03

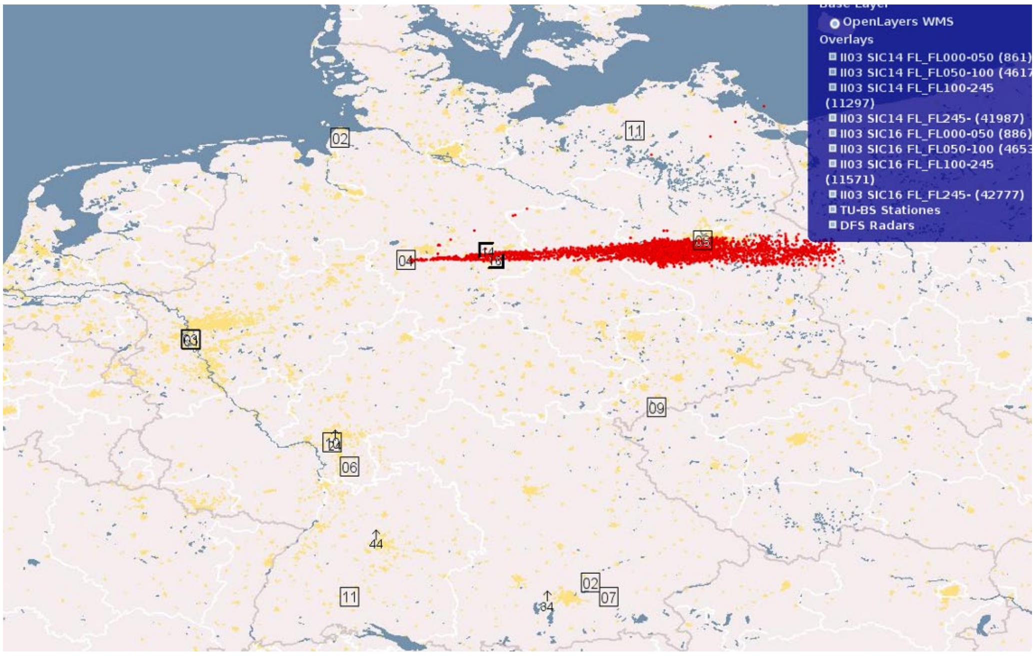

Figure 3-77: Positions of Aircraft interrogated with II Code 03

Figure 3-77 shows the Deister radar station interrogating with II code 03. Notable is the perfect beam form of the positions of aircraft being interrogated while the radar is pointing towards the Braunschweig monitor stations. In the map, Deister is still marked with the II code 04 but Deister radar as part of the German Cluster North is currently allocated to II code 03 (see Appendix B for a complete list of II/SI codes).

There is a thin beam at about 30° left of the main beam. This beam is due to either multipath effects or a gap in the side lobe suppression, enabling the Braunschweig station to receive interrogations not directed towards it.

3.2.2.5 Positions of Aircraft interrogated with II Codes 04 - 09

On 10.03.2010 there were no interrogations with II codes 04 to 09.

3.2.2.6 Positions of Aircraft interrogated with II Code 10

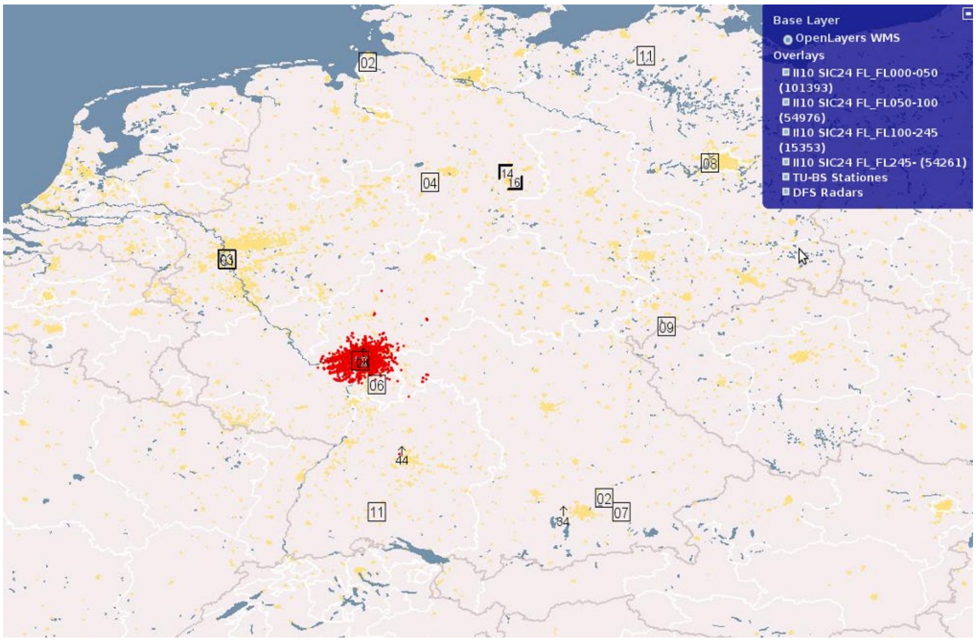

Figure 3-78: Positions of Aircraft interrogated with II Code 10

Figure 3-78 shows the Frankfurt station receiving many interrogations with II code 10. As already stated in section 3.1.2.4.3 (Figure 3-10), this code is associated with the MLAT interrogators of the new Precision Approach Monitoring of Frankfurt airspace system (PAM-FRA) which consists of several sensors and interrogation facilities covering Frankfurt TMA and a large area around.

These MLAT interrogations are radiated via wide-aperture antennas (omni-directional or sector type) and will be received by any aircraft within range. Interrogations of one or more of these facilities are received by the network receiver on the ground as well.

3.2.2.7 Positions of Aircraft interrogated with II Code 11

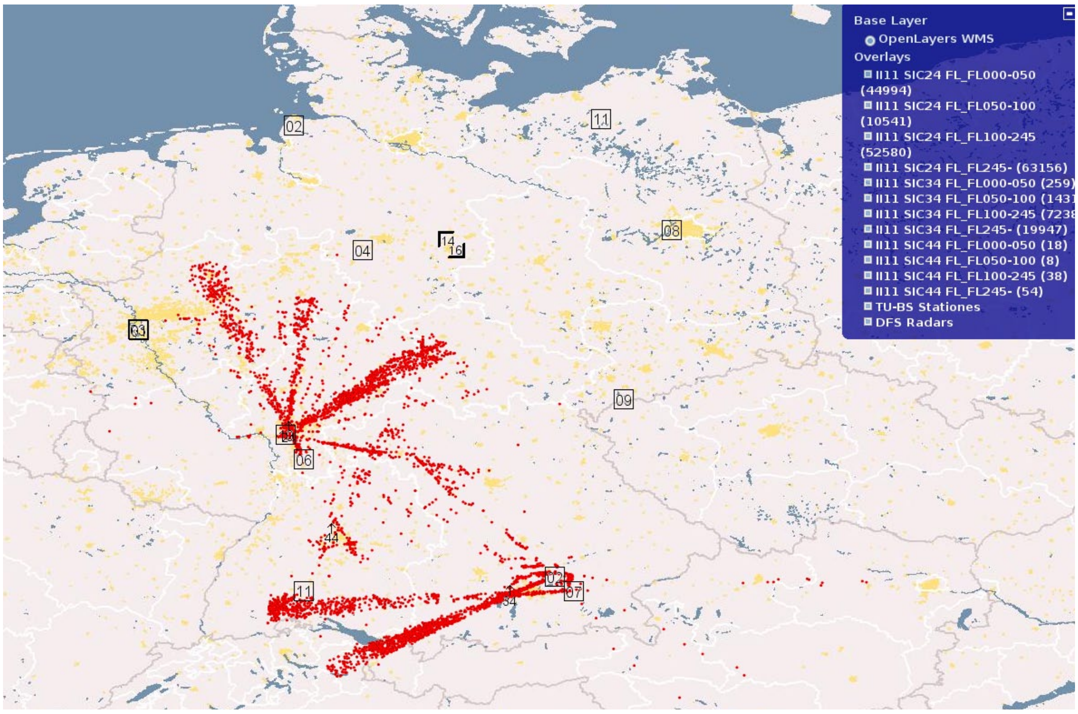

Figure 3-79: Positions of Aircraft interrogated with II Code 11

According to Figure 3-79 radars using II code 11 (German Cluster South) are located in:

- Frankfurt, forming many beams probably due to reflections
- in Gosheim (North west of Lake Constance) forming a thin beam to the Stuttgart monitor station (SIC 44)
- two radar stations near Munich

3.2.2.8 Positions of Aircraft interrogated with II Code 12

On 10.03.2010 there were no interrogations with II code 12.

3.2.2.9 Positions of Aircraft interrogated with II Code 13

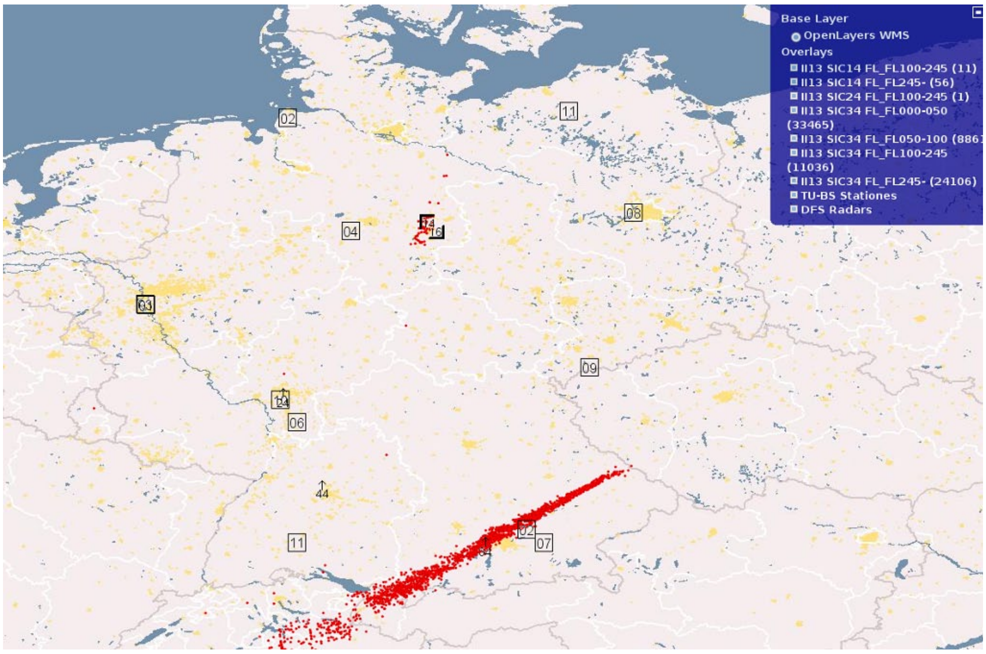

Figure 3-80: Positions of Aircraft interrogated with II Code 13

The II code 13 is reserved for the German Air Force. The German Air Force Großer Arber radar is interrogating with II code 13. Another radar station forms the thin beam in Braunschweig.

3.2.2.10 Positions of Aircraft interrogated with II Code 14

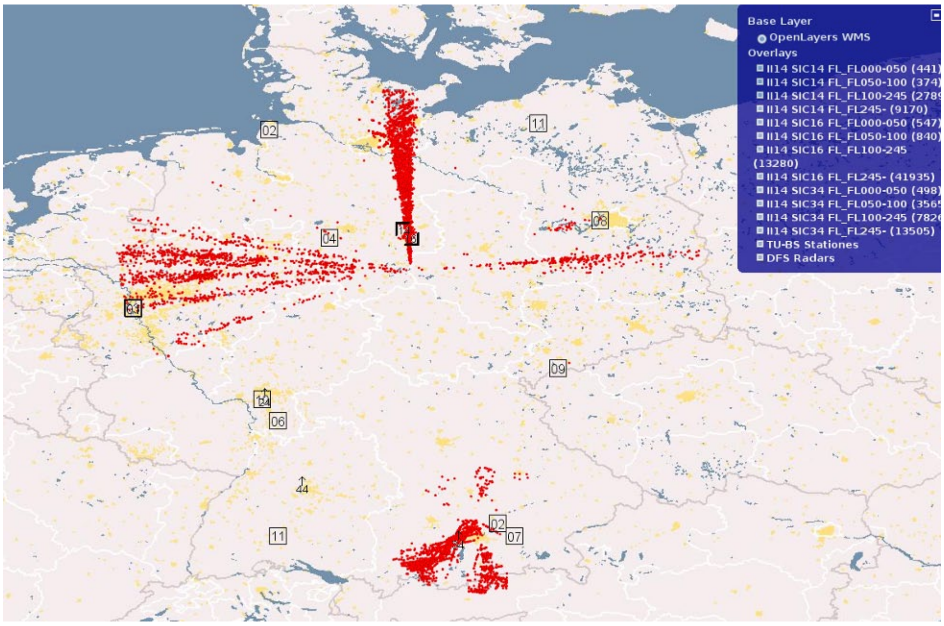

Figure 3-81: Positions of Aircraft interrogated with II Code 14

Figure 3-81 shows that the Brocken radar is interrogating with II code 14. The main beam is directed towards the Braunschweig monitor stations, located approx. 60 km to the North of the radar site. The figure also proves that interrogations that were not directed to a receiver station are received, even though the ground station receiver respects side lobe suppression. Why the side lobe suppression does not prevent the reception of the stray interrogations is subject to further research. One possible explanation is given in section 3.3.3 (see Figure 3-98).

Another reason may be multipath effects induced by ground structures near the radar station. The Brocken is the highest peak of the Harz mountain range and also the highest peak of Northern Germany (see Figure 3-82).

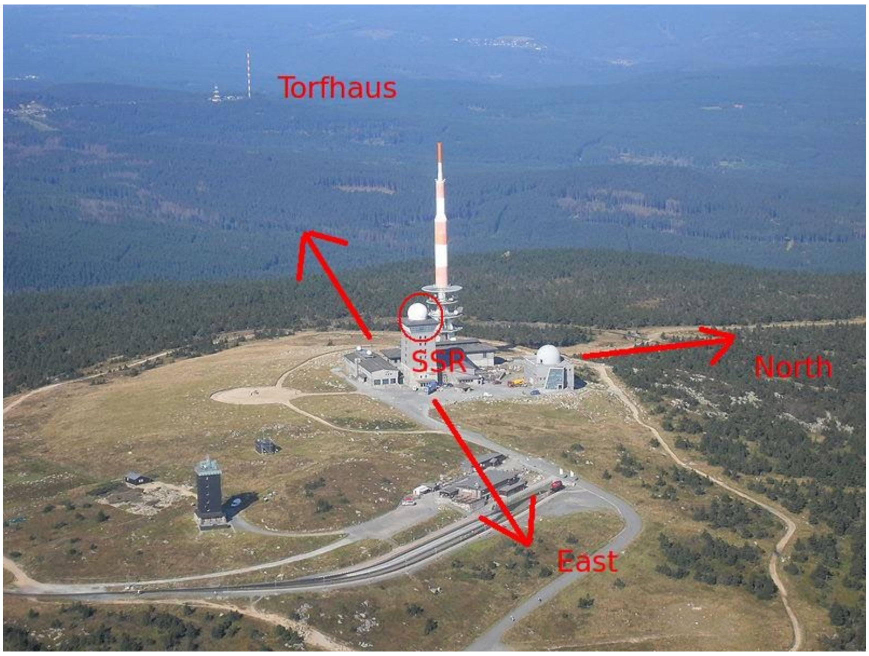

Figure 3-82: Brocken SSR

The peak at its altitude of 1,141 m (3,743 ft) is above the tree line. The SSR antenna is located on the roof of the "Brockenhotel" at an elevation of about 50 m above ground. The other buildings are:

- The "Brocken" transmitter is a facility for FM- and TV-transmissions on a 123 m tall, freestanding steel-tube tower. (Northwest of the SSR)
- The Brocken Museum with an unused radome atop. (Northeast of the SSR)
- The weather observatory tower southeast of the SSR.
- The "Torfhaus" transmitter towers for FM and TV. The "Torfhaus" ridge has an altitude of 821 m, the tallest of the three towers is 280 m high

Assuming the receivers cannot detect side lobe interrogations, the observed interrogations must be main beam reflections caused by reflectors to the west and to the east of the Brocken radar.

To which extent the above identified buildings cause these reflections remains subject of further studies.

There are also one or more radars operating with II code 14 near Munich.

3.2.2.11 Positions of Aircraft interrogated with II Code 15

On 10.03.2010 there were no interrogations with II code 15. This II code is assigned to military AWACS (Airborne Warning and Control System) operations.

3.2.3 Radio Load on Mode S Channels

Mode S messages on both the 1030 MHz and the 1090 MHz channel cannot always be decoded correctly by the respective receiving unit (transponder, radar station, multilateration ground station): Messages can be disturbed by other simultaneously received Mode A/C, Mode S, TCAS, or military messages. Non-ATC interference, such as very close mobile phone base stations or other transmitting devices with malfunctions may for example also disturb reception on the Mode S channels. Components of the receiving equipment or antennas can change their properties or even fail. Decoding software may be overloaded or crash.

For the development and operation of Mode S receivers it is thus important to have a precise knowledge of the real Mode S radio load. For this reason, an analysis using artificially generated messages representing future Mode S radio load is presented here. These statistics evolved during the long-term analysis in the course of the MOSTDONT project. They were also used to improve and control the receiving equipment employed by the TU Braunschweig within this study.

3.2.3.1 Test Messages

It is straight-forward to count the number of received messages. However, equally interesting is the number of sent but not received messages, because this permits to calculate a reception probability. That was realized by randomly feeding 100 additional test messages per second at low power (-80 dBm) into the antenna cable of the Braunschweig stations. The test messages are UF11-All-Calls and DF11-Squitter. Thereby the transmission of a far distant aircraft is simulated without significantly increasing the radio load in the air itself by these additional messages. The test-messages are detected by the Mode S monitoring software and the number of correctly received test-messages is counted.

3.2.3.2 Daily Radio Load

Figure 3-83 shows an automatically generated daily radio load statistics. As an example, one day was chosen on which all the reception facilities of the TU Braunschweig were in operation, arbitrarily the choice fell on the 25 April 2010.

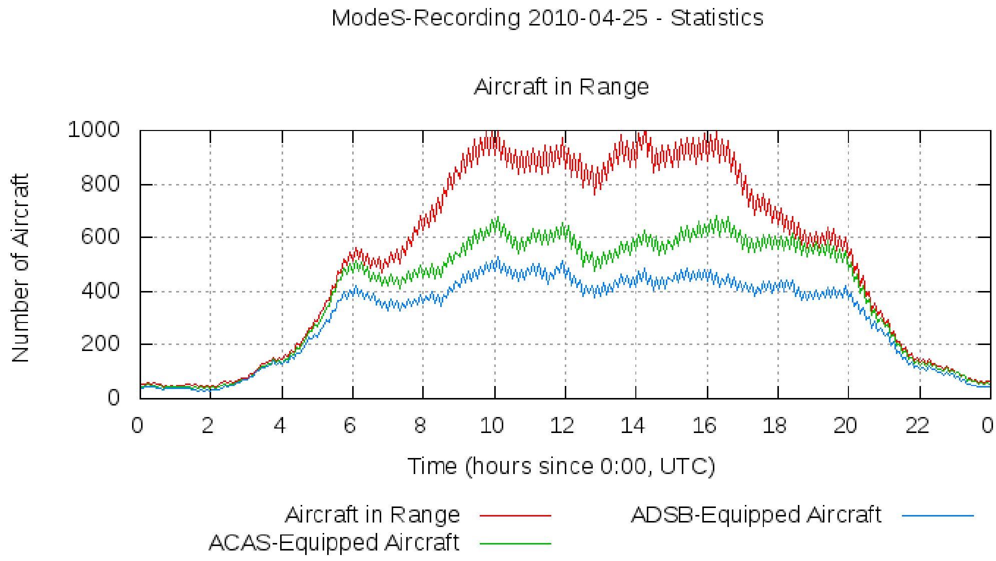
ModeS-Recording 2010-04-25 - Statistics
Aircraft in Range
Number of Aircraft
1000
800
600
400
200
0
0 2 4 6 8 10 12 14 16 18 20 22 0
Time (hours since 0:00, UTC)
Aircraft in Range
ACAS-Equipped Aircraft
ADSB-Equipped Aircraft

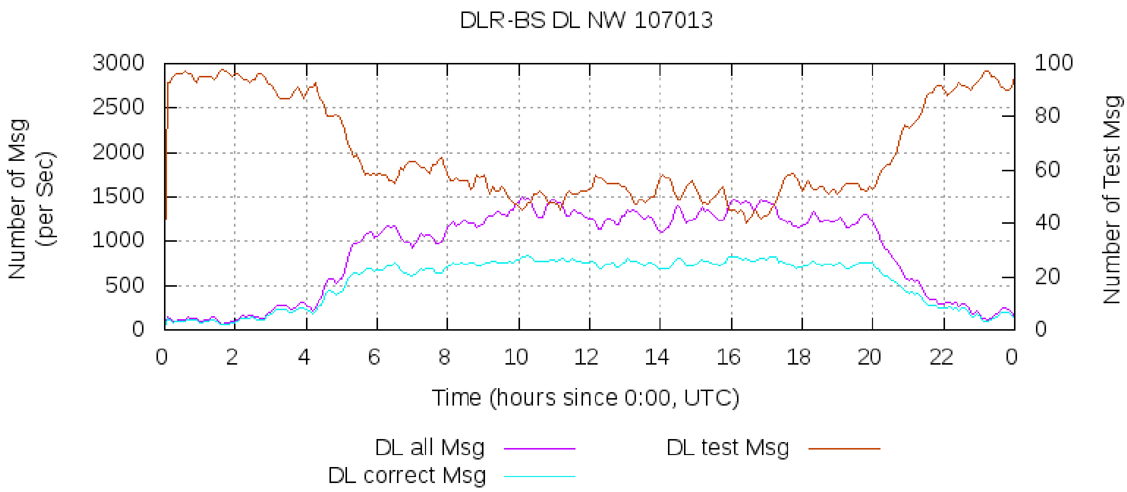
DLR-BS DL NW 107013
Number of Msg (per Sec)
3000
2500
2000
1500
1000
500
0
100
80
60
40
20
0
Number of Test Msg
0 2 4 6 8 10 12 14 16 18 20 22 0
Time (hours since 0:00, UTC)
DL all Msg
DL correct Msg
DL test Msg

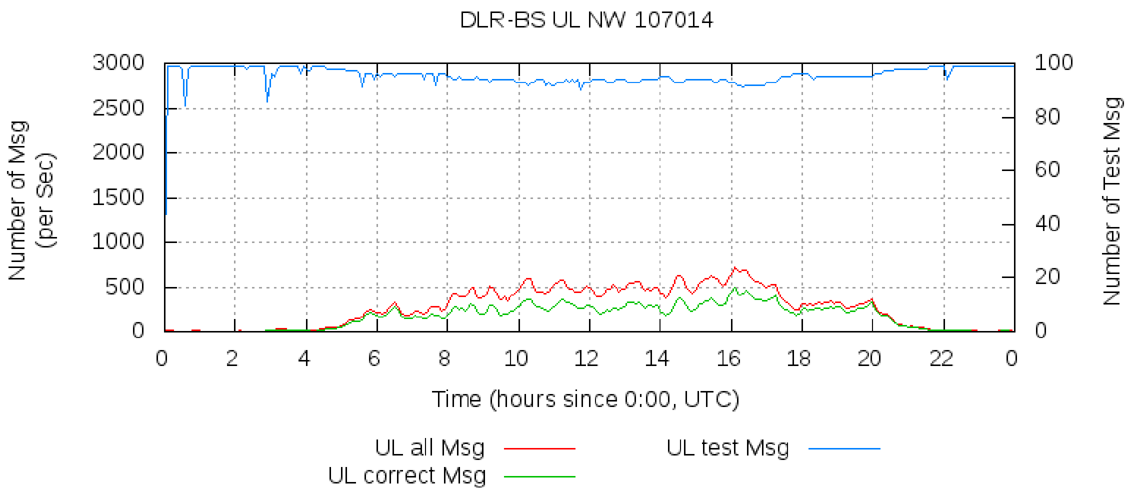
DLR-BS UL NW 107014
Number of Msg (per Sec)
3000
2500
2000
1500
1000
500
0
100
80
60
40
20
0
Number of Test Msg
0 2 4 6 8 10 12 14 16 18 20 22 0
Time (hours since 0:00, UTC)
UL all Msg
UL correct Msg
UL test Msg

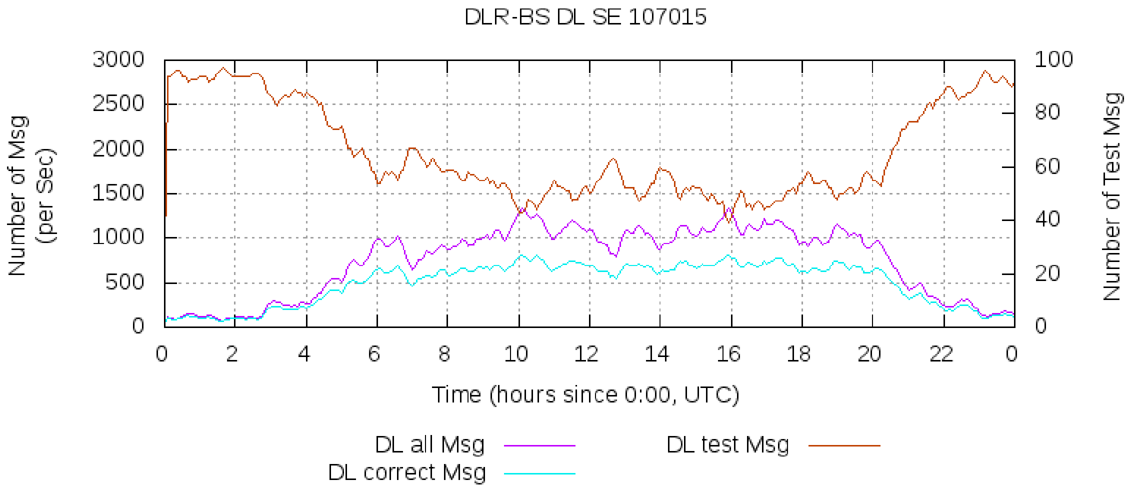
DLR-BS DL SE 107015
Number of Msg (per Sec)
Number of Test Msg
3000
2500
2000
1500
1000
500
0
100
80
60
40
20
0
0 2 4 6 8 10 12 14 16 18 20 22 0
Time (hours since 0:00, UTC)
DL all Msg
DL correct Msg
DL test Msg

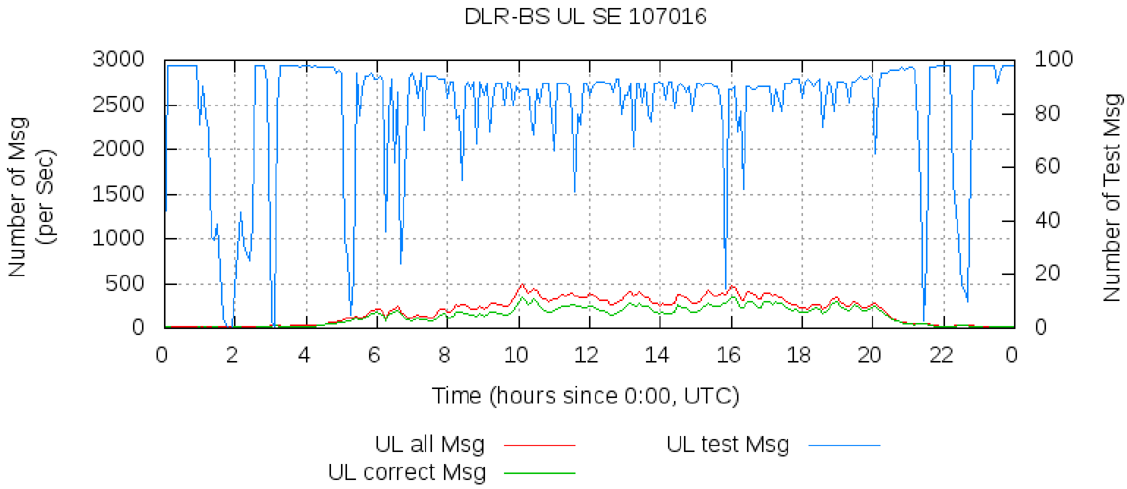
DLR-BS UL SE 107016
Number of Msg (per Sec)
Number of Test Msg
3000
2500
2000
1500
1000
500
0
100
80
60
40
20
0
0 2 4 6 8 10 12 14 16 18 20 22 0
Time (hours since 0:00, UTC)
UL all Msg
UL correct Msg
UL test Msg

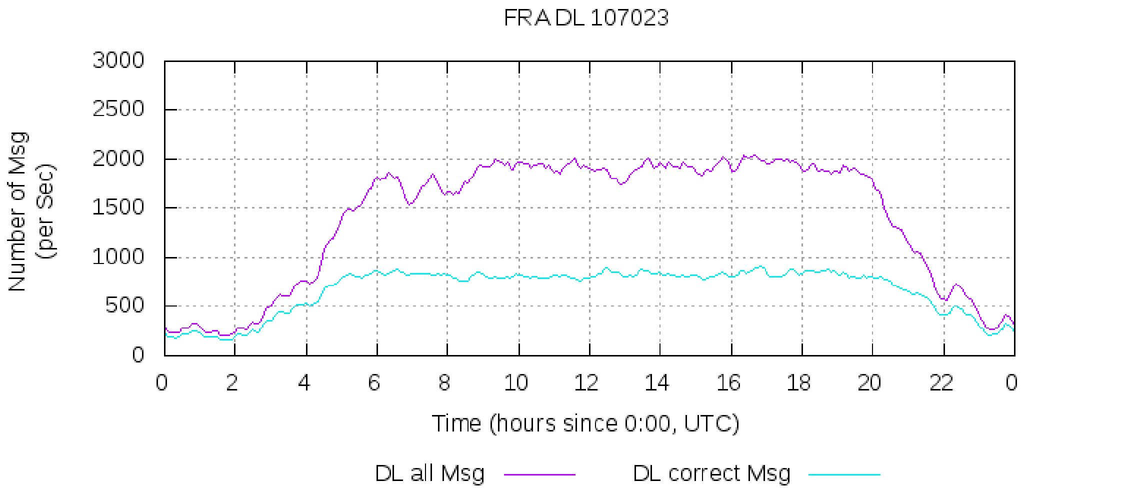
FRA DL 107023
Number of Msg (per Sec)
3000
2500
2000
1500
1000
500
0
0 2 4 6 8 10 12 14 16 18 20 22 0
Time (hours since 0:00, UTC)
DL all Msg
DL correct Msg

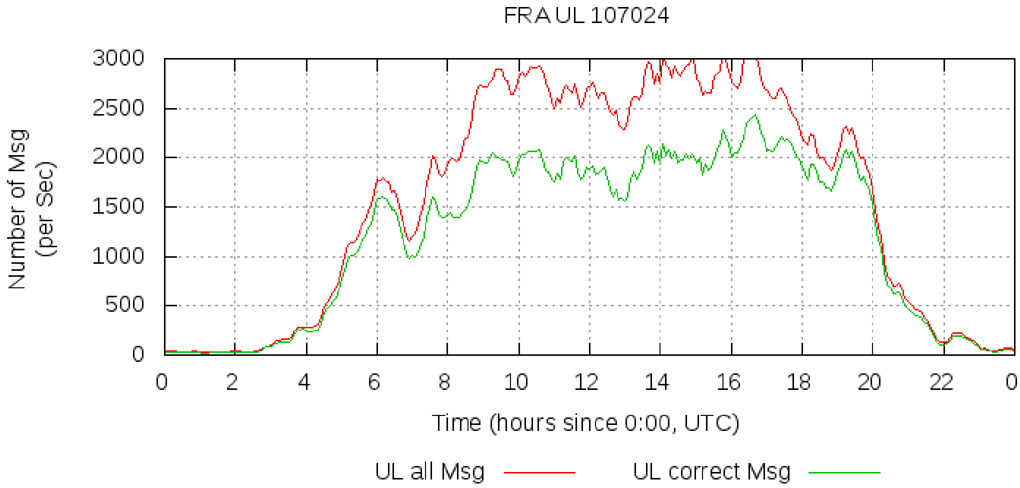
FRA UL 107024
Number of Msg (per Sec)
3000
2500
2000
1500
1000
500
0
0 2 4 6 8 10 12 14 16 18 20 22 0
Time (hours since 0:00, UTC)
UL all Msg
UL correct Msg

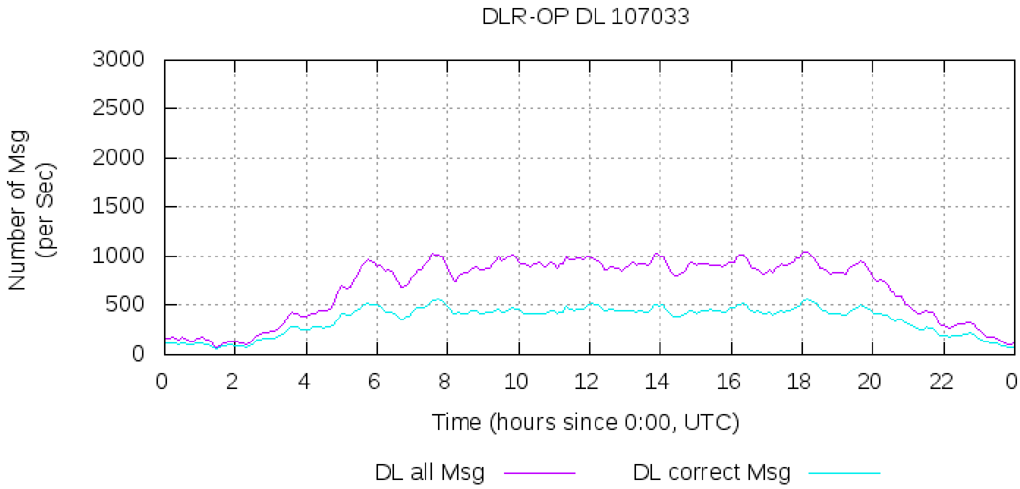
DLR-OP DL 107033
Number of Msg (per Sec)
3000
2500
2000
1500
1000
500
0
0 2 4 6 8 10 12 14 16 18 20 22 0
Time (hours since 0:00, UTC)
DL all Msg
DL correct Msg

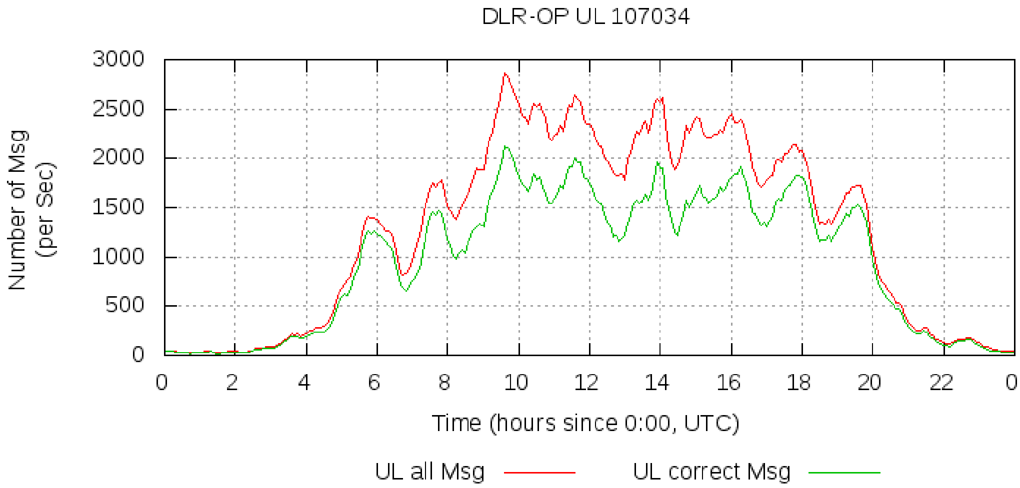
DLR-OP UL 107034
Number of Msg (per Sec)
3000
2500
2000
1500
1000
500
0
0 2 4 6 8 10 12 14 16 18 20 22 0
Time (hours since 0:00, UTC)
UL all Msg
UL correct Msg

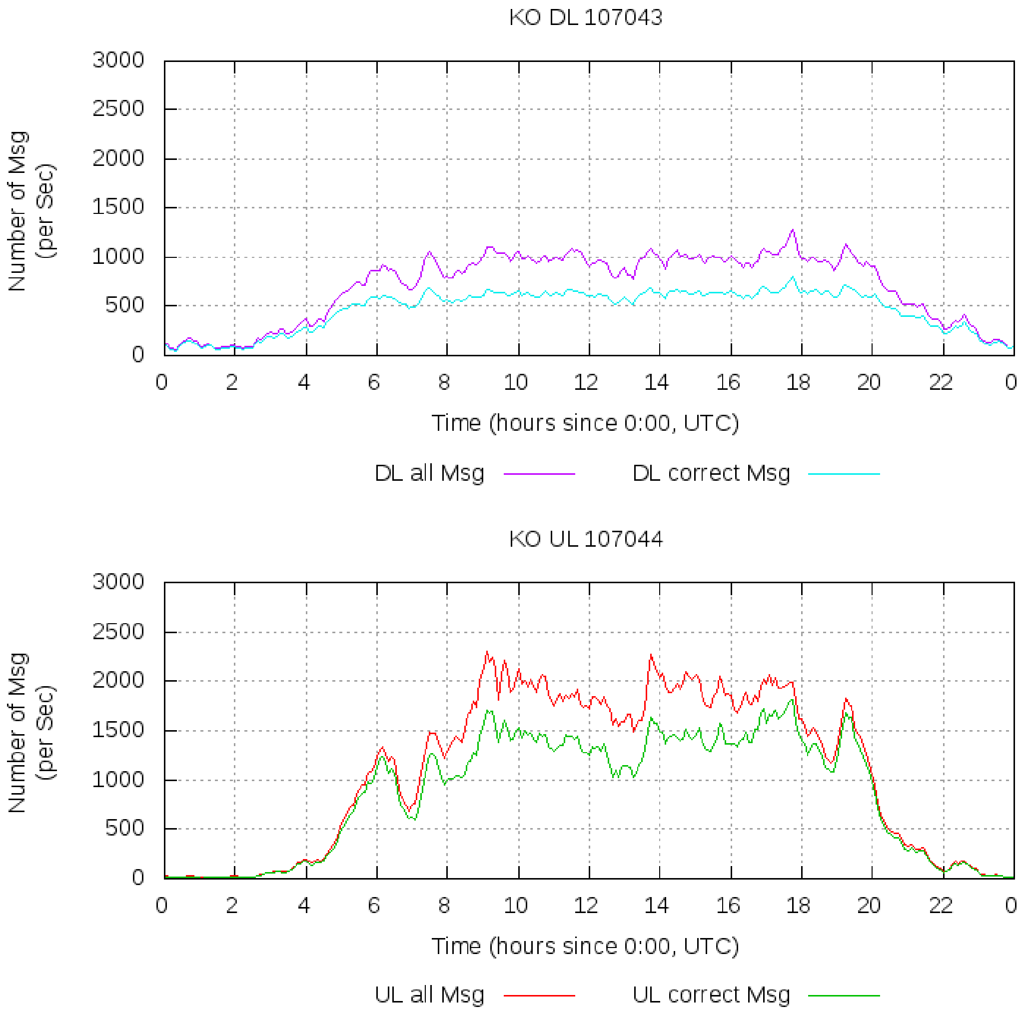

Figure 3-83: Daily Radio Load Statistic

Beginning from May 2008, the Mode S Monitor-Network was set up starting with a dual station in Braunschweig using sector antennas to the North-west and South-east. The stations in Braunschweig were supplemented by stations in Frankfurt, Oberpfaffenhofen, and Korntal near Stuttgart in August 2008.

The first chart of Figure 3-83 depicts the total number of aircraft simultaneously seen by all 5 stations. Aircraft seen by two stations are counted only once. As in all other charts the statistics are plotted over the time of day in UTC. The chart shows that between 8 a.m. and 6 p.m. 800 to 900 Mode S equipped aircraft (yellow) were simultaneously within range of the network of TU Braunschweig. Most of them are equipped with TCAS (blue), 60% also transmit ADS-B (brown). The curves oscillate in ten-minute intervals, because the list of known aircraft is cleared every 10 minutes from aircraft that left the reception range.

The other charts plot the radio load of each receiver during the course of day. The chart DLR-BS DL NW 107013 (the second one) in Figure 3-83 shows as a violet curve (left scale) the total number of received messages per second by the downlink receiver north-west at the DLR Braunschweig tower. Between 7 a.m. and 8 p.m. about 1,500 messages per second were received. The light-blue curve below shows the rate (messages per second) of correctly received messages, checked by the CRC check of the AP/PI-Field. In the respective time period around 700 messages per second can be found to be correct. Clearly, a large part of the messages was not received correctly.

The brown curve with its scale on the right ordinate plots the number of the 100 test messages per second which were received without error in any bits. Between 7 a.m. and 8 p.m. these are only about 40%. This implies that in times with high radio load only about 40% of the real received messages with -80 dBm are not disturbed by other signals within the monitored time period. The statistics of the test messages also shows that the reception probability depends on the channel load: At night, when few aircraft are flying and therefore only a limited number of messages are being sent, the reception probability is almost 100%. *Note: The test signals are not included in the red and blue curves.*

The chart DLR-BS UL NW 107014 (the third one) in Figure 3-83 plots the statistics on the uplink channel in Braunschweig NW. The red curve shows the rate of all uplink messages (left ordinate), which are approximately 500 messages per second during daylight hours. The green curve describes the rate of CRC-correct messages, about 400 messages per second. The reception probability (blue curve) of uplink test messages does not drop as much during daytime as on the downlink channel. This is due to a lower radio load in the uplink channel. Also, in the uplink channel only the preamble of a message is amplitude-modulated, the message itself is using a differential phase shift key modulation, which is more robust against interference of amplitude modulated Mode A/C signals.

The next two charts show the plot of the Braunschweig south east receivers. The Uplink test signal generator was only partial functional and did not reliably send test signals as shown in chart DLR-BS UL SE. Nevertheless, even the partial test signals yielded valuable information; therefore this is included in the plots. Only the receivers in Braunschweig were fed with test signals.

The other charts show the other receiver stations in Frankfurt (FRA), Oberpfaffenhofen (DLR-OP) and Korntal (KO). Most downlink messages are received in Frankfurt. There, the relationship between received and read messages is the worst. The data of all recipients make up the number of simultaneously observed aircraft (first chart).

3.2.3.3 Statistics over a Long Time Period

The receiver units are connected via Internet to TU Braunschweig. In order to save transfer rate and hard disk space, the original concept foresaw that already the receivers filtered out unnecessary message formats. Therefore, the filtered formats do not appear in the statistics. From August 21st to November 13th 2009, UF00, UF04, UF05, UF11, UF20 and UF21 (all formats except UF16 uplink) were filtered out. In Braunschweig, UF11 formats were not filtered out, since the test signals are UF11.

In November 2009 the hard disk capacity and the network capacity was extended to serve the needs of the MOSTDONT project. As a consequence all defined formats, which are DF00, DF04, DF05, DF11, DF16 – DF21, DF24 and UF00, UF04, UF05, UF11, UF16, UF20, UF21, UF24, are now accepted and recorded by the monitor network. By combining more than 800 daily statistics, Figure 3-85 was generated. The values from every single daily statistic between 11 a.m. and 12 a.m. UTC were taken into account.

Comparing the charts BS (Braunschweig) and FRA (Frankfurt) of the statistics over a long time period may lead to the hypothesis, that about 700 correctly read messages are the maximum number the employed COTS industry downlink receiver is able to handle. This hypothesis is only supported by the shown observations, it is not proven nor experimentally checked and therefore remains a hypothesis. The ability to read messages depends on the design and tuning of the receiver station and the characteristics of the surrounding traffic.

The theoretical maximum downlink capacity is far larger with approx. 8000 messages per second, since the duration of a short downlink message is 64 µs and that of a long message 120 µs. Uplink messages are almost 4 times shorter, the duration of a short uplink message is 19.75 µs and that of a long uplink message 33.75 µs. Therefore, the probability of message interference is lower than on the downlink channel and a receiver can decode more messages.

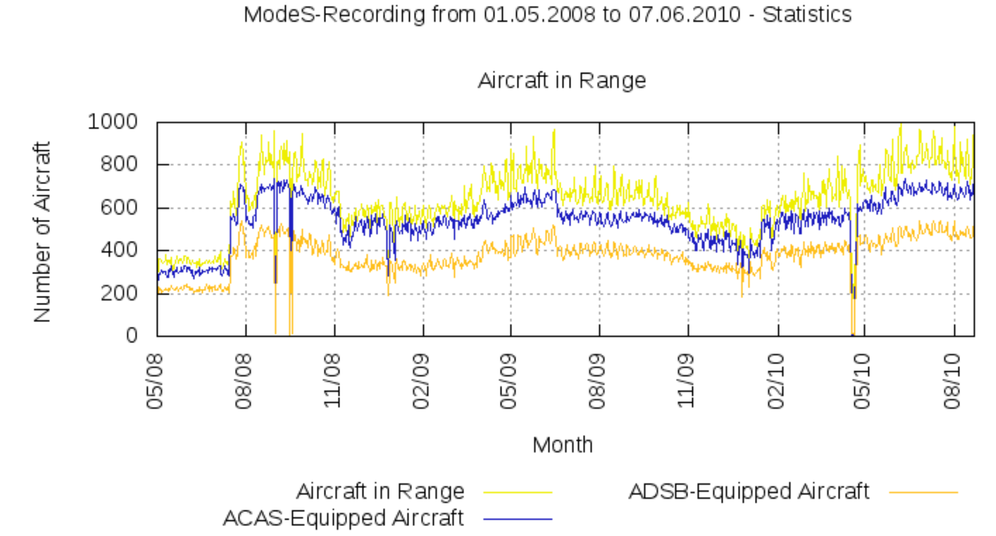

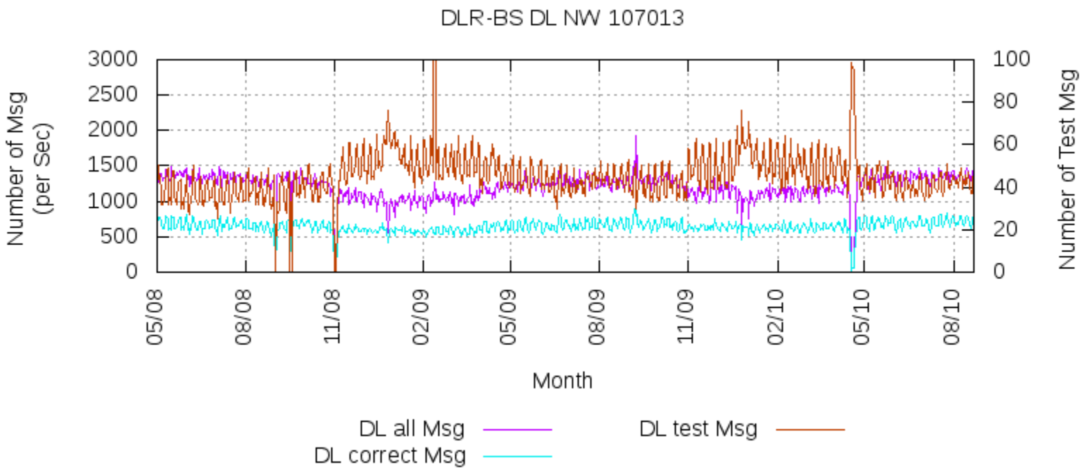

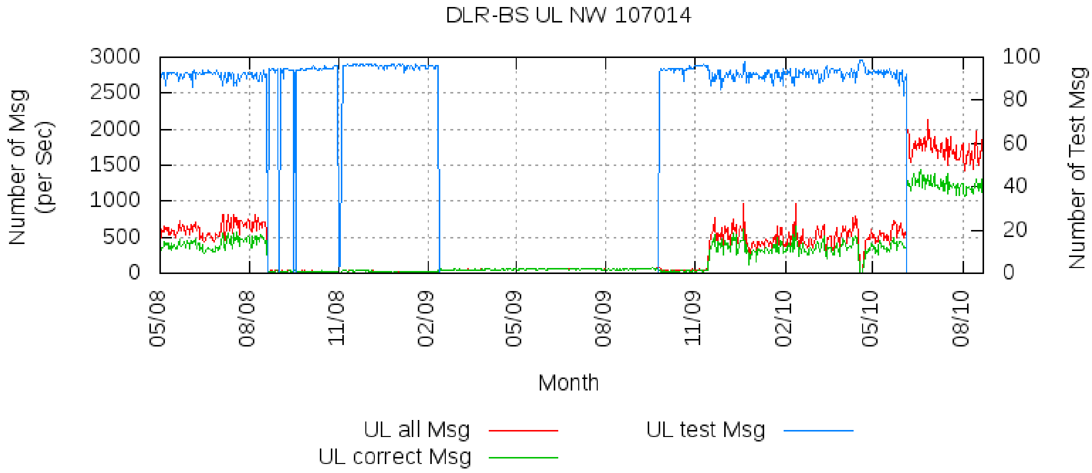
DLR-BS UL NW 107014
Number of Msg (per Sec)
Number of Test Msg
Month
05/08 08/08 11/08 02/09 05/09 08/09 11/09 02/10 05/10 08/10
UL all Msg
UL correct Msg
UL test Msg

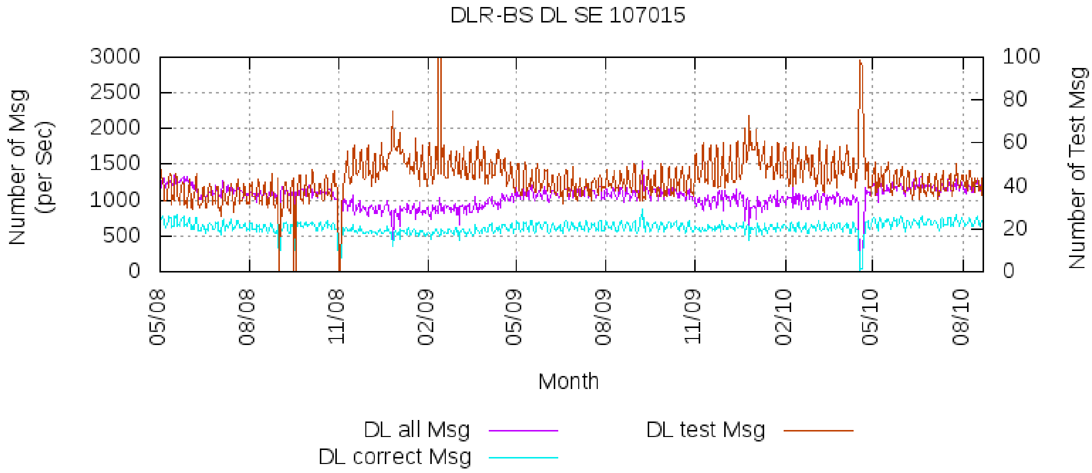
DLR-BS DL SE 107015
Number of Msg (per Sec)
Number of Test Msg
Month
05/08 08/08 11/08 02/09 05/09 08/09 11/09 02/10 05/10 08/10
DL all Msg
DL correct Msg
DL test Msg

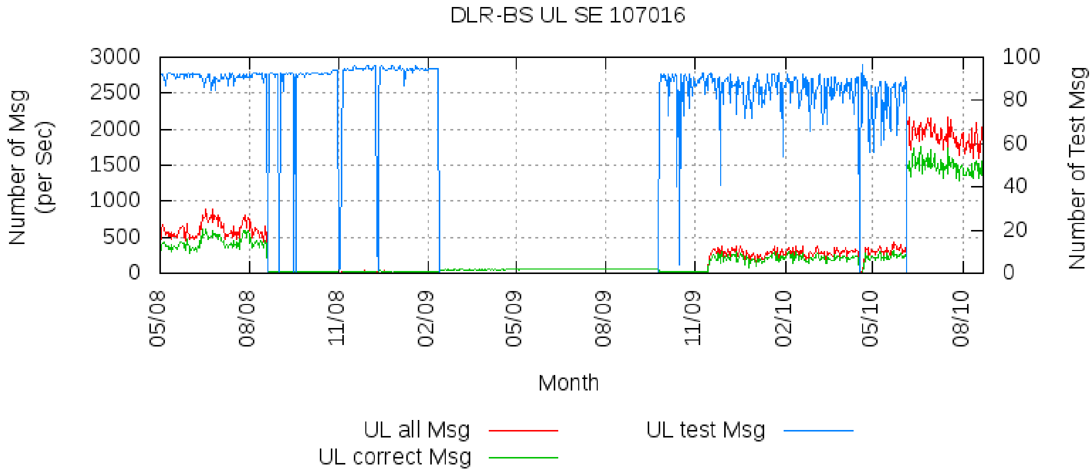
DLR-BS UL SE 107016
Number of Msg (per Sec)
Number of Test Msg
Month
05/08 08/08 11/08 02/09 05/09 08/09 11/09 02/10 05/10 08/10
UL all Msg
UL correct Msg
UL test Msg

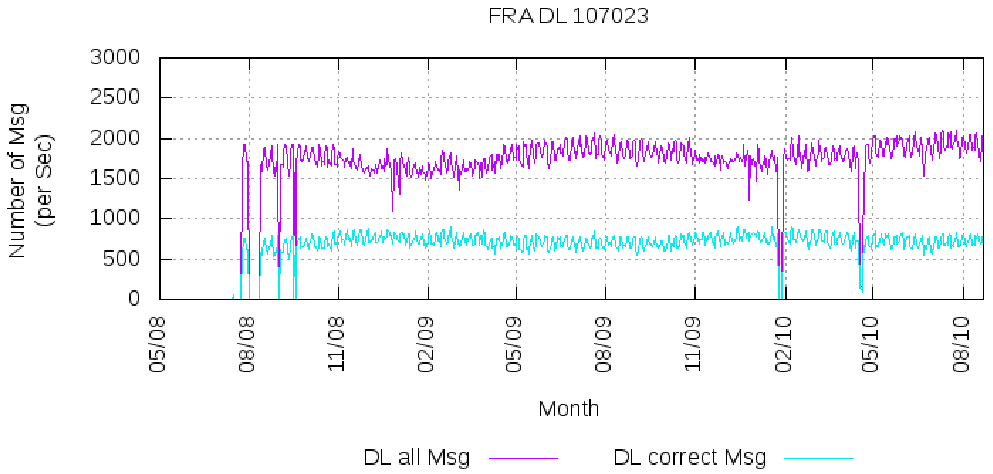
FRA DL 107023
Number of Msg (per Sec)
3000
2500
2000
1500
1000
500
0
05/08
08/08
11/08
02/09
05/09
08/09
11/09
02/10
05/10
08/10
Month
DL all Msg
DL correct Msg

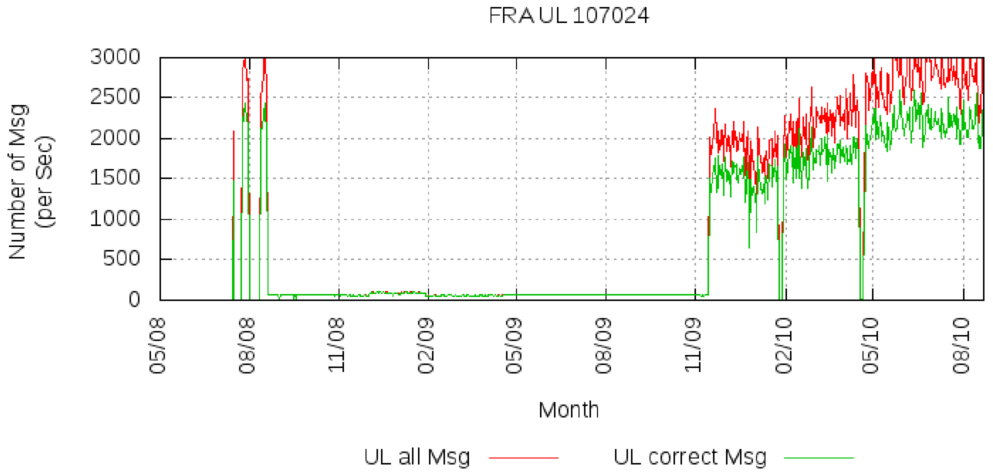
FRA UL 107024
Number of Msg (per Sec)
3000
2500
2000
1500
1000
500
0
05/08
08/08
11/08
02/09
05/09
08/09
11/09
02/10
05/10
08/10
Month
UL all Msg
UL correct Msg

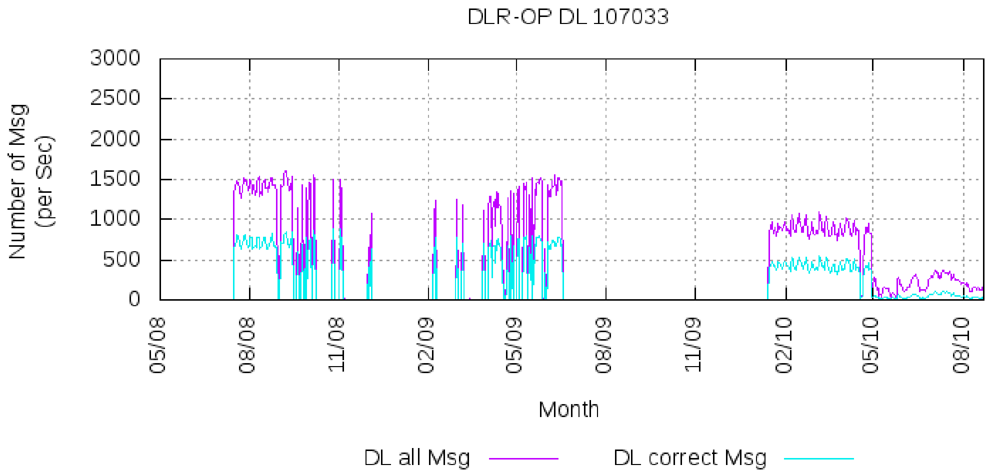
DLR-OP DL 107033
Number of Msg (per Sec)
3000
2500
2000
1500
1000
500
0
05/08
08/08
11/08
02/09
05/09
08/09
11/09
02/10
05/10
08/10
Month
DL all Msg
DL correct Msg

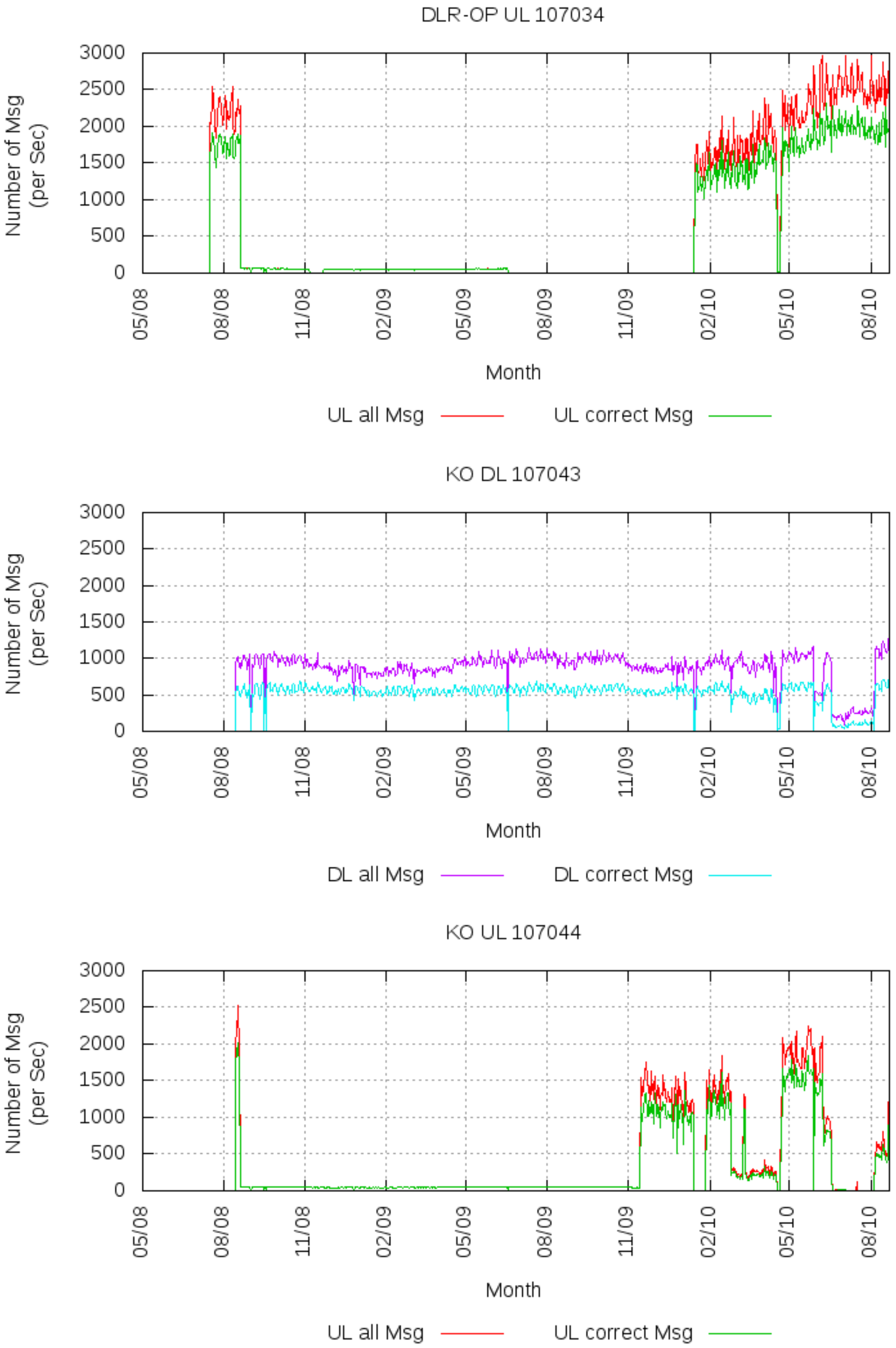

Figure 3-84: Statistics on Radio Load over a Long Time Period

These charts also document the time periods of proper operation of each single station. The filtering of Uplink messages from August 21st, 2008 until November 13th, 2009 is shown as well as temporary local off-line periods of network stations. For example, the Oberpfaffenhofen station was off-line for a long period, since the antenna had to be removed to enable a DLR experiment. The shutdown of German airspace in April 2010 because of volcanic ashes is clearly visible as a major drop in all stations.

The charts also show regular variation of traffic load with the frequency of one week (the continuous distortion on every graph) and with the frequency of one year.

Figure 3-85 contains the same graphs as Figure 3-84 but the ordinates are rescaled to enlarge the plots from August 21st, 2008 to November 13th, 2009 when most of the uplink telegrams were filtered.

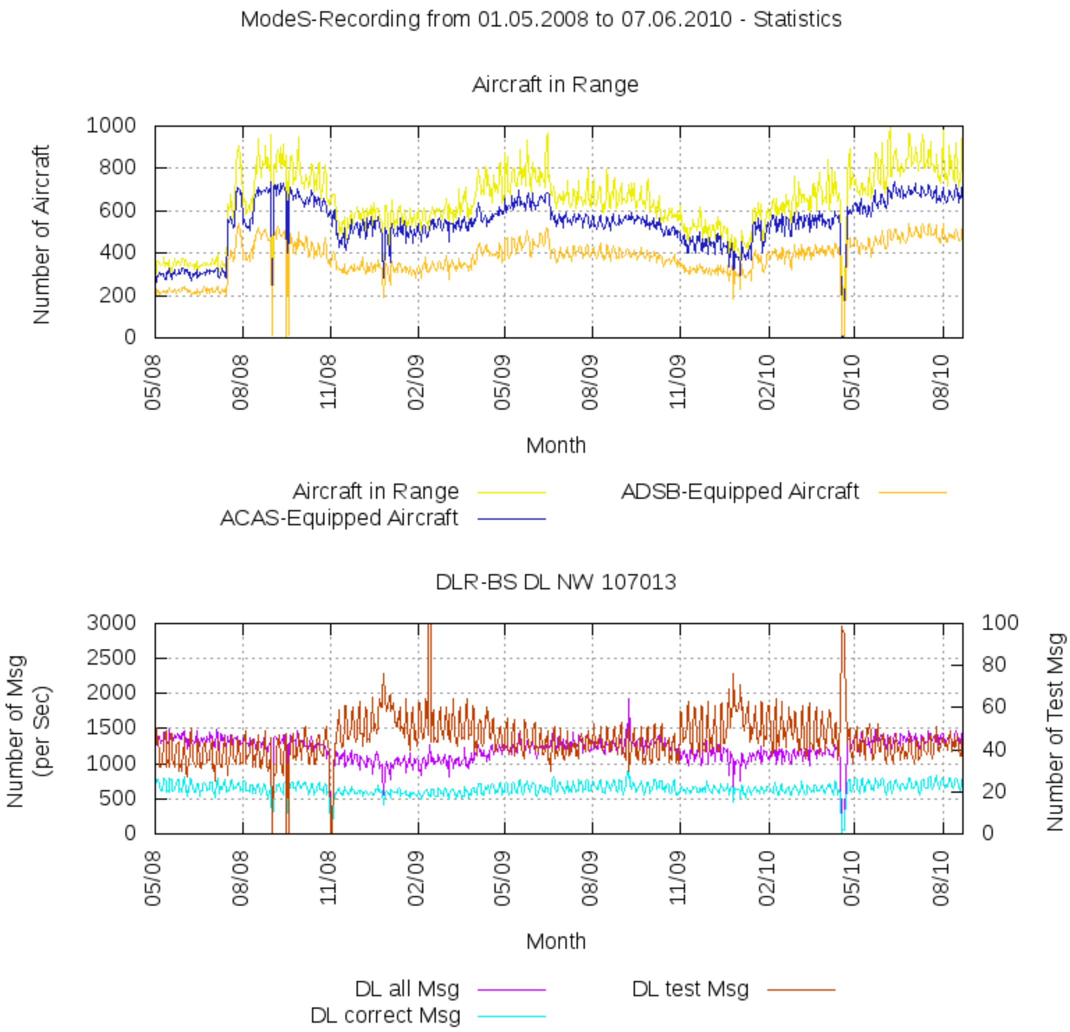

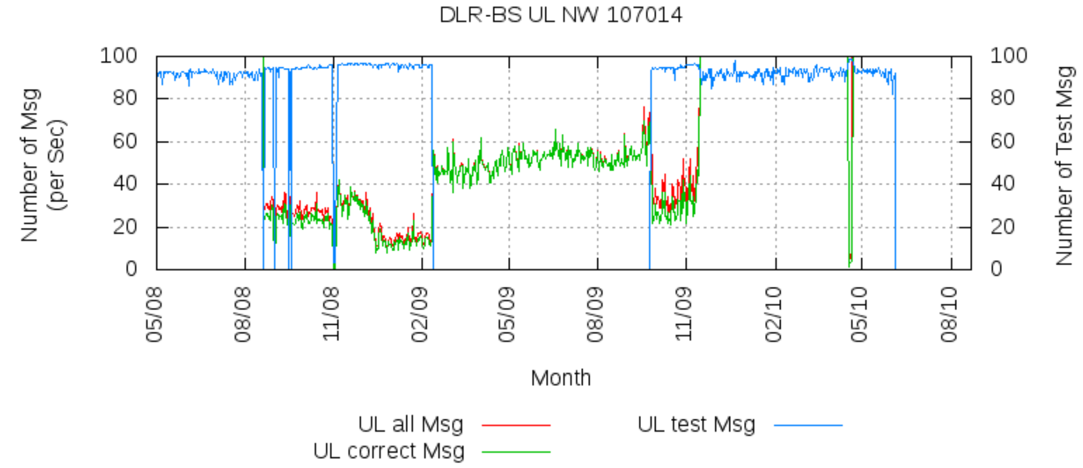
DLR-BS UL NW 107014
Number of Msg (per Sec)
Number of Test Msg
100
80
60
40
20
0
05/08
08/08
11/08
02/09
05/09
08/09
11/09
02/10
05/10
08/10
Month
UL all Msg
UL test Msg
UL correct Msg

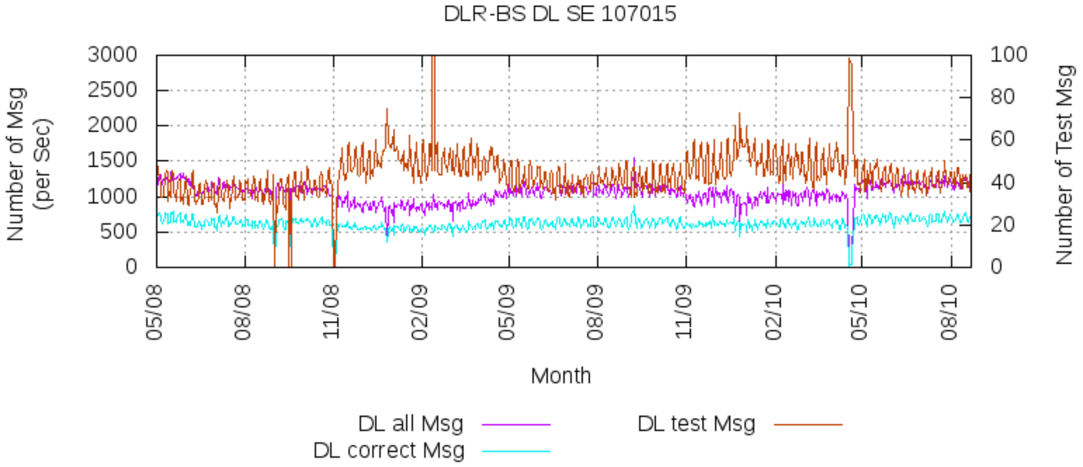
DLR-BS DL SE 107015
Number of Msg (per Sec)
Number of Test Msg
3000
2500
2000
1500
1000
500
0
100
80
60
40
20
0
05/08
08/08
11/08
02/09
05/09
08/09
11/09
02/10
05/10
08/10
Month
DL all Msg
DL test Msg
DL correct Msg

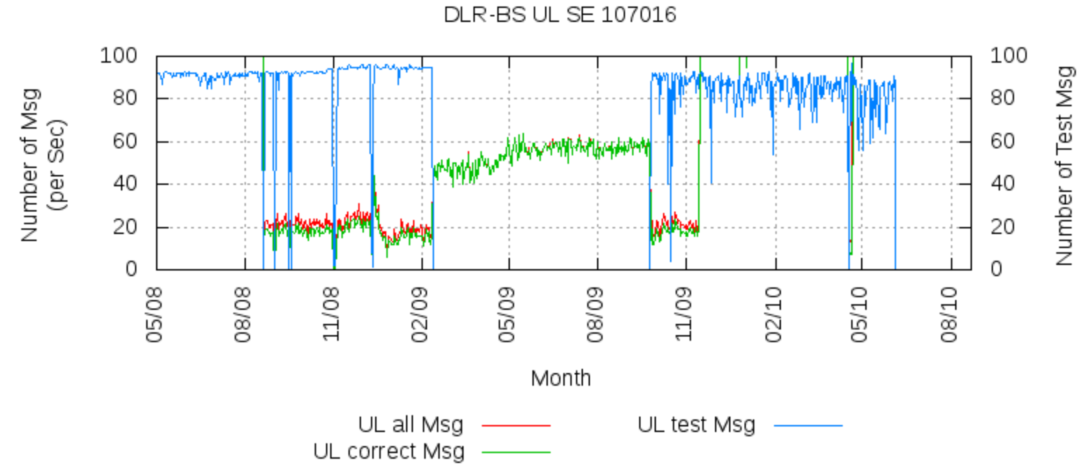
DLR-BS UL SE 107016
Number of Msg (per Sec)
Number of Test Msg
100
80
60
40
20
0
05/08
08/08
11/08
02/09
05/09
08/09
11/09
02/10
05/10
08/10
Month
UL all Msg
UL test Msg
UL correct Msg

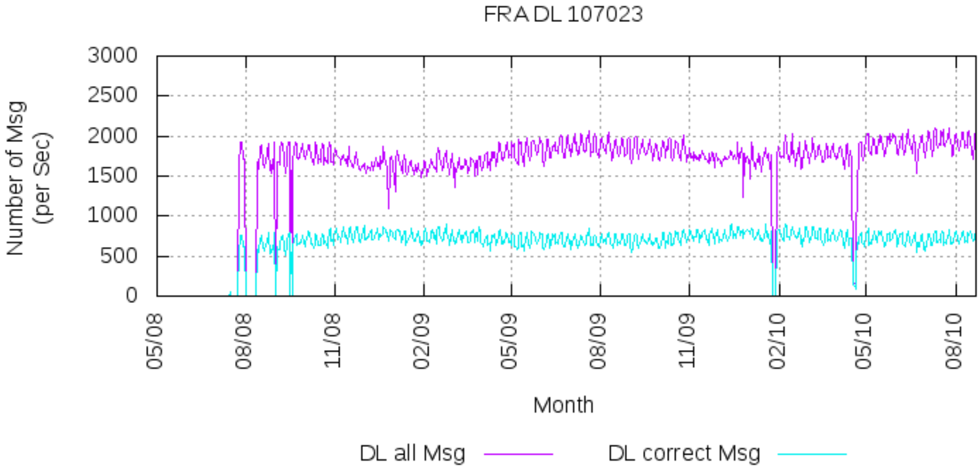
FRA DL 107023
Number of Msg (per Sec)
3000
2500
2000
1500
1000
500
0
05/08
08/08
11/08
02/09
05/09
08/09
11/09
02/10
05/10
08/10
Month
DL all Msg
DL correct Msg

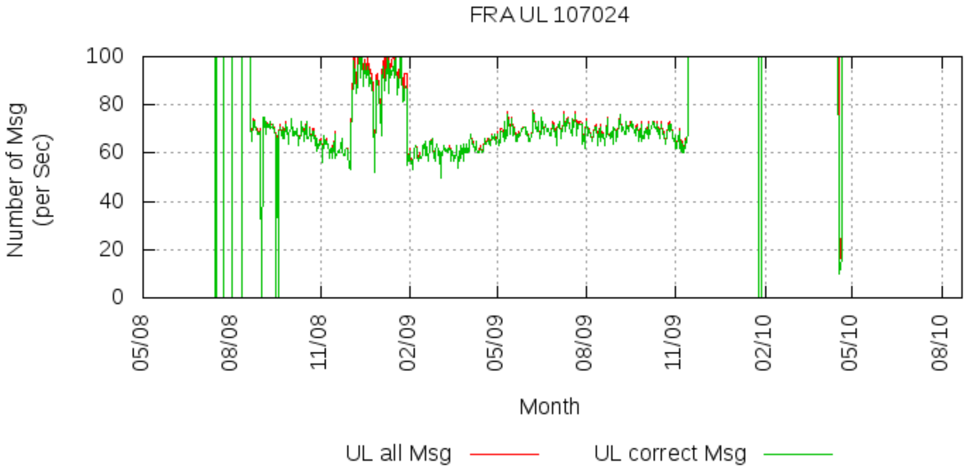
FRA UL 107024
Number of Msg (per Sec)
100
80
60
40
20
0
05/08
08/08
11/08
02/09
05/09
08/09
11/09
02/10
05/10
08/10
Month
UL all Msg
UL correct Msg

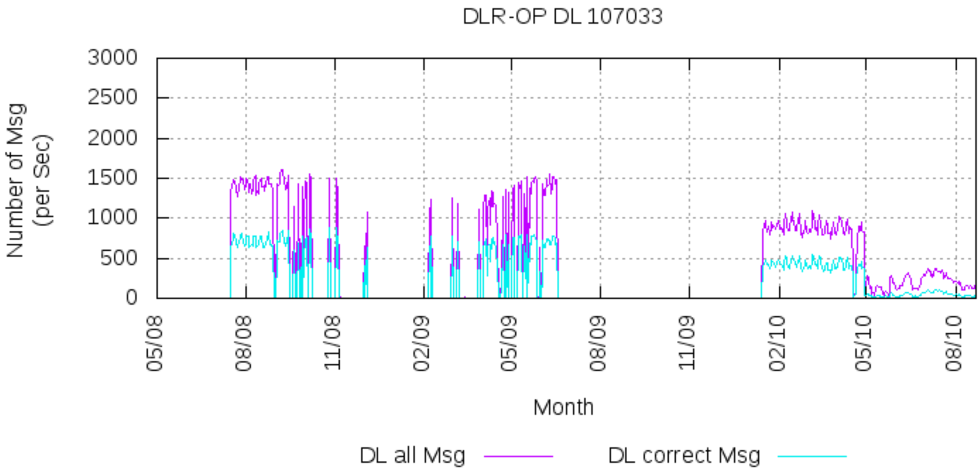
DLR-OP DL 107033
Number of Msg (per Sec)
3000
2500
2000
1500
1000
500
0
05/08
08/08
11/08
02/09
05/09
08/09
11/09
02/10
05/10
08/10
Month
DL all Msg
DL correct Msg

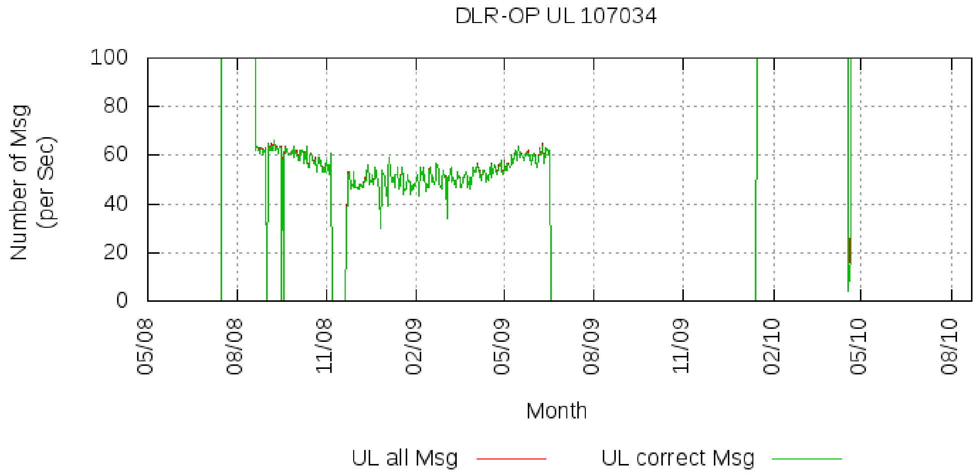

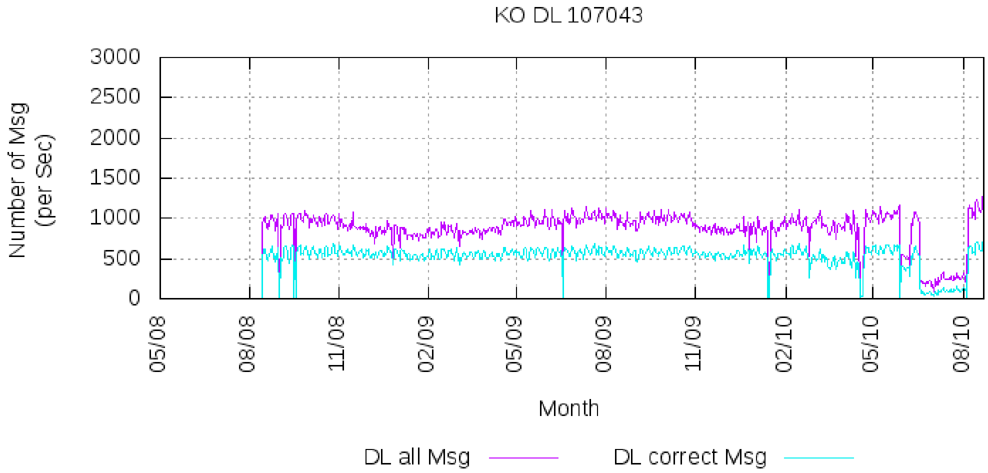

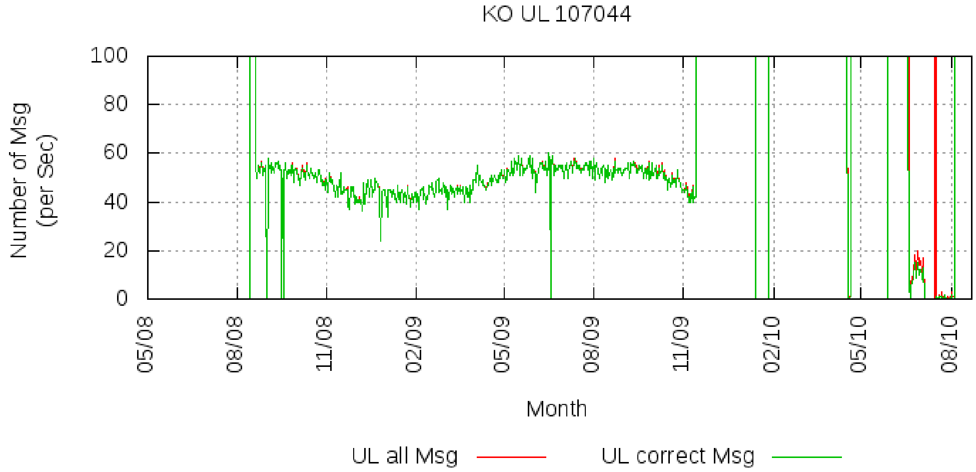

Figure 3-85: Statistics over a long time period, y-axis on uplink messages rescaled

3.2.3.4 Signal Amplitudes

The receiver stations include a basic signal amplitude measurement facility, i.e. for every Mode S message the signal amplitude is recorded by the station. The means of measurement as well as the scaling differ significantly for the uplink and downlink receivers. The receiver manufacturer has not documented details on how the signal amplitude is measured. For the MOSTDONT measurements the Braunschweig receiver stations were calibrated with defined input signals. The calibration curve of the Braunschweig station was then taken to compute dBm-like values for the other receivers. *Note: This process cannot replace individual calibration, and the results of the Non-Braunschweig stations have to be considered as being non-calibrated.*

As an example, one day was chosen on which all the reception facilities of the TU Braunschweig were in operation. Arbitrarily, the choice fell on April 25th 2010, as it is shown in Figure 3-86.

The charts plot the number of messages per second with given amplitude. The graph was computed by counting the number of messages for each signal amplitude value from 11 a.m. to 12 a.m. UTC on that specific day. The hourly rates were divided by 3,600 to obtain the average number of messages per second.

The characteristic zigzag shape is likely to be due to the amplitude quantisation and computation within the receiver.

The low numbers of messages in Braunschweig can be explained with a fault in the downlink channel, which was later determined and eliminated. The current signal amplitude statistics from Braunschweig are shown in Figure 3-87.

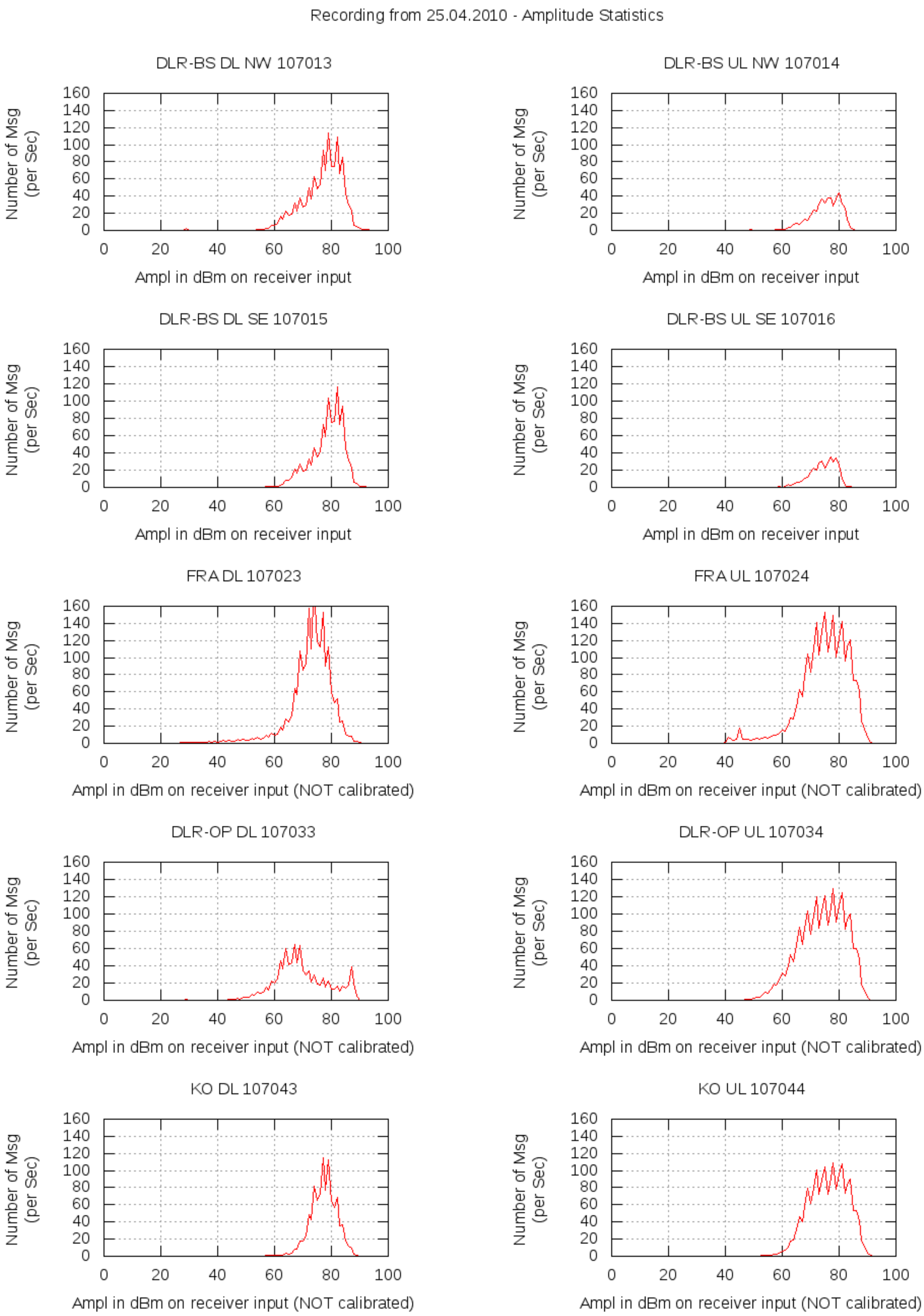

Figure 3-86: Amplitude statistics

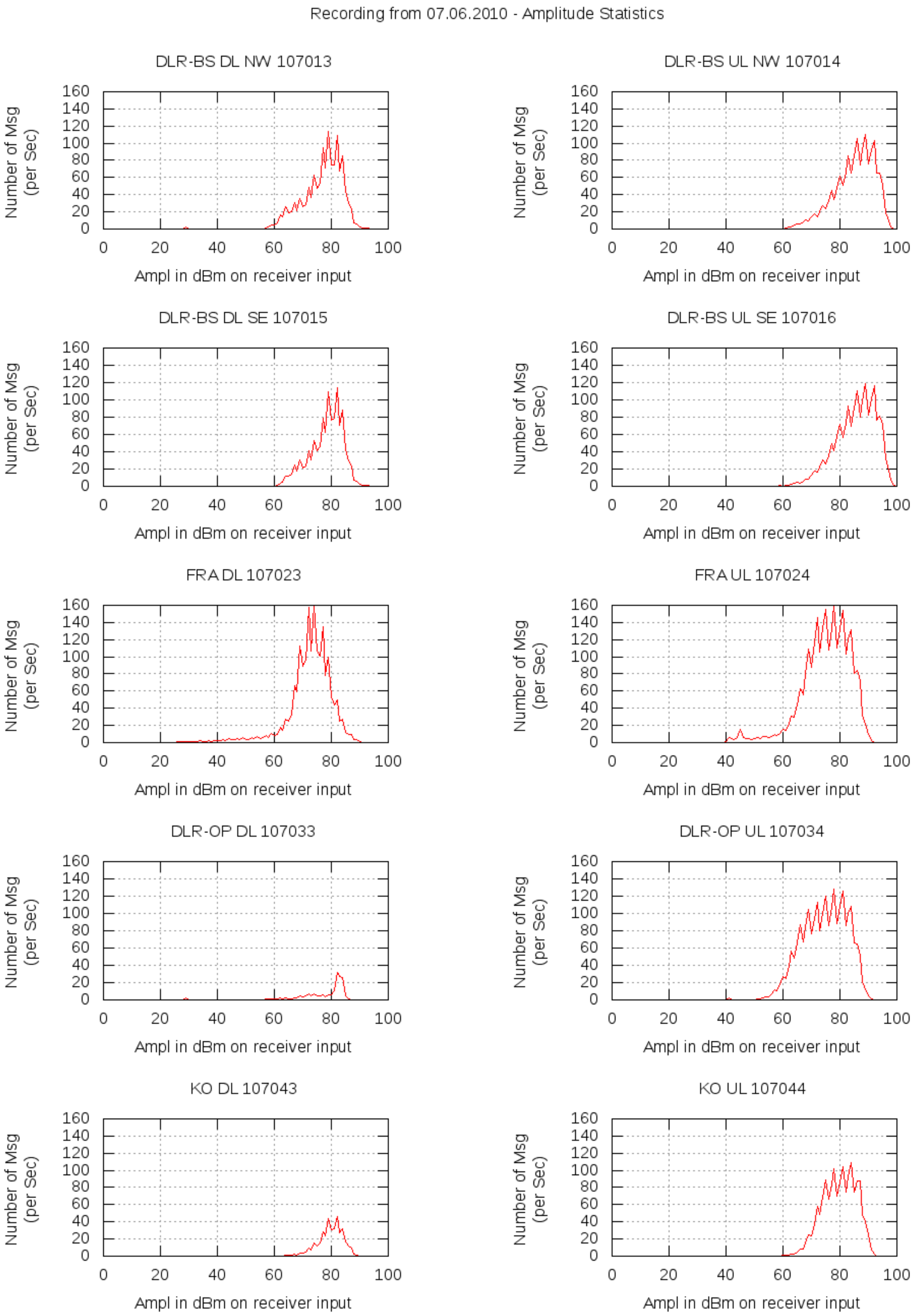

Figure 3-87: Amplitude statistics from Braunschweig, fully functional downlink channel

Figure 3-88 shows the distribution of Uplink and Downlink formats. Apparently, the main source of radio load is caused by TCAS with its UF00/DF00 surveillance interrogations.

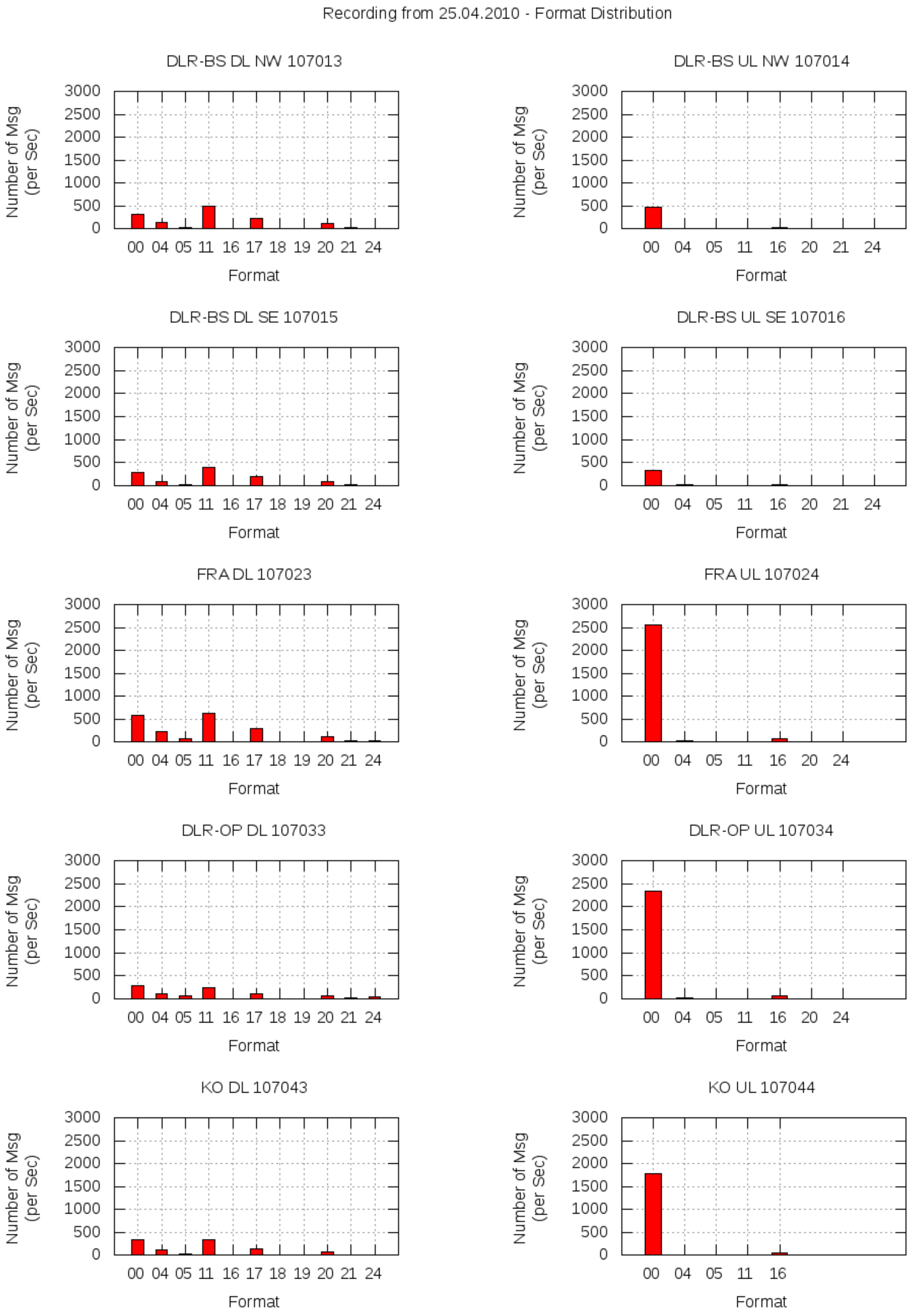

Figure 3-88: Format Distribution

Unfortunately in Figure 3-88 the Braunschweig stations were subject to a malfunction, which caused the low number of Uplink messages. In May 2010 this was corrected and the number of received messages in the Uplink channel achieved values almost as high as in Frankfurt as shown in the following figure:

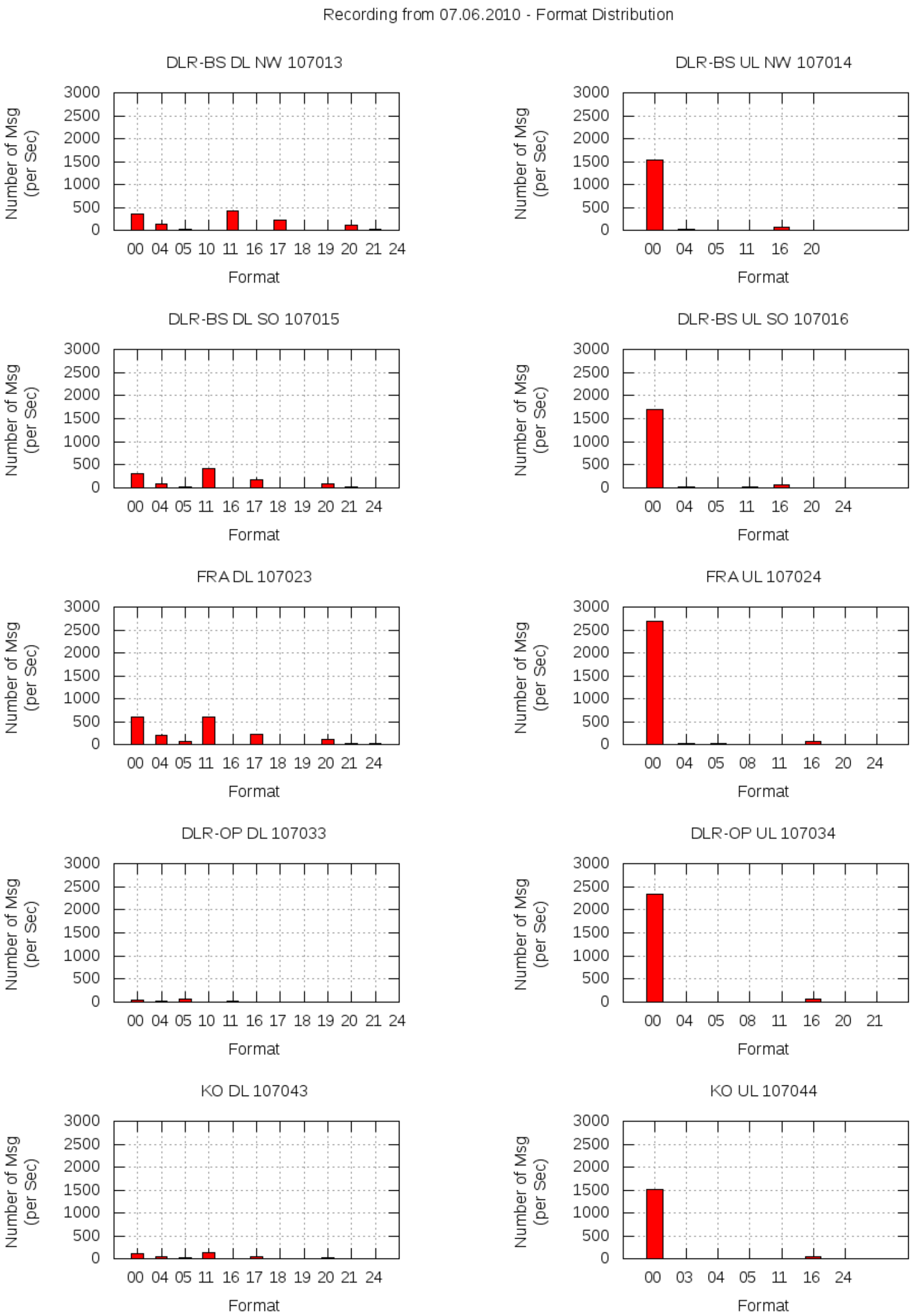

Figure 3-89: Format Distribution (normal function)

On this day, however, both the downlink receiver in Oberpfaffenhofen and the Korntal installation was undergoing maintenance work.

3.2.4 Summary of Findings

Figure 3-84 shows that Figure 3-83 is a good example for daily radio load statistics representing the current channel load as observed on a longer period. The daily statistics show that Mode S ground station reception probability decreases as radio load on the channel increases. During daytime the reception probability of weak Mode S signals (-80 dBm) in the 1090 MHz channel is dropping to 40%.

Since radio load is an issue, it is not advisable to further increase the radio load by introducing new applications on the 1030 MHz and 1090 MHz channels. Higher radio load causes more messages to interfere with each other, and therefore in high radio load regions more sensitive receivers might yield even less readable messages. This is also shown by Figure 3-87 which shows that most messages are below the level of -80 dBm.

Figure 3-88 shows that on the downlink channel, main contributors to the channel load are TCAS (DF00), responses to all calls (DF11) – induced by TCAS and ground interrogators including MLAT – and extended squitters (DF17) with ADS-B information. The uplink channel is predominantly used for TCAS interrogations (UF00).

TCAS is the main contributor to channel load, followed by ADS-B. It is therefore advised to perform detailed radio load impact analysis when considering the broadcast of additional information through extended squitter messages in order to protect the quality of service of legacy and new ATC 1030/1090 MHz based surveillance systems.

3.3 Side Lobe Suppression

3.3.1 Theory of Operation

Depending on the radar antenna design, transmissions from a radar station may be present not only in the main beam dwell (the so-called boresight, i.e. the direction towards which the antenna is pointing) but also at some angles off the centre line. Although these side-lobe transmissions have a significantly lower power, a transponder may still receive these interrogations and reply. This causes unwanted load on the downlink channel and must thus therefore be prevented.

In Mode A/C, such unwanted replies to side lobe interrogations are avoided by transmitting with a separate, non-directional antenna a P2 pulse with each interrogation that is weaker than the interrogation's P1 pulse inside the main beam dwell but stronger than any P1 on the side lobes.

For Mode S, P2 is transmitted as part of the interrogation at the same level as P1. While a pure Mode A/C transponder will interpret this as a side lobe interrogation and not reply, a Mode S transponder sees this as the beginning of a Mode S interrogation and waits for the P6 pulse that contains the Mode S data.

Therefore, a different method for side lobe suppression is applied for Mode S interrogations: A P5 pulse is generated (again, from a different, non-directional antenna) that lies on top of the sync phase reversal (SPR) part of the P6 pulse.

If the P5 pulse is weak compared to the interrogation (this is the case inside the main beam dwell), this will have little effect on the signal. However, if P5 is stronger than P6, the SPR will be distorted up to a point where a transponder is not able to correctly detect it. This is called "masking the SPR".

This distortion occurs because the P5 pulse is not phase-aligned with P6. But as the next sub-section shows, the change in phase signal will vary with each interrogation, depending on the exact phase-relation between P5 and P6. This relation varies depending on the target's bearing, altitude, and distance and cannot be limited by the radar station in any way.

3.3.2 P5 Effects on Sync Phase Reversal

Depending on the phase relation between P6 and P5, different amplitude and phase curves will result. The following pictures show the time span shortly before start of P5 until shortly after end of P5. *Note: The SPR in these figures is located at 6.2 ns.*

The normalized strength of P6 is set at 100% and that of P5 is set at 150%. The SPR duration is set at approx. 80 ns.

Without any P5, the amplitude and phase curves of P6 will then have the following form:

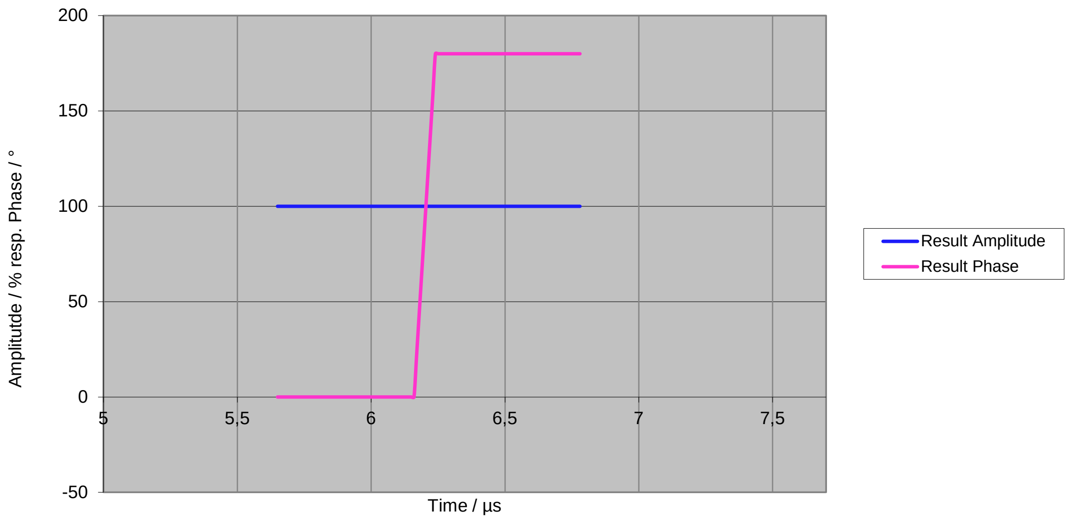

Figure 3-90: P6 Amplitude and Phase without P5

With P5 at a level of 150% and having the same phase as P6, the resulting amplitude will first rise to 250% (sum of P6 and P5). After the SPR, the two pulses have opposite phases, so the resulting amplitude will be the difference, i.e. 50%, until P5 ends. Then, the resulting amplitude will be back to 100%.

The resulting phase curve will first remain steady as both P5 and P6 have the same phase. After the SPR, the strong P5 signal will still dictate the resulting phase which will thus be the same as before the SPR. During SPR, however, a small change in phase will occur. The reversal to 180° will be delayed until P5 ends.

The following figure shows the simulated results:

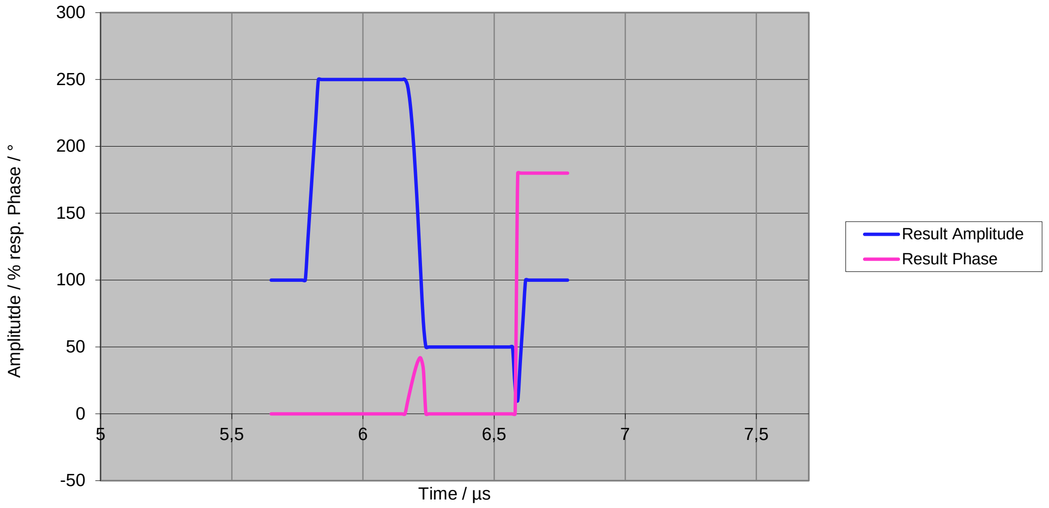

Figure 3-91: P5 with same phase as P6

If P5 has the exact opposite phase of P6, this picture is inverted. Now, the phase reversal will occur directly when P5 starts. Then, the SPR will cause a short variation of phase but well below 180°:

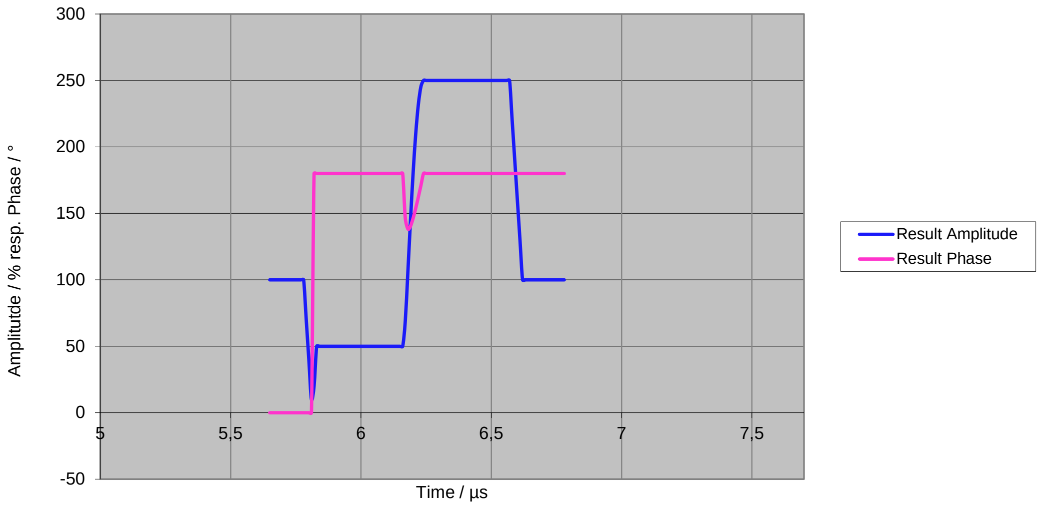

Figure 3-92: P5 with 180° phase difference vs. P6

If the phase difference between P5 and P6 is set at 90°, the phase curve will contain three steps. The start of P5 will cause an increase of approx. 55°. The SPR will then cause another 70° and the remaining 55° occur at the end of P5:

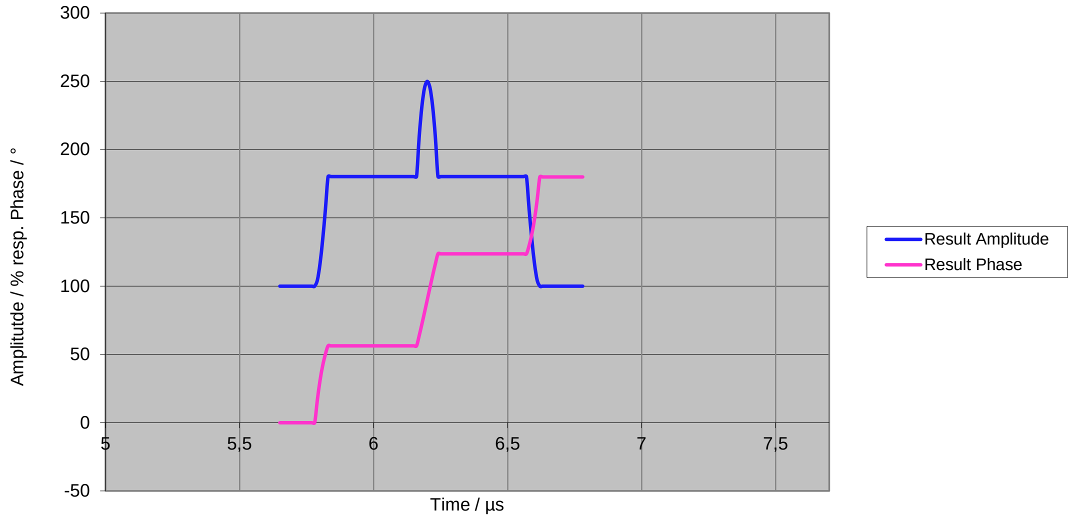

Figure 3-93: P5 with 90° phase difference vs. P6

This is a significant observation since such a signal might not be suppressed by a transponder that accepts the 70° phase shift as the trigger point for the SPR. In this case, the side lobe suppression will not work and the transponder will reply.

There are numerous other curves depending on the combination of P5 pulse strength and phase relation vs. P6 as shown in the following sample plots:

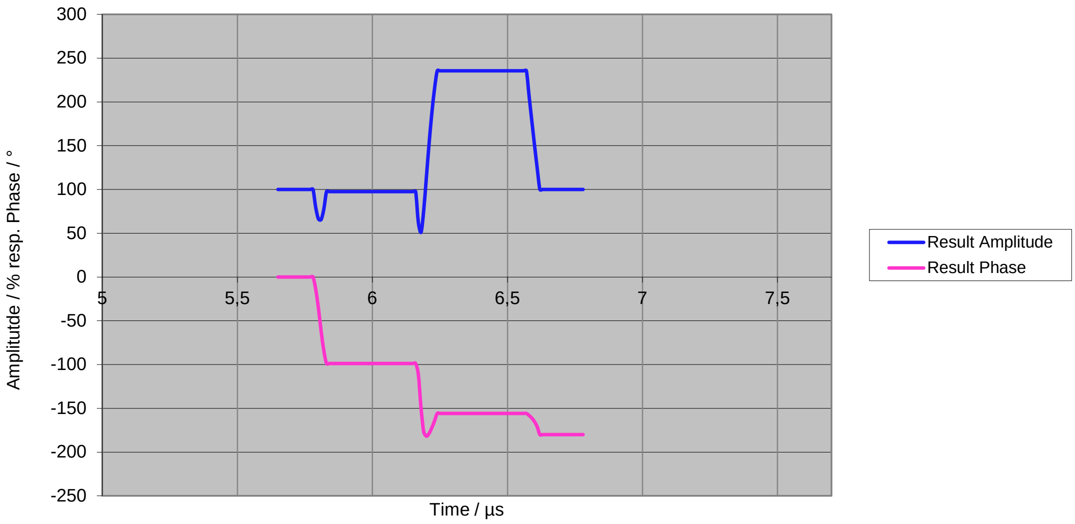

Figure 3-94: P5 with 220° (= –140°) phase difference vs. P6

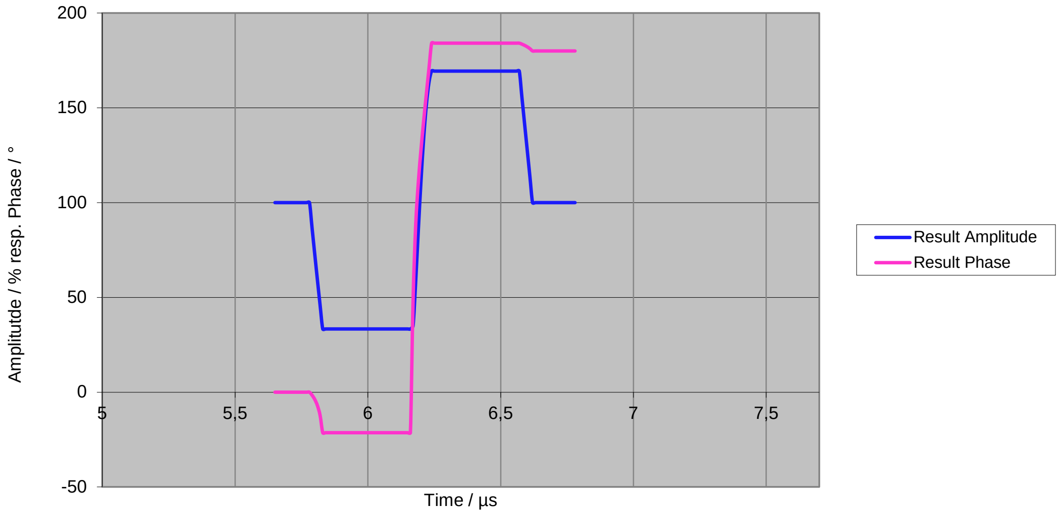

Figure 3-95: P5 at 70% of P6 with 190° phase difference

As stated above, any phase relation between P5 and P6 is possible. This will depend on the aircraft's bearing from the radar station, its altitude, and its distance. There is no means by which a radar station can control what phase relation is present at the receiver location.

3.3.3 Measured Signals-in-Space

The following plots are samples for actual side lobe suppression as received in the air. Although several real-life distortions are visible, the principle curves as gained from the simulation can be observed. (The blue line is the amplitude, the magenta line the phase.)

The first plot shows a P5 with approx. 30° phase difference vs. P6. The three-step change of phase is clearly visible. The simulated plot (shown next to the measured curves) looks very similar:

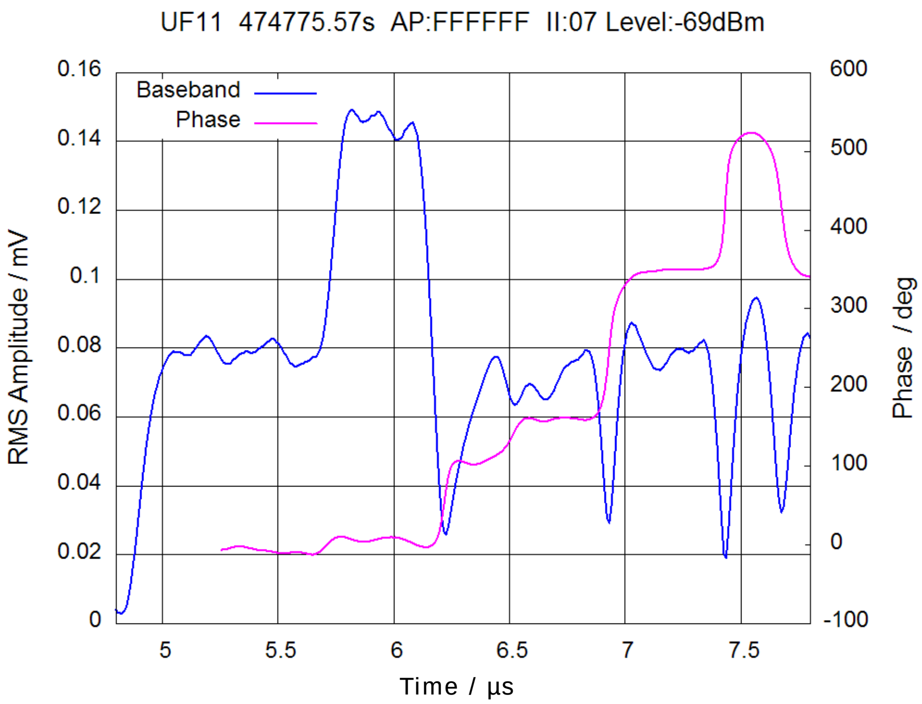

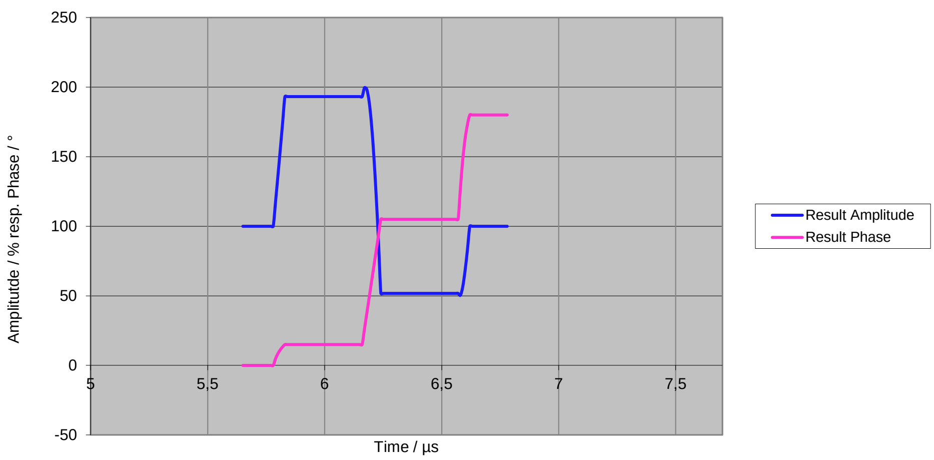

Figure 3-96: P5 with approx. 30° phase difference

In the next plot, the phase difference is approx. 170° and P5 is not much stronger than P6. With a simulated strength of 100 (same as P6), the simulated plot provides a very close match to the measured signal. In this case, the phase change at the SPR position is still approx. 90° which may be large enough for a transponder to accept this interrogation.

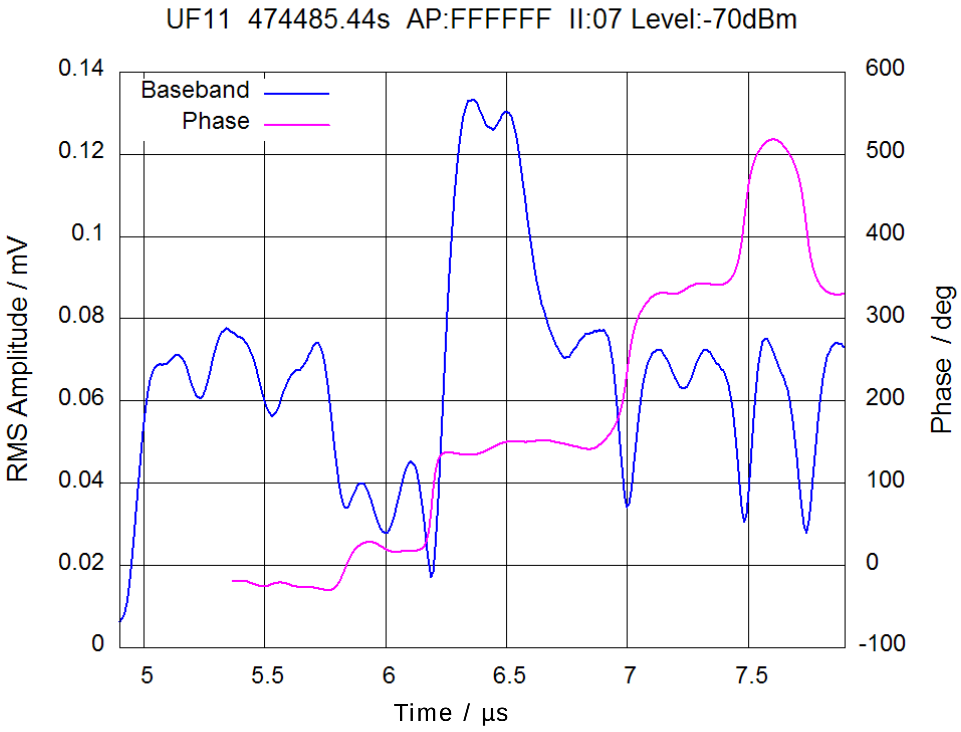

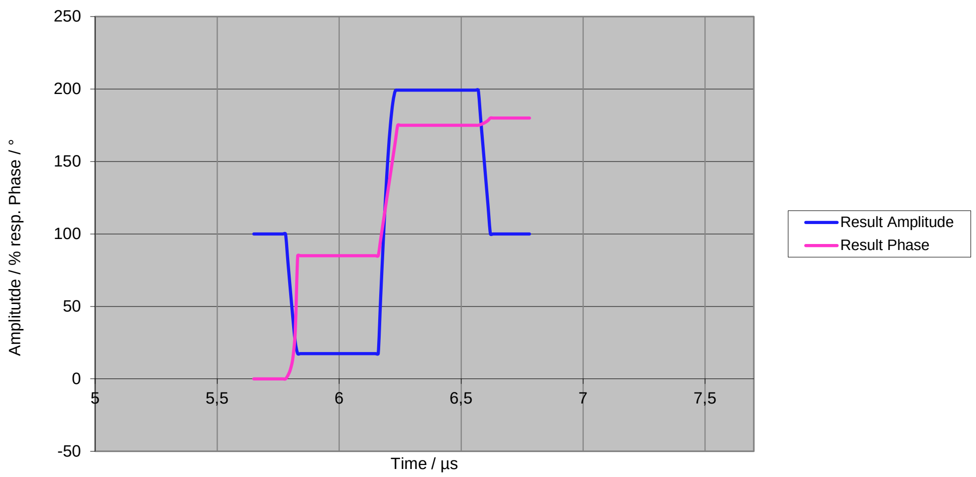

Figure 3-97: P5 at same level as P6 with approx. 170° phase difference

There are even cases where the phase change during SPR exceeds 180° due to the P5 pulse:

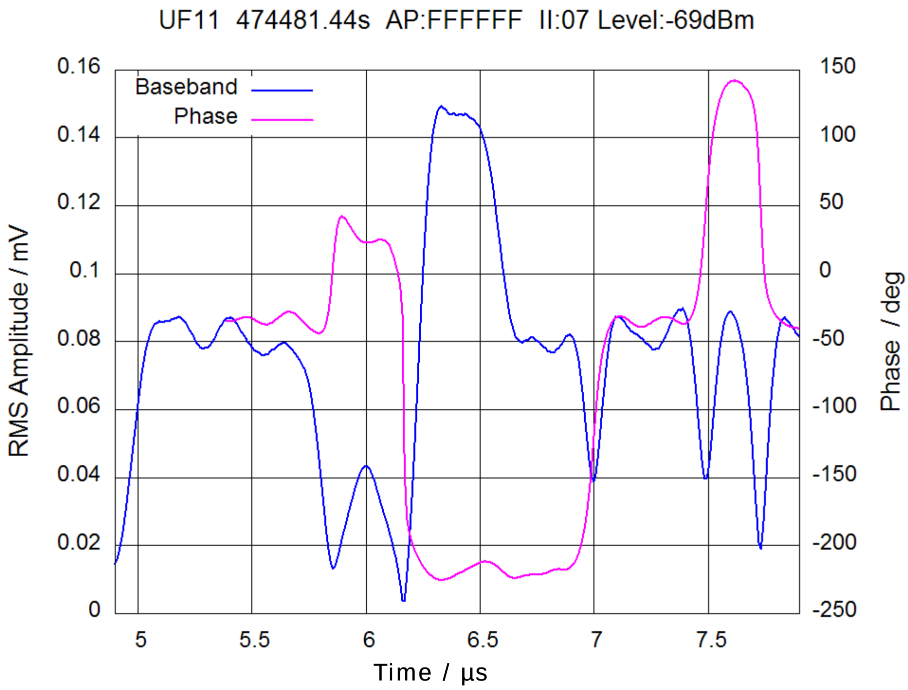

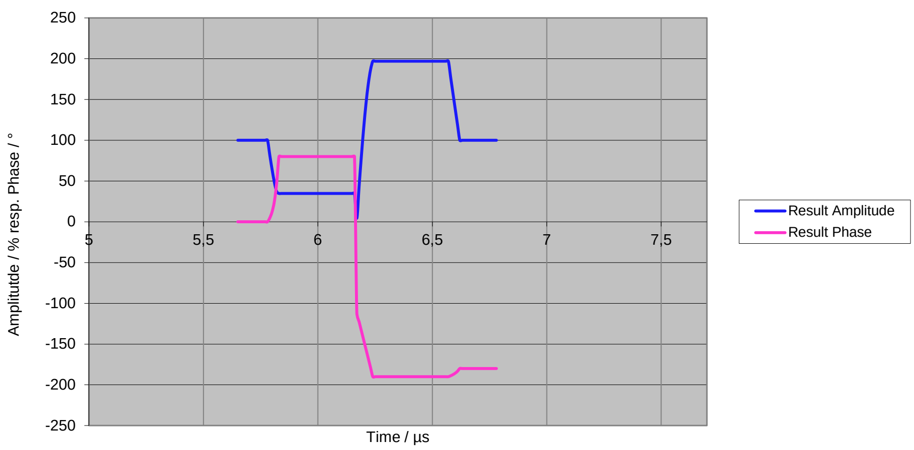

Figure 3-98: P5 at same level as P6 with approx. 160° phase difference (P6 turning anti-clockwise)

3.3.4 Discrepancies in Specifications

The side lobe suppression requirements as given in ED-73C do not provide details on how a transponder is expected to behave under certain circumstances.

The required reply behaviour for Mode S side lobe suppression with a difference between P5 and P6 in the range -12 dB to +3 dB is not defined, at all:

3.8.3 Side Lobe Suppression, Mode S Formats

a. Side lobe suppression for Mode S formats is characterised by the reception of P5 overlaying the location of the sync phase reversal of P6.

b. Given an interrogation which would otherwise require a reply, the transponder shall

(1) have a reply ratio of less than 10% at all signal levels between MTL+3dB and -21 dBm, if the received amplitude of P5 exceeds the received amplitude of P6 by 3 dB or more;

(2) have a reply ratio of at least 99% at all signal levels between MTL+3dB and -21 dBm, if the received amplitude of P6 exceeds the received amplitude of P5 by 12 dB or more.

NOTE: *The P5 pulse inhibits recognition of the sync phase reversal so that further decoding of the interrogation does not take place. There is, therefore no reply, but the transponder does not enter the suppression state.*

One may believe that there is a gradual transition from no reply (at +3 dB) to 100 % replies (at -12 dB). But this is actually not specified and a transponder would be fully compliant even if it did not reply to any interrogation with a P5 at P6 - 11 dB.

Even more problematic is that ICAO Annex 10, Volume 4 uses a different set of requirements:

3.1.2.1.5.2.5 *Pulse amplitudes*. The amplitude of P_2 and the amplitude of the first microsecond of P_6 shall be greater than the amplitude of P_1 minus 0.25 dB. Exclusive of the amplitude transients associated with phase reversals, the amplitude variation of P_6 shall be less than 1 dB and the amplitude variation between successive chips in P_6 shall be less than 0.25 dB. The radiated amplitude of P_5 at the antenna of the transponder shall be:

a) equal to or greater than the radiated amplitude of P_6 from the side-lobe transmissions of the antenna radiating P_6; and

b) at a level lower than 9 dB below the radiated amplitude of P_6 within the desired arc of interrogation.

This clearly defines the maximum level of the P5 pulse within the desired arc of interrogation at -9 dB below the P6 pulse amplitude.

These two different specifications are in clear contradiction. A transponder is fully compliant with ED-73C if it does not reply to any interrogation where a P5 pulse of, e.g. -11 dB compared to P6 is present. A radar station, however, would be compliant to ICAO Annex 10 if it sets the P5 level to -10 dB compared to P6. The result would be two devices fully compliant to their respective standards that will not work together.

3.3.5 Summary of Findings on Side-Lobe-Suppression

Unlike SLS for Mode A/C, where a simple comparison between the level of two pulses (P1 and P2) will allow a clear distinction between main lobe and side lobe interrogations, the SLS for Mode S is more complex.

It is not possible for a transponder to measure the level of the P5 pulse and compare it with that of the P6 pulse. Instead, the SPR quality (i.e. the duration of the phase reversal and its correct point of time within P6) will decline as the level of P5 increases. However, this distortion has a variety of different effects depending on the phase relation.

The problem is that similar distortions can occur as a result of multipath effects. A transponder that is optimised to handle disturbed interrogations (thus being less prone to multipath interference) will be more likely to reply to side lobe interrogations and vice versa.

Therefore, it is not practicable to specify (or rely on) any kind of behaviour of a transponder when P5 is with a certain "grey" area. There should be only one lower limit below which a P5 regardless of its phase relation to P6 will never have an effect strong enough to block acceptance by the transponder and an upper limit above which the SPR will be distorted so much that an acceptance is very unlikely (as demonstrated above, it is not possible to block ALL replies).

Testing compliance with these requirements, however, will only be possible if the test equipment is able to simulate any phase relation between P5 and P6. A test case should cover the entire range, e.g. in steps of 5° phase difference.

Another observation was made during analysis of ground recordings. Figure 3-70 to Figure 3-82 in section 3.2 show that a receiver which respects side lobe suppression (SLS) is still receiving some interrogations out of side lobes if reflections of the main beam weaken the effect of the SLS.

3.4 Laboratory Measurements

3.4.1 Test Equipment Signals

Three transponder test units were examined regarding the characteristics of their interrogation signals:

Figure 3-99: BF-Goodrich SDX-2000

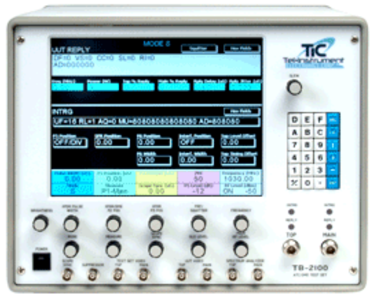

Figure 3-100: TiC TB-2100

Figure 3-101: Aeroflex IFR-6000

These units represent typical transponder test equipment that is used for both development and qualification testing (SDX-2000, TB-2100) and transponder ramp testing (IFR-6000).

Each unit provides slightly different capabilities, but all include means to test Mode S transponders with interrogation signals that include side lobe suppression pulses.

The following figures show the video signal of the interrogations created by these units:

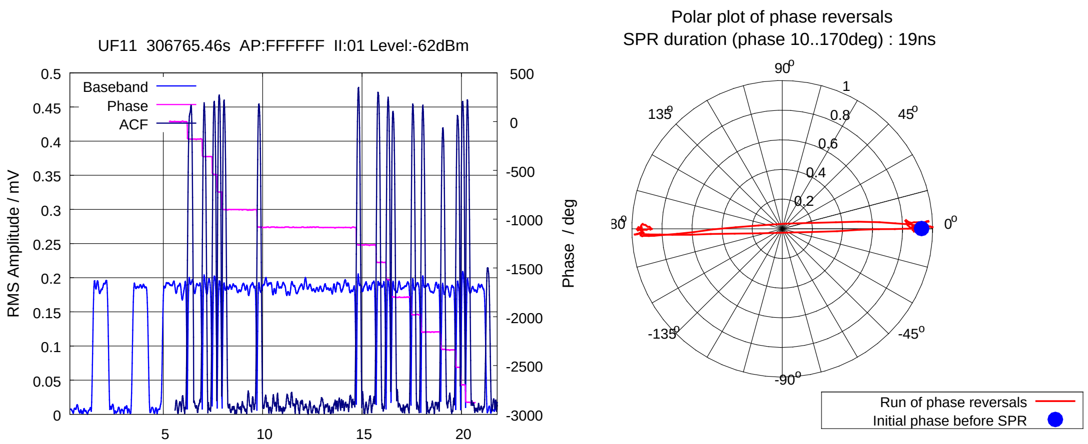

Figure 3-102: IFR-6000 (no P5)

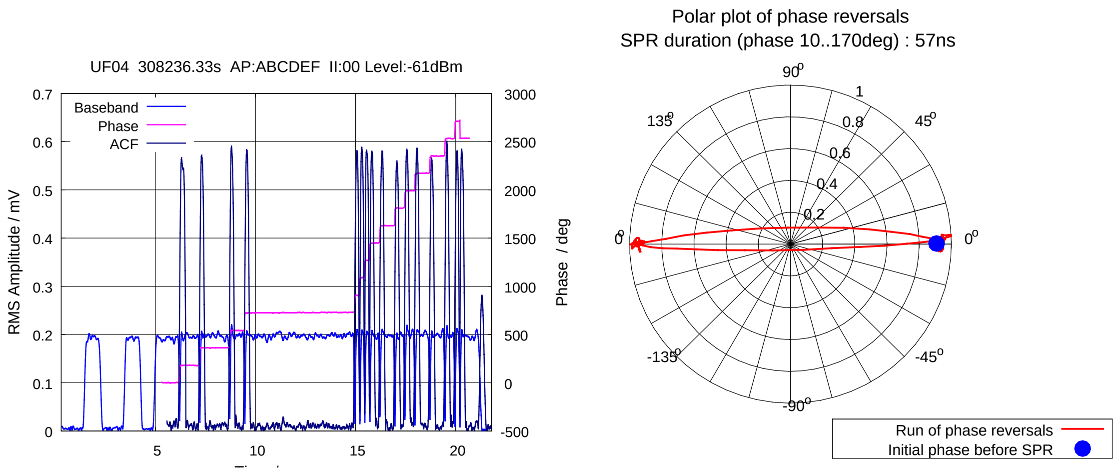

Figure 3-103: SDX-2000 (no P5)

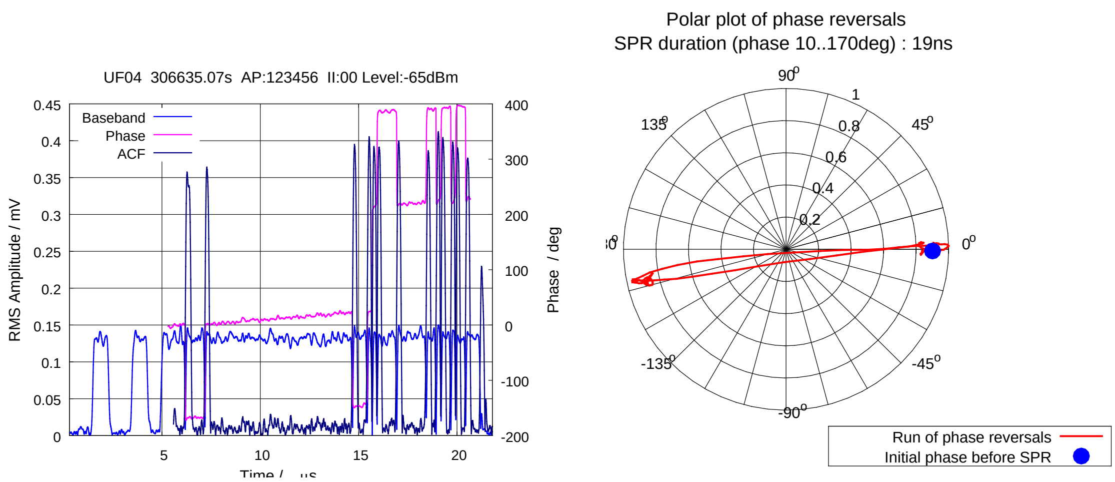

Figure 3-104: TIC-2100 (no P5)

These plots clearly show that all three units perform a fast phase shift with a complete amplitude drop to nearly zero. One can see from the polar plot that the tested TIC-2100 unit has a slight frequency offset. This is even more evident in the following figure that shows a complete interrogation:

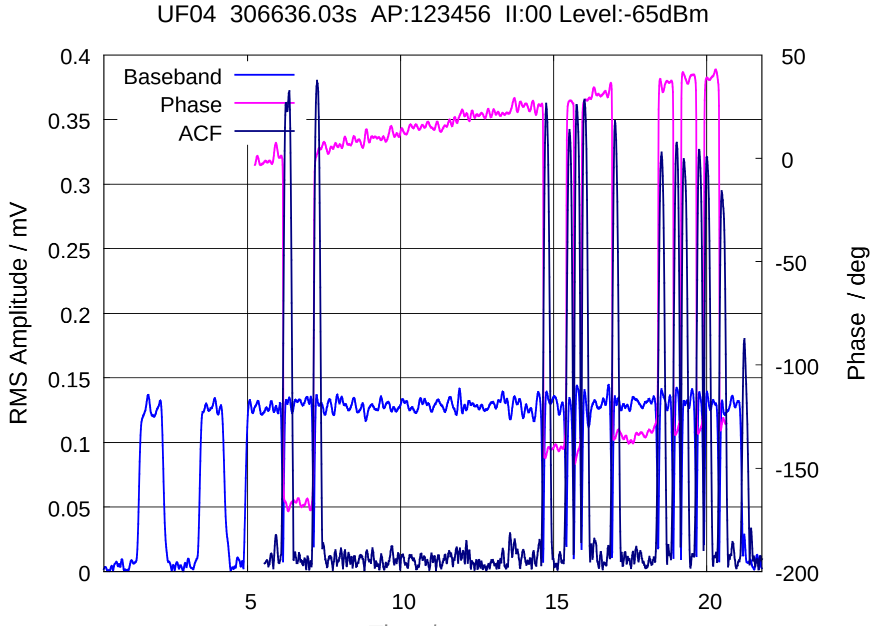

Figure 3-105: TIC-2100 Frequency Offset

This offset was calculated to be approx. 10 kHz and probably due to incorrect calibration.

Further investigation of the test signals, including activated side lobe suppression (SLS), revealed the following characteristics:

TB-2100:

- SPR duration approx. 28 to 57 ns
- SPR with almost complete amplitude drop to zero
- 3 different P5/P6 phase relations (slowly shifting over time)
- Frequency offset (approx. 10 kHz) on calibrated unit

SDX-2000:

- SPR duration approx. 38 to 57 ns
- SPR with almost complete amplitude drop to zero
- 7 different P5/P6 phase relations
- Phase change always in same direction

IFR-6000:

- SPR duration approx. 10 to 38 ns
- SPR with almost complete amplitude drop zero
- Phase change always in same direction
- SLS test not possible

Testing the SLS with the IFR-6000 was not possible as that unit only generates SLS signals when it is connected to a replying transponder. Since the test receiver cannot reply to interrogations, the IFR-6000 could not be triggered to generate interrogations with P5 SLS.

Apparently, none of these units is able to simulate the I/Q modulation technique (see section 3.1.2.4) that most radar stations apply. Referring to the phase reversal sequences defined in section 3.1.2.4.1, the following signatures apply for the test units:

TB-2100:	$b_k(1)$ with hard phase keying
SDX-2000:	$b_k(5)$ with hard phase keying
IFR-6000:	$b_k(6)$ with hard phase keying

Another important observation is that both the TB-2100 and the SDX-2000 have only a small number of possible phase-relations between P5 and P6 (the slow shift in this over time with the TB-2100 is most likely due to its 10 kHz frequency offset). This means that these devices would not support the test of any possible phase relation that was recommended in section 3.3.5.

3.4.2 Reply Rate Limiting

One aspect to be investigated by the study was a potential detrimental effect due to high interrogation rates that may cause a reduced reply rate on existing transponders.

Note: this only refers to interrogations that were correctly decoded and that required a reply from the transponder. The number of interrogations that a transponder receives and has to decode is much higher, see section 3.2.3 for those statistics.

The recorded data from WP2100 was analysed to determine the maximum reply rate required for a transponder at any given time. This analysis revealed that the number of interrogations to which a transponder had to reply (interrogations with broadcast address or interrogations addressed to the test aircraft) always stayed well below the ED-73C thresholds (e.g. 50 Mode S replies within 1 second). The maximum reply rate load during the flight trials was approx. 8 interrogations per second and even this for only very brief moments.

Nevertheless, the reply rate capabilities of three transponder types that are widely used in General Aviation were investigated.

3.4.2.1 Increased Mode A/C Reply Rate

- standard Mode A/C test
- starting at 1200 interrogations per second

  Note: Class 2 transponders (such as Transponder #1) are only required to have a capability of 1000 replies per second.
- then increasing at certain steps, recording the reply rate
- test equipment: SDX-2000

Interrogation Rate	Transponder #1	Transponder #2	Transponder #3
1200 / s	100 %	94 %	96 %
1250 / s	99 %	90 %	92 %
1500 / s	85 %	75 %	76 %
2000 / s	60 %	56 %	60 %
2400 / s	50 %	47 %	50 %

3.4.2.2 Increased Mode S Reply Rate

- 500 Mode A/C interrogations per second from one test equipment (TIC)
- starting with 50 Mode S interrogations (16 long) from other test equipment (SDX) – test condition according to ED-73C, section 3.4.2.b.1
- then increasing Mode S rate at certain steps, recording the reply rate and output power

Mode S Interrogation Rate	Transponder #1 [1)]	Transponder #2	Transponder #3
50 / s	100 %	100 % at 131 W	100 % at 77 W
60 / s	85 %	100 % at 131 W	100 % at 77 W
100 / s	51 %	100 % at 131 W	100 % at 75 W
200 / s	25 %	100 % at 131 W	100 % at 61 W

[1)]: output power remained constant (value not recorded)

Note: Measured power is approx. half of actual power due to test setup.

3.4.2.3 Mode S Reply Rate with increased Mode A/C Reply Rate

- 50 Mode S interrogations (16 long) from one test equipment (SDX)
- starting with 500 Mode A/C interrogations per second from other test equipment (TIC)
- then increasing Mode A/C rate, recording the reply rates for Mode A/C and Mode S

Mode A/C Interrogation Rate	Transponder #1		Transponder #2		Transponder #3	
	Mode S	A/C	Mode S	A/C	Mode S	A/C
500 / s	100 %	100 %	100 %	100 %	100 %	100 %
600 / s	100 %	100 %	100 %	100 %	100 %	100 %
1200 / s	100 %	100 %	100 %	95 %	100 %	97 %
2000 / s	100 %	60 %	100 %	58 %	100 %	- [1)]

[1)]: measurements varied between 50% and 100%, no stable value could be established

3.4.2.4 Mode S Reply Rate with increased Burst Rate

- 500 Mode A/C interrogations per second from one test equipment (TIC)
- one burst of 4 Mode S interrogations (2 long) within one second at an interrogation rate of 2500/s from other test equipment (SDX)
- then increasing number of messages in Mode S burst, recording the reply rate and output power

# of messages in Mode S burst	Transponder #1 [1)]	Transponder #2	Transponder #3
4	100 %	100 % at 131 W	100 % at 83 W
10	100 %	100 % at 130 W	100 % at 72 W
15	67 %	100 % at 127 W	100 % at 70 W
20	50 %	100 % at 122 W	100 % at 67 W
30	33 %	100 % at 109 W	100 % at 58 W
60	17 %	100 % at 81 W	100 % at 39 W
80	13 %	100 % at 67 W	100 % at 33 W

[1)]: output power remained constant (value not recorded)

Note: Measured power is approx. half of actual power due to test setup.

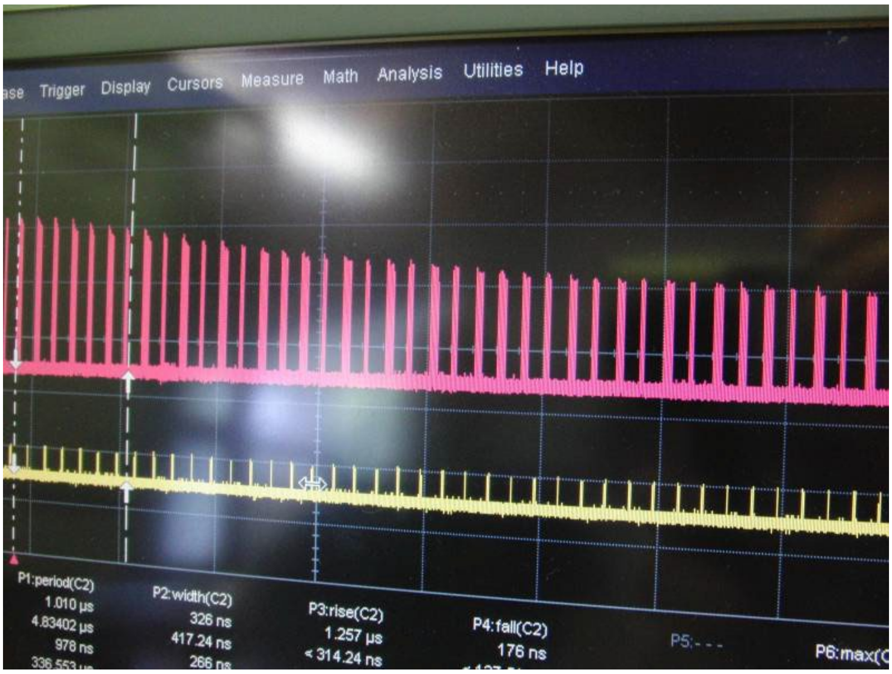

Figure 3-106: Reduction of Mode S Reply Power (Transponder#2)

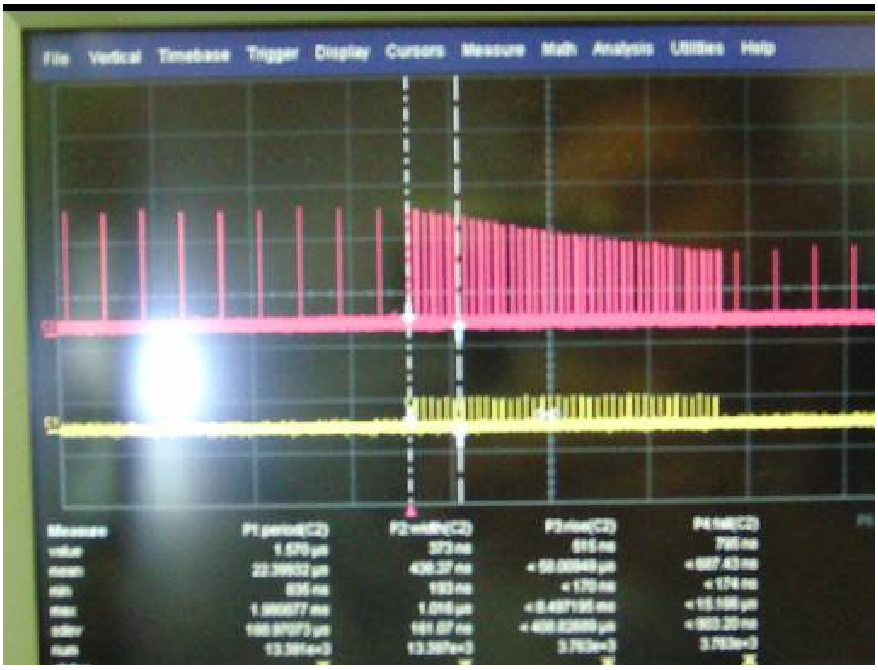

Figure 3-107: Reduction of Mode S Reply Power (Transponder #3)

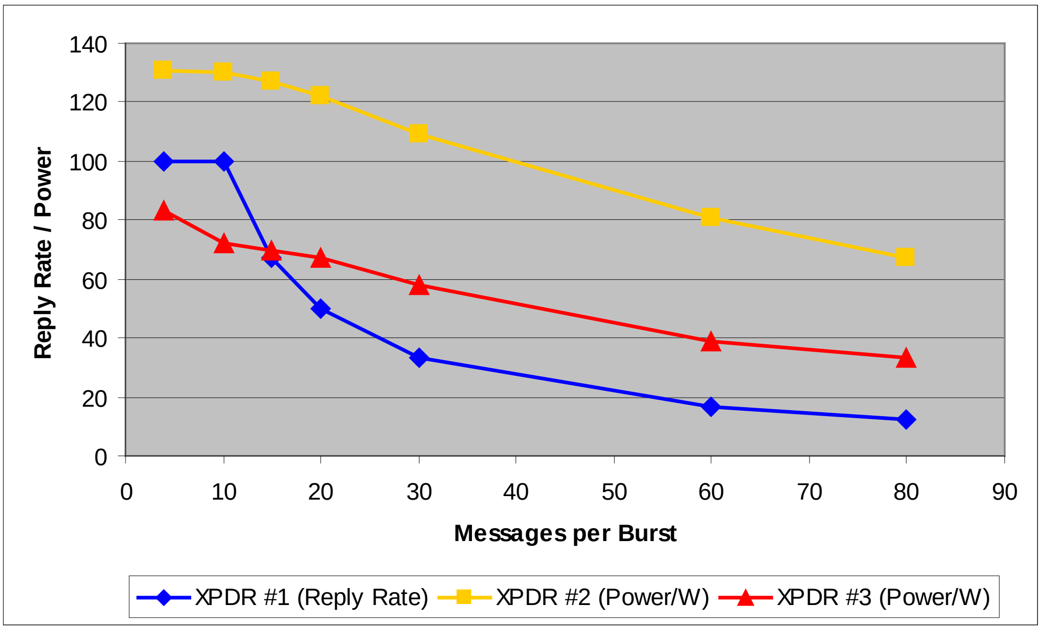

Figure 3-108: Transponder Reply Rate Limiting

3.4.2.5 Summary of Results

The tests clearly show that the three tested transponders exceed the requirements of ED-73C regarding their reply rate capabilities. Two units reduce their transmission power when the number of replies exceeds a certain threshold. The other transponder (#1) seems to have a hard-coded limit and does not reply to any excess interrogations.

The limits when performance starts to be degraded, however, are well above the maximum load observed during the MOSTDONT trials (by a factor of approx. 10). Therefore, reply rate limitation does not seem to be an issue of concern for transponder operation.

3.5 Interference of Radar and TCAS

3.5.1 TCAS Function and Communication

TCAS is an autonomous system on board of aircraft. This means that the TCAS-device itself on an aircraft must survey surrounding traffic. Upon detection of a collision risk, the TCAS-device issues a Resolution Advisory (RA) to its pilot.

Figure 3-109: Announcing of Addresses

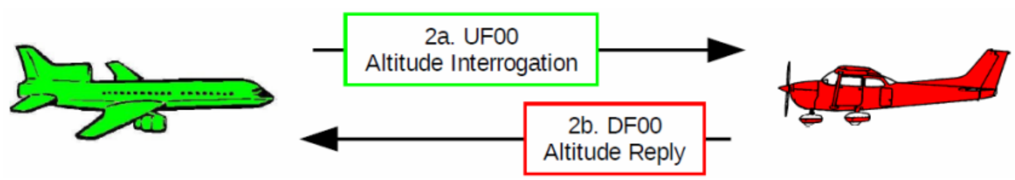

Figure 3-110: Green asking Red for its Altitude

The most important TCAS communications are shown in Figure 3-109 and Figure 3-110 and will be explained in the following paragraphs. The figures depict two aircraft, an airliner equipped with TCAS and therefore with Mode S and a General Aviation Aircraft equipped with Mode S.

A TCAS device monitors the presence of other aircraft by inquiring their Mode S secondary surveillance radar transponder; therefore TCAS uses the frequencies of the Mode S secondary surveillance radar 1030 MHz (Uplink) and 1090 MHz (Downlink) for all communication. Every Mode S equipped aircraft has a unique address and answers only if it is interrogated with this address. This way aircraft do not have to be addressed by pointing a narrow radar beam at them, but can be interrogated with individually addressed messages. This allows TCAS, which is not able to form a narrow beam, to communicate with surrounding aircraft. TCAS is also capable of surveying legacy aircraft with unaddressed Mode A/C (predecessor of Mode S) transponders in a less efficient way.

3.5.2 TCAS Surveillance

The TCAS device on an aircraft is autonomous, and therefore provides its own surveillance function. Firstly, an TCAS device must detect other aircraft in the vicinity. For this purpose every Mode S transponder regularly (up to 2 times a second) emits so called DF11-Squitter (Figure 3-109). DF is short for Downlink Format, which denotes a message in the 1090 MHz Downlink channel, 11 is the Format Number. If the aircraft is ADS-B equipped, it also emits a DF17-Squitter, a TCAS equipped aircraft also emits a so called UF16-32-TCAS broadcast (UF denotes the 1030 MHz Uplink channel, 32 the sub format). DF11, DF17 and UF16-32 all include the sender's address, and by this announce the address to surrounding aircraft.

If a TCAS knows about an aircraft in the vicinity, it can monitor it as shown in Figure 3-110. It sends UF00-Altitude-Requests which are answered by the Mode S transponder of the target with DF00-Altitude-Replies transmitting the current altitude. From the round trip delay of the message-pair TCAS computes the distance. TCAS starts a surveillance cycle every second.

TCAS can also estimate the bearing of the surveyed aircraft. This bearing estimate has a standard deviation of 5°. It is therefore only sufficient to display the other aircraft to the pilot on the horizontal situation display.

3.5.3 Test Approach

To find out whether the own aircraft is correctly recognised by surrounding traffic the natural approach would be to analyse the UF00 altitude interrogations. Unfortunately these do only contain the address of the target aircraft, not of the source. The reverse applies to DF00 altitude replies. So the surveyed aircraft (red) just replies to interrogations, no matter from where they come. The analysis of UF00 would only tell if an aircraft is surveyed, but not if everybody is surveying it.

Thus, UF16-32-TCAS broadcasts were recorded instead. The UF16-32-TCAS broadcast is sent via the top antenna every 8-10 s in all directions at full power.

The TCAS broadcasts are intended to let TCAS equipped aircraft in the vicinity know about the broadcasting TCAS aircraft, it is not read by a Mode S transponder. The UF16-32-TCAS broadcast contains the address of the sender. It is 112 bits long, while the UF00 is only 56 bit long; the UF16-32-TCAS broadcast is therefore more prone to superimposition by other signals.

If the experimental aircraft is able to receive UF16-32-TCAS broadcasts (which are longer and sent via the top antenna) from all aircraft in the vicinity, then these aircraft are also able to interrogate the experimental aircraft via UF00.

3.5.4 Radar Data

The positions of the other aircraft were taken from radar data supplied by LVNL for the time of the experimental flight. The data consists of ASTERIX CAT034 and ASTERIX CAT048 messages [http://www.eurocontrol.int/asterix].

The involved radars were:

Name	SAC-SIC	Latitude	Longitude
SCHIPOL_TAR_S	002-234	N52.31155694444	E4.7841725
RNLAF Volkel	025-176	N51.66012777777	E5.698294444444
RNLAF Twente	025-174	N52.27154444444	E6.900794444444
RNLAF Soesterberg	025-172	N52.13551666666	E5.276133333333
RNLAF Leeuwarden	025-170	N53.23206666666	E5.748738888888
RNLAF Woensdrecht	025-178	N51.45725277777	E4.352388888888

The data contains the position of radars and the plots of aircraft in polar coordinates relative to the radar. The plots of the different radars on the same aircraft were not merged to a system-track in the data.

For the analysis, the radar Soesterberg 025-172 was selected because it is in the centre of the analysed flight path. Within the obtained radar data the CAT048 was almost completely readable, 29 messages contained errors in the necessary data, while 3,609,507 were correctly read. Therefore, the extracted data is trusted.

3.5.5 Track Overview

The first Figure gives an overview of the radar range, the track of the research aircraft (Cessna 172 “D-EMWF”) and the traffic situation during an arbitrarily selected minute.

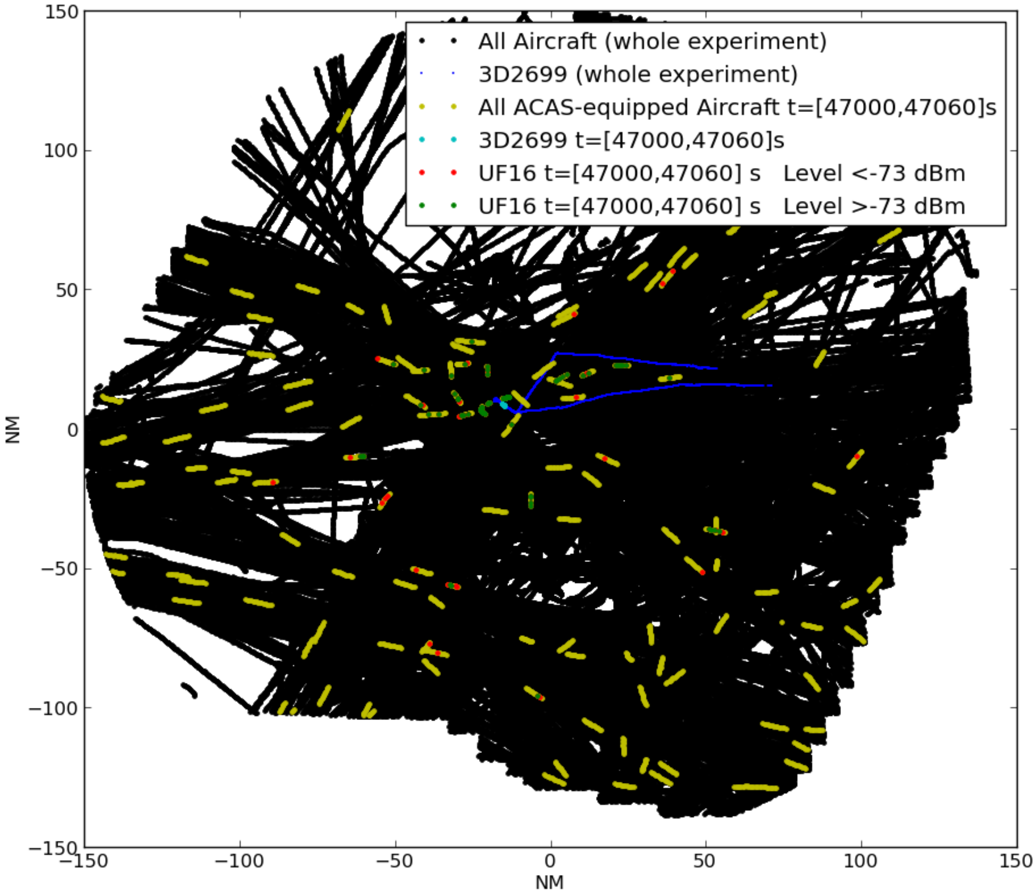

Figure 3-111: Overview of all tracks and tracks during one minute

Figure 3-111 combines CAT048 radar data from the Dutch radar RNLAF Soesterberg with 1030 MHz recordings taken with the on-board measurement antenna at the bottom side of the research aircraft. The axes are scaled in NM relative to the radar.

The black plots in the background show all aircraft (TCAS equipped and not TCAS equipped) that were in range of the radar during the recording period. This gives an impression of the range of the radar.

The thin blue radar track shows the research aircraft travelling though the range of the radar. Light blue are the plots of the research aircraft during the minute from 47000 s to 47060 s (seconds since midnight UTC). Shown in yellow colour are the radar plots of all the other TCAS equipped aircraft during that period.

The green plots indicate the positions of aircraft when sending UF16-32-TCAS broadcasts which were received by the research aircraft and which had a level stronger than -73 dBm – these would be read by a Mode S transponder. Shown in red colour are the positions of aircraft when sending UF16-32-TCAS-Broadcasts, that were received with a level weaker than -73 dBm, the research equipment is able to read them, a transponder is not.

Figure 3-111 indicates that some tracks of TCAS equipped aircraft do not contain any UF16-32-TCAS-Broadcasts. The question arises, if these are relevant for the function of TCAS.

3.5.6 Altitude of Research Aircraft

To understand the following graph it has to be noted that the research aircraft as a General Aviation aircraft was travelling below most TCAS equipped aircraft. Figure 3-112 shows that the altitude of the research aircraft remained below 3,500 ft.

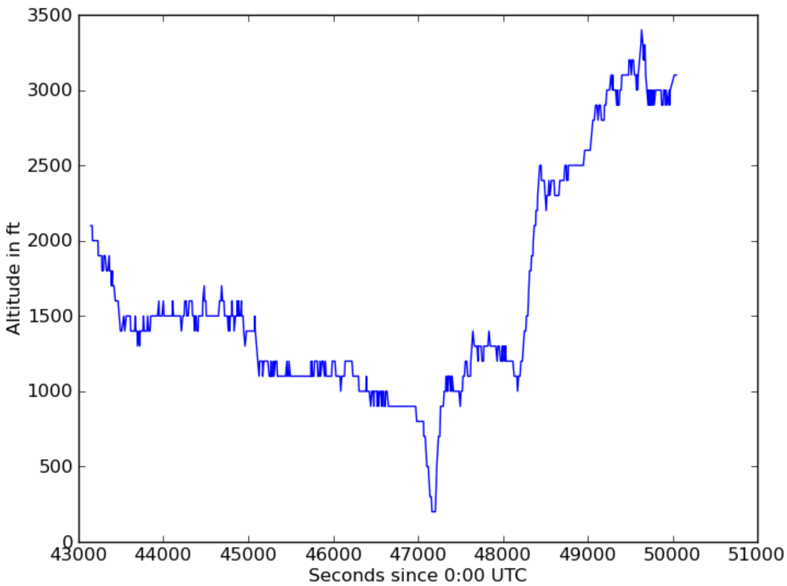

Figure 3-112: Altitude of Research Aircraft during the Experiment

Figure 3-113 shows that only about 14,000 of 365,435 plots of TCAS equipped aircraft are in the same altitude band. The large majority is way above. This was expected.

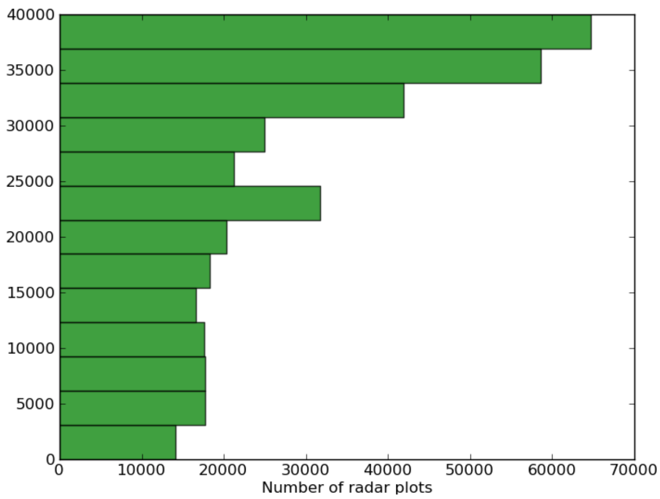

Figure 3-113: Number of Radar Plots of TCAS equipped Aircraft per Altitude Band

3.5.7 Plots relative to the Research Aircraft

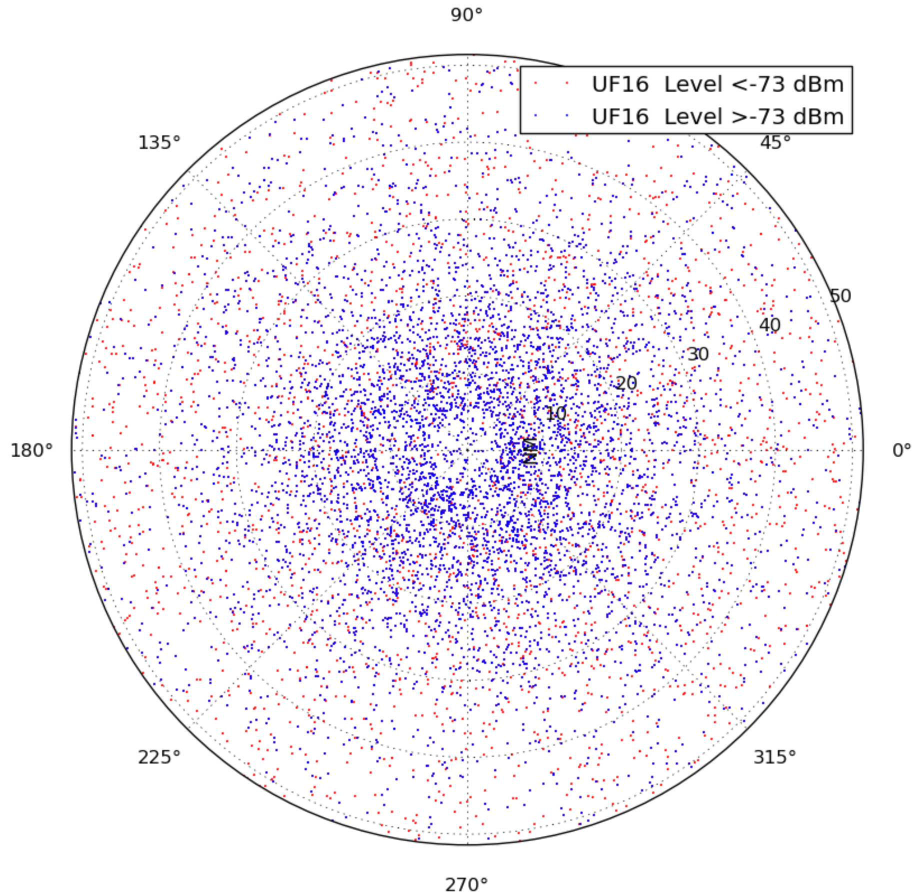

Figure 3-114: UF16-32-TCAS-Broadcasts relative to the Research Aircraft

Figure 3-114 shows a polar plot with the research aircraft at its centre heading towards 0° (towards right). Around the aircraft, the positions of all other aircraft when emitting an UF16-32-TCAS broadcast are plotted with their distance (in NM) and bearing relative to the research aircraft.

The figure covers the whole experimental flight through the range of the RNLAF Soesterberg radar. The relative distance and relative bearing from the research aircraft to the other aircraft were computed and plotted.

The red dots mark the positions of aircraft, from where UF16-32-TCAS-broadcasts were received with a power below the minimum trigger level (MTL) of a Mode S transponder of -73 dBm. These UF16 would probably not be read by the transponder. The blue dots mark received UF16 with a power above the MTL. These would probably be received by a Mode S transponder.

A blank spot above the research aircraft is visible. Within a range of 20 NM most receptions are above MTL. The figure cannot show plots for UF16-32-TCAS broadcasts that were not received by the measuring equipment, this shortcoming is addressed later on.

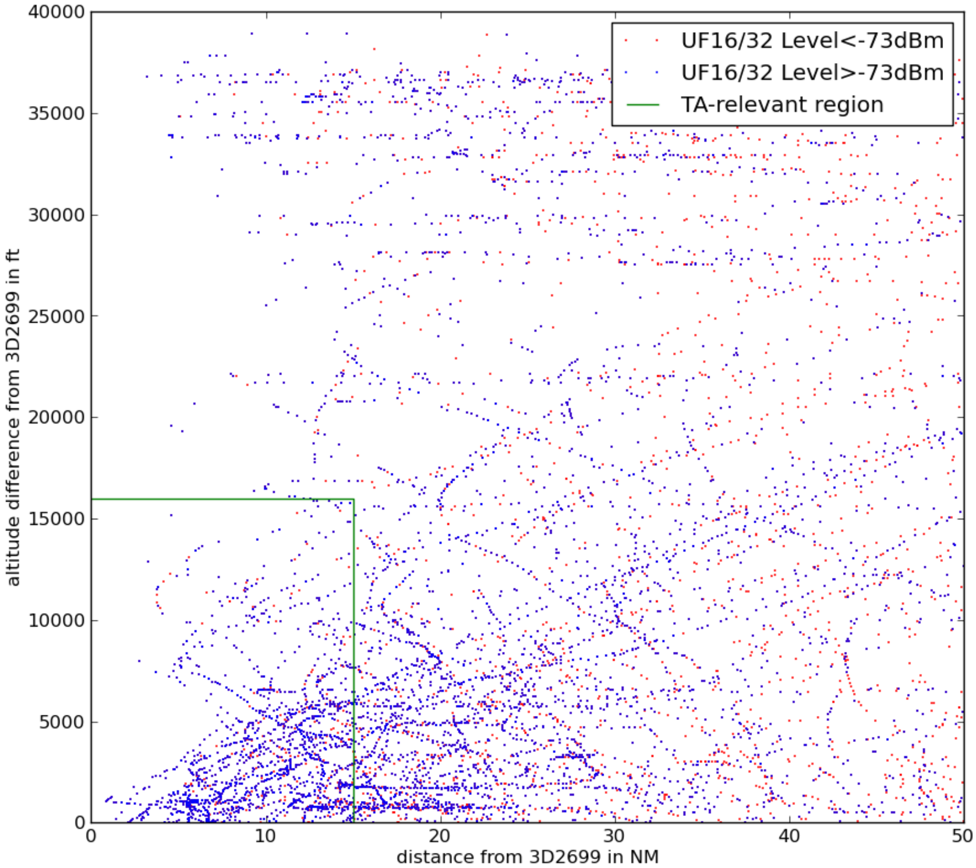

Figure 3-115: UF16-32-TCAS-Broadcasts relative to the Research Aircraft plotted over Distance and altitude

Figure 3-115 shows the sender's position of every received UF16-32-TCAS-Broadcast relative to the research aircraft at the origin of the graph. In contrast to Figure 3-114 the plot is based on distance and altitude. The TA-relevant region is marked as a green box. Within the TA-relevant region, most of the received UF16-32-TCAS-Broadcasts are above -73 dBm.

3.5.8 TA-relevant Region

TA is the Traffic Advisory issued by TCAS to the pilot up to 15 seconds before an RA. The TA does not just give advice to move in a certain direction, but draws the attention of the pilot to an upcoming threat. The RA is issued at maximum 35 second before the relative distance to the intruder and the relative altitude is dropping to zero. So about one minute is the minimum time TCAS needs to survey an intruder to give well timed warnings.

For TCAS the region of 15 NM and 16,000 ft is relevant.

The threshold of 15 NM has been concluded during the standardisation process of TCAS from the following consideration: Two aircraft converging with 500 kts each (1000 kts relative speed) are 16 NM apart one minute before the encounter.

The 16,000 ft barrier has been concluded from the experience of the TCAS-Monitoring-Program of IfEV, TU-Braunschweig, which recorded from April 2007 to August 2010 a total of 2,537 RA events in the period from April 2007 to August 2010. The highest observed vertical rate in an RA event was 16,000 ft/min climbing of an A320.

3.5.9 Reception Probability of TCAS equipped Aircraft

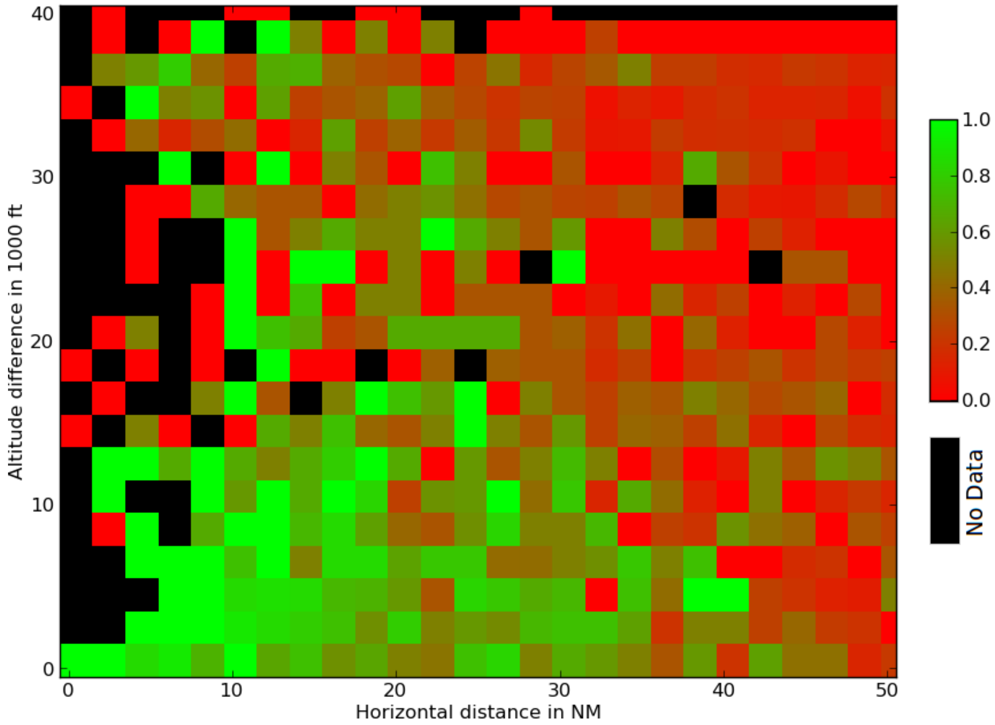

Figure 3-116: Reception Probability of TCAS equipped Aircraft with UF16-32-TCAS-Broadcasts with at least -73 dBm

Figure 3-116 shows the relative frequency of receiving a UF16-32 broadcast with a level of at least -73 dBm at the single (bottom) antenna of the research aircraft Cessna 172. It is formed using all TCAS equipped aircraft at a certain distance and relative altitude to the concerned aircraft, derived from the radar data.

For this purpose every minute of the flight is individually analysed. For every minute it is checked, if the research aircraft receives an UF16-32-TCAS broadcast from every TCAS equipped aircraft that was detected by radar. For one minute this process is shown in Figure 3-111, this has been repeated for all minutes of the experiment; the number of minutes any aircraft in a certain distance an altitude has been observed is summed up in Figure 3-116.

In Figure 3-116 the area around the research aircraft is divided into pixels of 2 NM * 2000 ft. A perfectly green pixel states that at a given distance and altitude UF16-32-TCAS broadcast messages from all TCAS equipped aircraft were received during the whole test. The more red a pixel is coloured, the more times TCAS equipped aircraft were not seen.

A black pixel indicates insufficient information, i.e., no radar plots of TCAS equipped aircraft were observed in that pixel.

The picture is based on the radar plots only from the RNLAF Soesterberg. All computations were relative to that radar, no multi-radar merging of tracks was performed. The research aircraft was travelling for 2 hours through the range of that radar, during that time 11358 UF16-32 were received.

Counting only the first UF16-32 per minute and per aircraft leaves 3349 UF16-32. In only 1330 of these cases a radar plot from the aircraft sending the UF16-32 existed within that minute. This is due to the fact that the research aircraft started out on the edge of the range of the radar. These 1330 UF16-32 with corresponding radar plots add green to the pixels on the figure. On the other hand, there were 14767 one-minute-track-snippets of TCAS equipped aircraft, where no UF16-32 was revived within the minute – these add red to the pixels.

A pixel represents a ring or a torus with squared diameter around the Radar. Therefore, the volume represented by one pixel is

$$V_{Pixel} = 2\pi\, r \cdot 2NM \cdot 2000\, ft$$

where r is the horizontal distance. The pixels on the right side thus represent a larger volume than the pixels on the left side, and therefore the more right a pixel is, the more likely an aircraft is observed within that pixel.

3.5.10 Conclusions

At total in the RA-relevant region (below 16,000 ft vertical distance, 15 NM horizontal distance) in 183 cases TCAS equipped aircraft were seen at least once per minute. There was a flying time of 216 minutes of TCAS equipped aircraft within the TA-relevant region in total.

85% of TCAS equipped aircraft were able to reach the experimental aircraft with UF16-32-TCAS broadcasts at a level of at least -73 dBm within one minute. Figure 3-116 shows that in no part of the TA-relevant region the reception of messages is impossible (except for the spots with no data).

The UF16-32-TCAS broadcast is a long transmission, and sent 6 times a minute. The UF00-Air-Air surveillance interrogation is a short transmission, and is repeated in case the interrogating aircraft is not receiving the answer.

The test thus shows that the experimental aircraft can be reached from an TCAS equipped aircraft. The question remains, if the replies reach the TCAS equipped aircraft. It also remains open, whether reception probability is sufficient right above the experimental aircraft. Within the TA-relevant region right above the research aircraft, there were not enough TCAS equipped aircraft. Aircraft flying high above the research aircraft had only a small chance of being received (upper left corner of Figure 3-116).

3.6 Non-Diversity Antenna

Smaller aircraft typically have only one antenna mounted at the bottom of the fuselage. In this section, the signal transmission on both 1030 MHz uplink and 1090 MHz downlink channels will be investigated using all available data sources. This gives some hints on the question if a non-diversity antenna operation is sufficient for the interaction of transponders with ground-based interrogators.

As already stated in section 3.1, a dedicated test flight to Amsterdam was performed flying VFR with a Cessna 172 aircraft ("D-EMWF") having such a single antenna installation. In addition to the 1030 MHz recordings gained from the measurement system, the ASTERIX radar data of all Dutch Mode S facilities was provided by LVNL. This allows also evaluating the downlink channel to a limited extent.

All other mission or ferry flights of the FCS "D-CFMD" flight calibration aircraft performed over Germany under IFR conditions revealed that there is sufficient signal strength received from the single bottom antenna during enroute and approach phase of a flight as shown in section 3.1.3.4, apart from weaker signals transmitted at greater off-boresight angles. A dedicated analysis of the 1090 MHz reception could not be done for any of those missions since no ASTERIX data from the German radars was made available to this study.

Apart from some general signal-in-space uplink channel analysis of the Amsterdam flight already given by section 3.1.3.6, this chapter also comprises the analysis of the ASTERIX radar data.

At Schiphol airport, the ASR "TAR1" (SAC/SIC: 002/234) uses the unique surveillance identifier SI28, whereas all other Dutch radars apply II07 in clustered mode. This makes things easier to assign received interrogations to that single facility.

3.6.1 Aircraft Antenna Locations

The following outlines in Figure 3-117 to Figure 3-120 show typical installation locations for transponder antennas on small aircraft with single antenna installations.

Parts of the antenna hemisphere are shadowed due to the fixed landing gear or the fuselage. A serious analysis of the antenna installed performance would require a *Method-of-Moments* computation which comprises the electromagnetic near-field conditions. The proper application of that method inherently implies a geometrical discretization of the aircraft body down to $\lambda/8$ (<4 cm), which is not part of this study.

Several flaps and other antennas influence the installed performance of the spare L-band antenna of the bigger flight inspection aircraft "D-DFMD" as well, of which the mounting point is comparable to Figure 3-118. However, the numerous data collected revealed that there is enough signal strength as shown in section 3.1.3.

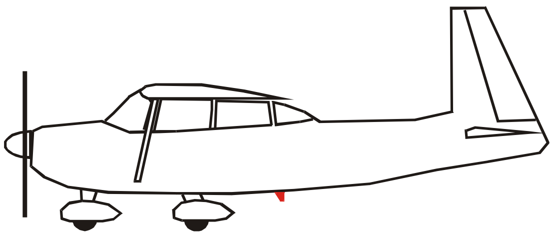

Figure 3-117: E-Class Aircraft

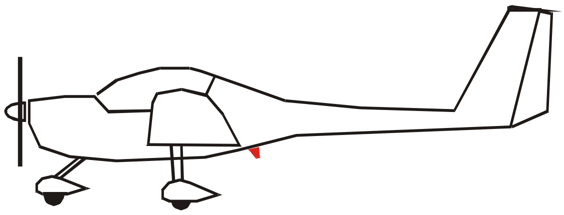

Figure 3-118: Motor-Glider/UL Aircraft

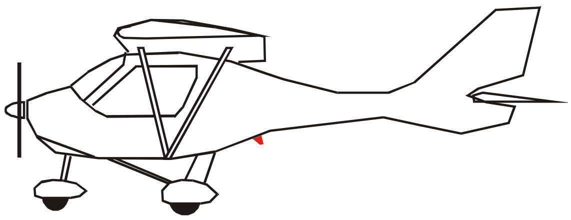

Figure 3-119: UL Aircraft (location variant A)

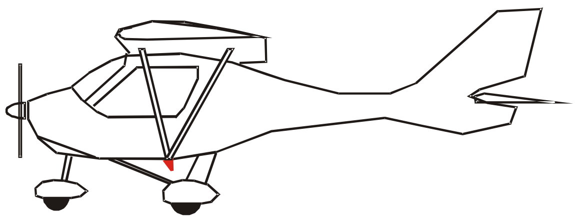

Figure 3-120: UL Aircraft (location variant B)

3.6.2 MSSR Antenna

A typical Large Vertical Aperture (LVA) MSSR antenna is constructed of several radiating vertical elements mounted on an aluminium spine in which all the feed cables and distribution networks are housed. This type of antenna is in widespread use across central Europe and therefore serves as a suitable example.

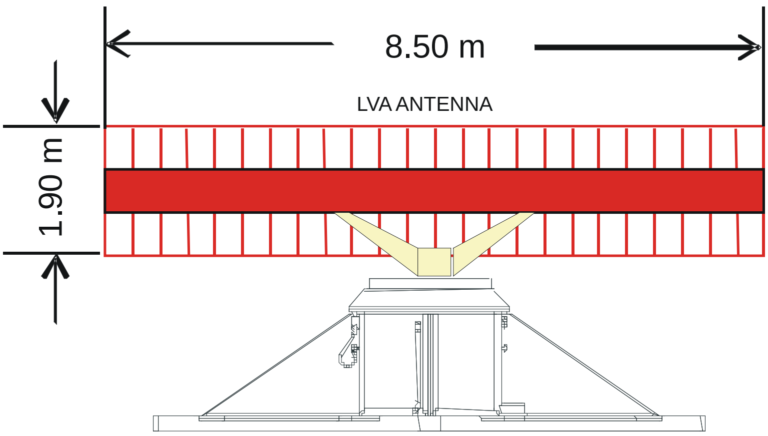

Figure 3-121: Large Vertical Aperture (LVA) antenna (source: DFS ATC Academy)

In Amsterdam Schiphol, the installation height of TAR1 is 22m above ground. At greater distances the antenna installation height becomes negligibly small. The vertical radiation pattern as shown in Figure 3-122 is positioned for maximum optimal range and minimum power transmitted towards the ground. It shows the vertical radiation displacement with the horizon level nominally set to -4 dB below the main beam, whilst the half power vertical bandwidth width is 10°. The sharp cut-off just below the horizon level is to reduce downward radiation reflecting off the ground and interfering with the main lobe within the near vicinity of the antenna mast.

However, the figure represents the computed far-field radiation pattern describing the propagation of plane electromagnetic waves. In a rough, obstacle-rich environment especially the effective lower boundary of the pattern might significantly differ from computations since there are no pure plane wave and far-field conditions at low elevation angles close to the horizon. Furthermore, the wave interacts with ground obstacles resulting in cross-polarizing effects. A complete description of all impacts cannot be raised by a closed theory but the resulting signal degradation can be measured on either side of SSR 1030/1090 MHz receivers.

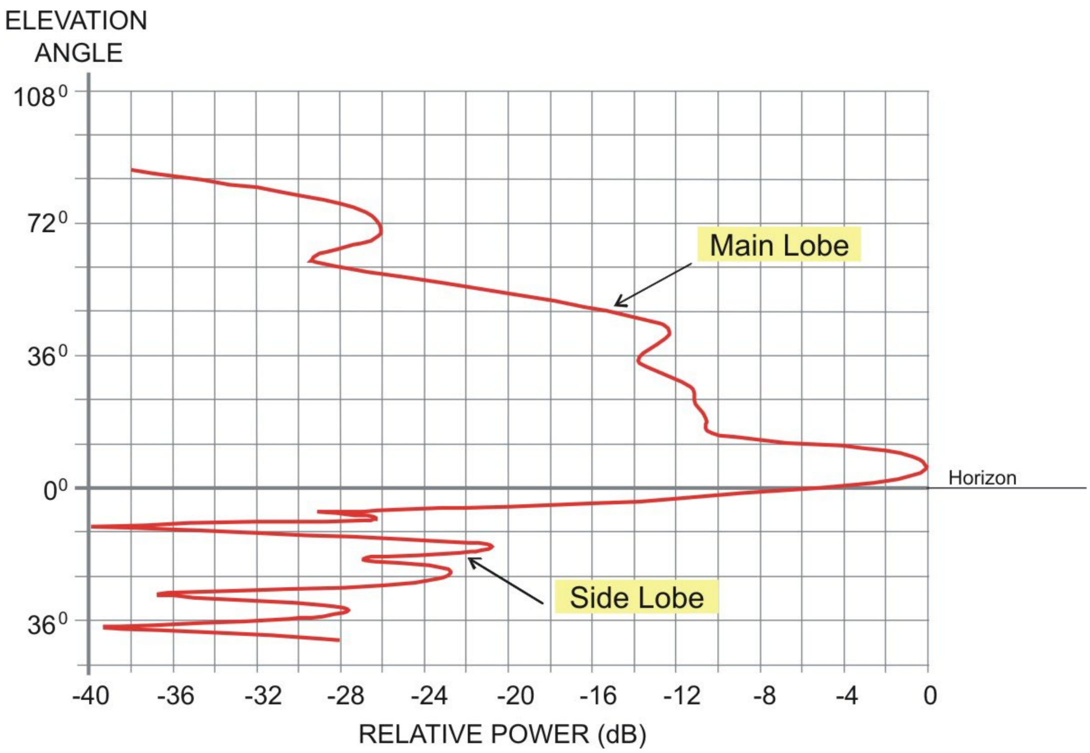

Figure 3-122: Vertical LVA antenna pattern (source: DFS ATC Academy)

3.6.3 Combined analysis of ASTERIX data and 1030 MHz recordings

To give an overview of the surveillance coverage of the TAR1 radar the observed traffic of opportunity on 2010-05-28 at any altitude is given by Figure 3-123, which forms a circle. Different receiving levels are expressed by colours according to the graph legend. As expected, the highest values appear close to the radar site. The track of dedicated flight is plotted by the dark green line and, regarding the distance only, the total flight is well within surveillance coverage of TAR1. Limiting the diagram to flight altitudes below 2000 ft, only a small portion of the original coverage remains as shown by Figure 3-124.

In order to show the maximum distance of targets at different altitudes the airspace is divided into altitude bands of 500 ft from ground up to 3500 ft. The traffic of opportunity flying within the bands that day is depicted by Figure 3-125. All aircraft are seen by TAR1 at their respective altitude. The plot and the radar at (0,0) are connected forming "range disks" for the altitudes bands given by the graph legend. The approach of the Cessna to Amsterdam Schiphol (EHAM) tracked by TAR1 starts in the upper right corner flying straight and then performing a left turn towards EHAM. Traffic visible to TAR1 in that direction could be observed mostly at 1000 ft and above.

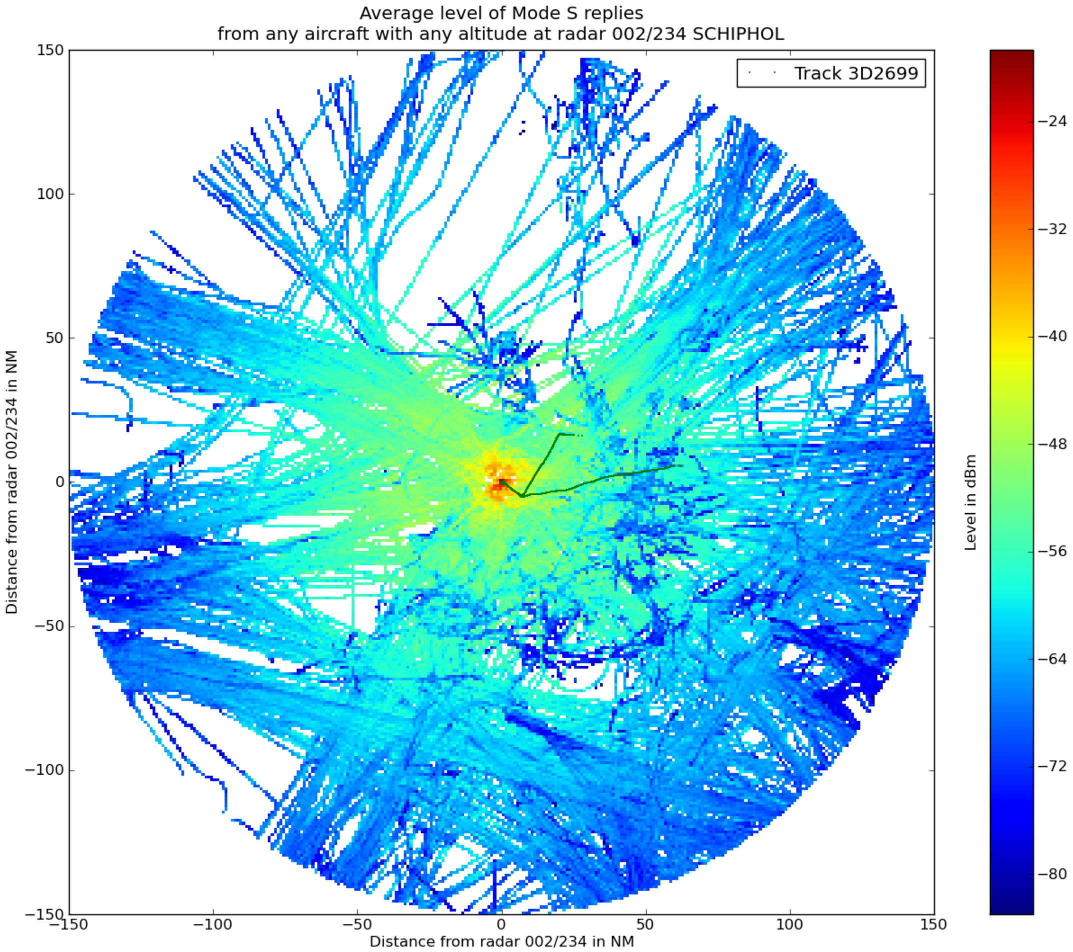

Figure 3-123: Surveillance coverage and levels on 1090 MHz at Schiphol TAR1

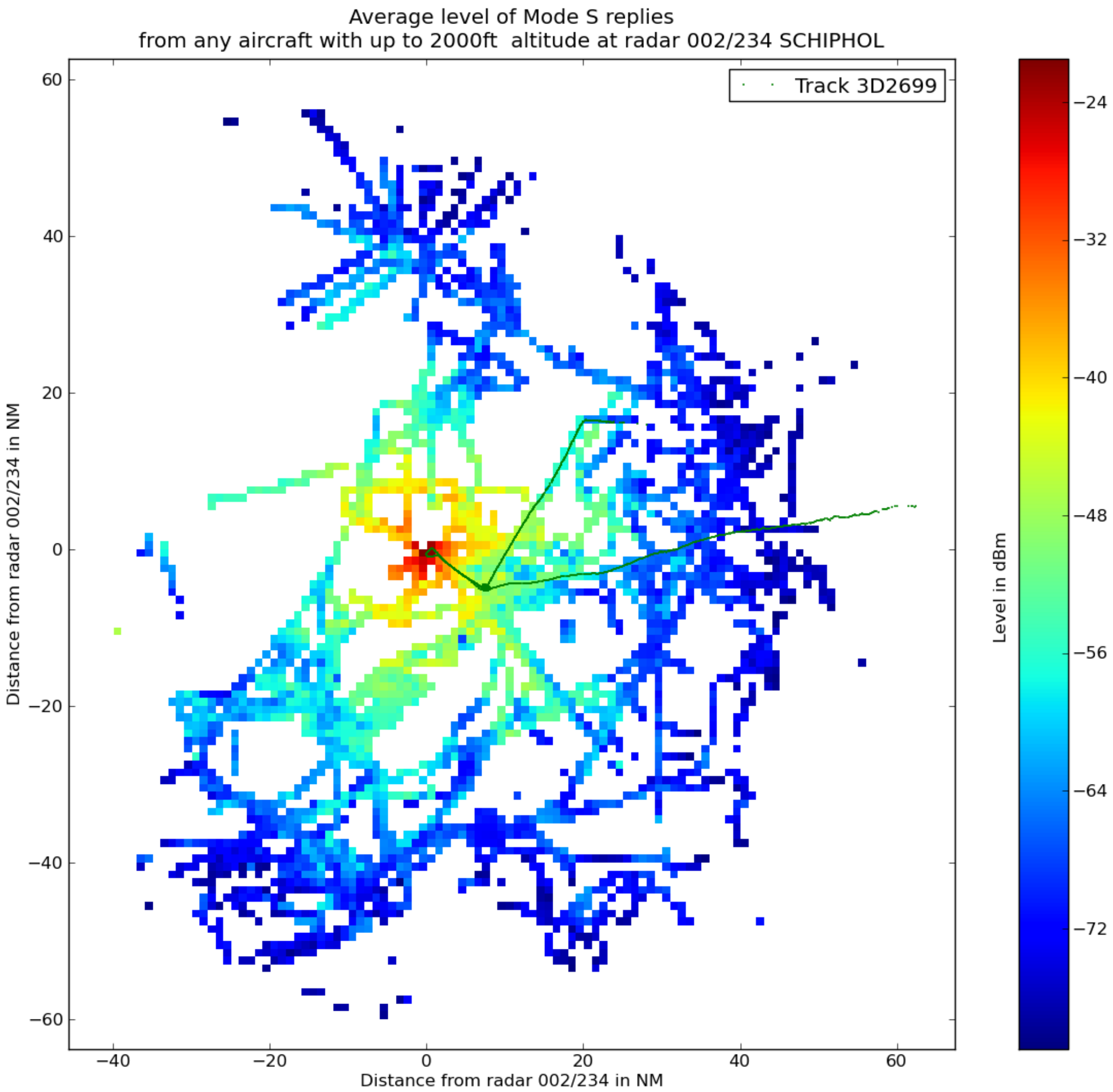

Figure 3-124: Traffic of opportunity at altitudes below 2000 ft

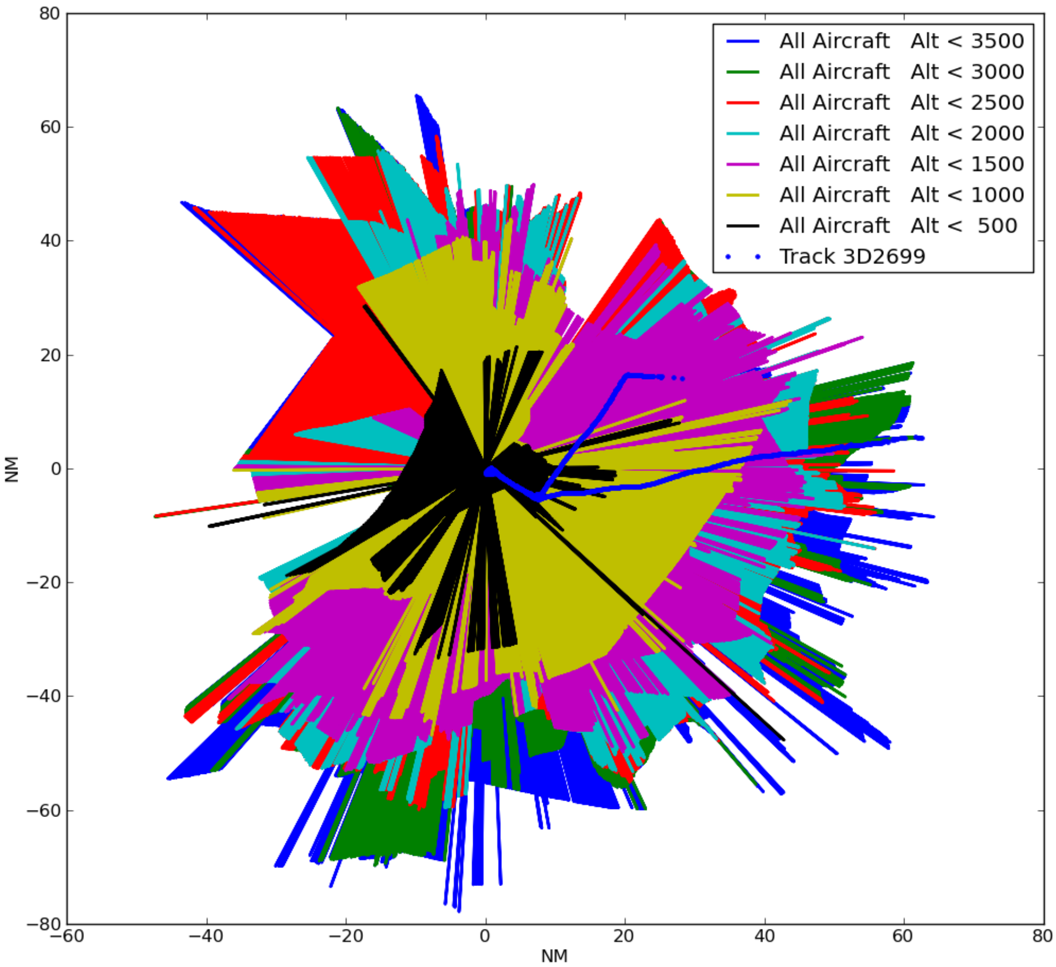

Figure 3-125: Ordinary traffic at low altitude bands observed by Schiphol TAR1

The transponder reply level distribution of D-EMWF for each available TAR1 plot is shown in Figure 3-126. Weak levels are to be observed at the beginning and end of the tracking, whereas the maximum was measured above runway 22 in the vicinity of TAR1. If there is no succeeding radar plot after 4 seconds, a red dot is added with the amplitude of the last plot, to mark the missing plot. Figure 3-127 shows a zoomed graph into the first critical region. As stated above, the initial and final outages occur when the aircraft is well within the nominal coverage since the distance is only 30 NM. However, due to the low altitude below 1500 ft, the free space propagation is constrained so the MSSR antenna pattern given by Figure 3-122 is not applicable at these low elevation angles. Generally, the incoming wave propagation direction is roughly parallel to the ground surface so the transponder antenna is radiated at negligible tilt angle. A top-mounted antenna would have been affected by the same low field strength than bottom antenna is.

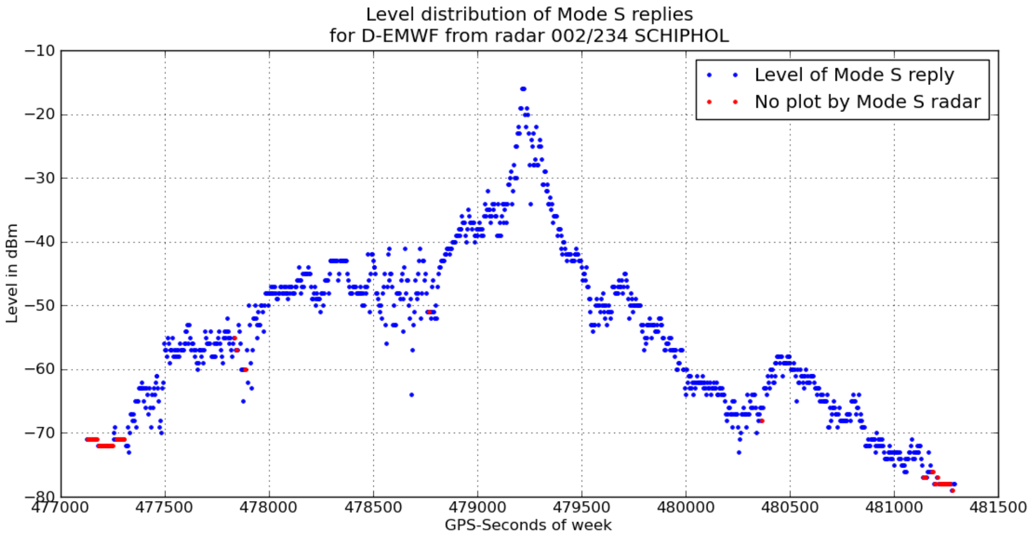

Figure 3-126: TAR1 Mode S level plots of Cessna 172 (D-EMWF)

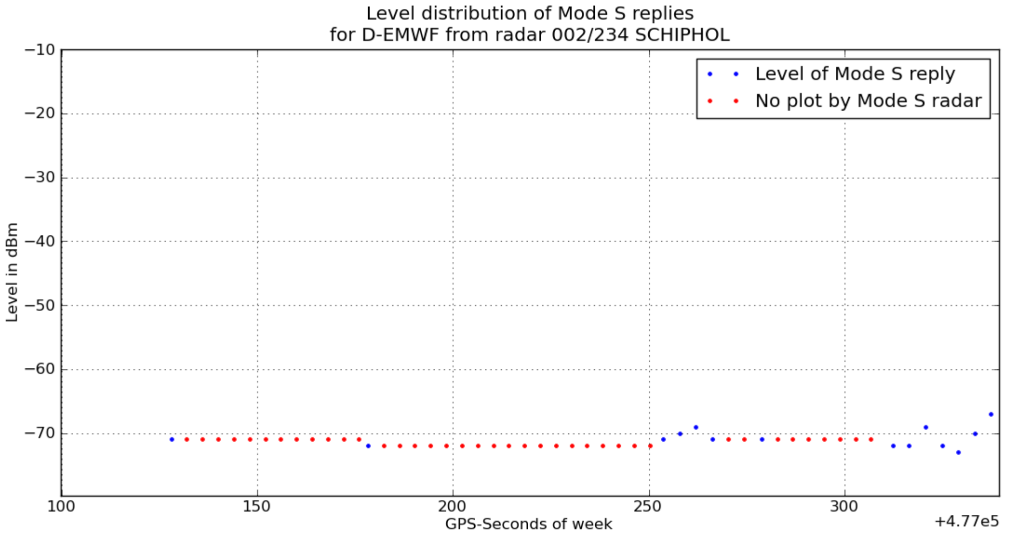

Figure 3-127: TAR1 outages at beginning of detection range

In Figure 3-128 a satellite photo of Amsterdam and Schiphol airport in the lower left is shown, in which the runway 22 fly-over of D-EMWF is visible. TAR1 resides at the airport and radiates over a wooded area and the city of Amsterdam towards the critical region where the signal strength is weak, noted at GPS time 477000 s onwards.

Since both the MSSR installation height and the flight altitude below 1500 ft at 30 NM distance is fairly low, the wave has to overcome several obstacles which affect its propagation.

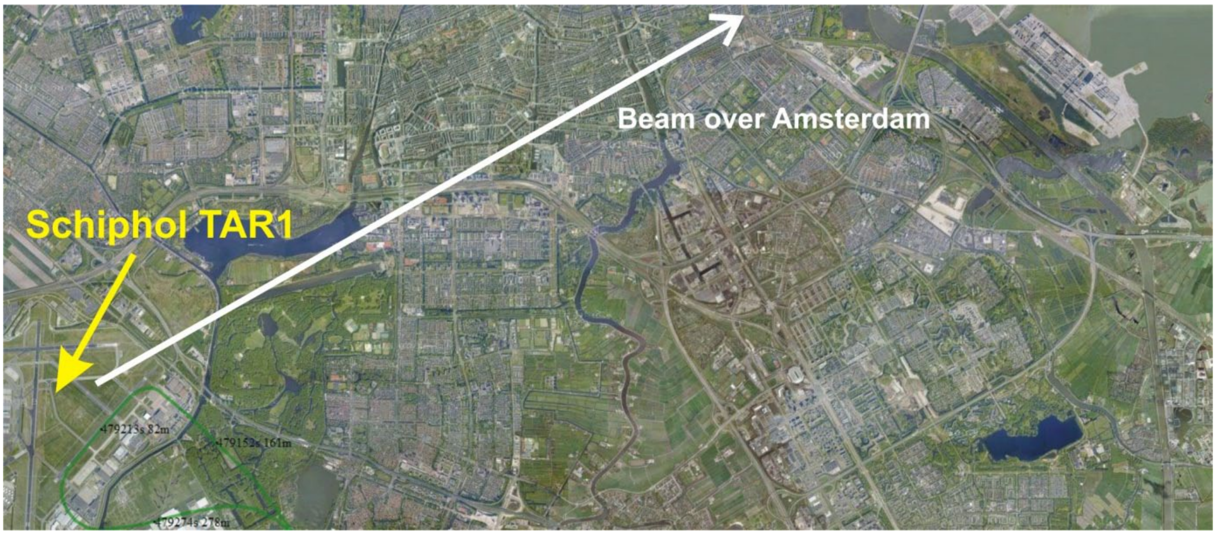

Figure 3-128: TAR1 Radiation over the city of Amsterdam

The corresponding beam sweeps on 1030 MHz comprising selective calls to D-EMWF and UF11 all-calls are depicted by Figure 3-129 covering 200 s each. Between 477000 s and 477250 s there are numerous selective calls detected by the measurement system and mostly above -73 dBm, but the radar plots of Figure 3-127 reveal that there are many gaps during that period. A received interrogation does not necessarily mean that the reply on 1090 MHz is understood by the radar: Since the radiated peak power on 1030 MHz is approximately 2 kW, Mode S transponders for smaller aircraft typically radiate only 250 W (for Class 1 units) on 1090 MHz, which is 9 dB below the radar power. And Class 2 transponders often radiate only 70 W.

If there is no reply received by the radar, it attempts to re-interrogate several times within one radar sweep before giving up. That behaviour is shown in Figure 3-130 selecting a certain beam sweep of the sequence that of the preceding figure. While the first attempts take place at the beginning of the beam dwell, there a succeeding interrogations also after the boresight passed by, which is normally not performed in case of success as shown in section 3.1.3.4 (e.g. Figure 3-25 ff).

Bit-identical interrogations of SI28 within 10 ms were accumulated to draw a re-interrogation bar diagram as given by Figure 3-130 , with a green bar indicating that one re-interrogation per sweep occurred, other colours show higher frequencies as given by the graph legend. The certain example at GPS time 477274 s is marked by a red line denoting that a sequence of six identical interrogations (1 + 5 re-int’s) in total were recorded by the measurement system. No reply was received from the transponder at that time at the radar site, as shown by Figure 3-127.

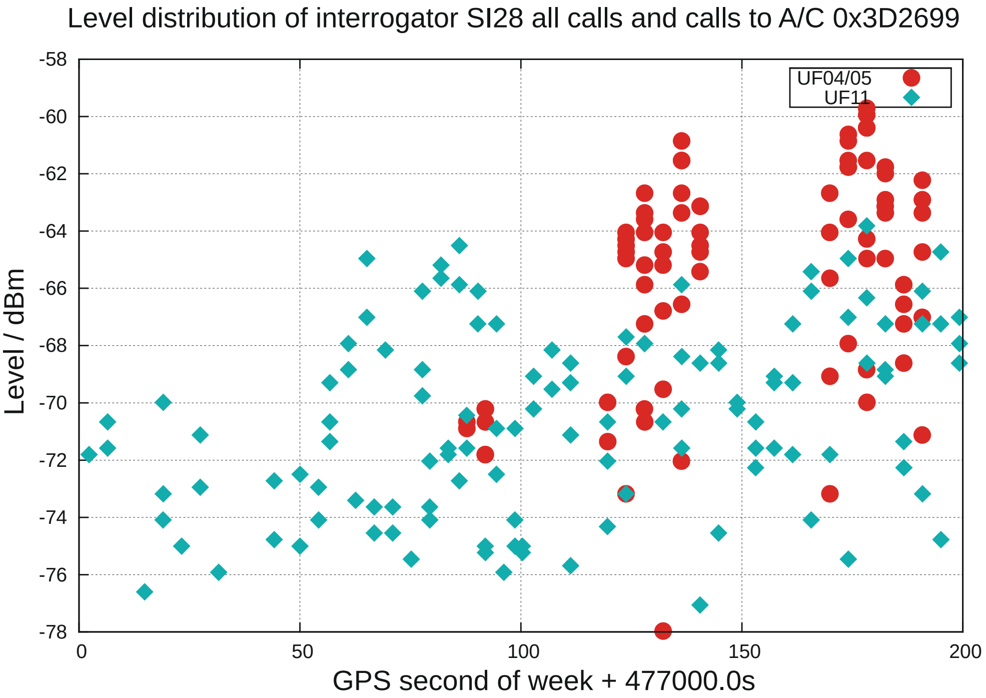

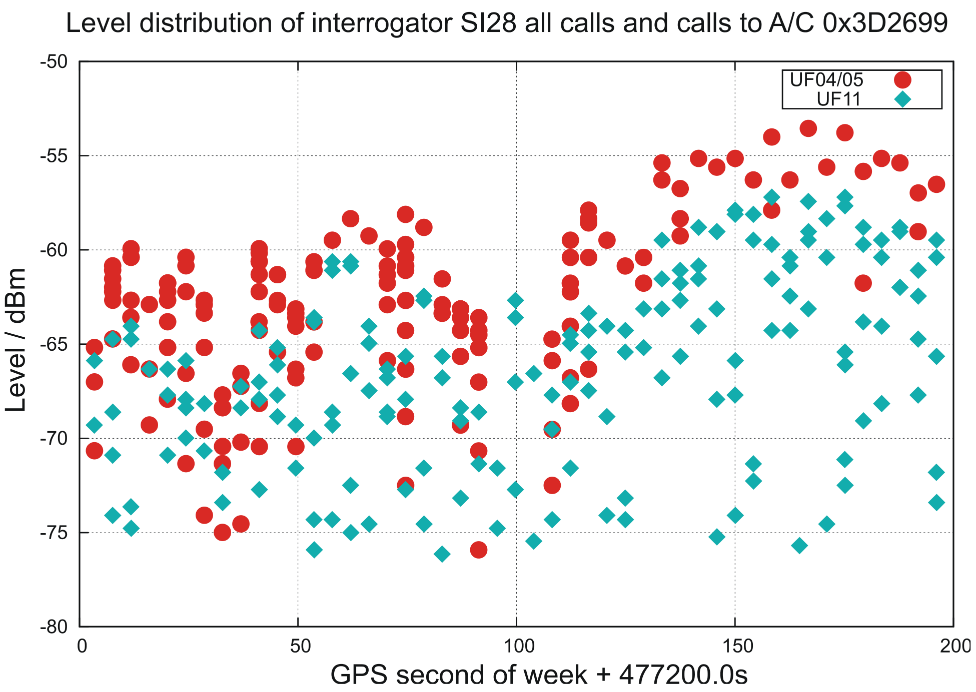

Figure 3-129: Corresponding radar sweeps observed airborne

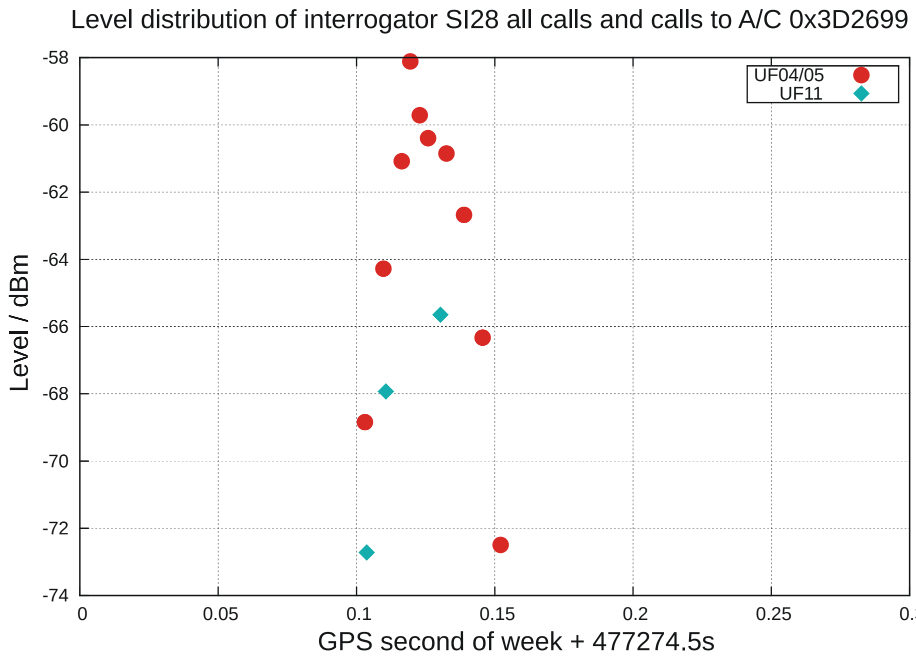

Figure 3-130: Radar sweep showing re-interrogations

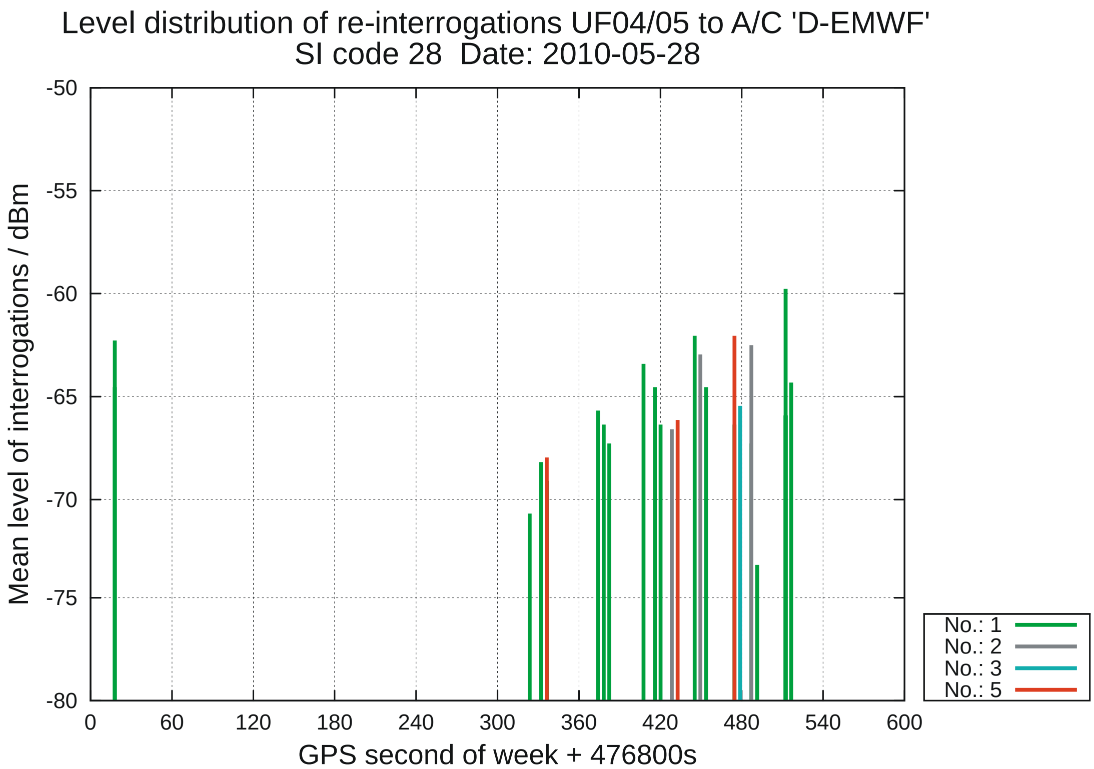

Figure 3-131: Frequency of re-interrogations

From GPS time 477350 s onwards the signal levels are strong enough either for the interrogations, shown in Figure 3-129 and Figure 3-132, and the replies gained from the ASTERIX data shown in Figure 3-126.

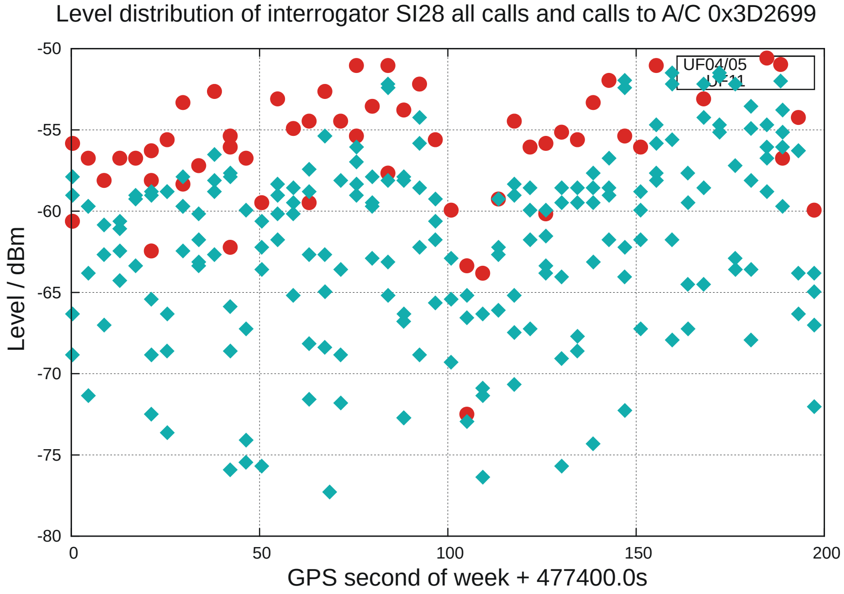

Figure 3-132: Succeeding sweeps indicating stronger reception levels

In the further course of Figure 3-126 there are some more missing plots around GPS time 477850 s, of which a higher resolution extract is given by Figure 3-133. Although the signal levels seem to be sufficient, the aircraft is not detected for a few beam sweeps.

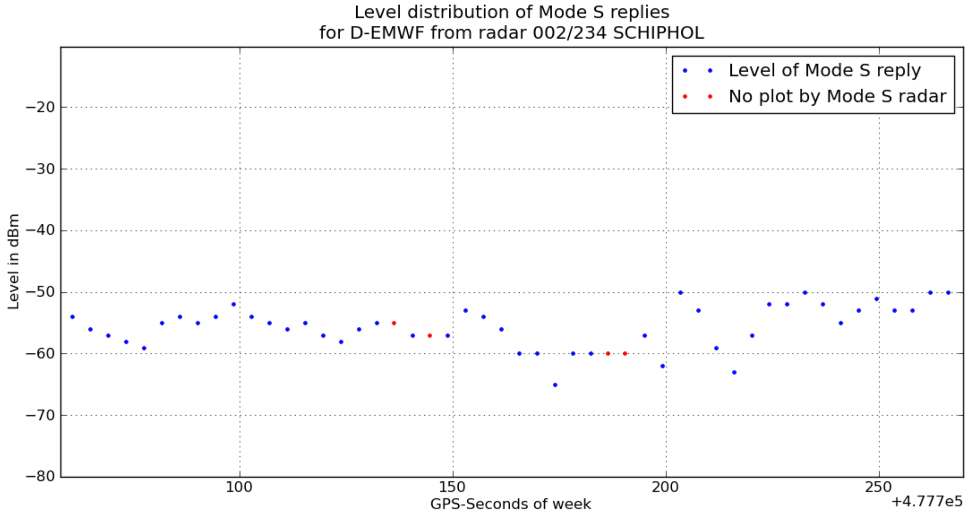

Figure 3-133: Outages over sea surface due to reflections

To find out the reason it is worth to view some video plots of incoming Mode S interrogations. In the following two diagrams of Figure 3-134 and Figure 3-135 a re-interrogated UF04 within one beam sweep at GPS time 477886.6 s is depicted. The signals are affected by reflections reaching relative levels roughly from -6 dB to -2 dB.

Already on the pulses P1 and P2 in Figure 3-134 the strong amplitude of a reflection becomes visible, which produces deep notches at the phase reversal positions of the succeeding P6. However, a zoom into the SPR region reveals that the reversal is accelerated from the common value 86 ns of that interrogator type (see also Figure 3-36) down to 48 ns. On the other hand, the first data pulse occurring after the SPR is slower. In the polar plot the effect of acceleration is expressed by a phase value being boosted from zero to a value below -180°.

In Figure 3-134 we observe that the SPR is accelerated by this multipath propagation, whereas it is heavily delayed beyond 200 ns as seen in the polar plot of Figure 3-135: A strong reflected pulse affects P1, P2 and the SPR within P6 in combination with a SLS P5. As to be seen in the polar plot the phase remains at the initial value for a long period before starting to advance.

The autocorrelation function ACF of the software demodulator has some remarkable side lobes, whereas its maxima amplitudes are unequally distributed. An artificial amplitude modulation, reaching 6 dB of depth, overlays pulse P6 and is generated due to the reflective environment.

As seen from the ACF curves which form the telegram data bits, the demodulation process is not too much impeded since the maxima are still clean and well above interference level. However, since the Mode S reply has 56/112 bit chips applying pulse position modulation, some necessary gaps may be filled up with reflected portions so a de-garbling process in the radar signal processor might fail to decode.

The reflected pulses P1 and P2 of both UF04 in that example nearly appear at the same time right after the respective direct pulses. Two beam sweeps later, at GPS time 477894.3 s the reflections evoke quite a different interference as shown in Figure 3-136: The differential runtime of the reflection is shorter than in the preceding examples, so P1 and P2 are already boosted within their duration. While the ACF process itself still remains untouched, there is a strong delay added to the SPR duration as depicted by the polar plot.

It is quite obvious that the scatter must originate from a plane reflector having an area of numerous square wavelengths, since the level is of notable strength. Flying at low altitude above a conducting sea surface as depicted in Figure 3-137 suggests that the reflections are very likely induced by that source.

Regarding the aircraft, reflections from ground may appear from different aspect angles below. The bigger the angular difference between direct and reflected wave is, the more a transmission between single transponder and radar antenna might suffer from degradations. In certain cases, antenna diversity might prevent the reflecting wave from interfering with the direct wave. However, the number of outages observed seen in the radar data is quite low, using the available data of the single flight performed with a smaller aircraft to Amsterdam. A dedicated multipath propagation investigation at certain areas may help to perform a Functional Hazard Assessment (FHA).

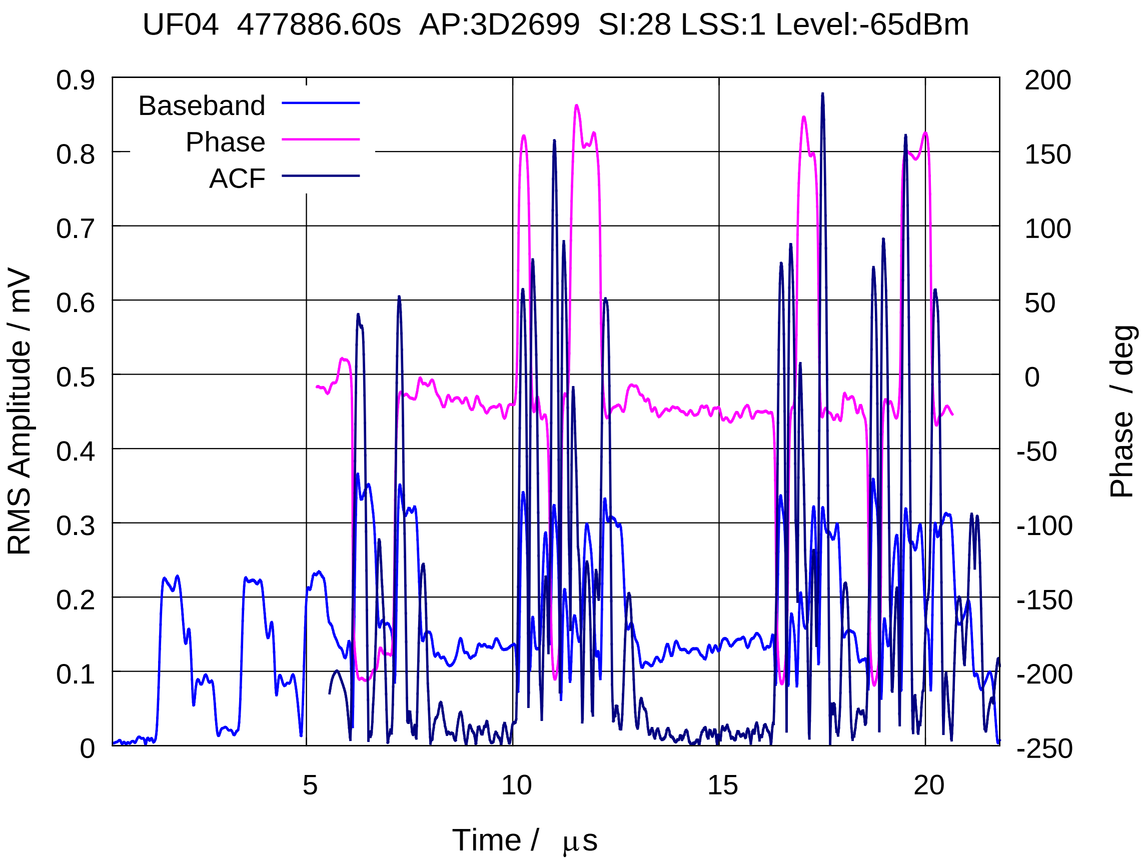

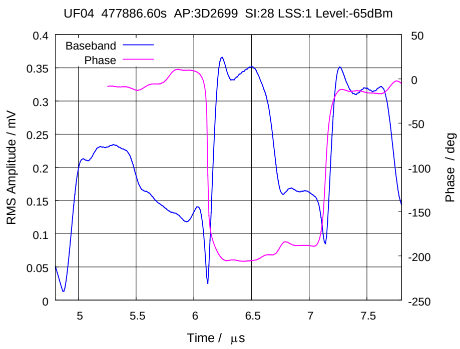

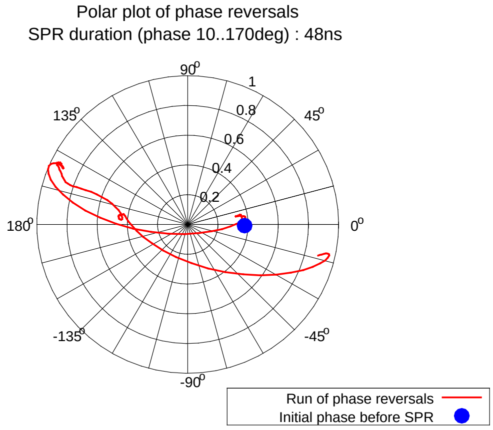

Figure 3-134: Video plot of multipath-affected interrogation UF04 (1)

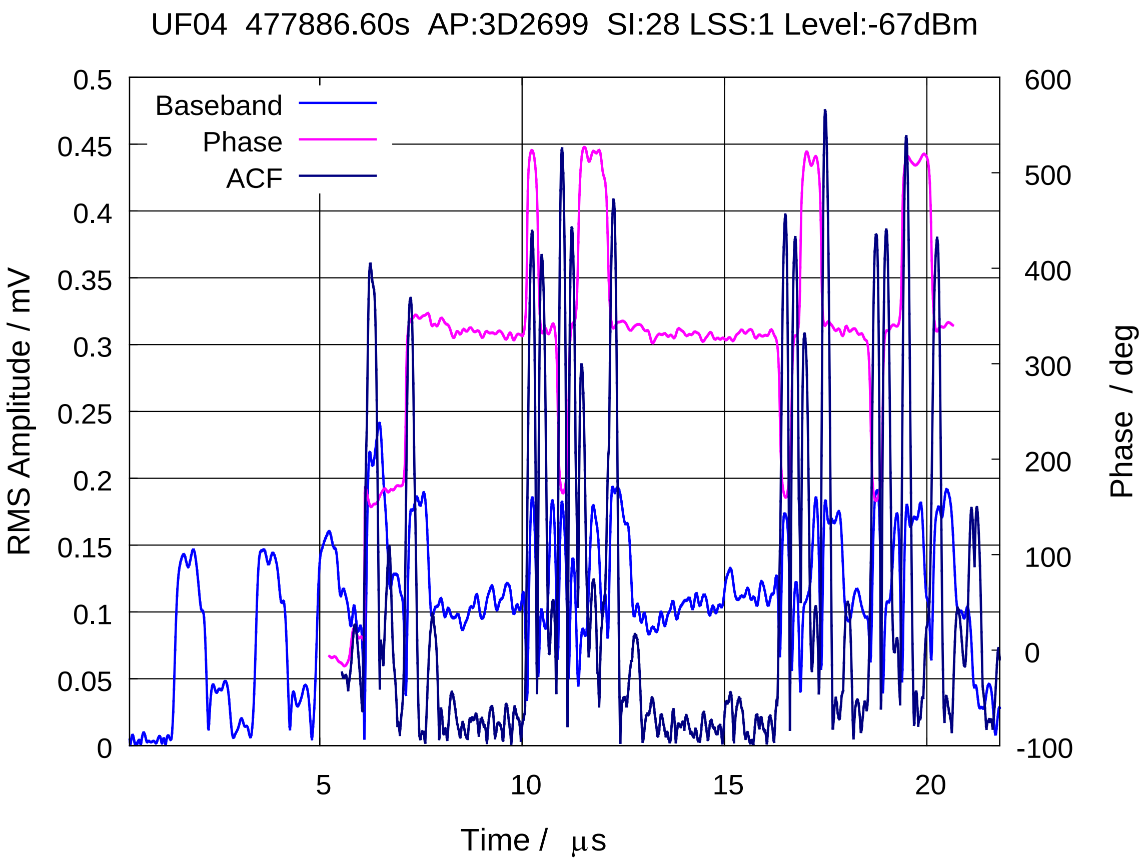

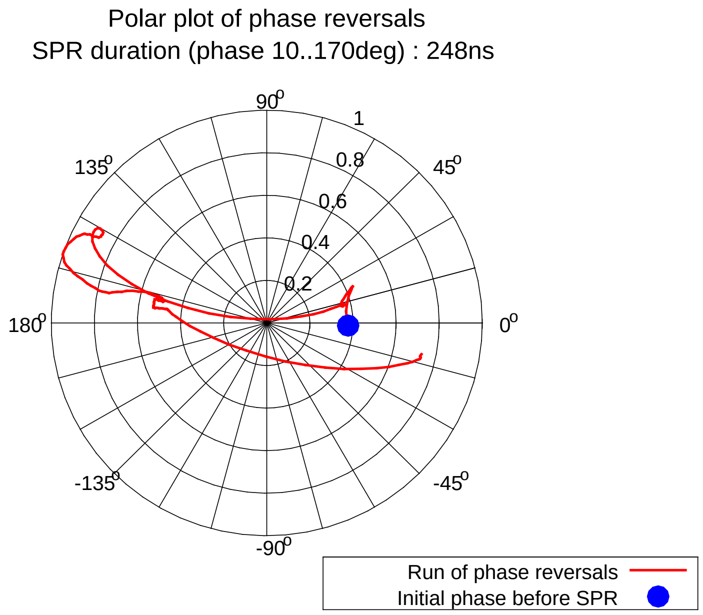

Figure 3-135: Video plot of multipath-affected interrogation UF04 (2)

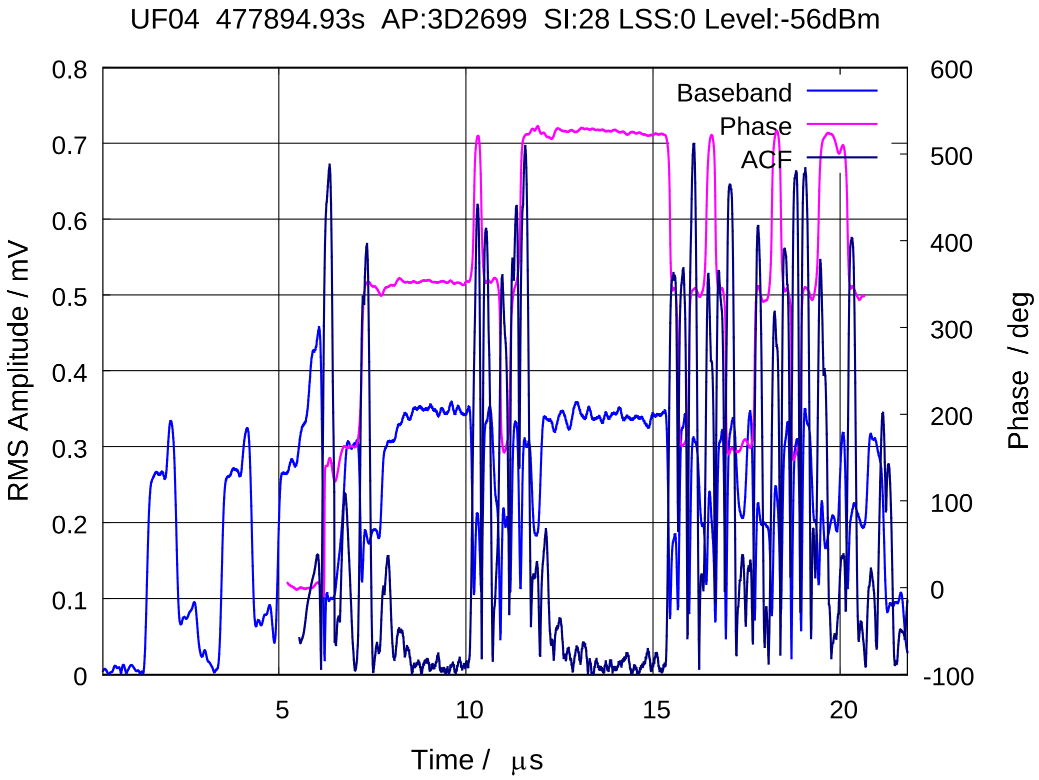

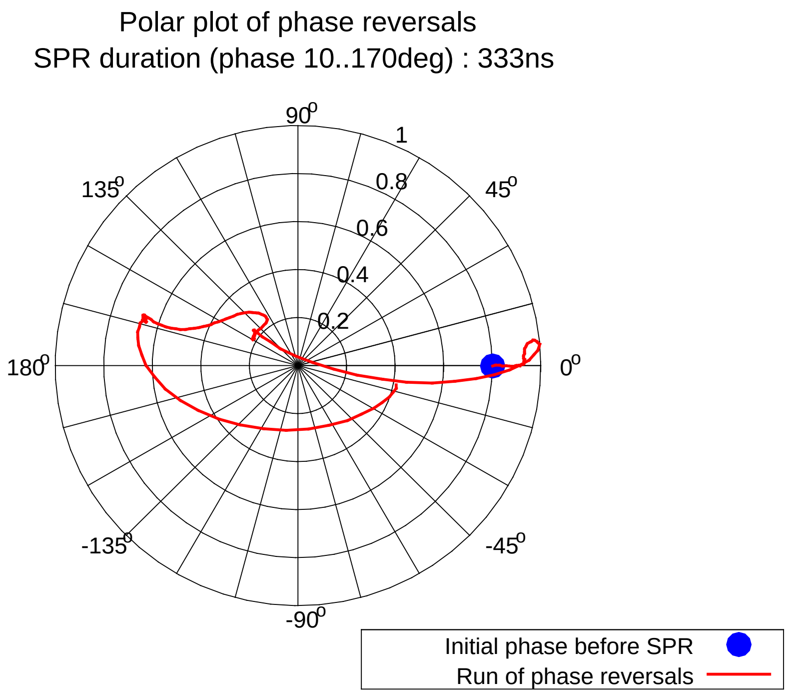

Figure 3-136: Video plot of multipath-affected interrogation UF04 (3)

Figure 3-137: Flight over sea surface (Markermeer)

4 SUMMARY AND CONCLUSIONS

4.1 Scope of Problem and Approach

The signal-in-space quality of a Mode S uplink telegram is mostly subjected to the performance of the phase reversals, especially to the quality of the SPR which is used to start the bit clock for the demodulation process. Any degradation of the SPR leads to a jittered determination of its point in time and consequently diminishes the remaining signal energy to accumulate the differential phase of succeeding bit chips. In total, the telegram demodulation is more likely to fail.

Generally, a signal-in-space is always the sum of the initial signal at the transmitter output and the transmission channel which includes the antenna installed performance of both the interrogator site and airborne. If wave propagation is based on an obstacle-free line-of-sight transmission, its contribution is a free-space loss in signal strength without additional interfering components.

A dedicated measurement system was developed to record and reconstruct the signal-in-space as far as possible. The system itself is not a spectrum analyser but a real measurement receiver for 1030MHz which stores a raw bandpass signal affected by the given RF/IF bandwidth limits of commercially available RF components. Since its constraints are known and depicted e.g. in sections 3.1.2 and 3.1.3.5, it is adequate to evaluate the signal-in-space to the greatest possible extent.

In order to obtain a reliable data basis of the Mode S uplink transmissions, more than 100 flight hours were performed across Germany with the FCS flight inspection aircraft “D-CFMD” plus an additional 4 hours spent on a dedicated flight to Amsterdam with a small aircraft Cessna 172 “D-EMWF”.

4.2 General Observations

Sufficient interoperability was observed between the transponder of “D-CFMD” and the MSSR radars within coverage during the flight tests as summarized in section 3.1.5.

This statement can be derived from on either the interference-free video examples given in section 3.1.3.4 (Figure 3-35) and investigations the radar sweeps as shown in the same section (Figure 3-19, Figure 3-34), separated for different interrogators by their II/SI codes. In most cases a regular interrogation scheme of selective UF04/U5 calls without immediate re-interrogations was found. This is an indication for both the uplink and downlink Mode S principle performing satisfactorily, regarding the directional transmission from the LVA radar antenna to the aircraft.

However, several signal characteristics measured during the campaign raise strong doubts on the interoperability of interrogators and transponders in all respective combinations.

As stated above, the clear detection of the SPR is the most critical task for a transponder to successfully detect a Mode S uplink telegram. Consequently, the analysis of the measurement data focuses on the evaluation of the phase reversals and in particular the SPR.

The measured variety of available interrogators was investigated on their specific phase characteristics resulting in a typical signature which then was classified: As depicted in section 3.1.2.4, different techniques to form a 2-PSK modulated signal exist. Interrogators using simple RF switches for the phase reversals perform best regarding the speed of reversals. Inherently, this technique is however inconsistent with ICAO Annex 10 (3.1.2.1.4.2.1) in that there shall be no amplitude modulation during phase transition. However, the AM actually has no effect on the DPSK demodulation performance.

Within the 3 dB bandwidth of the measurement receiver no telegram format found in the signal-in-space that would exceed the ICAO spectrum requirements (figure 3-2 in chapter 3 of Annex 10, Vol. IV).

There is a broad variety in the technique of generating phase reversals using quadrature modulators, since these can generate any complex bandpass signal. They can either copy the behaviour of a RF switch implementation, or perform phase accumulation in a particular direction using any kind of blending effects to advance the phase towards +/-180°. The blending effects applying orthogonal I/Q modulation for a specific period are used by some interrogators to generate an amplitude modulation-free P6 signal-in-space which meets the ICAO requirements. However, in a real transponder with bandwidth-limiting filters the effective phase transition to be fed into a DPSK demodulator will be temporally scaled and therefore extended. The longer a phase reversal takes the more energy is removed from a process detecting phase differences within a given chip length. Real transponders have bandwidth limits far below 2 * 10 MHz (as available with the measurement equipment employed for this study) and will therefore be subject to this issue.

A mechanically rotating interrogator transmits a side-lobe-suppression pulse P5 interfering with the SPR to prevent transponders from replying when located far outside the typical radar's 3° beam width, as shown by section 3.1.3.4 (Figure 3-24). However, the P5 leaks through P6 even if the radar selectively interrogates an aircraft. As a result, the duration of the SPR can either increase or decrease as shown in section 3.1.3.5. A strong rise of the SPR duration which could potentially harm the SPR detection was observed with certain radars, as shown in section 3.1.3.4. An addition of both the blending modulation (80 ns phase reversal duration) and the leakage of the P5 can boost the SPR duration to 250 ns and beyond, which then even exceeds a standard uplink chip length. Many inconsistencies of the signal-in-space and the phase reversal duration specified in ICAO Annex 10 were found, even considering the constraints of the measurement system. This behaviour is however limited to certain radar types and II/SI codes.

The masking effect of the P5 is inherently not of binary nature regarding the desired suppression effect. In fact, depending on the phase relationship between P5 and P6 becoming effective for the aircraft, it is an undefined transition. If applied to selective interrogations as seen in the examples described above, the probability to detect the affected UF04/05 within one beam sweep might decrease, depending on the applied DPSK demodulation technique.

Strictly speaking, the use of P5 below a certain off-boresight angle (e.g. at the point of -6 dB signal strength relative to the beam maximum) definitely increases the SPR duration to such an extent that the "80 ns" requirement of ICAO Annex 10 (3.1.2.1.4.2.1) is no longer fulfilled. Therefore, it might be necessary to disable the P5 during selective calls. However, other non-addressed aircraft receiving that specific interrogation from a side lobe are then blocked for a longer period since any received telegram having a valid SPR has to be decoded completed by the transponder.

Multipath propagation affecting turning radar antennas mostly occurs at low altitudes (e.g. section 3.1.3.6) touching lower boundary of the vertical antenna pattern which is in reality not identical with the computed LVA pattern as of Figure 3-121. If the aircraft operates at larger distances from the radar site and is above 10,000 ft no significant influence was determined.

Strong effects were found in radar transmissions above water (Amsterdam flight, section 3.1.3.6 and section 3.6.3 (Figure 3-134 to Figure 3-136) and close to the airport surface, induced by non-directional multilateration interrogators from various locations on the airport.

Some TCAS devices were found not to comply with the signal-in-space defined by ICAO as described in section 3.1.4. Several TCAS UF16 broadcast and UF00 interrogations show bad signal quality regarding phase, frequency and power stability. Deficiencies of the design and defective components are known to cause such effects. If the initial signal quality is as bad as observed in those transmissions, the signal-in-space reaching the aircraft antenna is even worse. Several concerned aircraft are identified by their Mode S addresses since the UF16-32 could be accurately read. Some of the radiated signals are unlikely to be detected by non-measurement equipment, e.g. transponders. However, this was not investigated in detail, so this will have to remain an assumption.

4.3 Single Antenna Installation

Section 3.6 provides measurements and analyses of limitations for non-diversity transponders on small aircraft that only use one antenna (located at the bottom of the fuselage).

For radar surveillance there are no significant issues on the basis of the single flight performed under real small aircraft conditions as shown in section 3.6.3. There is no significant difference for the top and bottom antenna in the line-of-sight between radar and aircraft. Higher elevation or tilt angles have to be reached before that difference becomes effective.

This may be the case if multipath propagation is induced from ground reflectors like conducting sea surfaces, since then a single bottom antenna casually experiences stronger scattering than a top antenna, depending on the angle of incidence. These issues could be further analysed in a dedicated investigation on multipath propagation on a larger data basis gained from smaller aircraft measurements in combination with radar data.

Regarding TCAS, no clear statement can be given having only the radar data available from the Amsterdam flight. Too few aircraft were flying above in the near vicinity as shown by Figure 3-116. As expected, the closer TCAS equipped aircraft generate sufficient signal strength, whereas the aircraft at 14000 ft or higher altitude difference have weak signals.

A more detailed discussion would require more data gained with smaller aircraft, having more air traffic at higher altitudes in the near vicinity.

4.4 Interference Issues

The Mode S channels, especially the 1090 MHz downlink channel have a high radio load. Most of this is introduced by the TCAS systems and ADS-B extended squitters.

Radars and receiving equipment listening on the channel must expect and deal with superimposing messages and lost messages. The certification process and test procedures should therefore include a loaded channel, many superimposing signals and reflections.

Current observations show that transponders have to handle more than 2,000 interrogations per second. TCAS devices must be designed to handle more than 3,000 replies. Both have to recover from unreadable messages or message not addressed to them as quickly as possible.

The radio load is expected to rise during the next years, since more aircraft are going to be equipped with ADS-B. Replacing conventional Mode A/C transponders with Mode S transponders will lower the radio load, since the surveillance of Mode S equipped aircraft by the TCAS devices introduces a much lower radio load.

The standardization of new applications using Mode S such as air-ground data link communications should be discouraged. The standardization of new extended squitter ADS-B formats should be limited. Applications under development such as multilateration should rely on passive reception of messages that are sent anyway, instead of interrogating aircraft.

4.5 Interaction of Radar, Transponder and Test Equipment

4.5.1 General Remarks

As seen from section 3.4.1 the investigated transponder test sets generate fast phase reversals which match the values of only few real interrogators as demonstrated in section 3.1.3.4 (Figure 3-35). The bandwidth of a transponder receiver, which is much more limited than in the used measurement equipment, modifies the phase reversals to be fed into the demodulation process. A signal-in-space complying with ICAO requirements may have a SPR duration of 80 ns. However, a bandwidth-limited receiver may extend the SPR duration to an unknown value. In combination with the observed SLS effect, the time-of-arrival (TOA) jitter might be much higher than that of a phase transition which was originally quick (<20 ns). Those quick phase transitions are only slightly prolonged by the receiver.

It depends generally on the RF/IF design, in particular on the filter bandwidth and the DPSK demodulation technique applied by the transponder if the device is interoperable with real radars. Since transponder test sets approximate only a very limited choice of real signals-in-space a general correct functioning cannot be taken for granted.

4.5.2 Recommended Changes to Test Equipment

The measurements on widely used transponder test equipment as presented in section 3.4.13.4.1 also show that typical characteristics of real radar interrogations cannot be simulated sufficiently. This is because those devices generate signals following the ICAO Annex 10 definition which does not reflect real environmental conditions.

The following changes to test equipment are thus recommended:

1. Support of blending I/Q DPSK modulation with adjustable phase reversal duration and adjustable amplitude drop.
2. Multipath-affected signal synthesis which allows to overlay an echo signal of each interrogation at adjustable time and phase offsets and with adjustable amplitude.
3. Support of different phase modulation sequences (see section 3.1.2.4.1).

All these requirements cannot be realized using the available hardware of current test sets. A fully digital signal synthesis is required to adjust the parameters of a desired bandpass signal to be converted to 1030MHz.

4.6 Recommendations to Organizations

The following sections concern the relevant certification standards and organizations contributing to develop and change them.

4.6.1 ICAO Aeronautical Surveillance Panel (ASP)

Changes to ICAO Annex 10, Volume IV:

Although Annex 10 states that *"There shall be no amplitude modulation applied during the phase reversal"* (3.1.2.1.4.2.1), it specifically refers to amplitude transients in defining the characteristics of the phase reversal (see note in figure 3-1):

> *"The 90-degree point of a phase reversal can be approximated by the minimum amplitude point on the envelope amplitude transient associated with the phase reversal and the phase reversal duration can be approximated by the time between the 0.8 A points of the envelope amplitude transient."*

This discrepancy should be resolved.

The blending phase reversal capability within 80ns on Mode S interrogations was introduced by some manufacturers to comply with the spectrum requirements given by figure 3-2 for a telegram having all bits set to “one”. However, valid Mode S interrogations do not have 56/112 telegram “one”-bits. Using a proper observation time for the DFT to compute the spectrum as stated in 3.1.2.3, there was no spectrum violation found even in the signal-in-space with the shortest phase reversal duration. It is strongly recommended to clarify the prerequisites of time/frequency conversion and spectrum measurements, since the result is strictly bound to an observation time.

Any transponder receiver will cause internal amplitude drops due to their limited RD/IF bandwidth which is far below that of the measurement system employed in the study. Consequently, all phase reversal durations will be extended, but the originally slow SPR might cause an unacceptable jitter to the SPR TOA.

It is therefore recommended to remove the strict zero-amplitude drop criterion and to replace it with a more realistic value, since any amplitude drop will not degrade the DPSK demodulation performance.

This might encourage manufacturers to speed up their phase reversals to meet examples seen in sections 3.1.2.4.3 and 3.1.3.4.

Changes to DOC 8071, Volume III (***Testing of Surveillance Radar Systems*** **) :**

The material of the still valid “First edition 1998” (see [RD18]) is old and out-dated in many parts. Moreover, it only covers the testing of radars but does not reflect current implementations of new surveillance technologies like multilateration or ADS-B.

This document should clearly state when and if a flight inspection should be performed. Contradictory details as following are given in the appendixes of the manual.

Appendix A “Flight Testing Methods” states:

> ***Periodic inspection***
>
> 2.8 Civil ATC PSR and SSR facilities, after being commissioned and set into operational service, do not require a periodic flight inspection. Instead, the radar performance parameters described in this manual shall be re-assessed at regular intervals by RTQC or by preventive/ corrective maintenance. Only in cases of specific problem investigation should it thus be necessary to perform measurement campaigns including flight checks.

In contrast to this, Appendix F “Secondary Surveillance Radar” prescribes procedures for commissioning and routine SSR flight inspection as follows:

> 2.5 Routine flight inspections are conducted to determine that the facility performance continues to meet specifications and satisfies operational requirements. The recommended frequency for routine flight inspection is 120-day intervals, plus or minus 30 days, from the initial or annual inspection. In cases where there is a satisfactory record of performance of an equipment, an Administration may extend the interval up to as much as 365 days. On the other hand, routine inspections at lesser intervals than 120 days may be needed if there are doubts about equipment performance at a given site.

While the manual generally recognizes Mode S as a newer SSR technology, it does not refer to its special characteristics and the differences to Mode A/C. Especially Mode S due do signal complexities and SLS issue needs to be monitored on a regular basis to ensure continuous interoperability.

The ancient section in Appendix F “A photographic method of recording received signals” proposes how to monitor the SSR downlink channel video signal. This should be removed completely or replaced by a system having those capabilities as of the measurement system described in this report, since this can be easily adapted to 1090 MHz. Furthermore, the technology is applicable for both Mode S and Mode A/C.

In case of a specific problem investigation it is useful to monitor the signal-in-space on 1030 MHz (airborne) as done for this study and on 1090 MHz (ground). As seen in section 3.1.3.6 it is beneficial to identify critical areas during flight inspection, e.g. at lower altitudes in TMAs where the coverage is poor. DOC 8071 should provide an indication of current measurement capabilities.

Generally, it is proposed to review Doc 8071 Volume III and develop amendments to cover new technologies.

4.6.2 EUROCAE WG-49 / RTCA SC-209

This joint working group is responsible for the development of the ED-73/DO-181 transponder MOPS. The changes proposed in the following refer to this document.

Amplitude drop issue

Alike ICAO Annex 10, the current ED-73C also seems to assume a phase reversal with a drop in amplitude during phase reversal: It describes in section 5.5.8.1 a test method for protocol checks stating:

> *"... a simple diode detector is adequate for manual determination of the location of phase reversals in a 0 dBm signal..."*

and later:

> *"The phase transitions within P6 will cause amplitude modulation that can be easily observed"*

Since existing interrogators apply different methods for phase reversal (hard keying with strong amplitude drop or I/Q blending with little to no amplitude drop), the standards should reflect this and not make any assumptions on modulation technology. Furthermore, this might be misleading, since it unintentionally suggests an inadequate method for using the amplitude for demodulation instead of the phase.

Side Lobe Suppression Criteria

There is a clear contradiction between the side lobe suppression criteria as given in ICAO Annex 10 and ED-73C (see section 0):

While ICAO Annex 10 states that no reply shall occur when P5 > P6 + 0 dB (upper threshold) and always reply when P5 < P6 - 9 dB (lower threshold), ED-73C specifies these limits to be 3 dB (upper) and -12 dB (lower).

Also, the required transponder reply behaviour in the range between lower and upper threshold is not defined.

The following changes are thus recommended:

1. Change ICAO Annex 10 and ED-73C to use the same thresholds.
2. Specify expected behaviour of transponder between lower and upper threshold values, e.g. gradual reduction of reply rate. *Note: the safest option would be to state that an interrogator cannot rely to any reply above the lower threshold.*

The working group must become aware that commercially available transponder test sets generate ideal signals which may considerably differ from real signals-in-space.

Only a few real interrogators radiate phase transitions comparable to those test sets. **However, the interoperability between approved transponders, complying with the MOPS, and existing radars must be sufficiently ensured.**

Therefore, it is proposed to introduce new transponder test set capabilities to synthesize multipath propagation effects and blending phase modulation, as stated in section 3.1.2.4.

In case of a strong SLS effect overlaying the SPR at the beam boundary there might be an additional error contribution to the TOA determination and to the subsequent reply delay. The “Mode S Reply Delay and Jitter” limits specified in section 3.72 of ED-73C may be exceeded, so their actual values should be measured under dedicated SLS test conditions. This may be extended to certain multipath-affected signal conditions.

In general, the MOPS should determine one or more worst-case interrogations, e.g. out of the variety given by this study, which is still suitable to elicit a reply. Those reference signals should then be generated by a suitable transponder test set.

All discrepancies between ICAO Annex 10 and ED-73, as stated above, should be resolved.

4.6.3 Air Navigation Service Providers (ANSPs)

An ANSP indirectly contributes to the certification standards by delegating representatives to the respective working groups.

Since the overdue revision of DOC 8071 (Part III) is likely to require an uncertain amount of time, it is suggested that ANSPs should not wait to develop suitable activities to maintain or improve the surveillance service quality level, given the fact that highly suitable analytical measurement tools as described in this study are available today. Wherever poor MSSR performance is detected, e.g. by means of EUROCONTROL SASS-C ("Surveillance Analysis Support System for ATC-Centre")-like tools with assessment on the basis of ordinary traffic, special mission flight inspections might be carried out. The prime subject of investigations should be the signal-in-space, referenced to the processed (ASTERIX) radar data.

Periodic radar flight inspection is not carried out by most civil ANSPs. In contrast to this, flight inspection of terrestrial navigation aids consumes numerous flight hours which are mostly spent on ILS and on instrument flight procedure inspection. Since these flights all take place in radar airspace a passive SSR measurement system could run in parallel at no additional flight time cost. This allows a continuous monitoring of the SSR signal-in-space performance, covering both rotating MSSR facilities and fixed MLAT interrogators.

Aircraft TCAS signals could then be also monitored on ground from elevated sites which are not subjected to multipath degradations. Amplitude and phase stability measurements as shown in this study can assist to identify poor interrogators violating certain ICAO requirements and forming a potential hazard. Far beyond conventional TCAS production line tests this would be continuously performed under real world operational conditions, as an additional safety net element in the complex world of ATC surveillance and safety.

Appendix A Measurement Equipment

Aircraft and primary avionics transponder used for the measurement campaign:

Hawker Beechcraft King Air B300, Registration number "D-CFMD"

Transponder: Rockwell-Collins TDR-94D, ICAO 24-bit Address (hex): 3CCE6F

Cessna 172, Registration number "D-EMWF"

Transponder: Becker BXP6401-2-(01), ICAO 24-bit Address (hex): 3D2699

Transponders used in the Laboratory:

Transponder #1:

Manufacturer:	Becker
Type:	BXP 6401-2
P/N:	BXP6401-2-(01)
S/N:	00475
Classification:	ETSO-C112a, Class 2, Level 2es

Transponder #2:

Manufacturer:	Garmin
Type:	GTX 328
P/N:	011-01684-00
S/N:	13K010109
Classification:	ETSO-2C112b, Class 1, Level 2s

Transponder #3:

Manufacturer:	Funkwerk Avionics
Type:	TRT800H
P/N:	800ATC-H-(201)-(201) with Mod. 2/5/8/10/11
S/N:	30505510
Classification:	ETSO-2C112a, Class 1, Level 2es

Appendix B Interrogator Code Assignment in Europe

The following Interrogator Codes were assigned during the MOSTDONT trials in the relevant area (Source: [RD17] ICAO CNS Supplement - SSR Mode S Interrogator Code (IC) Allocations for the EUR Region, Edition 1.6, EUROCONTROL).

Mode S Station	ALLOCATED CODE II	SI	Effective Date	OPERATOR	REMARKS/REFERENCE
GERMANY					
Auersberg North Cluster main	03		02/07/2008	DFS	MICA/ALLOC358
Auersberg North Cluster fallback	09		02/07/2008	DFS	MICA/ALLOC364
Deister	04		02/08/2007	DFS	MICA/ALLOC271
Deister North Cluster main	03		02/07/2008	DFS	MICA/ALLOC359
Deister North Cluster fallback	09		02/07/2008	DFS	MICA/ALLOC365
Düsseldorf Süd South Cluster main	11		02/07/2008	DFS	MICA/ALLOC352
Düsseldorf Süd South Cluster fallback	09		17/12/2008	DFS	MICA/ALLOC416
Frankfurt Süd South Cluster main	11		02/07/2008	DFS	MICA/ALLOC353
Frankfurt Süd South Cluster fallback	09		17/12/2008	DFS	MICA/ALLOC417
Gosheim South Cluster main	11		02/07/2008	DFS	MICA/ALLOC354
Gosheim South Cluster fallback	09		17/12/2008	DFS	MICA/ALLOC418
Götzenhain	14		05/02/2004	DFS	MICA/ALLOC072, TRD
Großhaager Forst South Cluster main	11		02/07/2008	DFS	MICA/ALLOC355
Großhaager Forst South Cluster fallback	09		17/12/2008	DFS	MICA/ALLOC419
München Süd South Cluster main	11		02/07/2008	DFS	MICA/ALLOC356
München Süd South Cluster fallback	09		17/12/2008	DFS	MICA/ALLOC420
Neunkirchner Höhe South Cluster main	11		02/07/2008	DFS	MICA/ALLOC357
Neunkirchner Höhe South Cluster fallback	09		17/12/2008	DFS	MICA/ALLOC421
Nordholz	02		01/08/2003	DFS	MICA/ALLOC269
Nordholz North Cluster main	03		02/07/2008	DFS	MICA/ALLOC360
Nordholz North Cluster fallback	09		02/07/2008	DFS	MICA/ALLOC366

Mode S Station	ALLOCATED CODE II	SI	Effective Date	OPERATOR	REMARKS/REFERENCE
GERMANY cntd.					
POEMS Düsseldorf N. North Cluster main	03		02/07/2008	DFS	MICA/ALLOC361
POEMS Düsseldorf N. North Cluster fallback	09		02/07/2008	DFS	MICA/ALLOC367
Schmooksberg	11		02/07/2008	DFS	MICA/ALLOC381
Schmooksberg North Cluster main	03		02/07/2008	DFS	MICA/ALLOC362
Schmooksberg North Cluster fallback	09		02/07/2008	DFS	MICA/ALLOC368
Tegel North Cluster main	03		02/07/2008	DFS	MICA/ALLOC363
Tegel North Cluster fallback	09		02/07/2008	DFS	MICA/ALLOC369
Büchel	01		02/07/2008	GAF	MICA/ALLOC385
Brockzetel BZ main	13		ad hoc 01/10/2007	GAF	MICA/ALLOC328, Cluster
Brockzetel BZ fallback		13	ad hoc 01/10/2007	GAF	MICA/ALLOC334, Cluster
Döbern DO main	13		ad hoc 01/10/2007	GAF	MICA/ALLOC329, Cluster
Döbern DO fallback		13	ad hoc 01/10/2007	GAF	MICA/ALLOC335, Cluster
Döbraberg DB main	13		ad hoc 01/10/2007	GAF	MICA/ALLOC330, Cluster
Döbraberg DB fallback		13	ad hoc 01/10/2007	GAF	MICA/ALLOC336, Cluster
Elmenhorst EH main	13		ad hoc 01/10/2007	GAF	MICA/ALLOC331, Cluster
Elmenhorst EH fallback		13	ad hoc 01/10/2007	GAF	MICA/ALLOC337, Cluster
Erbeskopf EK, main	13	13	ad hoc 01/10/2007	GAF	MICA/ALLOC332, Cluster
Erbeskopf EK, fallback		13	ad hoc 01/10/2007	GAF	MICA/ALLOC338, Cluster
Großer Arber GA, main	13		ad hoc 01/10/2007	GAF	MICA/ALLOC333, Cluster
Großer Arber GA, fallback		13	ad hoc 01/10/2007	GAF	MICA/ALLOC339, Cluster
Greding	14		05/02/2004	BWB	TRD-Station, MICA/ALLOC077
Erbach	14		ad hoc 07/05/2008	EADS	TRD-Station, MICA/ALLOC395
USH	14		05/02/2004	EADS	TRD-Station, MICA/ALLOC079
Ulm ULM	14		ad hoc 22/03/2007	EADS	TRD-Station, MICA/ALLOC281

Mode S Station	ALLOCATED CODE II	SI	Effective Date	OPERATOR	REFERENCE/REMARKS
BELGIUM					
Bertem Onmounted		08	17/12/2008	Belgocontrol	MICA/ALLOC408
Brussels		24	17/12/2008	Belgocontrol	MICA/ALLOC409
Liege	06		04/06/2009	Belgocontrol	MICA/ALLOC450
St Hubert Onmounted	05		15/09/2005	Belgocontrol	MICA/ALLOC113
EADS 2000I BE	14		04/07/2008	EADS BE	MICA/ALLOC398

Mode S Station	ALLOCATED CODE II	SI	Effective Date	OPERATOR	REFERENCE/REMARKS
FRANCE					
Auch		60	19/11/2009	DSNA	MICA/ALLOC481
Avranches		44	19/11/2009	DSNA	MICA/ALLOC482
Boulogne	10		15/02/2007	DSNA	MICA/ALLOC226
Charles de Gaulle	01		19/11/2009	DSNA	MICA/ALLOC484
Chaumont	04		31/08/2006	DSNA	MICA/ALLOC172
Grand Ballon		60	06/05/2010	DSNA	MICA/ALLOC506
Grasse		44	19/11/2009	DSNA	MICA/ALLOC483
Grenoble		28	17/01/2008	DSNA	MICA/ALLOC321
Marseille		13	ad hoc:05/08/2008	DSNA	MICA/ALLOC405
Montpellier	08		15/02/2007	DSNA	MICA/ALLOC240
Mont Ventoux		21	04/05/2009	DSNA	MICA/ALLOC469
Nevers	07		15/02/2007	DSNA	MICA/ALLOC233
Nice		05	04/05/2009	DSNA	MICA/ALLOC470
Paris Nord		12	17/01/2008	DSNA	MICA/ALLOC313
Paris Sud	03		15/02/2007	DSNA	MICA/ALLOC215
Pierre-sur-Haute	11		15/02/2007	DSNA	MICA/ALLOC237
Toulouse Blagnac		12	19/11/2009	DSNA	MICA/ALLOC485
Tours	09		17/12/2008	DSNA	MICA/ALLOC422
Cazeux CEV	14		01/06/2003	FAF	TRD-Station, MICA/ALLOC063
Toulouse Exp	14	62	ad hoc:06/02/2007	DSNA/DTI	TRD-Station, MICA/ALLOC059 & 258
Ymare	14		01/06/2003	Thales	TRD-Station, MICA/ALLOC060

Mode S Station	ALLOCATED CODE II	SI	Effective Date	OPERATOR	REFERENCE/REMARKS
LUXEMBOURG					
Luxembourg-TAR2	02		17/12/2008	AA Lux	MICA/ALLOC413
Luxembourg-TAR3	02		17/12/2008	AA Lux	MICA/ALLOC414

Note: TAR 2 and TAR 3 are clustered

Mode S Station	ALLOCATED CODE II	SI	Effective Date	OPERATOR	REFERENCE/REMARKS
POLAND					
Chrusciel	07		02/07/2008	PLAF NATO	MICA/ALLOC376
Suwalki	01		16/03/2006	PLAF NATO	MICA/ALLOC136
Zamosc	08		02/07/2008	PLAF NATO	MICA/ALLOC378

Mode S Station	ALLOCATED CODE II	SI	Effective Date	OPERATOR	REFERENCE/REMARKS
SWITZERLAND					
Geneva 1	06		ad hoc 08/11/2007	skyguide	MICA/ALLOC253
Geneva 2bis	02		ad hoc 08/11/2007	skyguide	MICA/ALLOC254
Holberg 1	05		ad hoc 08/11/2007	skyguide	MICA/ALLOC255
Holberg 2	01		ad hoc 08/11/2007	skyguide	MICA/ALLOC250
La Dôle	10		ad hoc 08/11/2007	skyguide	MICA/ALLOC251
Lägern	08		16/03/2006	skyguide	MICA/ALLOC266

Mode S Station	ALLOCATED CODE II	SI	Effective Date	OPERATOR	REFERENCE/REFERENCE
THE NETHERLANDS					
Schiphol TAR1		28	ad hoc 30/11/2007	LVNL	MICA/ALLOC344
Leeuwarden	07		15/09/2005	RNLAF	Clustered, MICA/ALLOC129
Soesterberg	07		15/09/2005	RNLAF	Clustered, MICA/ALLOC130
Twenthe	07		15/09/2005	RNLAF	Clustered, MICA/ALLOC131
Volkel	07		15/09/2005	RNLAF	Clustered, MICA/ALLOC132
Woensdrecht	07		15/09/2005	RNLAF	Clustered, MICA/ALLOC133

Mode S Station	ALLOCATED CODE II	SI	Effective Date	OPERATOR	REFERENCE/REMARKS
NATO					
AWACS	15		05/06/2002	NATO	MICA/ALLOC032

Appendix C Mode S Uplink and Downlink Formats

The following Uplink and Downlink Formats are currently defined for Mode S:

Uplink:

UF00	Short Air-Air-Surveillance (ACAS)
UF04	Surveillance Altitude Request
UF05	Surveillance Identity Request
UF11	Mode S-Only All-Call
UF16	Long Air-Air-Surveillance (ACAS)
UF19	(military use)
UF20	Comm-A Altitude Request
UF21	Comm-A Identity Request
UF22	(military use)
UF24	Comm-C (ELM)

Downlink:

DF00	Short Air-Air-Surveillance (ACAS)
DF04	Surveillance Altitude Reply
DF05	Surveillance Identity Reply
DF11	All-Call Reply
DF16	Long Air-Air-Surveillance (ACAS)
DF17	Extended Squitter
DF18	Extended Squitter from non-transponder equipment
DF19	(military use)
DF20	Comm-B Altitude Reply
DF21	Comm-B Identity Reply
DF22	(military use)
DF24	Comm-D (ELM)

EUROPEAN AVIATION SAFETY AGENCY
AGENCE EUROPÉENNE DE LA SÉCURITÉ AÉRIENNE
EUROPÄISCHE AGENTUR FÜR FLUGSICHERHEIT

Postal address
Postfach 101253
50452 Cologne
Germany

Visiting address
Ottoplatz 1
50679 Cologne
Germany

Tel +49_221_89990-000
Fax +49_221_89990-999
Mail info@easa.europa.eu
Web easa.europa.eu